STUDYING ANTARCTIC ORDINARY CHONDRITE (OC) AND MILLER RANGE (MIL) NAKHLITE METEORITES TO ASSESS CARBONATE FORMATION ON EARTH AND MARS

A Dissertation

by

MICHAEL ELLIS EVANS

Submitted to the Office of Graduate and Professional Studies of
Texas A&M University
in partial fulfillment of the requirements for the degree of

DOCTOR OF PHILOSOPHY

Chair of Committee,	Piers Chapman
Co-Chair of Committee,	Paul Niles
Committee Members,	Niall Slowey
	Kathryn Shamberger
	Ethan Grossman
Head of Department,	Shari Yvon-Lewis

May 2017

Major Subject: Oceanography

ABSTRACT

Carbonates are found in meteorites collected from Antarctica. The stable isotope composition of these carbonates records their formation environment on either Earth or Mars. The first research objective of this dissertation is to characterize the $\delta^{18}O$ and $\delta^{13}C$ values of terrestrial carbonates formed on Ordinary Chondrites (OCs) collected in regions near known martian meteorites. The second objective is to characterize the $\delta^{18}O$ and $\delta^{13}C$ values of martian carbonates from Nakhlites collected from the Miller Range (MIL). The third objective is to assess environmental changes on Mars since the Noachian period.

The OCs selected had no pre-terrestrial carbonates so any carbonates detected are presumed terrestrial in origin. The study methodology is stepped extraction of CO_2 created from phosphoric acid reaction with meteorite carbonate.

Stable isotope results show that two distinct terrestrial carbonate species (Ca-rich and Fe/Mg-rich) formed in Antarctica on OCs from a thin-film of meltwater containing dissolved CO_2. Carbon isotope data suggests the terrestrial carbonates formed in equilibrium with atmospheric CO_2 $\delta^{13}C$ = -7.5‰ at >15°C. The wide variation in $\delta^{18}O$ suggests the carbonates did not form in equilibrium with meteoric water alone, but possibly formed from an exchange of oxygen isotopes in both water and dissolved CO_2.

Antarctica provides a model for carbonate formation in a low water/rock ratio, near 0°C environment like modern Mars. Nakhlite parent basalt formed on Mars 1.3 billion years ago and the meteorites were ejected by a single impact approximately 11

million years ago. They traveled thru space before eventually falling to the Earth surface 10,000-40,000 years ago. Nakhlite samples for this research were all collected from the Miller Range (MIL) in Antarctica. The Nakhlite stable isotope results show two carbonate species (Ca-rich and Fe/Mg-rich) with a range of $\delta^{18}O$ values that are similar to the terrestrial OC carbonates. The Nakhlite carbonates have distinctly different, heavier $\delta^{13}C$ values from a presumed martian carbon reservoir. These carbonates cannot form in equilibrium at 15°C with the modern Mars atmospheric CO_2 (measured by the Curiosity rover) $\delta^{13}C = 46‰$, but may reflect kinetic carbonate formation from a high pH fluid. Alternatively, the Nakhlite carbonates may have formed with a lighter, early Amazonian atmosphere of $\delta^{13}C \approx 30‰$. Assuming the martian carbonates formed in a thin-film environment like the OC terrestrial carbonates, an oxygen mixing model predicts early Amazonian martian meteoric water $\delta^{18}O = -30‰$.

DEDICATION

I dedicate this work to my parents, who instilled in me a thirst for knowledge and a zest for life. They shaped my character to be confident, independent, and meticulous in all pursuits. My father modeled integrity with his work ethic that balanced professional and personal life. My love for family time stems from him. My mother has always been my greatest encouragement. She continues to model adult development with intelligence, humor, travel, outreach, and altruism.

I also dedicate this work to my children with the hope that they grow, and evolve, and expand with every breath. I hope they treat life as a long education experience, and make wise decisions without fear of wondering "What if …"

ACKNOWLEDGEMENTS

I acknowledge my Texas A&M University (TAMU) committee chair, Dr. Piers Chapman, for accepting me as his wayward graduate student and guiding my evolution in the Oceanography Department. I have greatly enjoyed his gentle coaching as a teacher, a researcher, and a colleague. I encourage all grads to seek his wisdom over "Beers with Piers".

I also acknowledge my NASA committee co-chair, Dr. Paul Niles, who crafted a scientist from an engineer. His focus redirected my outlook from "How" to "Why" with the assurance that "Science is SLOW". His assistance in coordinating NASA and TAMU logistics facilitated this successful research collaboration.

I credit Rick Socki, Darren Locke, and Dr. Tao Sun for teaching me the skills to accomplish this research in NASA's Light Element Analysis Laboratory (LEAL). I admire their patience, knowledge, and creativity in working to build, test, and maintain the finicky instruments and temperamental equipment.

I thank my committee members, Dr. Niall Slowey, Dr. Katie Shamberger, and Dr. Ethan Grossman for their guidance and support throughout the course of my TAMU education and research. I appreciate the faculty within Oceanography Department for their dedication to teaching excellence during my coursework. I acknowledge Dr. Debbie Thomas for her enthusiastic support (and comradeship on AGU runs).

My life at TAMU has been enhanced because of a close family of graduate students (especially Steph, Natalie, Chris, Cody and Kat) in the Oceanography

Department. From shared coursework to OCNG-252 TA meetings to exploring the Galapagos Islands to Friendsgivings to AGU with tailgates, football games, rallys, movie nights, “Mug Club” and pub crawls - I am thankful. I also developed dear friendships through church (especially Linda, Glenn, & Vinnie) and choir in College Station that enriched my soul. My heart resides in Aggieland.

Thanks to the Oceanography Department staff (especially Amy, Wendy, Janet and Debra) for their assistance with the paperwork that provided funding, benefits, and reimbursements for my educational expenses. This dissertation would not have been possible without the support of everyone.

CONTRIBUTORS AND FUNDING SOURCES

Contributors

This work was supervised by a dissertation committee with members of the TAMU College of Geosciences, including Dr. Piers Chapman (co-chair), Dr. Niall Slowey, and Dr. Katie Shamberger, of the Oceanography Department, and Dr. Ethan Grossman of the Geology and Geophysics Department. Dr. Paul Niles of NASA/JSC functioned as both co-chair of the dissertation committee and management supervisor of the student at NASA. All experimental work conducted for this dissertation was completed by the student independently in the NASA/JSC Light Element Analysis Laboratory (LEAL) located in Houston, Texas.

Funding Sources

Graduate study was supported by a stipend from Texas A&M University – Galveston as a Teaching Assistant (TA) for CHEM-117 Chemistry Lab for Engineers (Fall 2011 and Spring 2012), as a TA for OCNG-252 Oceanography Lab (Fall 2012, Spring 2013, and Fall 2013) and as a Graduate Assistant Lecturer (GAL) for OCNG-251 Oceanography (Fall 2014, Fall 2015, and Fall 2016).

Graduate study was also made possible with a scholarship from the family of Louis and Elizabeth Scherck for the 2015-2016 and 2016-2017 school years. Travel grants from the TAMU Oceanography Graduate Council (OGC) provided funds to present research at the 2014 American Geophysical Union (AGU) conference and at the

2017 Lunar Planetary Science Conference (LPSC). NASA provided funds to present research at the 2015 and 2016 AGU conference, and the LPSC in 2016 and 2017.

The remainder of my graduate funding was earned as salary while working as a summer scientist for Jacobs Engineering (Summer 2012) and as a NASA Pathways Graduate Student (Summer 2013, Jan-Aug 2014, Jan-Aug 2015, Jan-Aug 2016, Jan-May 2017).

TABLE OF CONTENTS

Page

LIST OF FIGURES

LIST OF TABLES

CHAPTER I

INTRODUCTION AND BACKGROUND

Understanding Mars

Why Study Mars?

Humans are exploring Mars to determine if life currently exists on that planet, or if life could have existed there in the past. Using Earth as a model for types of life that might exist now, or could have existed previously on Mars, it is necessary to identify "habitable" martian environments. The current martian environment is very cold and arid (similar to conditions in Antarctica on Earth), with little "habitable" environment. Surface geologic evidence from Mars demonstrates periods of past fluvial systems in the form of river channels, tributary networks, deltas, and lake beds. These features were formed by flowing, liquid water on the surface of Mars that is no longer present (although water ice currently exists at the poles). Obviously Mars has had dramatic changes in surface hydrology over geologic time, so understanding how water has moved from the surface to the subsurface, or from the surface to space, is necessary.

Carbonates require water to form. Rock cations combine with carbon dioxide (CO_2) in the presence of water to create calcite or aragonite (calcium based), magnesite (magnesium based), or siderite (iron based). Stable isotope values of carbon and oxygen in the carbonate reflect environmental conditions in the atmosphere and hydrosphere/cryosphere at the time of their formation. If former martian environmental conditions are discovered, then comparing them with modern values (as determined by

instruments orbiting Mars and on the surface) makes it possible to assess how the environment has changed over time. This knowledge aids interpretation of ancient martian "habitability" zones in the ongoing search for extra-terrestrial life.

This study measures the carbonates in martian meteorites known as "Nakhlites", which formed in lava flows on Mars 1.3 billion years ago and were ejected with a single impact on Mars 11 million years ago (Bridges et al., 2001). To assess the potential for terrestrial contamination of carbonates in the Nakhlites, an analysis of terrestrial carbonates formed on Ordinary Chondrite (OC) meteorites is first completed. The Antarctic environment provides an analog for carbonate formation in a low water/rock ratio, cold (near 0°C) environment similar to the modern martian environment. All of the meteorites (both Nakhlites and OCs) for this dissertation research study were collected in Antarctica. There are three objectives of this research:

1. Characterize the $\delta^{18}O$ and $\delta^{13}C$ values of terrestrial carbonates formed on Ordinary Chondrites (OCs) collected in regions near known martian meteorites
2. Characterize the $\delta^{18}O$ and $\delta^{13}C$ values of martian carbonates from Nakhlites collected from the Miller Range (MIL)
3. Assess environmental changes on Mars since the Noachian period

Mars Environmental Changes

Mars' geologic history is divided into Epochs using either crater count techniques or mineralogical techniques for dating (see Figure 1-1) (Jakosky and Phillips,

2001). The earliest period of Mars, known as Noachian (circa 3.7 - 4.6 Ga) was the most active geologically, with an active dynamo, volcanism and possibly a dense atmosphere similar to ancient Earth during the Hadean period. During this period the sun was approximately 25% less bright (Batalha et al., 2016, Wordsworth et al., 2017) and the planets of the inner solar system were pummeled by leftover accretion debris from 4.1-4.5 Ga, climaxing at the Late Heavy Bombardment (LHB) approximately 3.8-3.9 Ga (Abramov and Mojzsis, 2016), followed by a profound loss of atmospheric CO_2.

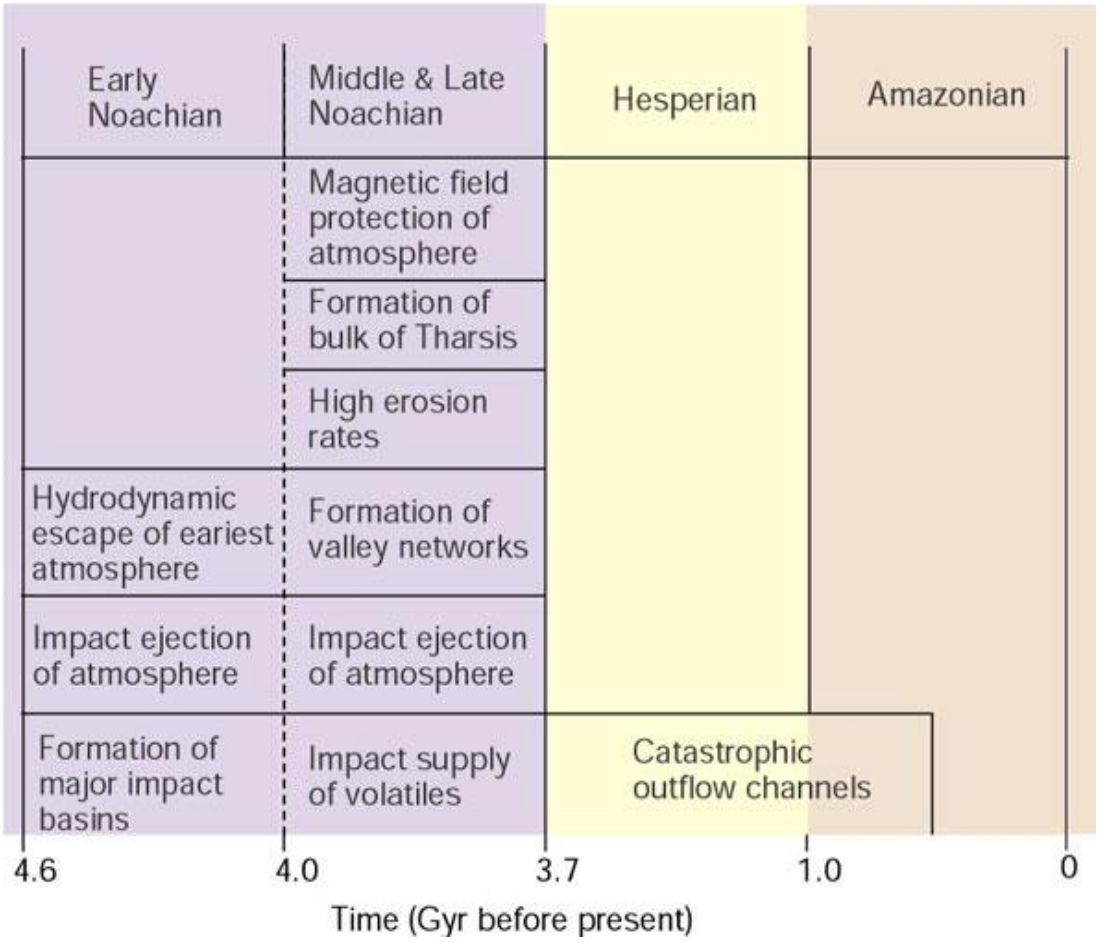

Figure 1-1: Mars Geologic Time (reprinted from Jakosky and Phillips, 2001)

During the late Noachian and early Hesperian period (circa ~1.0 - 3.7 Ga), fluvial systems formed on the surface. This period saw a dramatic decrease in volcanism and likely atmospheric CO_2 loss to space. By the current period, known as Amazonian (circa present to ~1.0 Ga), Mars was a "dead" planet with little geologic activity and a much thinner, CO_2-rich, atmosphere (Grady et al., 2007).

Mars is more likely to host, or have hosted, habitable environments if liquid water was available for long periods of geologic time. Geologists believe that martian fluvial and evaporite deposits on the surface (Poulet et al., 2005) indicate the presence of past surface water (likely Late Noachian into the Hesperian Epoch), at least for brief geologic periods (see Figure 1-2) (Lammer et al., 2008). Mars clearly exhibits geologic features of fluvial erosion (Carr, 1996), sedimentary layered deposits (Malin and Edgett, 2000), clay and phyllosilicate deposition (Ehlmann et al., 2013), and aqueous mineral deposition such as carbonates (Morris et al., 2010) and sulfates (Gendrin et al., 2005).

Modern water ice has been detected at the poles (Bibring et al., 2004) and in the subsurface of Mars (Boynton et al., 2002). Recurring Slope Lineae (RSL) are features of melted brine flows under the surface on sunlit hills, which currently occur seasonally on Mars (Chevrier and Rivera-Valentin, 2012).

As shown in Figure 1-2, the Viking Landers 1 (VL1) and 2 (VL2), launched in 1975 and retired in 1982, (NASA, 2017a) measured current martian surface pressure varied (with an 8^{th}-order harmonic fit of data) from ~6.8 mb to ~9.9 mb over a 660 sol (sol is a martian day) period (Hourdin et al., 1995).

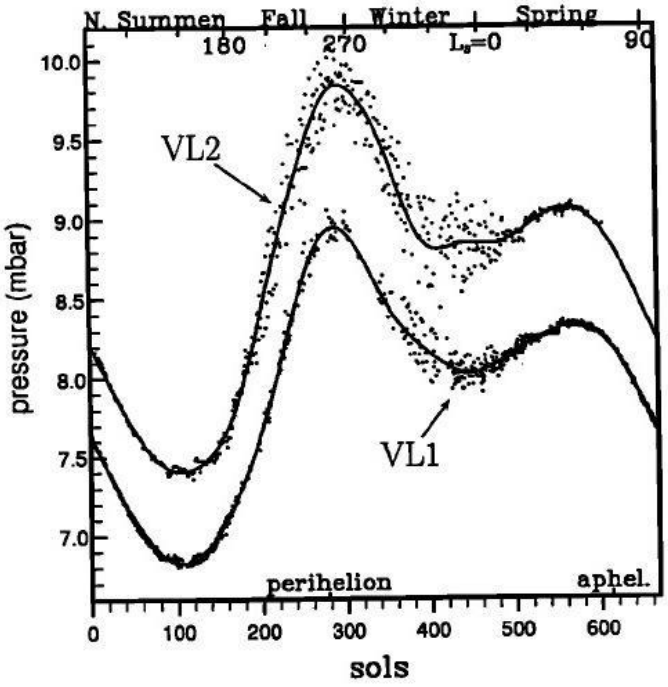

Figure 1-2: Mars Surface Pressure (reprinted from Hourdin et al., 1995)

Figure 1-3 demonstrates the typical zonally averaged temperature variation shortly after solar zenith on modern Mars at all latitudes during the northern hemisphere summer (Haberle et al., 2001). The warmest temperature near the equator (~280°K) is above the freezing point of water (273°K).

Given the current environmental conditions and the phase behavior of H_2O (as shown in a phase diagram (Figure 1-4), liquid water is mostly unstable to boiling or freezing on the current martian surface. An important, but often overlooked, distinction of water phase stability on Mars is the low amount of water vapor in the atmosphere. The partial pressure of water vapor is the critical factor, not just surface pressure (Niles, 2017). Perhaps 29% of the entire martian surface could support liquid water near zenith

(for a few hours) on an average of 37 sols each year if surface ice is available for melting (Haberle et al., 2001).

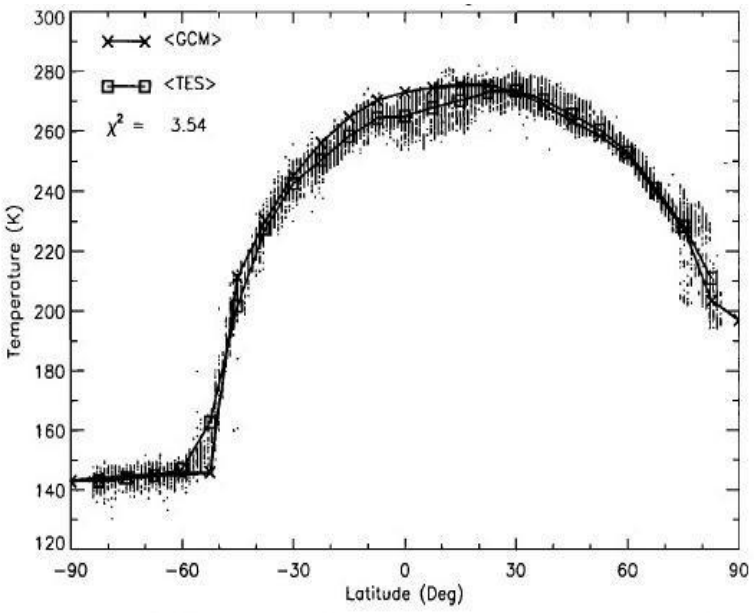

Figure 1-3: Mars Near Zenith Surface Temperatures (reprinted from Haberle et al., 2001)

Early 1-D radiative convective models of the martian atmosphere predicted a high concentration of CO_2 (up to 5 bars) that could have raised surface temperatures in ancient Mars to 0°C (Haberle, 1998), but a newer 3-D climate model with parameterized CO_2 ice cloud microphysical and radiative properties suggests the ancient martian climate was never above the freezing point of water (Forget et al., 2013).

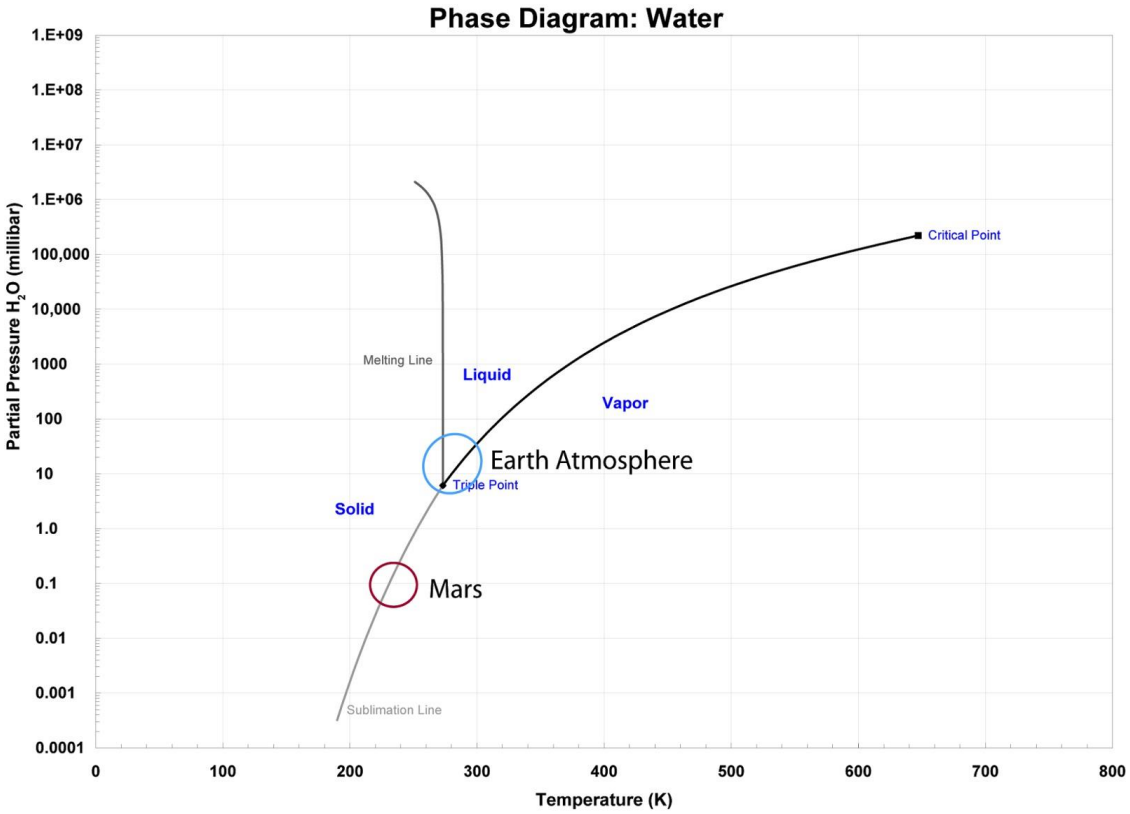

Figure 1-4: Mars Typical Surface Temperature (reprinted from Niles, 2017)

With the latter model, brief periods of warming from impacts of volcanism would create liquid water despite the below freezing surface temperature. If, however, the martian atmosphere was once dense enough for phase stable liquid water, where did the CO_2 go? The CO_2 must have either 1) escaped to space, or 2) been trapped in different reservoirs on Mars.

A warm, wet ancient Mars with a dense atmosphere (>1 bar) would produce large volumes of sedimentary carbonates on the surface, yet little evidence of surface carbonate lithology exists (Pollack et al., 1987). Some researchers suggest that vast carbonates formed early in the Noachian, and were then buried by lava flows in the late

Noachian and Hesperian (Wray et al., 2016). Others suggest the ancient atmosphere was less dense (<1 bar) and the missing CO_2 can be accounted for with loss to space and Hesperian carbonate formation (Hu et al., 2015). Another theory concludes from measurements of surface sulfur and in-situ sulfates (Clark et al., 1976, Squyres et al., 2004) that ancient Mars possessed an acidic environment (Hurowitz et al., 2006), which would be hostile to carbonate deposition (Fairen et al., 2004).

Mars may have accreted with much water, perhaps enough to cover the entire planet with a Global Equivalent Layer (GEL) of 10 km (Raymond, 2006). Modern Mars has only a GEL only 20-30m in ice-caps and regolith, so much water was either lost to space or could be buried in unknown reservoirs. A study suggests water is trapped in a 500m GEL thick deposit of serpentine in the southern hemisphere, based on measurements of the magnetic field with the Mars Global Surveyor (Chassefiere et al., 2013). Serpentine is formed from the aqueous weathering of basalts, and it releases H_2 gas. The H_2 gas would be lost to space with an enrichment of the atmospheric D/H ratio, which has been measured (Owen et al., 1988). Martian minerals formed in equilibrium with the ancient martian atmosphere have a D/H ratio 5 times greater than similar species on Earth due to the loss of H to space (Watson et al., 1994). Measurements of the δD in martian meteorites (Nakhlites) have not successfully reproduced this high enrichment, probably due to rapid contamination of samples from exchange of hydrogen with the terrestrial atmosphere (Hallis et al., 2012).

A model of the greenhouse gas composition of early Mars suggests that atmospheric methane (CH_4) could provide sufficient global warming to raise surface

temperature significantly (Wordsworth et al., 2017). The methane source could be serpentization of olivine-rich crust, volcanism, or atmospheric thermochemistry following large meteorite impacts. The authors conclude:

> "Our results suggest that with just over 1 bar of atmospheric CO_2, a few percent of H_2 and/or CH_4 would have raised surface temperatures to the point where the hydrological cycle would have been vigorous enough to explain the geological observations".

Isotopic studies of the gas Xenon (Xe) suggest 50-90% of the martian atmosphere was lost to space from 4.0 Ga to 4.3 Ga (which is <0.5 billion years after accretion to the end of the LHB) (Jakosky and Jones, 1997). Possible Mars volatile sinks, and reservoirs for volatiles are shown in Figure 1-5.

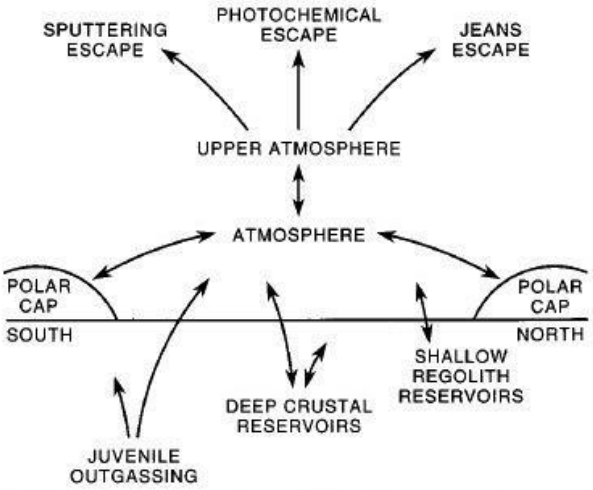

Figure 1-5: Mars Volatile Sources, Sinks and Reservoirs (reprinted from Jakosky and Jones, 1997)

Atmospheric models suggest nonthermal escape processes could have removed 10-100 mbar of CO_2 since 4.1 Ga (Chassefiere et al., 2013, Lammer et al., 2013). A

model of the martian upper atmosphere suggests < 300 mbar of CO2 has escaped to space since the LHB (Hu et al., 2015). If the early Noachian atmosphere was dense (>1 bar), these processes are insufficient to account for the thin Amazonian atmosphere of <10 mbar, driving the ongoing search for an ancient carbon reservoir sink.

Using ages based on crater count, the large fluvial features on Mars were created by liquid water flowing on the surface during the Late Noachian and Early Hesperian periods (Fassett and Head, 2008). If much of the martian atmosphere was lost in the Early Noachian period, it is challenging to explain the timing of these features. Mars climate modelers have fallen into two groups: "Cold" early Mars or "Warm" early Mars, yet neither group has successfully created compelling solutions to the dilemma.

A possible timeline of martian atmospheric loss is given in Figure 1-6 (Lammer et al., 2008).

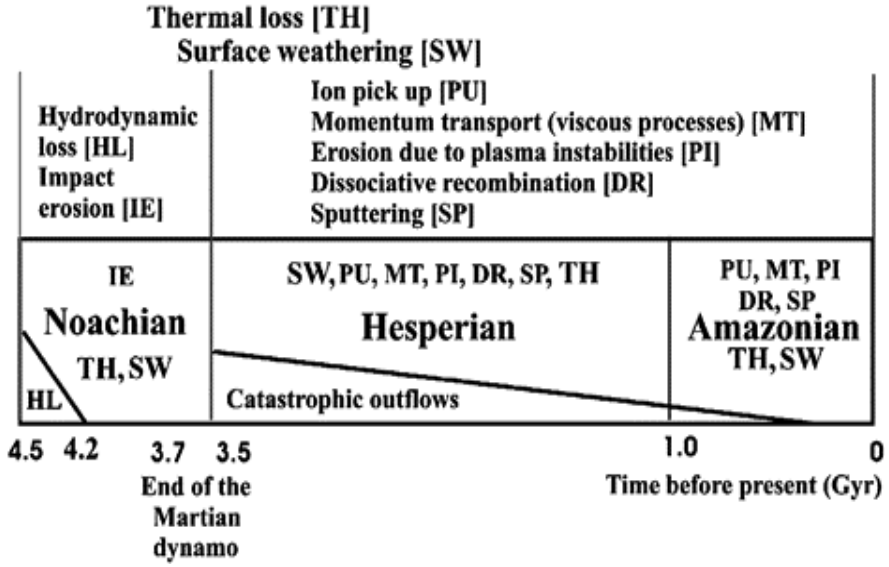

Figure 1-6: Mars Atmospheric Escape Processes (reprinted from Lammer et al., 2008)

Past instrument measurements on the surface and in orbit around Mars have detected only trace carbonates in the dust (Bandfield et al., 2003, Bibring et al., 2005). From measurements with the Mars Global Surveyor (MGS) Thermal Emission Spectrometer (TES) (Christensen, 2001 et al.):

> "There is no evidence for large-scale (tens of kilometers) occurrences of moderate-grained (> 50-μm) carbonates exposed at the surface at a detection limit of ~10%"

More recent studies, however, are identifying larger carbonate deposits on Mars. Basalts altered by low temperature fluid during the late-Noachian to early-Hesperian periods (before or during valley network formation) in the Nili Fossae region may contain carbonates representing ~0.25 – 12 mbar of atmospheric CO_2 (Edwards and Ehlmann, 2015). Mars Reconnaissance Orbiter (MRO) data from the Compact Reconnaissance Imaging Spectrometer for Mars (CRISM) instrument, outcrops of carbonate in the Huygens basin northwest of Hella and other regions have been found. These outcrops occur in the rim, walls, and ejecta of craters within Late Noachian rock (Wray et al., 2016). Often the carbonates are mixed with Fe/Mg-phyllosilicates, which are hard to distinguish using near-IR spectrometers on orbital satellites. The most recent compilation of martian carbonates discovered on the surface is given in Figure 1-7 (Green is prior reported Mg-carbonates, orange is prior reported Fe/Ca-carbonates, dark blue is study reported Fe/Ca-carbonates).

Studying the isotopic composition of martian secondary minerals can provide insight into ancient aqueous environments, and potentially address the issue of habitability. This information, coupled with estimates for the ancient martian

atmosphere, lithosphere, and hydrosphere/cryosphere, can increase understanding of the carbon cycle and how carbon dioxide reservoirs on Mars have changed over time. Climate scientists on Earth use remote sensing and direct measurements of pristine samples in a terrestrial lab.

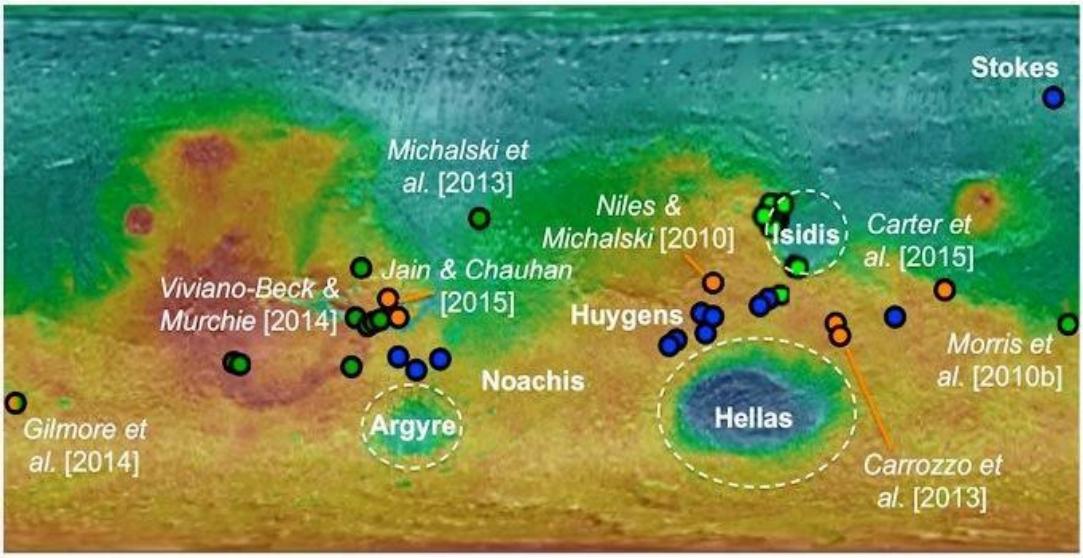

Figure 1-7: Mars Surface Carbonates (reprinted from Wray et al., 2016)

Until a successful Mars sample return mission brings pristine samples to Earth, robotic missions in orbit and on the surface are the best tools for investigating Mars. NASA's Mars Science Laboratory (MSL) launched on November 26, 2011 and landed on Mars August 6, 2012, delivering the unmanned rover "Curiosity" (NASA, 2017a). This mobile science laboratory is capable of studying Mars geology and chemistry directly, but still lacks the capability to return samples to Earth (see Figure 1-8).

An important component of Curiosity is the Sample Analysis at Mars (SAM) instrument suite. This package of 3 instruments includes a Quadrupole Mass Spectrometer (QMS), a Gas Chromatograph (GC), and a Tunable Laser Spectrometer (TLS) (see Figure 1-9) (NASA, 2017a). The TLS measures carbon and oxygen isotopes in carbon dioxide from the martian atmosphere and from the regolith (Grotzinger et al., 2012).

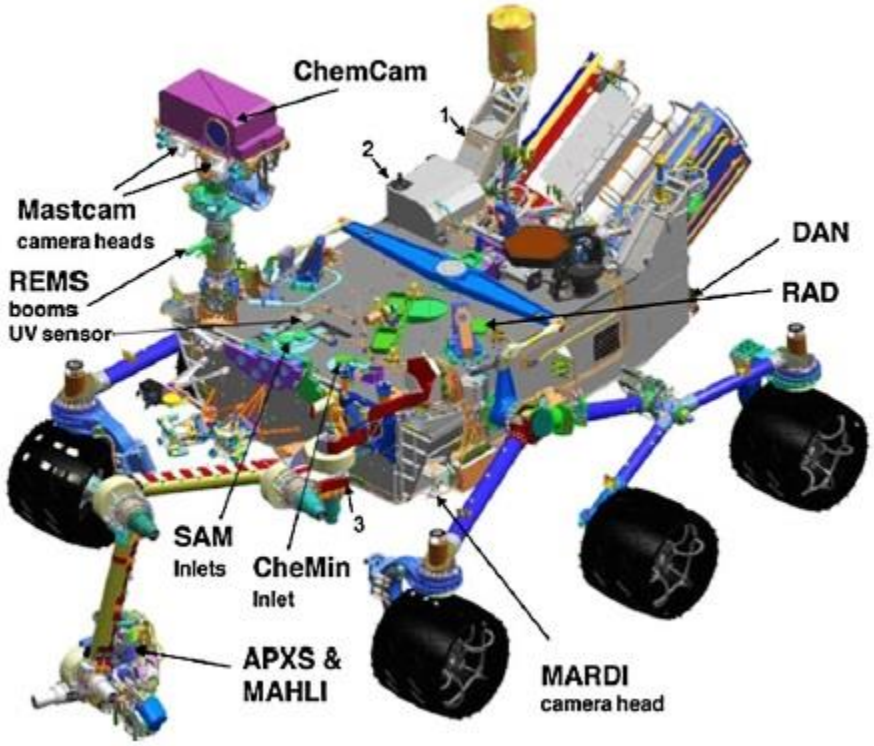

Figure 1-8: Curiosity Rover Component of MSL (reprinted from NASA, 2017a)

Analysis of a wide range of rock samples collected from the martian surface will eventually be necessary to fully decrypt the evolution of the martian environment. Lacking returned samples from a NASA mission, the only available martian rocks are

meteorites. These are rocks that have been delivered to Earth via impacts on the martian surface.

Figure 1-9: The SAM Instrument Suite (reprinted from NASA, 2017a)

Meteorites

Meteors are named from the Greek word for "things in the air", and when they fall to Earth they are called meteorites. If a meteor entering the atmosphere is followed to the ground and collected, it is called a "Fall". If a rock on the ground is collected and later determined to be a meteorite, it is called a "Find".

Although meteorites fall over the entire Earth surface, they are mostly lost through terrestrial geologic processes. Falls into the ocean or terrestrial soils are rapidly weathered and integrated into the lithosphere. Observed falls over populated areas can be rapidly recovered by humans, but meteorite "finds" are mostly recovered from either

the Sahara Desert region of northern Africa or the ice fields in Antarctica. Over 66,000 meteorites have been collected in Antarctica by a group funded by the National Science Foundation (NSF) Antarctic Search for Meteorites (ANSMET) (Institution, 2017) (see Figure 1-10). These meteorites exhibit water and ice weathering and secondary mineral deposition from interactions between rock minerals and the terrestrial hydrosphere.

Figure 1-10: ANSMET Collection Sites (reprinted from Institution, 2017)

Meteorite Types

Three techniques are used to characterize a meteorite: 1) Petrographic analysis of the physical and optical characteristics of minerals, 2) Chronological analysis of the residence time on Earth via radiogenic decay or time of exposure to cosmic rays, and 3) Chemical analysis of the stable isotopes of carbon, oxygen and hydrogen or ratios of elements that differ between planetary bodies. Three broad categories of meteorites are now recognized: 1) Undifferentiated (chondrites), 2) Differentiated silicate-rich (DSR), and 3) Iron (Urey and Craig, 1953, Wasson, 1985, Wasson, 2012).

Undifferentiated Meteorites

Undifferentiated meteorites, known as "chondrites", are composed of molten drops of material (chondrules, from the ancient Greek word for a grain) that cooled and fused together as stone. Within this category are Carbonaceous Chondrites (CC) (Type C), Ordinary Chondrites (OC) (Types H, L, and LL), and Enstatite Chondrites (EC) (Type E). They are the most common category of finds (66.8%) and falls (81.7%) (Grady, 2000). Most consist of chondrules, a fusion matrix (thought to be from the original solar nebula), and Calcium-Aluminum Inclusions (CAI). The chondrules have a wide range of sizes, textures and compositions. The CAIs generally contain refractory minerals. The variety in chondrules (size, composition and texture) suggests they formed in multiple episodes of condensation and melting early in the life of the solar system (Milone and Wilson, 2008).

Chondrites are further categorized based upon petrology, which indicates the alteration to which they have been subjected prior to landing on Earth. The alteration

range is from 1-7. Types 1-2 have been aqueously altered, with Type 1 showing more alteration than Type 2. Type 3 is considered unaltered. Types 4-6 reflect increasing thermal metamorphism (alteration by heating). A Type 7 chondrite is poorly defined, but generally reflects significant meteorite alteration with complete obliteration of the chondrules (Twelker, 2017). CCs have mostly undergone aqueous alterations (Types 1-4), while OCs and ECs demonstrate thermal alteration (Types 3-6) (Van Schmus and Wood, 1967).

Further designations in the NASA meteorite collection indicate "weathering" categories: A (minor rust haloes, particles or stains), B (large rust haloes and extensive rust stains on internal fractures), C (severe rustiness with metal particles mostly rust stained), and E (evaporite minerals visible on the fusion crust) (Velbel, 1988).

In general, chondrites seem to have formed on a parent body smaller than 100km in diameter, since the materials fractionated rather than melted (not enough heat from accretion or radioactive decay). The CAIs and chondrules are depleted in volatiles. The favored theory of creation is that the solar nebula accretion formed the matrix and CAIs, with secondary processes (shock events and weathering) forming the chondrules (Milone and Wilson, 2008).

CCs

Carbonaceous Chondrites contain relatively large amounts of carbon and organic material (including amino acids) making them black or gray in color. They are relatively fragile and fragment easily during atmospheric entry. The most famous recent falls are

"Allende" (1969 in Mexico) and "Murchison" (1969 in Australia). The iron in CCs is the most oxidized of any chondrite. An old naming scheme groups similar meteorites, e.g. CI for Ivuna, CM for Mighei, CO for Ornans, CV Vigarano) and now combines the numeric petrographic types (following the van Schmus system) (Van Schmus and Wood, 1967). These meteorites are aqueously altered (Types 1-2) indicating the presence of liquid water on the parent world, which may be primitive C-type (carbonaceous) or D-type (dark, from low albedo) asteroids (including the martian moons Phobos and Deimos) (Casper, 2017).

OCs

Ordinary Chondrites are the most common "fall" and "find" meteorites, hence their name. These stony meteorites are rich in the mineral olivine and are thermally altered only (No Type 1-2). OCs are divided into three distinct groups based upon metal mineralogy: H chondrites (highest total iron 48.8%, with lower silicate iron oxide), L chondrites (total iron 43.6% with higher silicate iron oxide than H), and LL (lowest total iron 7.3%, highest silicate iron oxide) (Grady, 2000). Type H OCs may originate from the mid-region of the asteroid belt, the type L OCs may originate from the Gefion family in the outer main belt, and the type LL OCs may originate from the Flora region of the inner main belt (Binzel et al., 2015). A representative view of the asteroid belt is given in Figure 1-11 (Darling, 2017).

ECs

Enstatite meteorites are named for the mineral enstatite ($MgSiO_3$), and are classified by high iron (EH) and low iron (EL). The iron in the ECs is the least oxidized of any chondrite. These are rare and comprise only 1% of the fall meteorite collection. ECs have only thermal alteration (No Type 1-2) (Casper, 2017, Milone and Wilson, 2008).

Differentiated Meteorites

Differentiated meteorites experienced density separation of component materials while the large parent body (with a gravity field) was molten. The silicates floated to the surface of the system while the denser molten metals sank to the center.

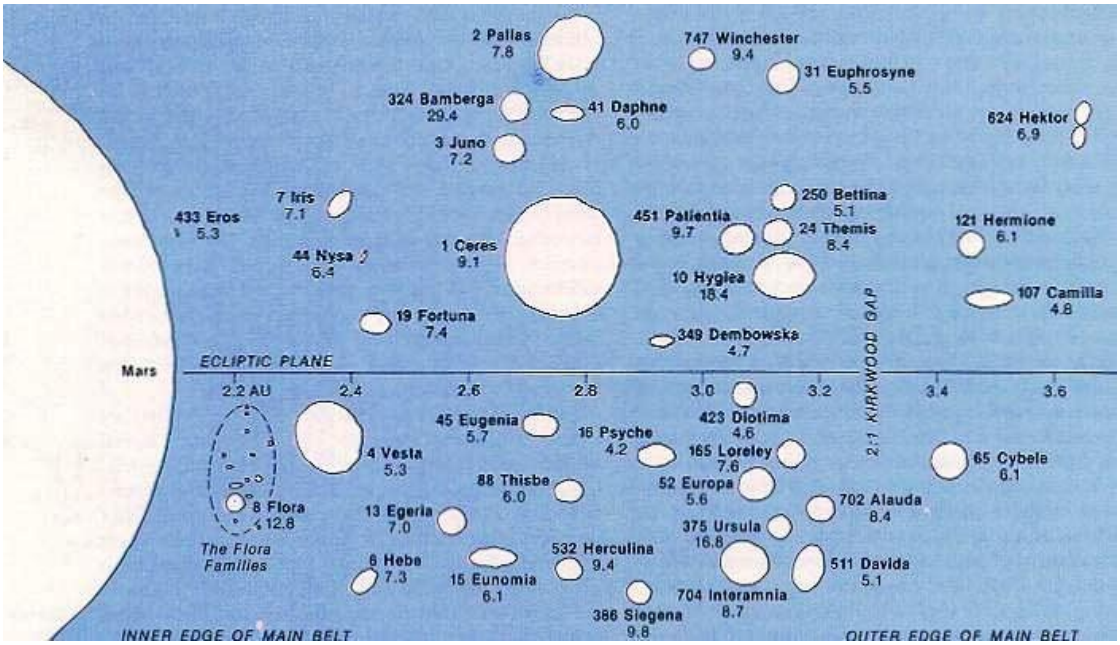

Figure 1-11: Interesting Objects in the Asteroid Belt Between Mars and Jupiter (relative size and shape only) (reprinted from Darling, 2017)

Differentiated Stony Meteorites

This group is known as Differentiated Silicate-Rich (DSR) meteorites, and is divided into two subgroups. The Achondrite subgroup has low metal content and includes classifications for ureilites, diogenites, aubrites, howardites, eucrites, lunar, and martian SNCs (discussed below). The Stony-Iron subgroup has high metal content and is further divided into two classifications for pallasites and mesosiderites (Milone and Wilson, 2008).

A group of differentiated meteorites, named for their defining types of Howardite, Eucrite, and Diogenite (HED), are thought to have been formed on the asteroid 4 Vesta (Wiechert et al., 2004). The meteorite ALH 84001 was thought to have been HED (Dreibus et al., 1994) before its martian origin was identified (see Chapter 4).

Differentiated Iron Meteorites

These meteorites have high iron and nickel content, and are divided into 13 classifications (based upon relative abundance of other elements) (Milone and Wilson, 2008).

Mars Meteorites

Planetary scientists study martian meteorites as they are the only martian surface samples available; however these are problematic (see discussion later). They are created on Mars and then altered. Alterations are from weathering on Mars, impact ejection from the martian surface, re-entry through the Earth atmosphere, and terrestrial

weathering. As of January, 2017, 183 identified martian meteorites have been collected on the Earth (Society, 2017), many from Antarctica (see Figure 1-12) (NASA, 2017b).

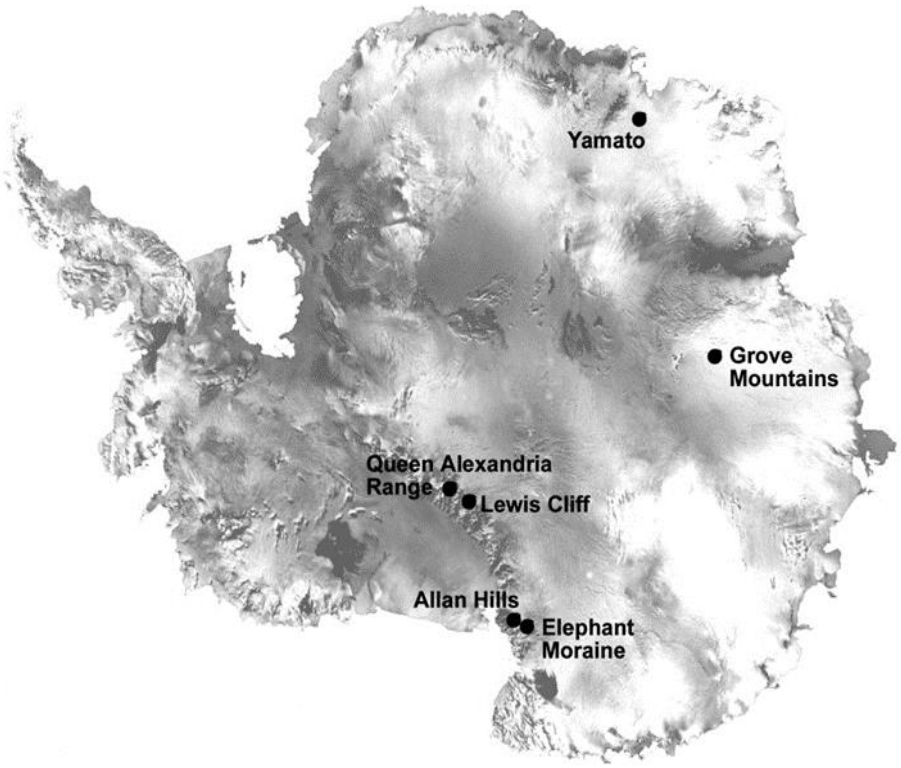

Figure 1-12: Martian Meteorite Sites in Antarctica (reprinted from NASA, 2017b)

Martian meteorites are igneous in origin, and are classified as differentiated DSRs (see discussion above). They are often identified by measuring their chemical composition. They exhibit unique iron oxide/manganese oxide (FeO/MnO) ratios, as well as potassium/lanthanum (K/La) and gallium/aluminum (Ga/Al) ratios. Geologists often characterize the martian meteorites based upon rock texture, presence of trapped gas suspected to be from the martian atmosphere, and presence of unique Rare Earth Elements (REE). Martian meteorites are generally mafic with an abundance of iron (Fe)

and magnesium (Mg). They are low in silica (Si) and alumina (Al) with many interstitial minerals. They are much younger in age than igneous meteorites from asteroids, which date to the formation of the solar system.

It is speculated that perhaps 4-8 asteroid impact events on Mars (in the past 20 million years) have been large enough to eject material into space that leads to meteorites on Earth (Nyquist et al., 2001). The formation age of the rock on Mars is determined with radiometric dating by measuring ratios of Rb-Sr, Sm-Nd, Lu-Hf, and Ar-Ar. The ejection age of the rock from the martian surface is determined with Cosmic-Ray-Exposure (CRE) age measurements; these measure changes in isotopes of He, Ne, and Kr that are affected by high-energy cosmic rays striking the rock. Controversy exists over many measurements of both formation age and ejection age, especially with Shergottites (Bouvier et al., 2005, Bogard and Park, 2008). Age chronology analysis is affected by how much the meteorite was altered by weathering, impact, or ejection on the martian surface, and also by atmospheric re-entry and weathering on the Earth surface. Identified martian meteorites demonstrate unique groups when crystallization, or formation, age is plotted against ejection age (see Figure 1-13) (Nyquist et al., 2001).

Meteorite geologists grouped a set of three odd achondrite types together based on their common mineralogy. Labeled as the Shergottite-Nakhlite-Chassigny (SNC) category of meteorites, some speculated that they might be of martian origin (Wood and Ashwal, 1981). The martian origin of SNC meteorites was firmly established by

studying the atmospheric gases that were trapped in EET 79001 and comparing them to values measured by the NASA Viking landing (Bogard and Johnson, 1983).

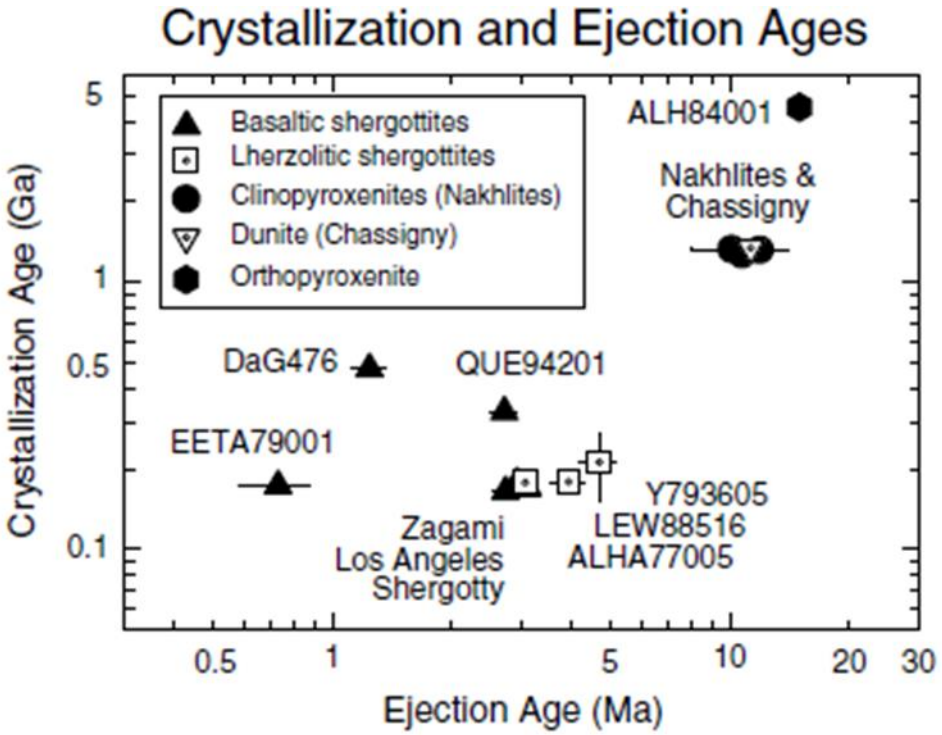

Figure 1-13: Mars Meteorite Formation & Ejection ages (reprinted from Nyquist et al., 2001)

Shergottites

The first broad group of identified martian meteorites is called “Shergottites”. The group includes the meteorites Shergotty, Zagami, ALH 77005, EET 79001, LEW 88516, QUE 94201 and Y 793605. They resemble terrestrial basalts on Earth. Some have large olivine crystals, or contain high calcium pyroxene, or low calcium pyroxene. Shergottites exhibit severe shock and display unique martian minerals such as pigeonites, maskelynite, stishovite, and ringwoodite (Milone and Wilson, 2008).

Shergottites are relatively young meteorites with formation ages from 175 Mya to 475 Mya, and ejection ages from 0.7 Mya to 20 Mya (Nyquist et al., 2001), although recent studies suggest ancient (~4.1 Ga) formation ages that differ from prior results (Bouvier et al., 2008, Bogard and Park, 2008). Proponents of older Shergottite age argue prior studies were skewed by terrestrial contamination.

Nakhlites

A second group of martian meteorites, called "Nakhlites", is named after a famous witnessed fall over Egypt in 1911. The Nakhla meteorite fragmented into approximately 40 pieces that show little terrestrial contamination (McBridge and Righter, 2011). They were formed on Mars 1.3 Ga and ejected from a common impact on Mars approximately 11 million years ago. Nakhlites contain secondary minerals commonly formed in low temperature aqueous environments such as carbonates, sulfates, and amorphous silicate material (Bridges et al., 2001). They are largely composed of augite (Milone and Wilson, 2008). Many are found in Antarctica. The class of Nakhlites is composed of 13 meteorites: Nakhla, Lafayette, Governador Valadares, NWA 817, NWA 998, NWA 5790, paired Miller Range (MIL) samples MIL 03346, MIL 090030, MIL 090032, MIL 090136, and paired Yamato (Y) samples Y 000593, Y 000749, and Y 000802 (McCubbin et al., 2013). A total of 34 meteorites of similar petrology and the same CRE age indicate a common ejection date from Mars approximately 11 million years ago.

Chassignites

Chassignites (a class composed of meteorites Chassigny, Brachina and NWA 2737), also have a formation age of approximately 1.3 billion years ago (1.3 Ga) (Nyquist et al., 2001, Korochantseva et al., 2011). The Nakhlites and Chassignites are believed to have formed by partial remelting of a common LREE depleted source (Debaille et al., 2009, McCubbin et al., 2013). Both groups may have been ejected from the same impact (Eugster et al., 2002, Korochantseva et al., 2011). Slight geochemical differences (pyroxene trace element ratios) between the Nakhlites and Chassignites lead some authors to propose they were not formed co-magmatically (Wadhwa and Crozaz, 1995), but others believe the minor differences can be caused by an invasion on a Cl-rich fluid to a single magma source after formation of the cumulus and olivine (McCubbin et al., 2013).

Other SNCs

Three unique martian meteorites defy easy classification. First, the Dhofar 019 has the oldest CRE of 20 million years, and has a highly depleted siderophile element composition. Second, NWA 7034 contains a breccia texture and extreme oxygen isotope values, making it a class unto itself. Third, the Allan Hills 84001 (ALH 84001) is a unique martian meteorite found on December 27, 1984 in Allan Hills, Antarctica. It was originally considered part of the HED group, then the SNC group, but is now considered unique (Borg, 1999). It is much older than other martian meteorites, having formed on Mars approximately 4.5 billion years ago (~4.5 Ga), and was ejected from

Mars approximately 16 million years ago. It landed on Earth approximately 13,000 years ago (Gaines et al., 2009). The bulk of ALH 84001 is orthopyroxene, and it contains old carbonate globules (formed ~3.9 Ga) and polycyclic aromatic hydrocarbons (PAHs) of suspected martian origin. These organics lead NASA scientists to publish research claiming the meteorite contained fossilized martian bacteria (McKay et al., 1996), which motivated then US President Bill Clinton to make a special address announcing the discovery. Subsequent research determined the evidence showed crystallographic artifacts, not fossils (Wickramasinghe, 2015).

Meteorite Curation

Meteorites collected by the ANSMET team in Antarctica are frozen and transferred to freezers at McMurdo Station. They are later shipped to Port Hueneme, California and transported to Houston in containers that keep the samples frozen. Once delivered to JSC, the samples are transferred to freezers.

The samples are transferred to a N_2 cabinet in the Antarctic Meteorite Processing Lab (MPL) when ready for characterization. Once thawed, they are weighed, measured, photographed and visually analyzed. After initial processing they are transferred to nylon or Teflon bags. The larger samples are stored in N_2 cabinets at room temperature, and the small samples <200g are placed in stainless steel cabinets with no nitrogen flow. A special N_2 cabinet was constructed for the large meteorite LEW 85320, which is growing the Mg-rich carbonate nesquehonite while in storage (Righter et al., 2014).

Stable Isotope Analysis

General Stable Isotope Background

A discussion of the major processes impacting the carbon and oxygen isotopes on Earth or Mars begins with a basic review of stable isotope geochemistry, then a specific discussion of each process. An excellent discussion of stable isotope fractionation is given in two well known reference works (Hoefs, 2009, Faure, 1986). Stable isotope measurements are reported in "delta" (δ) notation:

$$\delta^{18}O = [(R_x - R_{std}) / R_{std}] \times 1000 \qquad \text{eq. 1-1}$$

where R is the $^{18}O/^{16}O$ ratio

The fractionation factor, α, defines the exchange of isotopes between two species in equilibrium.

$$\alpha_{A\text{-}B} = Ra / Rb \qquad \text{eq. 1-2}$$

$$\Delta_{A\text{-}B} = \delta^{18}O_A - \delta^{18}O_B \approx 1000 \ln \alpha_{A\text{-}B} \qquad \text{eq. 1-3}$$

(the approximation in eq. 1-3 is generally valid when $\delta^{18}O_A - \delta^{18}O_B$ is small)

Standards

The standard for terrestrial water measurements of oxygen isotopes is "Vienna Standard Mean Ocean Water" (SMOW or VSMOW) which was created based on samples from the Potomac River NBS-1. The standard for oxygen isotopes in carbonate materials, and carbon isotopes in general, is Pee Dee Belemnite (PDB) or Vienna PDB (VPDB) if calibrated via NBS-19. The oxygen isotope values are related between standards (Coplen, 1988):

$$\delta^{18}O_{VSMOW} = 1.03091 * \delta^{18}O_{VPDB} + 30.91 ‰ \quad \text{eq. 1-4}$$

$$\delta^{18}O_{VPDB} = 0.97001 * \delta^{18}O_{VSMOW} - 29.99 ‰ \quad \text{eq. 1-5}$$

Mass Dependent and Independent Fractionation

General isotope fractionation is based on the preferential movement of isotopes between species based on the difference in their energy level. The energy level is associated with the mass of the isotopes. Most element isotopes follow "Mass Dependent Fractionation" (MDF); however, O, Mg and S do not strictly fractionate in this manner. The expected MDF fractionation for ^{18}O to ^{16}O is twice that of ^{17}O to ^{16}O because of the doubled mass difference between the species. The oxygen "Mass Independent Fractionation" (MIF) is determined by measuring the triple isotopes of oxygen (Clayton et al., 1976), which requires instrumentation capable of detecting small quantities of ^{17}O. Plotting the $\delta^{17}O$ versus $\delta^{18}O$ creates a straight line unique for planetary bodies (Matsuhisa et al., 1978). From this plot, the term $\Delta^{17}O$ is defined as the MIF:

$$\Delta^{17}O = \delta^{17}O - (\lambda * \delta^{18}O) \quad \text{eq. 1-6}$$

where λ is defined by the system (Assonov and Brenninkmeijer, 2005)

For Earth, the "Terrestrial Fractionation Line" (TFL) is generally λ=0.52 but can vary from 0.50 to 0.53 (see Figure 1-14). On Mars, the λ=0.52 (same as Earth) but there is an offset of $\Delta^{17}O$=0.321‰ based on measurements from silicates in martian meteorites (Franchi et al., 1999).

Terrestrial MIF of oxygen is evident in the formation of ozone in the stratosphere (Mauersberger et al., 1999), other atmospheric gases (Thiemens, 1999), desert sulfates (Bao et al., 2000) and volcanic sulfate aerosols of polar ice (Baroni et al., 2007).

Martian carbonates have distinct $\Delta^{17}O > 0.3‰$ (ranging from 0.5‰ to 0.9‰), which is interpreted as carbonate exchange with atmospheric CO_2 undergoing MIF, and not from equilibrium formation with the silicates (Farguhar and Thiemens, 2000, Shaheen et. al, 2015).

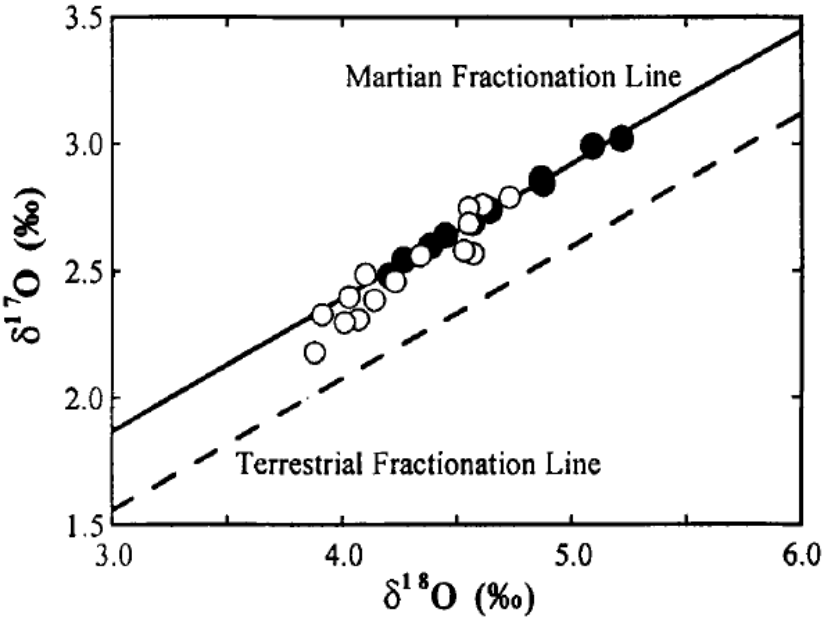

Figure 1-14: Mars and Earth MIF (reprinted from Franchi et al., 1999)

Temperature

Stable isotope fractionation varies with temperature. It is zero at very high temperature ($\alpha=1$) because the high energy of all particles distributes the isotopes

uniformly. Fractionation increases with lower temperature. Thus, $\alpha = f(1/T)$ at low temperatures, and $\alpha = f(1/T^2)$ at high temperature (T is in degrees K) (Hoefs, 2009).

Fractionation Mechanics

In equilibrium isotope exchange, the heavier isotope is enriched where there is a stronger bond or higher oxidation state. For carbon dioxide (CO_2) and calcite in equilibrium, the stronger bonds in CO_2 are enriched in ^{18}O, whereas the calcite is relatively depleted in ^{18}O. Non-equilibrium kinetic effects impact isotope exchange in only one direction. Biological processes and diffusion have kinetic effects which favor the light isotope. With the evaporation of water, the vapor is the less dense phase. The vapor is enriched in ^{16}O, which means it is depleted in $\delta^{18}O$. The liquid is the denser phase, and it is enriched in $\delta^{18}O$. Evaporation equilibrium fractionation (aka distillation) between seawater ($\delta^{18}O = 0‰$) and water vapor predicts the vapor should be depleted in ^{18}O with $\delta^{18}O = -9‰$ at 25°C, but kinetic effects enhance the depletion to $\delta^{18}O = -13‰$ (Craig and Gordon, 1965). Predicted gas kinetic diffusive fractionation can be calculated using Graham's Law:

$$\alpha'_{\text{light-heavy}} = (\text{mass}_{\text{heavy}} / \text{mass}_{\text{light}})^{0.5} \qquad \text{eq. 1-7}$$

e.g. for carbon in methane:

$$\alpha'_{\text{light-heavy}} = (17/16)^{0.5} = 1.030 = 30‰ \text{ enrichment in } ^{12}C \qquad \text{eq. 1-8}$$

Earth Oxygen Isotopes

The stable isotopes of oxygen are ^{16}O, ^{17}O, and ^{18}O ("triple isotopes" of oxygen). The relative oxygen isotope abundance in VSMOW is: $^{16}O = 0.99985$, $^{17}O = 1/2632 = 0.00038$, and $^{18}O = 1/498.7 = 0.0020052$ (Pilson, 2012). Oxygen isotope measurements use VSMOW for seawater and VPDB for rocks. These measurements are studied in processes involving water (atmosphere, hydrosphere, and lithosphere), paleothermometry and geothermometry.

Biology

Most marine organisms that create carbonate shells fractionate oxygen in equilibrium between H_2O and $CaCO_3$, but a few have "vital effects" that alter the predicted equilibrium oxygen isotope fractionation (see Figure 1-15) (Sharp, 2007, Anderson, 1983).

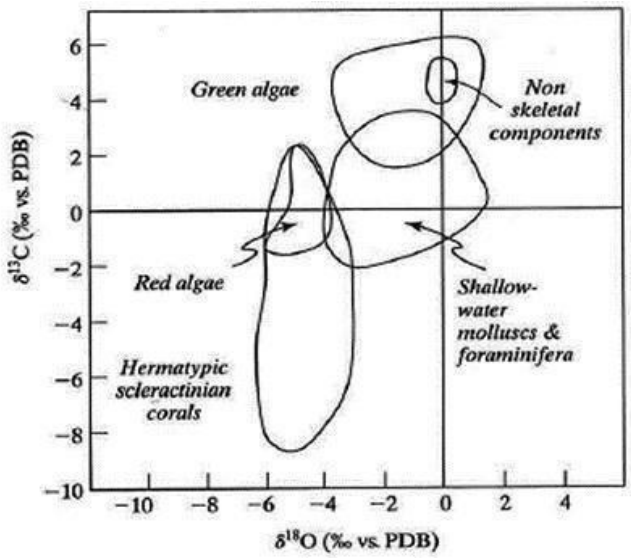

Figure 1-15: Vital Effect Fractionation in Earth Organisms (reprinted from Sharp, 2007)

The Atmosphere

Biological respiration from organisms preferentially consumes ^{16}O from the atmosphere, leaving an enrichment of ^{18}O in the atmosphere. This is called the "Dole Effect". Although first noted in 1936 (Dole, 1936), it was accurately measured in 1975 as $\delta^{18}O_{O2} = +23.5‰$ (Kroopnick and Craig, 1972). The terrestrial contribution is 22‰ to 27‰ and the oceanic contribution is between 17‰ to 19‰ (Bender et al., 1994). The predicted equilibrium fractionation between O_2 and water is 6‰, so the oxygen in the atmosphere is not in equilibrium with the ocean surface (Urey, 1947).

The atmospheric CO_2 is $\delta^{18}O_{CO2} = +41‰$, which is in equilibrium with seawater but not atmospheric O_2 (Keeling, 1961). The southern hemisphere has a regional enrichment of atmospheric CO_2 $\delta^{18}O = 2‰$ due to the large volume of ocean in the southern hemisphere ($\delta^{18}O_{seawater} = 0‰$) versus northern hemisphere with more land area ($\delta^{18}O_{meteoricwater} < 0‰$) (Hoefs, 2009).

Ozone (O_3), O_2, and CO_2 in the Earth atmosphere follows MIF based on photochemical reactions (Thiemens et al., 1995). The ^{17}O in the atmosphere with this MIF is depleted relative to oxygen created only by photosynthesis/respiration by 0.2‰. The total depletion varies with biological productivity and stratospheric mixing. The ^{17}O anomaly can thus be used as a tracer for biological productivity (Luz et al., 1999).

The Hydrosphere

Rayleigh fractionation, which involves the distillation of oxygen isotopes in evaporation and condensation, is important in Earth's hydrosphere. If the isotope exchange is in a closed system, the fractionation between phases does not alter the total reservoir $\delta^{18}O$ since the total number of isotopes remains the same. In an open system, however, the reservoir $\delta^{18}O$ changes over time due to the loss of specific isotopes from the system. Rayleigh fractionation models water evaporation (distillation) and condensation on Earth as closed systems. Enrichment of one phase creates depletion in another, but the total reservoir $\delta^{18}O$, and thus the total number of ions for each isotope, in the reservoir remains constant. Consider seawater at the equator: the light isotope ^{16}O is preferentially evaporated over the heavy isotope ^{18}O, so the water vapor is depleted in $\delta^{18}O$. The residual seawater is enriched in $\delta^{18}O$. The water vapor creates rain, which is a process that preferentially condenses the heavy isotope ^{18}O, leaving the water vapor further depleted in $\delta^{18}O$. As the water vapor moves farther from the equator, or farther inland, the vapor cloud and the rain condensation get progressively lower in $\delta^{18}O$. Since much of the ^{18}O depletion of the vapor cloud occurs at high latitude and altitude, temperature is an effective parameter to predict the $\delta^{18}O$. Modeling the condensation of rain from a vapor cloud in a closed system provides insight to the $\delta^{18}O$ variation of each phase (water vapor, instantaneous liquid "rain", and residual water). The model varies based upon the parameter "f", which is the amount of vapor remaining after rain has precipitated from the vapor cloud (see Figure 1-16) (Broecker and Oversby, 1971, Dansgaard, 1964).

Rivers weather continental rock and collect organic debris (which is an important component of exchange with carbon isotopes) before re-entering seawater. Lower ^{18}O rain becomes meteoric water feeding fluvial systems. For example, rivers in northern Asia are created from rain that is depleted in $\delta^{18}O$ due to the great distance from the ocean source that created the water vapor. They become significantly lower, or"rained out", in $\delta^{18}O$ as water vapor travels inland across Russia. The $\delta^{18}O$ values for the rivers discharging into the Eurasian Basin of the Arctic decrease from west to east (from the Ob River with $\delta^{18}O$ = -16.3‰ to the Indigirka River, with $\delta^{18}O$ = -23.8‰) (Bauch et al., 2005). The ^{18}O depleted rain in polar regions ($\delta^{18}O_{rain}$ < -40‰) creates more depleted glacial ice, seen in Figure 1-17 (Dansgaard, 1964, Pilson, 2012).

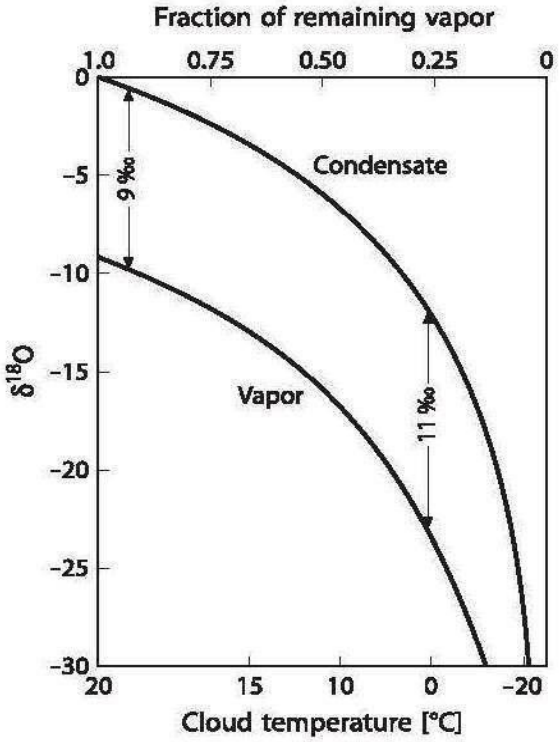

Figure 1-16: Rayleigh Fractionation (reprinted from Broecker and Oversby, 1971)

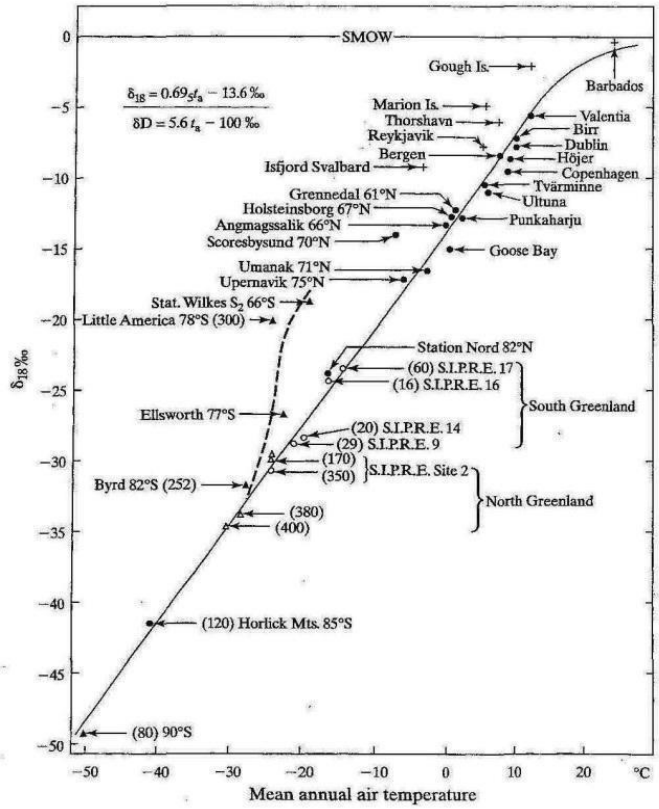

Figure 1-17: $\delta^{18}O$ vs. Mean Air Temperature (reprinted from Pilson, 2012)

Evaporation increases the salinity and ^{18}O enrichment of seawater. Modern salinity values typically are measured with electrical conductivity instruments and the value is reported without any units. Older salinity measurements, based upon evaporation or titration, reported the presence of dissolved ions in water as parts-per-million, ppm. Ocean seawater generally has a salinity of about 35, whereas freshwater has a salinity of zero (0).

Lower $\delta^{18}O$ rainfall creates fluvial runoff that decreases the salinity of seawater and reduces $\delta^{18}O_{seawater}$. Thus, $\delta^{18}O_{seawater}$ and seawater salinity can be correlated (see

Figure 1-18). The $\delta^{18}O_{VSMOW} = 0‰$ (by definition), but variation in $\delta^{18}O_{seawater}$ is predicted by salinity measurements in seawater (Craig and Gordon, 1965).

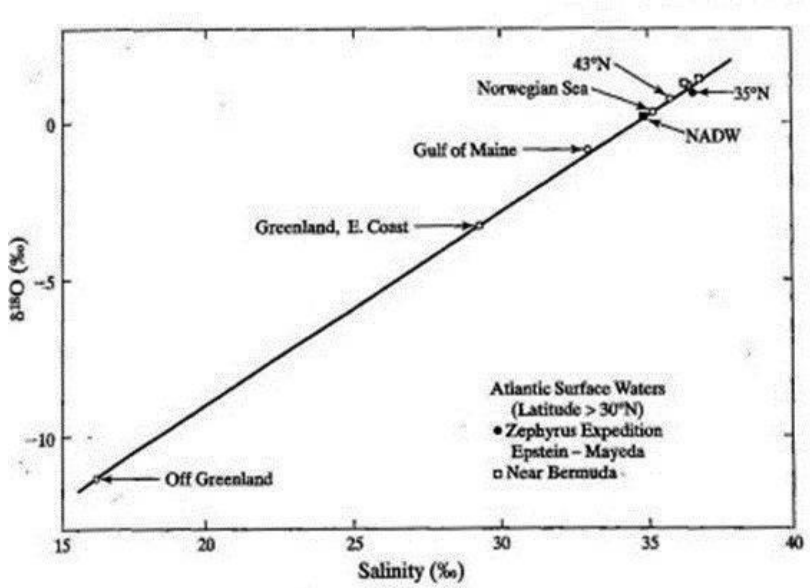

Figure 1-18: $\delta^{18}O$ vs. Salinity (reprinted from Craig and Gordon, 1965)

Sea ice formation does not affect sea level, but it does alter the salinity and $\delta^{18}O$ of seawater. When sea ice is formed, the dissolved salt ions in seawater are excluded from the ice lattice in a process known as "brine rejection". The salinity of the seawater in the immediate vicinity is thus increased with the salt ions from the sea ice. The formation of sea ice also enriches the $\delta^{18}O_{seawater}$. Water is a unique fluid because the solid phase is less dense than the liquid phase at the freezing point (Thurman et al., 2011). This phenomenon makes aquatic life possible in cold climates, since the ice floats on the surface and provides thermal insulation to the liquid water below. Equilibrium melting of ice causes fractionation that enriches $\delta^{18}O_{seawater} = +3.1‰$

(O'Neil, 1968). Kinetic effects, however, reduce the enrichment to only about 2.6‰ (Pilson, 2012). Melting of sea ice reverses the enrichment of $\delta^{18}O_{seawater}$ and reduces seawater salinity.

Glacial ice formation (ice over continental land mass) impacts sea level, seawater salinity and $\delta^{18}O_{seawater}$. Evaporation of water vapor from seawater decreases sea level, increases the salinity of the seawater, and enriches $\delta^{18}O_{seawater}$ due to Rayleigh fractionation. The water vapor creates lower $\delta^{18}O$ snow that precipitates at high latitude and elevations. Snow that doesn't melt compacts over time to create glacial ice. It is estimated that the Pleistocene glacial maximum sea level was 120 m lower than the current level, $\delta^{18}O_{seawater}$ was +1.25‰, and $\delta^{18}O_{glacialice}$ was -40‰ (Fairbanks, 1989). If all of the current glacial ice melted today, the predicted global $\delta^{18}O_{seawater}$ would change to -1‰ (Pilson, 2012) due to runoff from the depleted precipitation. Sea level would rise by 216 feet, or 72 m (Geographic, 2013).

The oxygen isotopes of global seawater are in equilibrium with the hot seafloor crust at spreading centers and mid-ocean ridges where $\delta^{18}O_{silicatecrust} \approx +5.7‰$ (Muehlenbachs and Clayton, 1976, Eiler, 2001). Depleted meteoric water ($\delta^{18}O_{meteoric} \approx$ 0 to -40‰) mixes with the seawater to reduce $\delta^{18}O_{seawater}$. Thermohaline circulation tends to mix the global ocean so that the average seawater oxygen isotope value creates SMOW. Surface waters vary more than deep water due to local evaporation, precipitation, and runoff. Despite the average value for global seawater, distinctive deep water masses exist within the oceans. North Atlantic Deep Water (NADW) and Antarctic Bottom Water (AABW) are two of these water masses characterized by

distinct oxygen isotopic values, salinity, temperature, and nutrient content (see Figure 1-19). Using the $\delta^{18}O$ and salinity as tracers of water mass provides a tool to predict mixing circulation within the global ocean (Pilson, 2012).

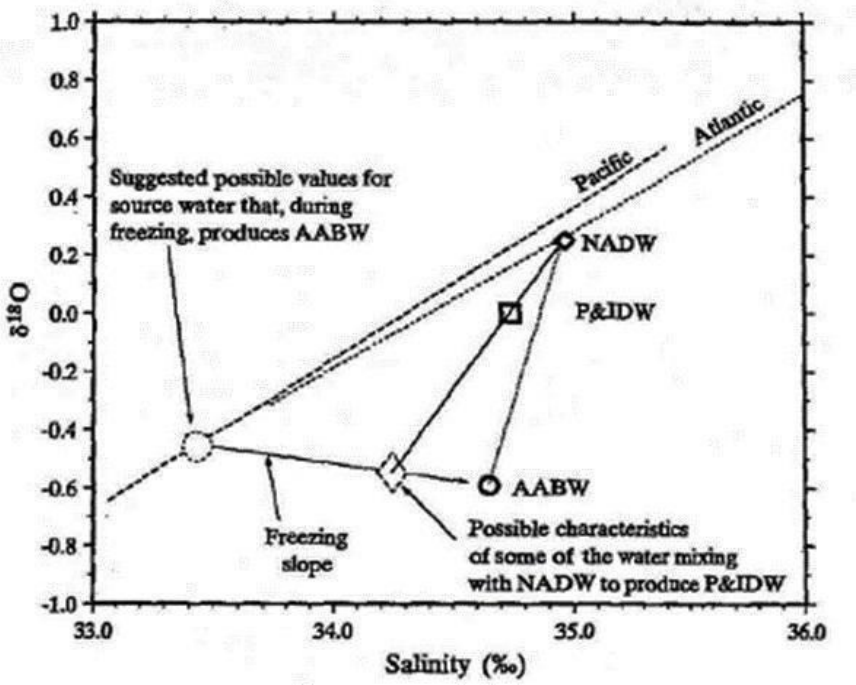

Figure 1-19: $\delta^{18}O$ and Salinity as Water Mass Tracers (reprinted from Pilson, 2012)

Average ocean $\delta^{18}O_{seawater} = 0‰$ is the basis of VSMOW. Meteoric waters are created from precipitation. The oxygen, $\delta^{18}O$, and hydrogen, δD (^{2}H), isotopes of meteoric waters can be correlated. Deviations from the Meteoric Water Line (MWL) occur with hydrothermal rock-water exchange and evaporation in closed basins (Craig, 1961).

Generally:

$\delta D = A * \delta^{18}O + B‰$ (A and B based on humidity) eq. 1-9

Slope, A: At 25°C

At 100% humidity, A=8 ($\alpha D/\alpha O = 76/9.3$).

At 50% humidity, A=4.5

Intercept, B "D-excess": B=10 at avg. humidity,

B>10 for dry areas,

B<10 for humid areas

The surface ocean water has $\delta^{18}O_{water} = 24.2‰$ based on the atmospheric $\delta^{18}O_{O2} = 23.5‰$ ("Dole effect") and the fractionation of 0.7‰ for gas dissolution (Quay et al., 1993). Dissolved O_2 concentration in saturated surface waters is approximately 210 µmoles/kg (depending on temperature). If photosynthesis dominates the surface waters, the $\delta^{18}O_{water} < 24‰$ due to excess creation of O_2 (the water will be supersaturated in O_2). If respiration dominates the surface waters, the $\delta^{18}O_{water} > 24‰$ due to excess consumption of ^{16}O (the water will be undersaturated in O_2). Respiration and consumption of dead organic matters consumes dissolved O_2 and creates an enriched $\delta^{18}O_{water} > 30‰$ at the oxygen minimum depth (approximately 1 km). The dissolved O_2 concentration drops to ≈ 150 µmoles/kg at the oxygen minimum and then increases in deep water ≈ 270 µmoles/kg from downwelling of surface waters (see Figure 1-20). Deep water reflects downwelled surface $\delta^{18}O_{water} \approx 26‰$ (Kroopnick and Craig, 1972).

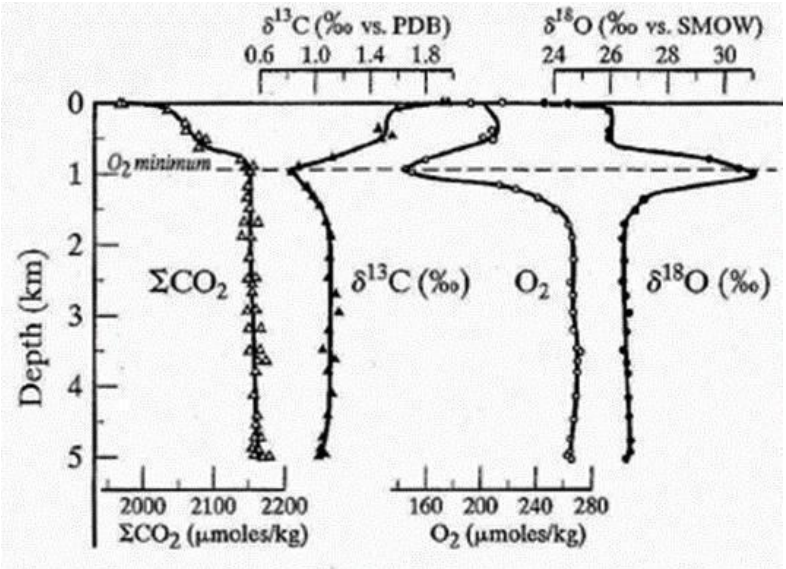

Figure 1-20: $\delta^{18}O$ and $\delta^{13}C$ Changes with Ocean Depth (reprinted from Kroopnick and Craig, 1972)

The Lithosphere

The bulk Earth $\delta^{18}O \approx +5‰$ based on measurements of silicates (Muehlenbachs and Clayton, 1976) and ordinary chondrite meteorites (Clayton and Mayeda, 1999) that are assumed to reflect the primitive Earth. In general, oxygen isotopes in the Earth crust fractionate with the heavy isotope enriched in the species with the stronger bond (Broecker and Oversby, 1971).

Carbonates

Oxygen (and carbon) isotopes are measured from CO_2 released by carbonates in the laboratory. The CO_2 gas is created when the carbonate is dissolved in phosphoric acid. Harold Urey established that oxygen isotope fractionation between $CaCO_3$ and water depended on temperature (Urey, 1947), and empirical paleo-temperature equations

were developed for inorganic calcite (McCrea, 1950), mollusks and other biogenic carbonates (Epstein and Lowenstam, 1953), and pelagic foraminifera (Emiliani, 1955). Pleistocene climate change (approximately the recent 500,000 years) is reconstructed by correlating changes of carbonate $\delta^{18}O$ with Antarctica ice cores (Petit et al., 1999) and other radiogenic dating techniques (Faure, 1986).

Using changes in ^{18}O of biogenic carbonates is problematic. First, some organisms, such as enchinoderma, asteroidea, ophiuroidea, and crinoidea, do not secrete carbonate shells in equilibrium with seawater (see Figure 1-15) (Faure, 1986). Second, both water temperature and water isotopic composition impact $\delta^{18}O_{carbonate}$, such as during periods of glaciation or in regional areas of high fluvial runoff. One solution to this is to measure both pelagic and benthic foraminifera deposited together, with the assumption that the deep ocean water does not change in temperature (recorded in the benthic forams) (Kahn, 1981). Volumetric mass balance predicts the change in $\delta^{18}O$ is 2/3 from glacial ice volume and 1/3 from seawater temperature change (Craig and Gordon, 1965, Emiliani and Shackleton, 1974).

Terrestrial carbonates formed in equilibrium with seawater create $\delta^{18}O_{rock} = 28‰$ (25°C) to 35‰ (0°C) (using the VSMOW standard) based on temperature dependent fractionation between calcite and water (Bottinga, 1968, Chacko et al., 1991).

On the seafloor, carbonates are lithified and compacted. Cementation and diagenesis alter the $\delta^{18}O$ through isotope exchange between the sediments and meteoric waters. Deep burial also causes dissolution and recrystallization from increased

temperature and pressure. Generally, these processes cause a depletion of $\delta^{18}O_{rock}$ up to 25‰ (more discussion on diagenesis and metamorphism below).

The field of "Oxygen Isotope Stratigraphy" evolved to measure the $\delta^{18}O_{carbonate}$ and reconstruct the temperature of the seawater in which the carbonate formed. It is important to understand the contribution to $\delta^{18}O$ from temperature variation and the contribution to $\delta^{18}O$ from glacial ice volume, since each alters $\delta^{18}O$ in the same direction (Grossman, 2012).

Precambrian seawater temperature has been reconstructed using $\delta^{18}O$ measurements of chert and carbonates (Perry, 1968). Paleozoic records have been created from brachiopod shells and marine sediments (Popp et al., 1986) and conodonts (Joachimski et al., 2009), and Mesozoic records are created with macrofossils such as bivalves, belemnites, and brachiopods (Urey et al., 1951, Hudson and Anderson, 1989). Cenozoic measurements of the $\delta^{18}O$ in planktonic and benthic forams establish accurate climate estimates for the past 65 million years (Zachos et al., 2001).

Igneous Silicates

Mantle xenoliths (Zhang, 2001b) and unaltered basalts formed along a Mid-Ocean Ridge (Muehlenbachs and Clayton, 1976) are thought to represent the bulk Earth silicate, with $\delta^{18}O_{silicatecrust} \approx +5.7‰$ Oxygen isotopes in granites vary more than in basalts due to variation in the magma source and secondary alterations. "High" granite rocks have $\delta^{18}O_{rock} > 10‰$ and reflect low temperature isotopic fractionation with meteoric water from sedimentation or weathering. "Low" granite rocks have $\delta^{18}O_{rock} <$

6‰ and reflect high temperature and high pressure interactions such as remelting or recrystallization. Mantle peridotites (olivine and pyroxene) have $\delta^{18}O_{rock} \approx +5.2‰$, Ocean Island Basalts (OIB) (pyroxene and plagioclase) $\delta^{18}O_{rock} \approx +5.5‰$, and Mid-Ocean Ridge Basalts (MORB) (pyroxene and plagioclase) $\delta^{18}O_{rock} \approx +5.7‰$. "Normal" granite rocks have $\delta^{18}O_{rock}$ from 6‰ - 10‰ reflecting their unaltered igneous origin, such as continental granites (quartz) $\delta^{18}O_{rock} \approx +6.1‰$ (Muehlenbachs and Clayton, 1976).

Correlations between $\delta^{18}O_{rock}$ and $^{87}Sr/^{86}Sr$ ratio are used to distinguish crustal contamination (mixing of mantle material with re-melted crustal material) from source contamination (recycling of subducted material) (Marshall et al., 1999).

Quartz (SiO_2) with a higher vibration frequency of 1.64×10^{13} sec^{-1} is enriched in ^{18}O relative to periclase (MgO) with a lower vibration frequency of 1.18×10^{13} sec^{-1}.

Earth Carbon Isotopes

The stable isotopes of carbon are ^{12}C and ^{13}C. The isotope ^{14}C is radioactive with a half-life of approximately 5730 years, and is used to measure the age of organic material. In "delta" notation:

$$\delta^{13}C = [(R_x - R_{std}) / R_{std}] \times 1000 \qquad \text{eq. 1-10}$$

where R is $^{13}C/^{12}C$ ratio

Carbon isotopes are measured with the VPDB standard. The relative abundance of carbon isotopes is ^{12}C=0.989, ^{13}C=0.011, and ^{14}C=variable, very small amount (Hoefs, 2009). A summary of the carbon on Earth (see Figure 1-21) reflects that most

organic processes prefer ^{12}C, which causes a depletion of $\delta^{13}C$ in the organic material produced (Mateo et al., 2006).

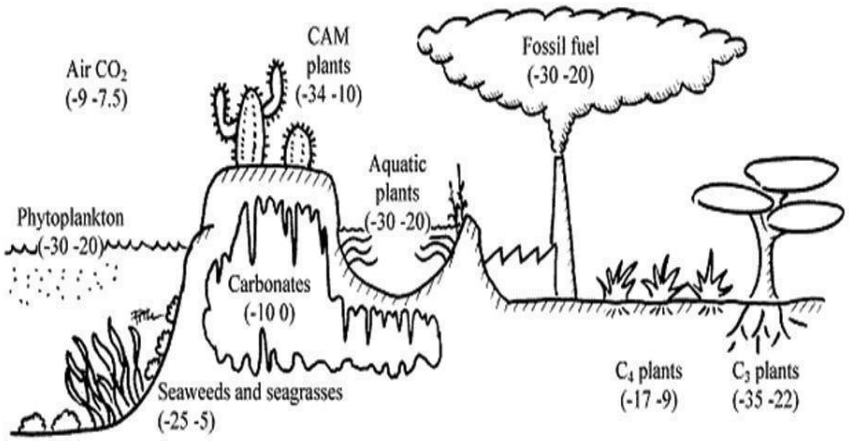

Figure 1-21: Earth $\delta^{13}C$ reservoirs (reprinted from Mateo et al., 2006)

Biology

Plant photosynthesis consumes CO_2 preferentially using ^{12}C (which creates a depletion of $\delta^{13}C_{plant}$ relative to $\delta^{13}C_{CO2}$). Photosynthesis favors ^{12}C in consumption of CO_2, causing an enrichment of $\delta^{13}C$ from +4‰ to +27‰, and is evident in the summer atmosphere over each hemisphere (Wingate et al., 2007).

The older type of plants, known as "C3", appeared on Earth in the late Paleozoic and Mesozoic (250 mya) periods. They flourish in moderate climates with abundant water, since they lose 97% of their absorbed water to transpiration. C3 plants currently comprise approximately 95% of the Earth's plant biomass and include plants such as rice and barley (Raven and Edwards, 2001). C3 leaves fractionate $\delta^{13}C$ = -20‰ (Ghashghaie and Badeck, 2014).

"C4" plants evolved later, perhaps in the Oligocene (38 mya), in response to higher temperatures and arid environments. They utilize a more efficient chemistry for photorespiration than C3 plants. C4 plants have a distinctive leaf structure, and the more drought tolerant "crassulacean acid metabolism" (CAM) plants developed spines (e.g. cacti). C4 examples include corn (maize), sugarcane and crabgrass (Nickell, 1993). C4 plants fractionate $\delta^{13}C$ = -4‰ (less than C3 plants) (Ghashghaie and Badeck, 2014).

Carbon isotopes (often studied along with nitrogen isotopes) are also used in diet studies to determine organism migration - "You are what you eat". The $\delta^{13}C$ of animal tissue reflects the $\delta^{13}C$ of the primary food source. Some organisms, such as Red Sea corals, do not correlate well due to differences in biogenic pathways that deliver the food to the tissue.

The Atmosphere

The 2014 atmospheric CO_2 $\delta^{13}C \approx$ -8‰ (Cuntz, 2011). In 1955, the atmospheric CO_2 $\delta^{13}C$ was = -7‰. The depletion of $\delta^{13}C$ in CO_2 results from the burning of fossil fuels, which started approximately in the 1750s with the Industrial Revolution. Fossil fuels are significantly depleted in $\delta^{13}C$ (due to their large composition of C3 plants). As they are burned, they cause a reduction (or isotopically "lighter") in the atmospheric $\delta^{13}C_{CO2}$. This is known as the "Seuss Effect" (Keeling, 1979).

The bulk Earth $\delta^{13}C \approx$ -6‰, based largely on meteorite studies (Grady and Wright, 2006). Volcanic eruptions provide CO_2 and CH_4 to the atmosphere. The CO_2 is in equilibrium with the hot lava before eruption, and the fractionation between CO_2 and

graphite is ≈ 5‰ at 1000°C (Friedman and O'Neil, 1977). Magma composition changes with regional integration of country rock or plume evolution from the mantle. Measurements of the $\delta^{13}C_{CO2}$ from Mt. Etna show a progressive increase in $\delta^{13}C_{CO2}$ since 1970 (each measurement numbered in Figure 1-22). This chemical change in the released CO_2 reflects a change in the $\delta^{13}C$ magma source, estimated to be from -9‰ to -6‰ (Chiodini et al., 2011).

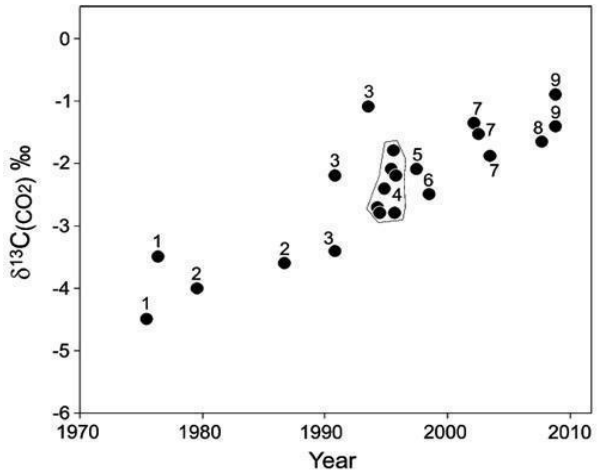

Figure 1-22: $\delta^{13}C$ changes of Mt. Etna Released CO_2 (reprinted from Chiodini et al., 2011)

The Hydrosphere

Water does not contain any carbon, but dissolved inorganic carbon (DIC) in seawater is composed of mostly HCO_3^- ions, with some CO_3^{2-} ions and small amounts of dissolved CO_2. Marine plant photosynthesis enriches the $\delta^{13}C_{DIC}$ of surface waters by up to 2‰ (through preferential consumption and storage of ^{12}C in tissues). The young NADW (recently formed from cooling surface waters near Labrador) varies from

$\delta^{13}C_{DIC} \approx +0.5$ to +1‰, and older Pacific water (traveling the globe via thermohaline circulation) can decrease to $\delta^{13}C_{DIC} \approx -0.5$ from the addition of organic material and its oxidation as it falls through the water column (see Figure 1-20) (Kroopnick, 1985).

Marine plants are enriched in $\delta^{13}C \approx +10$‰ compared to terrestrial plants, and thus $\delta^{13}C$ can be a tracer for carbon source. Phytoplankton $\delta^{13}C$ varies across the global ocean by 15‰, but there is significant $\delta^{13}C$ depletion in southern ocean plankton. The reasons for this depletion are unknown (Pilson, 2012).

Meteoric waters flush organic material into the ocean via fluvial networks. The debris includes C3 and C4 plants, which are depleted in ^{13}C. Continental runoff of meteoric waters ($\delta^{13}C$ = -17‰ to -26‰) carry the lower $\delta^{13}C$ into seawater, and also provide lower $\delta^{13}C$ to sediment pore water during diagenesis.

The Lithosphere

The bulk Earth $\delta^{13}C \approx -5$‰, based largely on meteorite studies and comparisons to diamonds from kimberlite eruptions. Volcanoes release CO_2 to the atmosphere. The CO_2 is then returned to the lithosphere via the ocean to form carbonates or organic matter sediments (Grady and Wright, 2006).

Carbonates

In general, the heavy carbon isotope ^{13}C is enriched where the oxidation state of inorganic carbon is +4 (such as CO_2 and $CaCO_3$), but ^{13}C is depleted in organics such as CH_4 where the carbon oxidation state is -4. Organisms that create carbonate shells are

often in equilibrium with the oxygen isotopes of seawater (see Figure 1-15), but not in equilibrium with the carbon isotopes of DIC. Carbonate shells are thus lower in $\delta^{13}C$ relative to equilibrium values (Hoefs 2009, Faure, 1986).

The $\delta^{13}C$ of DIC and of carbonates reflects changes in the environment. Increasing the burial rate of organic carbon in the sediments causes the $\delta^{13}C$ to increase. The closing of the Laurasian seaway (approximately 323 mya in the Carboniferous Period during the formation of Pangea) increased $\delta^{13}C$ DIC by 2‰ (Grossman et al., 1993). The "dinosaur killer" comet impact at the KT boundary (approximately 65 mya) is thought to have shut down primary production, causing a decrease in $\delta^{13}C$ due to respiration and lack of photosynthesis (Koch et al., 1992). Carbonate shells also record episodic Ocean Anoxic Events (OAE) which create a brief enrichment of $\delta^{13}C$ DIC due to decline of respiration (Saltzman et al., 2004).

Sediment Alterations

Interpreting measurements of carbon and oxygen isotopes can provide insights into the formation and alteration environment of carbonate sediments as they are lithified.

Diagenesis

Diagenesis is the physical, chemical and/or biological alteration of sediments at low temperature. After carbonate sediments form on the seafloor, the oxygen and carbon isotopes can be altered in two ways: cementation or dissolution/recrystallization.

Factors influencing the isotopic exchange between rock and fluid include temperature, isotopic composition of the cementing fluid, fluid/rock ratio, and stability of the carbonate mineral.

Early cements are added from abiotic carbonate deposition in the pores of the sediments, and the cement may be in equilibrium with ocean water. Shallow marine sediments initially interact with seawater, then with $\delta^{18}O$ depleted (Rayleigh) and ^{13}C depleted (C3/C4) meteoric waters. Late cements form at higher temperature with more kinetic energy for fractionation. Recrystallization of unstable minerals to more stable minerals, such as from aragonite to calcite, or from high-Mg calcite to low-Mg calcite, also fractionates the isotopes (Sharp, 2007).

In deep sediments, the temperature and pressure increase and water is squeezed from the sediment pores. Generally, the $\delta^{18}O_{rock}$ decreases with increasing temperature. The $\delta^{13}C_{rock}$ varies greatly based on microbial activity. Trace elements can be added or removed, and complex isotope fractionation occurs (Hudson, 1977).

Carbonate Metamorphism

Metamorphism depends upon three factors: 1) pre-metamorphism composition of the protolithic rock, 2) effects of volatilization in increasing temperature, and 3) effects of rock-fluid isotope exchange with fluids and melts. Metamorphism tends to create lower $\delta^{18}O$ values and smaller $\delta^{18}O$ differences between minerals due to the high temperature environment (Baumgartner and Valley, 2001). The $\delta^{18}O$ values can be used to determine if a metamorphic system is closed or open. Dolomite, which is formed in

low temperature, anaerobic environments, is enriched with respect to calcite by 2-4‰ (Land, 1980). Dolomite is common in the geologic record, but not prevalent in the modern depositional environment. It has yet to be created in the laboratory under expected formation conditions, and there is controversy over what role biology plays in formation (Roberts et al., 2013).

Methane Production

Controversial measurements of methane in the martian atmosphere at the 10-60 ppbv level (Formisano et al., 2004, Mumma et al., 2009) have been refuted by other researchers (Zahnle et al., 2011), but discussions of possible biotic (Atreya et al., 2007) or abiotic (Oze and Sharma, 2005) origin continue. Understanding the process of creating methane on Earth provides insight into potential processes active on Mars.

Methanotrophs are unicellular organisms that live in aerobic or anaerobic environments and consume methane Methanogens are archaea that live in anoxic conditions (often in sediments, but also in hydrothermal systems) and produce methane as a metabolic byproduct. Biogenic methane has a $\delta^{13}C < -52‰$, and is not associated with larger simple alkanes such as ethane (C2) or propane (C3). Methane values of $\delta^{13}C < -120‰$ indicate depleted methane can be carbon source, not just a metabolic product, for archaea (Hoefs, 2009).

Methane can also be created at high temperature and pressure from the cracking of kerogen to form petroleum. Thermocatalytic methane has $\delta^{13}C > -52‰$ and is associated with larger simple alkanes such as ethane (C2), propane (C3), butane, (C4),

etc. (Whiticar, 1996). Methanogenesis, the process of creating methane with methanogens, causes an increase in $\delta^{13}C_{DIC}$ (~10‰) because the organisms preferentially metabolize ^{12}C to create methane (see Figure 1-23) (Clark and Fritz, 1997).

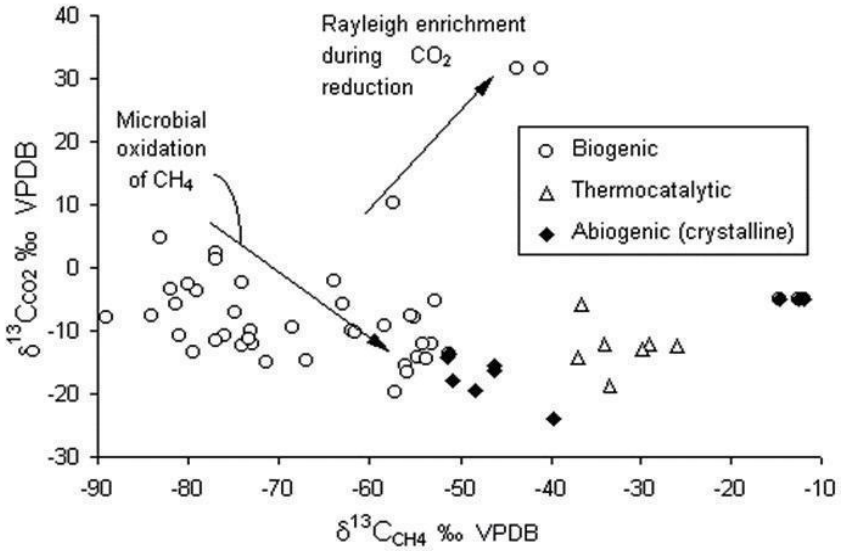

Figure 1-23: Methanogenesis Impacts on $\delta^{13}C$ (reprinted from Clark and Fritz, 1997)

Controversy exists over whether methane can be produced abiotically by combining molecular hydrogen (H_2) and CO_2 in the crust or mantle. The process of "serpentinization" creates H_2 when olivine from ultramafic rock is in contact with water (Wordsworth et al., 2017). In a study of the Rainbow ultramafic hydrothermal vent system along the Mid-Atlantic Ridge, it was found that H_2 at high temperature combines with CO_2 to form organic compounds through Fischer-Tropsch type (FTT) synthesis. Analysis of the vent fluids detected FTT reactions, which supports the hypothesis that

methane can be created by high temperature, aqueous weathering of silicates (Holm and Charlou, 2001).

Gas hydrates form on the seafloor and in permafrost. They are a large reservoir or carbon with unknown impacts on terrestrial, atmospheric $\delta^{13}C$ when released. Researchers suggest methane hydrate releases create sudden global warming cycles as recorded in the geologic record (Dickens, 2011).

Dissertation Research Goals

This dissertation research combines stable isotope measurements of carbonates, which are common in the field of oceanography, with space exploration for past habitable regions on Mars. The oceanographer toolset for determining Earth climate change is useful to explain possible evolution of environmental conditions on Mars.

The first research goal is to study carbonates from Mars to understand their formation conditions. Subsurface water on Mars altered martian rocks to create carbonates. The environmental conditions at the time of carbonate formation provide information about the martian climate and its evolution. When a large object impacted the surface of Mars, subsurface rocks (and their carbonates) were ejected into space. Some of these meteorites traveled to Earth and were trapped in Antarctic ice before being recovered and stored at NASA/JSC in Houston, Texas. Unfortunately, melt water from glacial ice in Antarctica penetrate~~s~~ and precipitates terrestrial carbonate~~s~~ and sulfates on the meteorites. The difficulty is thus identifying which carbonates formed on Mars and which formed on Earth.

The second research goal is to identify stable isotope "fingerprints" of terrestrial carbonates formed on meteorites in Antarctica. This study measures the $\delta^{18}O$ and $\delta^{13}C$ of OC terrestrial carbonates to identify them when found on martian meteorites. This identification allows separation of martian carbonate values from terrestrial carbonate values on meteorites collected in Antarctica. The selected OC meteorites have no extraterrestrial carbonates, yet when they were collected in Antarctica they were observed with secondary alteration minerals on their fusion crust. The meteorite (with low albedo) exposed on the glacial ice (with high albedo) warms and creates a thin-film layer of water around the grains. The atmospheric CO_2 dissolves in the meltwater film and interacts with the available cations (either from the meteorite or sea spray) to form carbonates. This cold (< 0°C), arid environment of Antarctica may also be a formation analog for thin-film carbonates created in martian the subsurface.

The third research goal is to assess how Mars environment conditions have changed, to contribute data towards answering the question of past habitability. By comparing the modern martian environment (measured with NASA orbiters and rovers) to the carbonate formation conditions, it is possible to determine how Mars has changed. If liquid water existed for long periods of geologic time on the martian surface (during the Hesperian period), the ancient atmosphere of Mars must have been denser than now. The current $\delta^{13}C$ and $\delta^{18}O$ values would be enriched (similar to modern δD) (Owen, 1988). The NASA Phoenix spacecraft (launched in 2007) measured the current Mars atmosphere $\delta^{18}O_{VSMOW}$=+31‰ and $\delta^{13}C_{VPBD}$=2.5‰. The NASA Mars Science Laboratory measured the current Mars atmosphere $\delta^{18}O_{VSMOW}$=+48‰ and

$\delta^{13}C_{VPDB}$=+46‰ (Webster et al., 2013). Thus, an older, denser atmosphere would be expected to have $\delta^{13}C$ and $\delta^{18}O$ values lighter, or less enriched, than the MSL measurements.

Prior published martian carbonate stable isotope values vary greatly. Using a single stage phosphoric acid digestion procedure to extract CO_2 (McCrea, 1950) from meteorite samples, carbonates from Mars and carbonates from terrestrial weathering can be mixed. Carbonates of different cation species can also be mixed in the extracted CO_2. This creates results that are difficult to interpret. Using stepped extractions, where the temperature and acid reaction time is varied, distinct carbonate species can be separated and analyzed (Al-Aasm et al., 1990, Shaheen et al., 2015). This dissertation research employs stepped extractions to separate carbonate species and to and compare $\delta^{13}C$ and $\delta^{18}O$ measurements between OC terrestrial carbonates and carbonates in martian MIL Nakhlites.

CHAPTER II

CARBONATE SAMPLE METHODOLOGY

NASA LEAL Facility

The NASA Light Element Analysis Laboratory (LEAL) is located at NASA – Johnson Space Center in Houston, Texas. This laboratory was constructed in the 1960s to provide geochemistry analysis of Apollo moon rocks. The current laboratory configuration is shown in Figure 2-1.

Figure 2-1: NASA LEAL Room Layout

Experiments for this study were conducted in the LEAL. Samples measured included carbonate standards, Ordinary Chondrite (OC) meteorites, and martian Miller Range (MIL) Nakhlite meteorites. Carbonate extractions had not been conducted in this laboratory recently, so new components were built and tested on the legacy systems. New pyrex glassline connections, Sample Tube (ST) heaters, Finger Tubes (FTs), pumps and cooling systems, and a GC with inlet and outlet connections were added.

General Procedure

The general procedure for creation, extraction, separation, and measurement of CO_2 from acidifed carbonates is given in Figure 2-2. Detailed procedures and explanations of system components are provided in Appendix B. This methodology follows prior procedures regarding phosphoric acid reaction of carbonate samples with stepped extractions of CO_2 (Al-Aasm et al., 1990); however, this is the first known research to extract carbonate species from reactions at both 30°C for 1 hour (Rx0), 30°C for 18 hours (Rx1), and 150°C for 3 hours (Rx2).

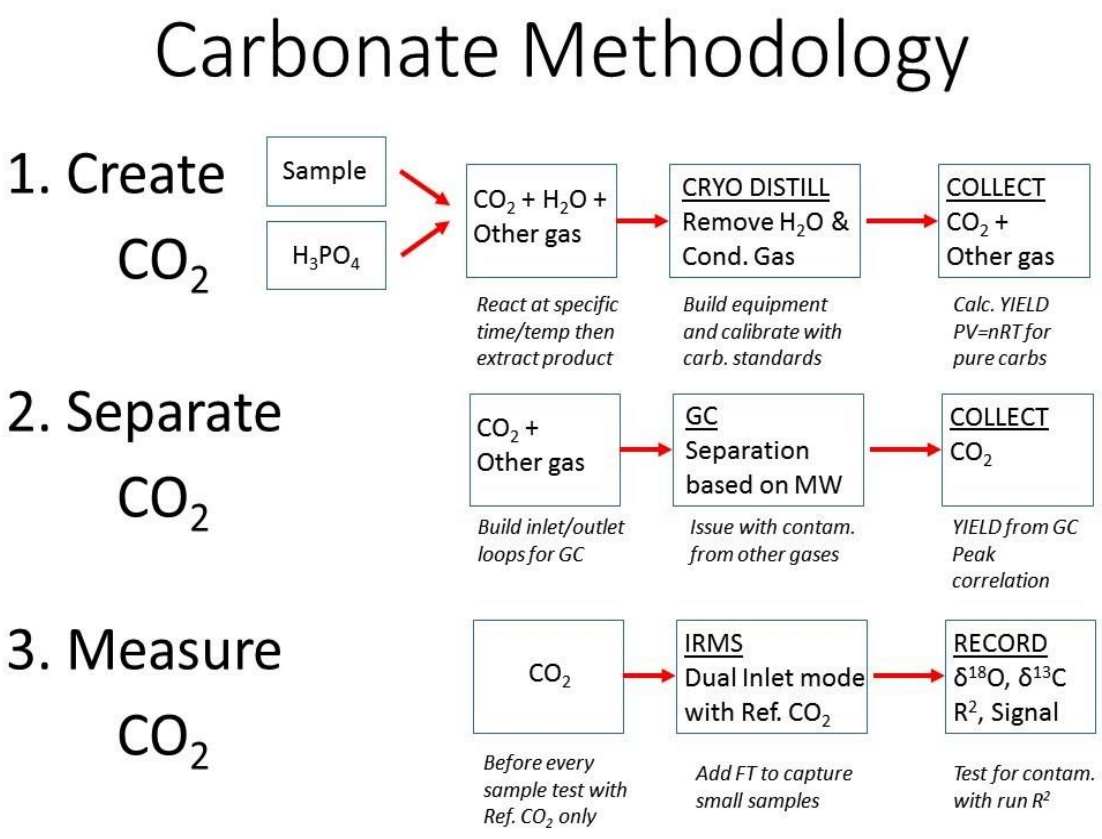

Figure 2-2: Summary of Carbonate Methodology

Additionally, this research works with extremely small samples of CO_2 from untested martian meteorites and compares the results to terrestrial carbonates formed on Ordinary Chondrite meteorites collected from Antarctica.

Each component of the system was tested individually before incorporation into the general methodology. Initially the acid was tested alone, then laboratory calcite standards were acidified, extracted, purified and measured alone to calibrate the system. Next, a laboratory siderite standard was created so that combination of calcite and siderite could be tested on the system. Finally, terrestrial regolith with the combinations of carbonates was test on the system as an analog for meteorite samples. Each of these tests was recorded in a labelled dataset.

Blank Acid Measurement

Before any carbonate reactions with acid were tested, the acid alone was evaluated to determine if it released gas when heated. This released gas is important because it contributes to the pressure gauge reading on the extraction line interpreted for Yield calculations (see discussion below). These measurements were recorded in a dataset known as "Acid_1".

Dataset Acid_1: Two samples were created with only acid (no carbonate or regolith). First, a ST containing 1.0ml of 100% phosphoric acid (H_3PO_4) was heated at 30°C for 18 hours and condensable gas was extracted in the same procedure followed for CO_2 samples. The pressure reading on the carbonate extraction line "fixed volume loop" P_{FTc}= 0.60 mbar. A second acid blank sample was heated to 150°C for 3 hours and

condensable gas was again extracted. The pressure reading on P_{FTc}= 0.56 mbar. It is thus concluded that the heated acid creates a condensable gas at both 30°C and 150°C that creates a slight pressure reading on FT_c of $P_{FTc} \approx 0.6$ mbar. Each of the single extraction carbonate standards (typical FT_c from 30-50 mbar) is corrected by reducing the apparent pressure by 0.6 mbar to calculate Yield (see "Predicting Sample CO_2 Yield with Ideal Gas Law" section, below). The multi-carbonate extraction Yield calculations were also reduced for the calcite and siderite P_{FTc} by 0.6 mbar. When extracting condensable gas from the acid added to terrestrial regolith (HIBB) without any carbonate, the 0.6 mbar P_{FTc} acid condensable gas contribution is noticed in both reactions (30°C and 150°C) (see "HIBB Regolith and Acid Alone" section, below).

Predicting Sample CO_2 Yield with Ideal Gas Law

A Collection Tube (CT) in the lab was first filled with deionized water and weighed to measure the known volume. The result is CT_k = 7.121 ml ± 0.302 ml (2σ standard deviation). The dried CT_k was then filled with CO_2 gas from a gas cylinder connected to the carbonate extraction line, and the pressure was recorded as P_1. The CT_k was sealed and the carbonate finger tube, FT_c was then evacuated to baseline and isolated from the system. The CO_2 in CT_k was expanded to fill the volume of FTc and its pressure gauge. This volume was then calculated using the ideal gas law at constant lab temperature:

$$P_1 * V_1 = P_2 * V_2 \qquad \text{eq. 2-1}$$

so

$$V_2 = (P_1 * V_1) / P_2 \qquad \text{eq. 2-2}$$

where V_1 is the volume of CT_k, V_2 is the volume of FT_c with its pressure gauge, and P_2 is the pressure reading on the FT_c gauge from the expanded CO_2, also called P_{FTc}. The average of 3 measurements for this volume is $V_2 = 8.49$ ml $\pm$ 0.16 ml (2σ standard deviation). This value was used for all initial calcite standard measurements to predict the moles of CO_2 in any sample based on the ideal gas law:

$$PV = nRT \qquad \text{eq. 2-3}$$

so:
$$n_p = P_2V_2 / RT \qquad \text{eq. 2-4}$$

where n_p is the predicted moles of CO_2 in the sample, R=8.314 J/mole°K = $8.314*10^4$ (ml mbar/mole°K), T is the absolute temperature of the lab during the CO_2 extraction, P_2 is the reading on the pressure gauge associated with FT_c, and V_2 is the volume of FT_c. The actual number of moles of carbonate in each sample is known from the weight of the sample and the Molecular Weight (MW_c) of the carbonate:

$$n_k = \text{wt. of sample} / MW_c \qquad \text{eq. 2-5}$$

Comparing the predicted moles of CO_2 to the number of moles of calcite weighed into each sample tube provides an estimate of Yield:

$$\text{Yield} = n_p / n_k \qquad \text{eq. 2-6}$$

The only direct measurement on the carbonate extraction line is the Pressure, P_{FTc}, for the FT_c. Manipulating the ideal gas law (eq. 2-3) and calculated moles (eq. 2-4) provides the predicted carbonate extraction line pressure, P_p:

$$P_p = (wt/MW_c) * RT/(V_2) * MR_c \qquad \text{eq. 2-7}$$

where MWc is the Molecular Weight of the carbonates (calcite = 110.09 g/mole and siderite = 115.86 g/mole), and MR_c is the mole ratio for moles of CO_2 created for each

mole of carbonate sample acidified with phosphoric acid (MR_c = 1.0 for all sample carbonates). Thus,

$$\text{Yield} = P_{FTc} / P_p \qquad \text{eq. 2-8}$$

Each Yield value and its associated stable isotope measurements are then compared to the known calcite stable isotope measurements to assess if fractionation occurred due to an incomplete reaction of all the calcite. Based on the calcite standard results for this system, a Yield > 90% is required to consider the associated stable isotope values as accurate.

Using carbonate standards, 26 successful measurements on single carbonate extractions and 6 successful measurements on multi-carbonate extractions were completed. Using the measured V_2 = 8.487 ml, the calculated Yield = 90%. The corrected stable isotopes for these samples indicate the carbonates were completely reacted with the acid to form CO_2 without fractionation; thus, the choice of V_2 is incorrect. The explanation is that the repeated measurements on the system reflect the true volume of the FTc and associated pressure gauge better than the simplistic calculated volume using the ideal gas law. Thus, the V_2 was empirically adjusted from 8.487 ml to 9.200 ml. With this adjusted V_2, the average Yield = 98% for all of the carbonate standard extractions. The results are given in Figure 2-3.

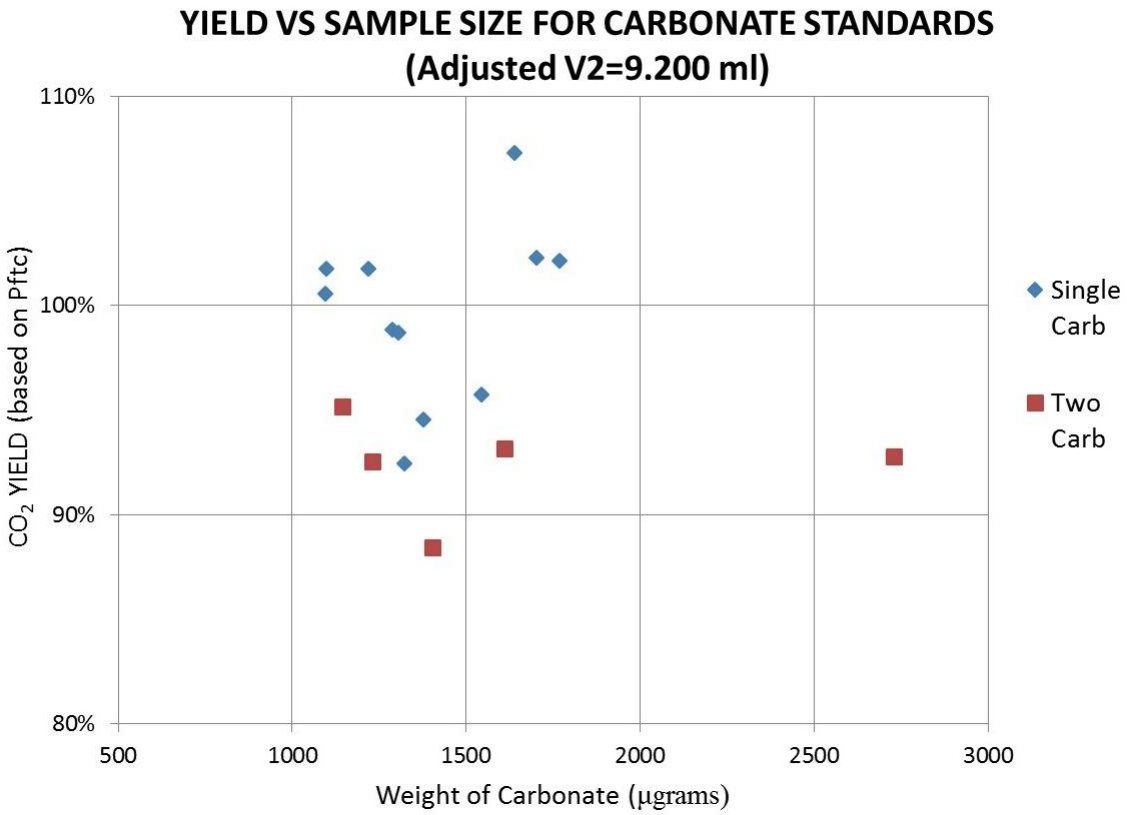

Figure 2-3: Summary of Carbonate Standard Yields

Carbonate Standard Results

The IRMS in "dual inlet" mode compares measurements of the unknown sample against a CO_2 reference gas of known stable isotope values. Each IRMS "run" consists of 8 measurements comparing the unknown sample to the reference gas. The average and standard deviation of each run is then computed for $\delta^{13}C$ and $\delta^{18}O$, and recorded for analysis. Before any unknown sample is loaded into the IRMS for analysis, a "CO_2 Zero Enrichment" run is completed comparing the reference gas to itself as an unknown. This provides confidence that the system is performing as expected and errors in the

measurements are low. Errors in the CO_2-Zero run identify leaks in the instrument or contamination in the system.

The LEAL has calcite standards with known stable isotope values for NBS-18, Joplin, and NASA1. There were no siderite standards before this study, but the Greenland IV siderite was chosen as a new standard. To complete this study, NASA1 calcites were run on the system components and the resulting stable isotope values were compared to the "known" values (aka "TRUE" values) to create an instrument fractionation factor (aka "β_{ins}"). There is a different β_{ins} for each reaction temperature. The NASA1 β_{ins} was applied to different calcite datasets. Differences between the β_{ins} corrected values and the "known" values implied fractionation in the system, and correction factors, or offsets, were produced to force the β_{ins} corrected values to match the "known" values. Three offsets were created: 1) FTc pressure offset for the phosphoric acid used in all reactions (see "Acid Alone" section, above) 2) $\delta^{13}C$ and $\delta^{18}O$ offset for sample transfers between system components (see "Calculate a GC Fractionation Offset" section, below) and 3) $\delta^{13}C$ and $\delta^{18}O$ offset for small CO_2 sample size (see "Calculate a Small CO_2 $\delta^{13}C$ Sample Size Offset" section, below).

A separate group of small sample calcite standards were prepared and tested (after all of the offsets were determined) to evaluate the total error and 2σ standard deviation in stable isotope value measurements. A summary of the carbonate standard datasets completed is given in Table 2-1.

A total of 42 carbonate standard samples (in all datasets) were weighed and acidified. From these samples, 30 successful stable isotope measurements were made in

24 single carbonate extractions and 6 multi-carbonate extractions (see Figure 2-4). Overall Yield for these 30 measurements is 98%.

Dataset	Standard	Type	Use
NBS18	NBS18	Calcite	comparison of 30C β_{ins}
NASA1_1	NASA1	Calcite	create 30C β_{ins}
NASA1_2	NASA1	Calcite	create 150C β_{ins}
NASA1_3	NASA1	Calcite	error on GC CO_2 peak correlation
JOPLIN	NASA1	Calcite	comparison of 30C β_{ins}
IV_1	none	Siderite	create new siderite standard
HIBBs_1	NASA1	Calcite	offset for GC and sample xfers
HIBBs_2	NASA1	Calcite	correlation for GC CO_2 peak to CO_2 sample size, and offset for small CO_2 sample size
HIBBs_3	NASA1	Calcite	correlation for GC CO_2 peak to CO_2 sample size, and error analysis of total stable isotope values
Acid_1	none	H3PO4	offset for Yield based on FTc

Table 2-1: Study Datasets

The multi-carbonate samples were created by combining a known calcite standard and the laboratory established IV siderite standard into a single ST. No regolith was included in these samples. The samples were then acidified and CO_2 was extracted in two steps: 1) After approximately 13 hours at 30°C, and 2) After 3 hours approximately 3.5 hours at 150°C. This multi-step extraction was the initial test for future meteorite extractions of unknown carbonates.

Instrument Corrections

It is essential to create a correction factor, known as a β-Instrument or "β_{ins}", which is unique for all acidifications, extractions and measurements on this system. It is specific for each type of carbonate sample and reaction temperature.

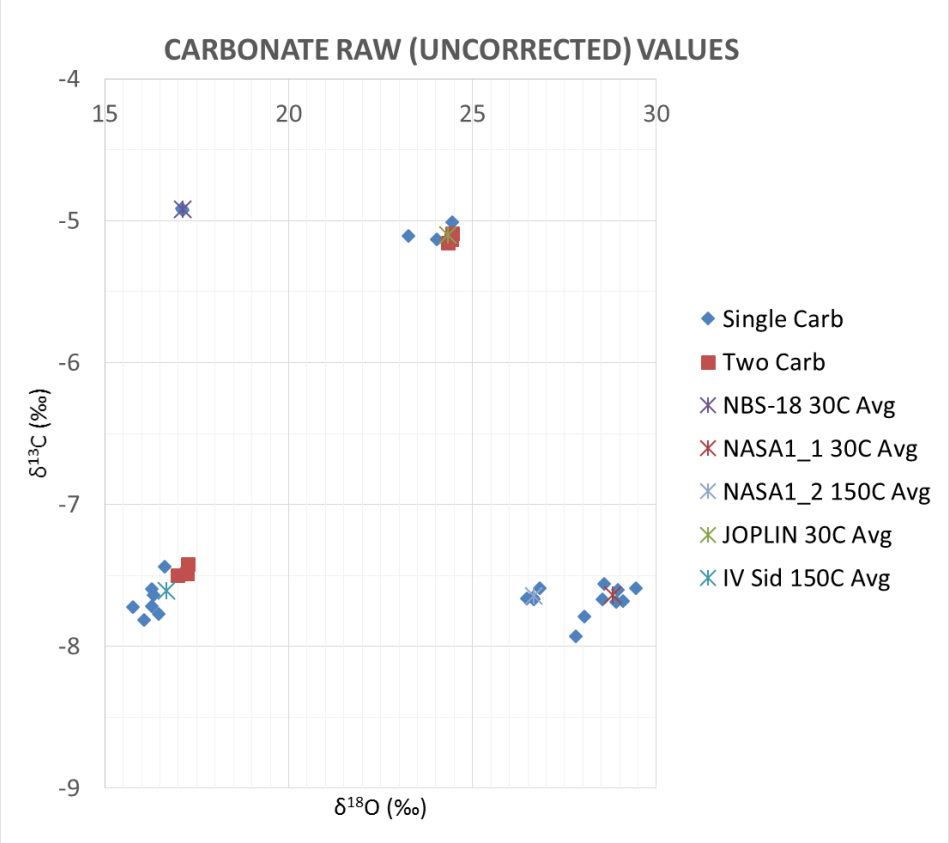

Figure 2-4: Single/Multi Carbonate Standard Extraction Raw Isotope Values

. The β_{ins} is calculated as:

$$\beta_{ins} = (\text{"Measured"} + 1000) / (\text{"True"} + 1000) \qquad \text{eq. 2-9}$$

where "Measured" is the $\delta^{18}O$ or $\delta^{13}C$ value from the IRMS, and "True" is the prior, known value of $\delta^{18}O$ or $\delta^{13}C$. Knowing the stable isotope β_{ins} for each carbonate and reaction temperature, the measured stable isotope values are corrected by:

$$\text{"Corrected"} = ((\text{"Measured"} + 1000) / \beta_{ins}) - 1000 \qquad \text{eq. 2-10}$$

IRMS measurements for 3 calcite standards (NBS-18, NASA1, and Joplin) and 1 siderite (Greenland IV) were collected. A 30°C β_{ins} for NBS-18 and NASA1, and a 150°C β_{ins} NASA1, were calculated for $\delta^{13}C$ and $\delta^{18}O$ using eq. 2-9. Each NASA1 β_{ins} was then applied to correct other datasets. Overall error analysis cannot be conducted with a dataset used to create a β_{ins}, since the error would be associated with the same measurements that were utilized to create the correction factor. Thus, the NASA-1 calcite 30°C extractions were separated into two datasets: NASA1_1 was used to calculate a β_{ins} for correcting the Joplin calcite. NASA1_2 was treated as an unknown and corrected with the β_{ins} from NASA1_1, but then error analysis was completed comparing the results of the corrected NASA1_2 values to the "known" values.

The NBS-18 carbonate standard was not used to correct any of the carbonate measurements in this study, but the β_{ins} calculations provided useful comparisons. The NASA1 calcite dataset NASA1_1 (30°C, no GC) was used to calculate a β_{ins} and correct the measurements for the Joplin calcite. It was also used to correct the other measurements of NASA1 calcite where the sample was treated as an "unknown" (for GC offset, small sample offset, and error calculations).

The dataset NASA1_2 (150°C, no GC) was used to correct the measurements for the IV siderite. Using a calcite to correct for siderite measurements is required due to

the lack of an available siderite standard. This creates an unknown error since fractionation factors for siderite are not available.

A summary of the carbonate measurements is given in Table 2-2.

Carbonate	NBS18	NASA1	NASA1	JOPLIN	IV
Type	Calcite	Calcite	Calcite	Calcite	Siderite
PRIOR d13C, ‰	-5.040	-7.799	-7.799	unknown	unknown
PRIOR d18O, ‰	7.160	19.094	19.094	unknown	unknown
Reference	RM 8543	??	??	n/a	n/a
Dataset (no GC)	NBS18	NASA1_1	NASA1_2	JOPLIN	IV_1
Rx_Temp, ^{0}C	30	30	150	30	150
Rx_Duration, hrs	12, 20	24	3, 26	13, 24	3
# Samples	2	5	4	5	12
Avg. YIELD	101%	99%	97%	93%	96%
Raw d13C, ‰	-4.92	-7.64	-7.65	-5.10	-7.61
d13C 2σ stdev, ‰	0.02	0.11	0.08	0.12	0.27
Raw d18O, ‰	17.11	28.82	26.65	24.34	16.68
d18O 2σ stdev, ‰	0.01	0.48	0.28	0.35	0.90
Treatment	Known	Known	Known	Unknown	Unknown
Bins Correction	PRIOR	PRIOR	PRIOR	NASA1_1	NASA1_3
BinsC	1.000122	1.000159	1.000156	n/a	n/a
2σ stdev	0.000018	0.000111	0.000076	n/a	n/a
BinsO	1.009876	1.009539	1.007417	n/a	n/a
2σ stdev	0.000008	0.000468	0.000268	n/a	n/a
Offset correction?	n/a	n/a	n/a	no	no
Corrected d13C, ‰	-5.04	-7.80	-7.80	-5.26	-7.76
d13C 2σ stdev, ‰	n/a	n/a	n/a	0.12	0.27
Corrected d18O, ‰	7.16	19.09	19.09	14.66	9.20
d18O 2σ stdev, ‰	n/a	n/a	n/a	0.35	0.89
d18O standard	VSMOW	VSMOW	VSMOW	VSMOW	VSMOW
d13C standard	VPDBD	VPDBD	VPDBD	VPDBD	VPDBD

Table 2-2: Single Carbonate Standard Runs

NBS-18 Calcite

The accepted value for NBS-18 calcite is $\delta^{13}C$ (VPDB) = -5.04‰ (Coplen et al., 2006) and $\delta^{18}O$ (VSMOW) = +7.16‰ (Verkouteren, 1999). These values were utilized to calculate a β_{ins} using equation 2-9 to compare to the NASA1_1 β_{ins}.

Dataset NBS18: Two samples of NBS-18 were weighed, acidified, and extracted at 30°C at an average reaction time of approximately 16 hours. No GC purification was completed on these samples. The average CO_2 Yield = 101%. The average "raw" measurements from the IRMS were $\delta^{13}C$ = -4.919‰ ± 0.018‰ (2σ) and $\delta^{18}O$ = +17.107‰ ± 0.008‰ (2σ) (see Figure 2-5). This creates a 30°C β_{ins} correction for $\delta^{13}C$ = 1.000122 ± 0.000018 (2σ) and $\delta^{18}O$ = 1.009876 ± 0.000008 (2σ).

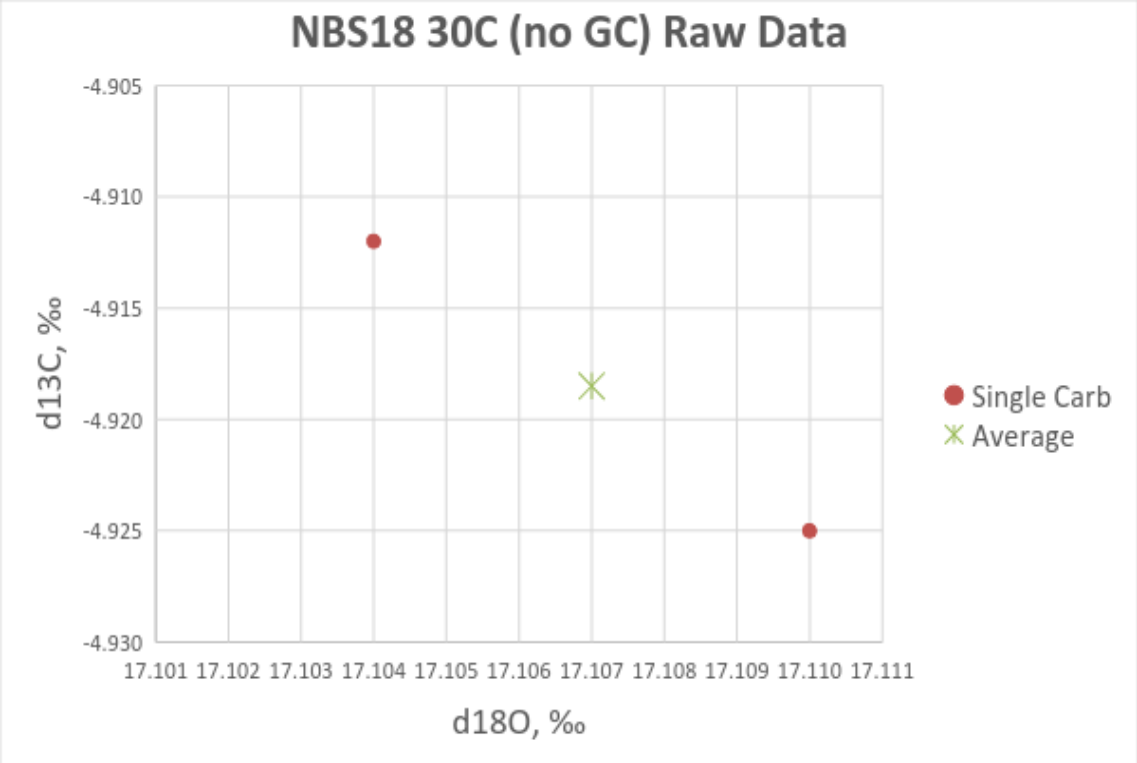

Figure 2-5: Dataset NBS18 Raw Isotopic Values

NASA1 Calcite

NASA1 calcite is an internal laboratory standard with previously measured stable isotope "true" values $\delta^{13}C$ (VPDB) = -7.799‰ and $\delta^{18}O$ (VSMOW) = +19.094‰. These known values were utilized to calibrate the extraction system and create a β_{ins} for the Joplin calcite and the IV siderite.

Dataset NASA1_1: Five samples of NASA1 calcite were weighed, acidified, and extracted at 30°C at an average reaction time of approximately 24 hours. No GC purification was completed on these samples. The average CO_2 Yield = 99%. The average "raw" measurements from the IRMS were $\delta^{13}C$ = -7.641‰ ± 0.110‰ (2σ) and $\delta^{18}O$ = +28.815‰ ± 0.477‰ (2σ) (see Figure 2-6). Using the prior "true" values for NASA1, these measurements create a 30°C β_{ins} correction for $\delta^{13}C$ = 1.000159 ± 0.000111 (2σ stdev) and $\delta^{18}O$ = 1.009539 ± 0.000468 (2σ stdev). This β_{ins} is used to correct the "raw" stable isotope measurements for the NASA1_2 dataset and the Joplin calcite, and also for all low temperature calcite extractions on all meteorite measurements.

Dataset NASA1_2: Fours sample of NASA1 calcite were weighed, acidified, and extracted at 150°C. Two samples were reacted for approximately 26 hours, and two samples were reacted for approximately 3 hours. The stable isotope measurements results were nearly the same, indicating that all of the calcite reacted with the acid within 3 hours and no further fractionation happened up to 23 hours later.

The NASA1_2 dataset average CO_2 Yield = 97%. These samples were not run on a GC for purification. The average "raw" measurements from the IRMS were $\delta^{13}C$ = -7.645‰ ± 0.075‰ (2σ) and $\delta^{18}O$ = +26.653‰ ± 0.279‰ (2σ) (see Figure 2-7).

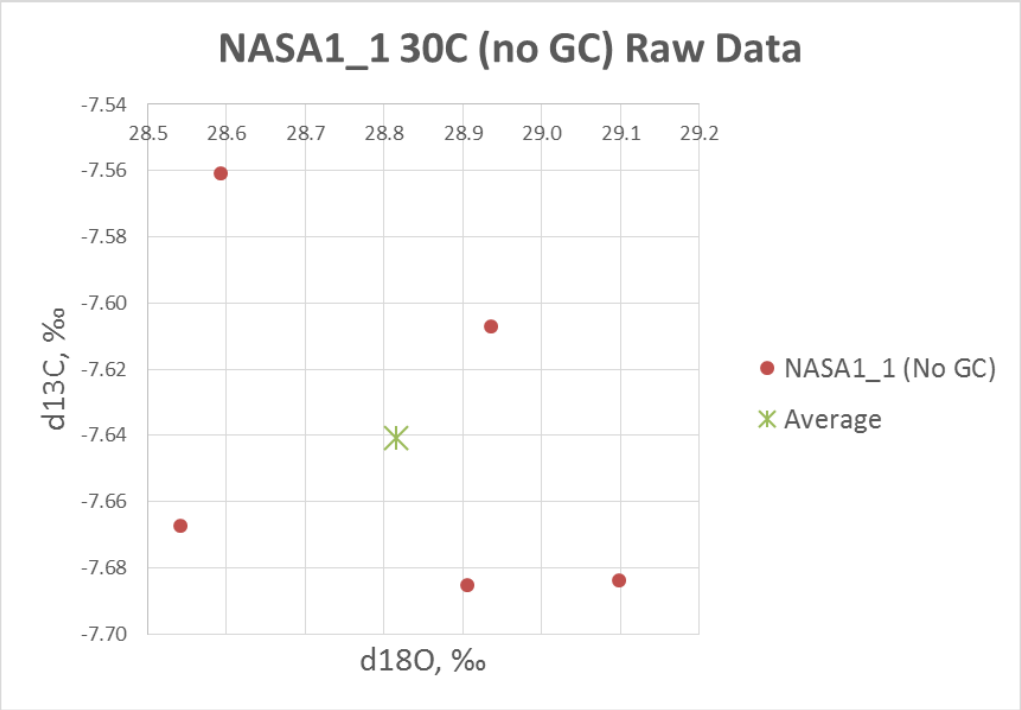

Figure 2-6: Dataset NASA1_1 Raw Isotopic Values

Using the prior "true" values for NASA1, these measurements create a 150°C β_{ins} for $\delta^{13}C$ = 1.000156 ± 0.000076 (2σ) and $\delta^{18}O$ = 1.007417 ± 0.000268 (2σ). This β_{ins} was used to correct the "raw" stable isotope measurements for the IV siderite, and also for high temperature (150°C) extractions on all meteorite measurements. The use of a high temperature calcite β_{ins} to correct for a siderite or magnesite extraction in meteorites of unknown carbonate may induce slight error, but analysis indicates the fractionation

difference between species is far less than the overall systemic and data errors encountered in the sample measurements.

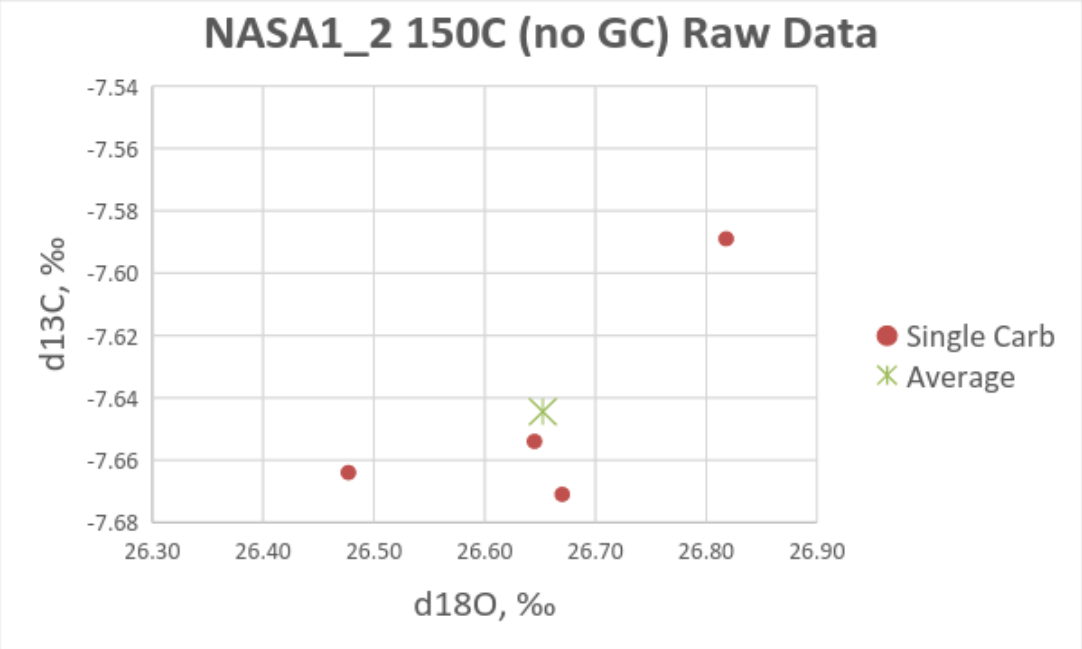

Figure 2-7: Dataset NASA1_2 Raw Isotopic Values

It is noted that the high temperature reaction (150 °C) fractionates the calcite by approximately $\delta^{13}C$ = -0.024‰ and $\delta^{18}O$ = -2.268‰ compared to the lower temperature reaction (30°C), as reflected in the "raw" stable isotope measurements. This is expected since there is generally less isotope fractionation at high temperature than at low temperature.

Joplin Calcite

Dataset Joplin_1: Joplin calcite has no previously reported set of stable isotope values for equilibrium reactions at 30°C. Five samples of Joplin calcite were weighed, acidified, and extracted at 30°C. Two samples were reacted for approximately 24 hours, and three samples were reacted for approximately 13 hours. There was so little variation between the Yield and stable isotope measurements that the total of all five samples was combined and averaged for analysis. No GC purification was completed on these samples. The average CO_2 Yield = 93%. The average "raw" IRMS measurements were $\delta^{13}C$ = -5.103‰ ± 0.0.057‰ (2σ) and $\delta^{18}O$ = +24.338‰ ± 0.176‰ (2σ) (see Figure 2-8). The Joplin_1 dataset was used to compare β_{ins} calculations to NASA1_1.

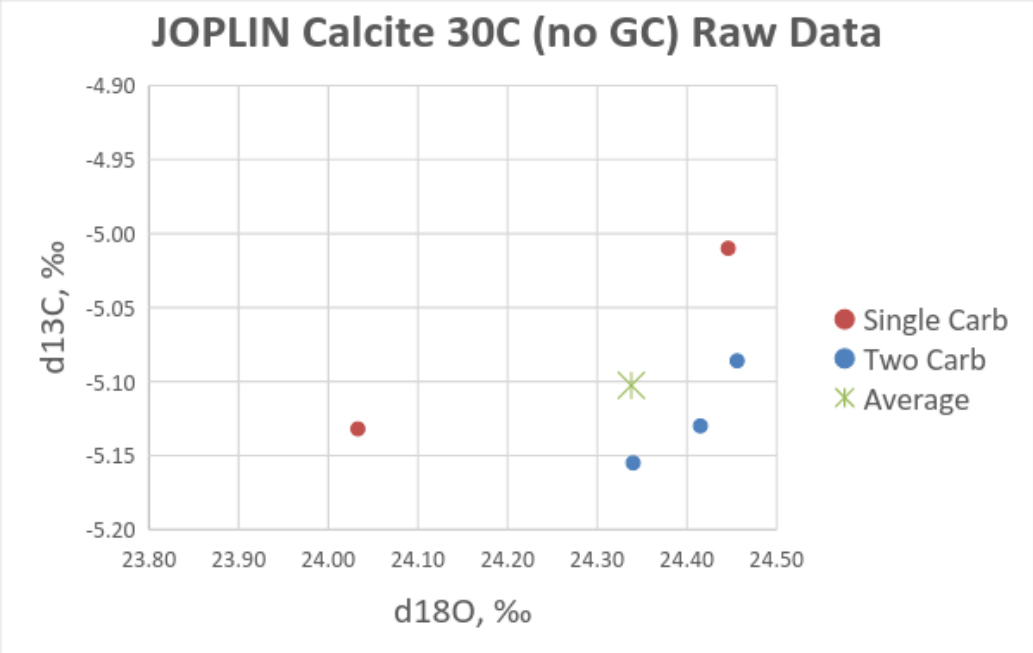

Figure 2-8: Dataset JOPLIN Raw Isotopic Values

Greenland IV Siderite

Dataset IV_1: Greenland IV siderite has no previously measured set of stable isotope values for equilibrium reactions at 30°C or 150°C. Four samples of IV siderite alone were weighed, acidified, and single extracted at 150°C at an average reaction time of approximately 3 hours. No GC purification was completed on these samples. The average of the samples CO_2 Yield = 95%. The average "raw" IRMS measurements for the single extractions were $\delta^{13}C$ = -7.702‰ ± 0.275‰ (2σ) and $\delta^{18}O$ = +16.487‰ ± 0.936‰ (2σ).

Six multi-carbonate samples of IV siderite were extracted (following calcite extractions at 30°C) at 150°C after an average reaction time of 3 hours. No GC purification was completed on these samples. The average CO_2 Yield = 96%. The average "raw" IRMS measurements for the multi-carbonate extractions were $\delta^{13}C$ = -7.544‰ ± 0.199‰ (2σ) and $\delta^{18}O$ = +16.816‰ ± 0.841‰ (2σ).

Combining the results of the ten IV siderite samples (single carbonate and mult-carbonate extractions), the average CO_2 Yield = 95%. The average "raw" measurements from the IRMS were $\delta^{13}C$ = -7.607‰ ± 0.272‰ (2σ) and $\delta^{18}O$ = +16.684‰ ± 0.895‰ (2σ). These results are shown in Figure 2-9.

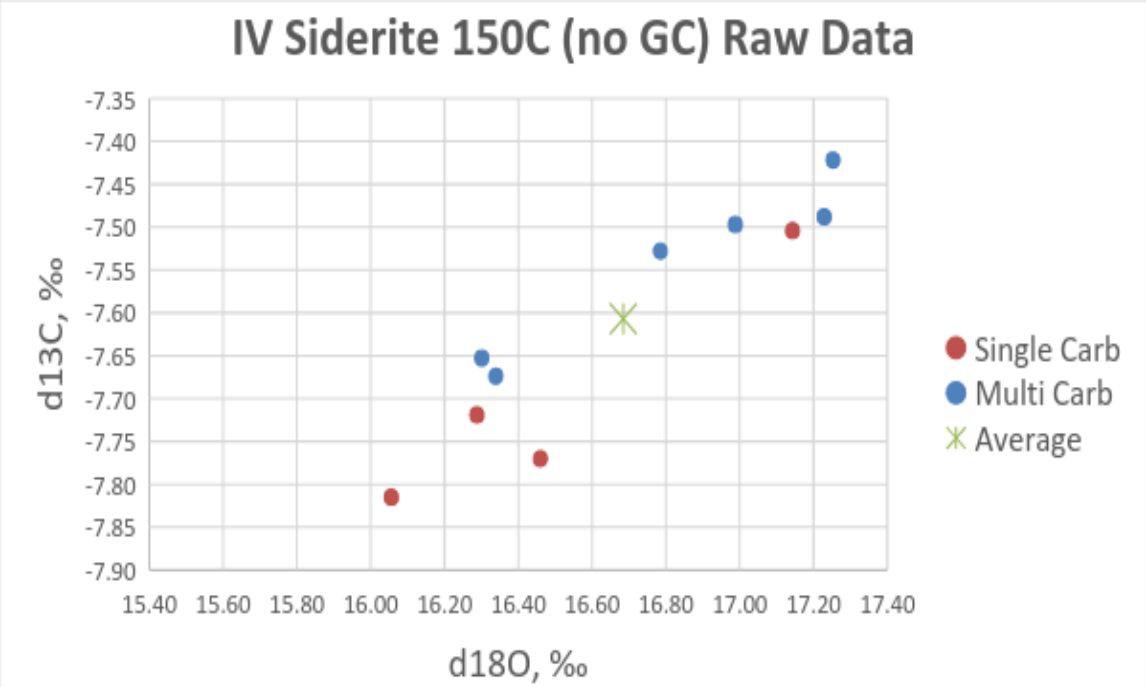

Figure 2-9: Dataset IV_1 Raw Isotopic Values

HIBB Regolith and Acid Alone

Dataset HIBB_1: A terrestrial regolith was tested to ensure that it contained no in situ carbonates. A carbonate sterile regolith was necessary to add known amounts of carbonate standard, then measure results to ensure the laboratory procedure produces expected results. The regolith acts as a surrogate for ground meteorites.

Eleven samples were created combining 1.0 ml of H_3PO_4 acid and HIBB terrestrial regolith. For Rx1, nine samples provided very slight condensable gas. For Rx2, seven samples provided very slight condensable gas

The acidified samples were reacted at 30°C for 18 hours (Rx1) before the first extraction. The samples were then heated at 150°C for 3 hours (Rx2) before the second

extraction. No GC was used for gas purification. The pressure for the condensable gas, P_{FTc}, collected from each extraction was consistent with the "acid-only" measurements, thus it is concluded the HIBB regolith contains no *in situ* carbonate that creates CO_2.

Known weights (and moles of CO_2 from eq. 2-4) of carbonate standards were added to the HIBB to create HIBBs ("spiked") samples that resembled meteorite powder for testing stable isotope fractionation and CO_2 Yield correlations on the GC.

CO_2 Fractionation by Transfer

Sample CO_2 is transferred between system components in CTs before stable isotope measurements are completed on the IRMS. The amount of fractionation created by transferring CO_2 reference gas between components was measured as described below.

IRMS Left Bellow to/from IRMS CT

To ensure all of the small volumes of meteorite sample CO_2 are transferred to the IRMS, a Finger Tube was attached to the IRMS Left Bellow (replacing the pressure gauge). CO_2 reference gas of known isotopic values was transferred from the IRMS left bellow to a CT on the left "sample" port of the instrument, then refrozen into IRMS left bellow FT_i. After thawing the FT_i, the change in signal on the Left Bellow reflects that 98% ± 1% of the CO_2 was recovered. The uncertainty is based in the change in signal on the Right Bellow, which was unchanged during the test. The reference gas CO_2 stable isotope values changed as follows: $\delta^{13}C = +0.08‰$, $\delta^{18}O = +0.16‰$, which reflects a slight loss of the lightest isotope of each molecule in the transfer.

IRMS Left Bellow to/from Carbonate Line FT_c

CO_2 reference gas was transferred from the IRMS left bellow to a CT on the left "sample" port of the instrument, then the CT was moved to the carbonate extraction line. The CO_2 was transferred to the FT_c and allowed to thaw so that a pressure reading could be taken. The CO_2 was then refrozen to FT_c, the CT was moved to the IRMS, and the CO_2 was refrozen into IRMS left bellow FT_i. The stable isotope values were measured before and after the complete transfer of CO_2. Four transfer were completed with the following results: Recovery = 95% (based upon left bellow signal), $\delta^{13}C$ = +0.26‰, $\delta^{18}O$ = +0.40‰. Thus, a slight but defined fractionation occurs in transfer between the IRMS to/from the carbonate line FT_c.

IRMS Left Bellow to/from GC

CO_2 reference gas was transferred from the IRMS left bellow to a CT on the left "sample" port of the instrument, then the CT was moved to the GC. The gas was run through the GC and collected and moved back to the IRMS for stable isotope measurement. A "pseudo" Yield determination was made based upon the change in the left bellow signal for the sample before and after the GC purification. Initially the Yield from the GC was <70% (based on change in IRMS left bellow signal), so the GC collection procedure was modified. The collected CO_2 contains Helium carrier gas, and it must be removed to transfer the CO_2 from the GC outlet loop to the CT. Initially the He was pumped away to a pressure of $1x10^{-1}$ mbar, but the pump away pressure was reduced to $1x10^{-2}$ mbar. The transfer time to freeze the CO_2 from the outlet loop to the

CT was increased from 3 minutes to 5 minutes. These modifications increased the pseudo Yield with runs using only the CO_2 reference gas from 70% to 105% in the final three transfer tests. The 3 final transfers were completed with the following results: Recovery = 105% (based upon left bellow signal), $\delta^{13}C = +0.16‰$, $\delta^{18}O = +0.49‰$. Thus, a slight but defined fractionation occurs in transfer between the IRMS to/from the GC which is nearly identical to the transfer to/from the carbonate extraction line. This lead to the creation of a "GC offset" for meteorite sample stable isotope measurements.

Carbonate CO_2 Separation with the GC

The single extraction and multi-step extractions on carbonate standards produced pure CO_2 and very little extraneous gas. The meteorite samples create CO_2 and other gases when acidified. Most of the incondensable gas is pumped away during the cryogenic extraction procedure on the carbonate line; however, condensable gases and CO_2 are frozen together when collected with a dewar of liquid N_2 (which has a condensation temperature of -196°C). These condensable gases can produce isobaric interferences and need to be separated from the CO_2 with a GC. Multiple tests were conducted with carbonate standards to assess the stable isotope value fractionation using the GC. The result of these GC fractionation tests, combined with the transfer fractionation between components, creates an "offset" applied to the measured sample CO_2 $\delta^{13}C$ and $\delta^{18}O$ values. It is also noticed that there is a fractionation based upon extraction of small CO_2 sample size (< 5 μmole CO_2), which required an additional "offset" to the stable isotope values.

Calculate a GC (and transfer) Fractionation Offset

HIBBs_1 dataset: The terrestrial, carbonate-free regolith, HIBB, is "spiked" with carbonate standards to create samples that resemble meteorite samples. This dataset was collected to better understand the effects of basaltic minerals during the acidification process. This also provided an opportunity to test extraction and purification of CO_2 before studying meteorites. Both calcite and siderite was added to create various combinations of HIBBs. The range of sample sizes were 5-56 μmoles for each carbonate species. The samples were acidified, and reacted in two conditions: Rx1 at 30°C for 18-20 hours, Rx2 at and at 150°C for 3 hours.

After the stepped extraction of each carbonate species, some of the samples were run on the IRMS ("dirty-only") without any GC purification. Some of these samples were then run on the GC for purification. This provided a comparison of stable isotope "dirty" values before-GC to "clean" values after-GC runs.

Other HIBBs samples were extracted and purified on the GC before running on the IRMS ("clean-only"). The β_{ins} corrected stable isotope measurements for all "dirty" and "clean" samples are given as a graph in Figure 2-10, and with errors as a table in Table 2-3. Using the carbonate extraction line pressure gauge on a known volume, the average Rx1 "clean" CO_2 Yield = 107% for four measurements. The average Rx2 "clean" CO_2 Yield = 95% for five measurements. The HIBBs_1 dataset raw values were then corrected with the appropriated β_{ins}: Rx1 using NASA1_1 dataset and Rx2 using NASA1_2.

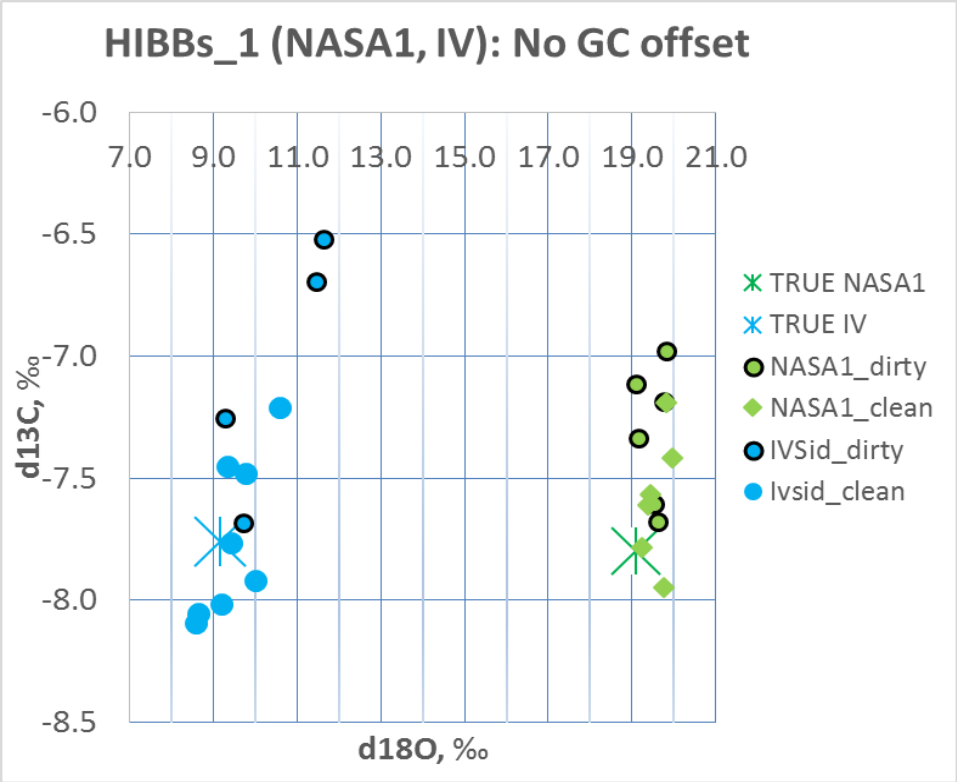

Figure 2-10: Dataset HIBBs_1 Corrected Isotopic Values (no GC offset)

HIBBs_1 , βins corrected							
Rx1 βins Basis	NASA1_1						
Rx1βinsC used (30C)	1.000159						TRUE
Rx1 βinsO used (30C)	1.009539	n	avg.	stdev (1σ)	stdev (2σ)	sterr (2σ)	ERROR
Rx1 Correct d13C "dirty"		6	-7.320	0.278	0.556	0.227	0.479
Rx1 Correct d18O "dirty"		6	19.512	0.306	0.612	0.250	0.418
Rx1 Correct d13C "clean"		6	-7.501	0.266	0.533	0.218	0.298
Rx1 Correct d18O "clean"		6	19.606	0.291	0.582	0.237	0.512
Rx2 βins Basis	NASA1_150						
Rx2 βinsC used (150C)	1.000156						
Rx2 βinsO used (150C)	1.007417						
Rx2 Correct d13C "dirty"		4	-7.038	0.531	1.063	0.531	0.722
Rx2 Correct d18O "dirty"		4	10.523	1.204	2.408	1.204	1.381
Rx2 Correct d13C "clean"		8	-7.791	0.330	0.660	0.233	-0.031
Rx2 Correct d18O "clean"		8	9.386	0.676	1.352	0.478	0.244

Table 2-3: Dataset HIBBs_1 Errors Before GC Offset

This dataset showed that a consistent, small fractionation was introduced during the GC separation of CO_2. To calculate a GC offset, only the "clean" β_{ins} corrected stable isotope values for Rx1 and Rx2 are employed. The "dirty" values were not included in this offset calculation since it was decided that no meteorite sample would be run "dirty" (based on IRMS run contamination from unknown gas using the unpurified meteorite sample). The average for the "clean" NASA1 calcite (Rx1) and Greenland IV siderite (Rx2) is:

$$\text{GC OFFSET: } \delta^{13}C = +0.104‰,\ \delta^{18}O = +0.406‰ \qquad \text{eq. 2-11}$$

The GC offset is (+), indicating the corrected measurements are isotopically heavy. To correct for this offset, the above values are thus SUBTRACTED to make the correction for fractionation in the GC and transfers.

Correlation GC CO_2 Peak Count to Sample Size

Using the carbonate extraction line FT_c pressure gauge provides an accurate method to predict the Yield of extracted CO_2 for samples where the only product is CO_2, such as with the carbonate standards alone or when the carbonate standards were added to HIBB regolith. This Yield method fails when the acidification creates other gases that are not separated cryogenically in the extraction process. After acidifying the meteorite samples, unidentified gases were created that froze together with the CO_2 in the CT. When thawed, these gases increased the pressure reading on FT_c and provided false values for Yield; thus a new method needed to be developed for predicting the sample CO_2 size.

Dataset HIBBs_2 and HIBBs_3 were created with NASA1 calcite added to the HIBB regolith to create the GC CO_2 peak count to CO_2 sample size correlation. Ten samples were weighed, acidified, and reacted at 30°C for 18 to 67 hours. The weighed carbonates created CO_2 samples ranging in size from 1.19 μm to 4.02 μm (which is the expected size of meteorite carbonate samples). The average CO_2 Yield = 93% (using the carbonate extraction line pressure gauge on the known volume). After extraction, these samples were then run on the GC for CO_2 separation from other condensable gases. Each GC CO_2 peak count was recorded, and a correlation with calcite sample size was created (see Figure 2-11). The equation (from the graph) provides an equation for predicting CO_2 sample size from measured GC peak as:

$$CO_2 \text{ size } (\mu m) = ((\text{GC Peak})^2 * 7.48E\text{-}14) + ((\text{GC Peak}) * 1.47E\text{-}6) \quad \text{eq. 2-12}$$

The error on this correlation is determined using the dataset NASA1_3, which was created from six samples of NASA1 calcite (no HIBB regolith) ranging in size from 1.8 μm to 7.5 μm of CO_2. The predicted CO_2 sample size (from equation 2-12) is compared to the actual CO_2 sample size (based upon calcite weight). The difference in predicted sample size of dataset NASA1_3 provides an error for the GC correlation created with datasets HIBBs_2 and HIBBs_3. The result is a range of errors from +6.4% to -4.6% in CO_2 sample size (±6%), with an average error of -0.2%.

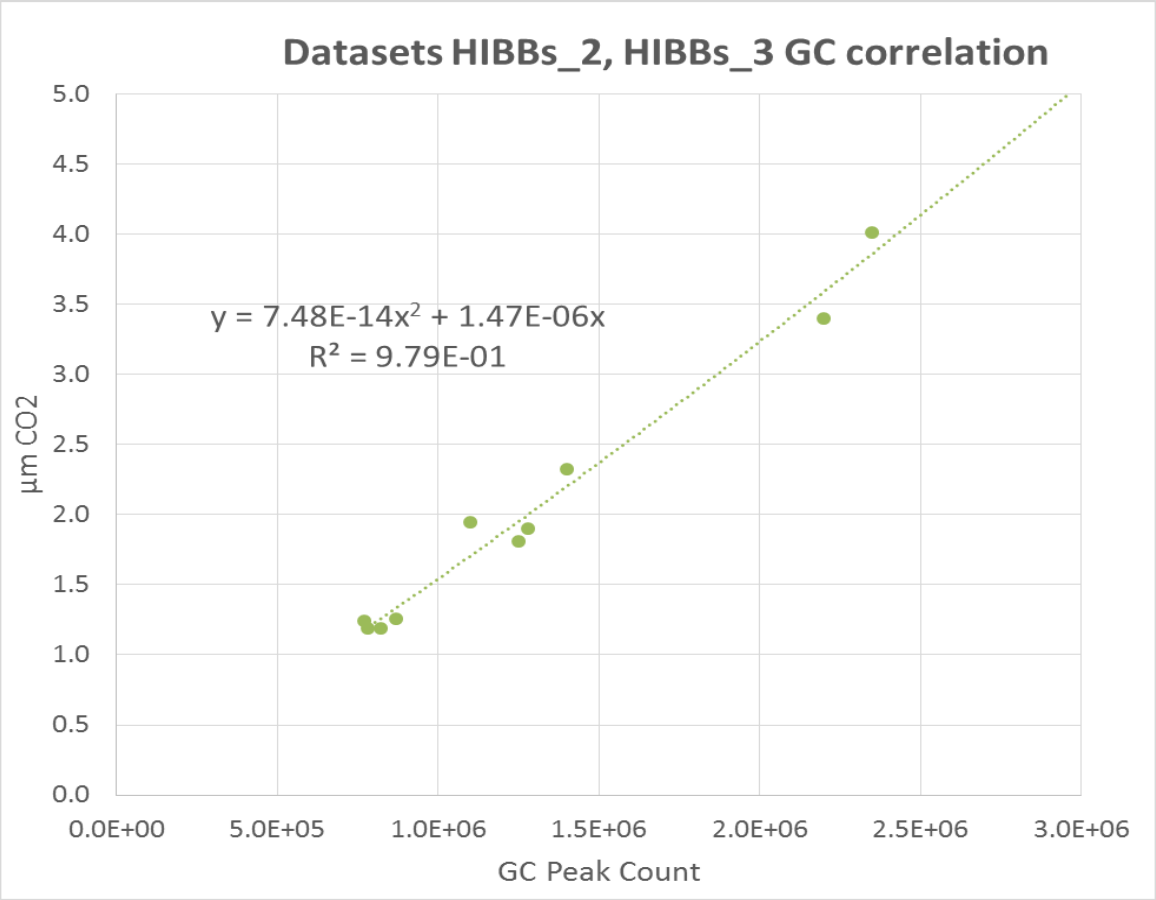

Figure 2-11: Correlation of GC Peak Count to CO_2 Sample Size

Small CO_2 Sample Size

As carbonate standard sample analysis was ongoing, it became apparent that small samples of CO_2 were consistently enriched in heavy isotopes relative to larger samples (even with the offset correction for GC and transfer fractionation).

The Mars Nakhlite meteorites contain martian carbonate of approximately 0.005% to 0.007% by weight, which generates a total of less than 1 µm of CO_2 from a 1g ground meteorite sample (see Chapter 4). An additional correction to the stable

isotope values is necessary based upon observations of additional fractionation in very small samples of CO_2 carbonate standards.

Small CO_2 Sample Size Impacts

Using dataset HIBBs_2 and HIBBs_3 (CO_2 sample size from 1.19 μm to 4.02 μm), the β_{ins} corrected stable isotope values with the GC offset is shown in Figure 2-12). The values consistently are heavier in $\delta^{13}C$, thus an offset is needed. The $\delta^{18}O$ values vary both heavier and lighter than the known value for NASA1 calcite, with an average of zero (0) from the standard. No offset for $\delta^{18}O$ is applied.

Calculate a Small CO_2 $\delta^{13}C$ Sample Size Offset

Only dataset HIBBs_2 is employed to calculate the small CO_2 sample offset. The dataset HIBBs_3 is used for error analysis on the results after all sample corrections are applied (corrections for β_{ins}, GC offset, and CO_2 small sample size offset). The error on the $\delta^{13}C$ stable isotope values is shown in Figure 2-13, and the value of the offset can be calculated with the following equation:

$$\delta^{13}C \text{ Offset} = -0.631 * \ln(CO_2 \text{ sample size}) + 0.9286 \qquad \text{eq. 2-13}$$

As with the GC offset, the small CO_2 sample offset causes the measured stable isotope value to be heavier than the true value. A correction for the CO_2 small sample offset is thus subtracted from the measured stable isotope value (causing the result to become lighter).

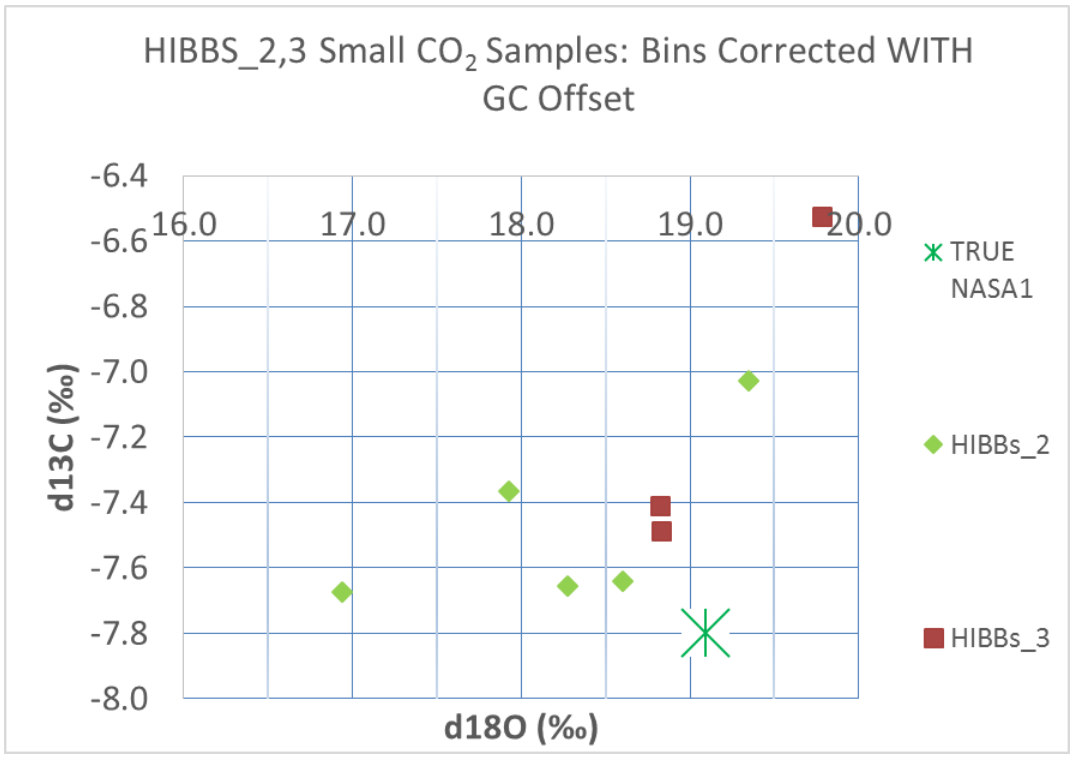

Figure 2-12: Dataset HIBBs_2,3 β_{ins}+GC Corrected Isotopic Values

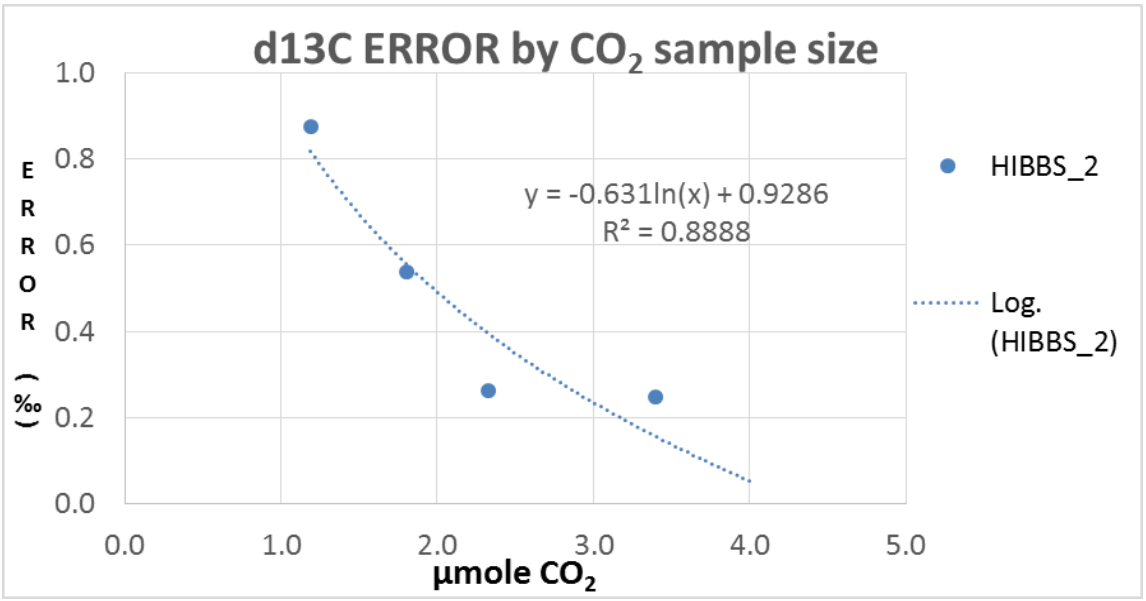

Figure 2-13: Dataset HIBBs_2 $\delta^{13}C$ Error Based on CO_2 Sample Size

In summary, the $\delta^{13}C$ raw, measured carbonate stable isotope values are first corrected with the β_{ins}, then the GC fractionation offset is subtracted, then the small CO_2 sample size offset is subtracted (if sample size < 5 μm). The $\delta^{18}O$ raw, measured carbonate values are corrected only with the β_{ins} and the GC fractionation offset.

Stable Isotope Measurement Error Analysis

Overall error analysis of the stable isotope measurements, including all corrections and offsets, is accomplished with dataset HIBBs_3. The major components of the error reported here include: 1) Uncertainty in the instrument fractionation β_{ins} correction, 2) Uncertainty in the GC transfer fractionation offset, and 3) Uncertainty in the small sample size offset. Three extremely small samples of NASA1 calcite were added to HIBBs and extracted, measured, and corrected with the process described above. After all of the modifications, the difference between the corrected stable isotope value and the TRUE value is calculated. The average of the differences and the standard deviation of the differences is then calculated for all three samples. A summary of the dataset HIBBs_3 results is given in Table 2-4. The stable isotope measurement error for the complete analytical methodology is then given as:

$$\text{ERROR} = \text{Avg. Differences} + \text{stdev } (2\sigma) \text{ of Differences} \qquad \text{eq. 2-14}$$

Thus, the error for $\delta^{13}C$ is 0.05 + 0.72 = 0.77‰. The error for $\delta^{18}O$ is -0.05 + 1.10 = 1.06‰. For future publications, this analysis error is reported as:

ERROR: $\delta^{13}C = \pm 0.77‰$, $\delta^{18}O = \pm 1.06‰$.

This error is caused by the extremely small size of the CO_2 samples extracted from the carbonates, coupled with separation of CO_2 from other gases on the GC. It is

based on measurements of known calcite standards. The magnitude of this error is consistent with prior reported martian carbonate stable isotope errors of ±1‰ to 2‰ (Wright et al., 1988, Wright et al., 1992, Grady et al., 2007).

HIBBs_3 Extraction Date	5/18/16	5/27/16	6/3/16	Avg	2σ stdev	
Sample Tube	380	381	375			
CO2 size (μmole)	1.95	1.90	1.19			
Raw d13C (‰)	-7.146	-7.223	-6.264	-6.878	1.066	
Raw d18O (‰)	28.954	28.955	29.917	29.275	1.111	
βins correct d13C (‰)	-7.304	-7.381	-6.422	-7.036	1.066	
βins correct d18O (‰)	19.232	19.233	20.185	19.550	1.101	
GC offset d13C (‰)	-0.100	-0.100	-0.100			
GC offset d18O (‰)	-0.410	-0.410	-0.410			
Size offset d13C (‰)	-0.508	-0.524	-0.819			
Size offset d18O (‰)	0.000	0.000	0.000			
CORRECTED d13C (‰)	-7.912	-8.005	-7.341	-7.753	0.718	
CORRECTED d18O (‰)	18.822	18.823	19.775	19.140	1.101	
TRUE d13C (‰)	-7.799	-7.799	-7.799			
TRUE d18O (‰)	19.094	19.094	19.094			ERROR
DIFFERENCE d13C (‰)	-0.113	-0.206	0.458	0.046	0.718	0.765
DIFFERENCE d18O (‰)	0.272	0.271	-0.681	-0.046	1.101	1.055

Table 2-4: Error Analysis from Dataset HIBBs_3

There is an observed co-variance feature in the results of this analysis that is often seen in other data during this study (e.g. Figures 2-21, Figure 2-22, and Figure 2-25). Increases, or heavier, $\delta^{13}C$ (upward on a graph) and increases, or heavier, $\delta^{18}O$ (rightward on a graph) can create a "smear" of data points. The nature of this co-variance is not understood.

CHAPTER III

STUDY OF ORDINARY CHONDRITES

Introduction

Purpose of this Study

Meteorites collected in Antarctica contain secondary minerals that could be formed before or after landing on Earth. To assess any environmental formation conditions on Mars, it is essential that the minerals analyzed be martian in origin. Ordinary Chondrites (OCs), collected from Antarctica, can provide a witness plate for potential terrestrial alteration. Certain types of OCs contain no pre-terrestrial carbonate, thus any carbonate alteration is almost certain to be terrestrial in origin. Furthermore, OCs are quite common and it is possible to study a larger population of samples from different regions on the continent (selecting OCs near where known martian Nakhlites have been collected).

The first objective of this study is to identify stable isotope characteristics of terrestrial carbonates formed on meteorites collected from Antarctica. Once the terrestrial characteristics are established, identification of non-terrestrial carbonates is easier. OCs of alteration type 3-6 with "e" weathering are excellent samples for characterizing terrestrial weathering products (see discussion in Chapter 1 for explanation of types).

The second objective of this study is to assess the formation mechanism of carbonates in a cold, arid environment. The Antarctic environment has many similarities

to Mars, and therefore a better understanding of carbonate formed in Antarctica can provide a model for understanding how Mars carbonates form. Studying terrestrial carbonate stable isotope values from OCs, a mixing model can be developed to predict the contribution of different reservoirs to the measured values. This model could then be applied to Mars carbonate values to assess the martian environmental conditions for carbonates formed on Nakhlites (see Chapter 4).

Interesting Terrestrial Meteorite Minerals

Ca-rich carbonates (usually calcite) are commonly found as secondary alteration products in meteorites; however, other secondary minerals are often found. One theory for Antarctic meteorite weathering is from slightly alkaline sea-spray. This aerosol, which is found far inland on Antarctica, deposits Ca^{+}, Na^{+}, and SO_4^{2-} ions on the meteorite. Then, when the meteorite is exposed on the surface of Antarctic glaciers, the high albedo rock absorbs sunlight and melts a small amount of ice to form liquid water. This water combines with the cations and anions to form carbonates and sulfuric acid, which alters the meteorite mineralogy (Hallis, 2013).

Nesquehonite

This is an alteration product created as a hydrated form of magnesite ($MgCO_3$). On Earth, it tends to decompose into magnesite from dehydration. The chemical equation is $Mg(HCO_3)(OH)*2H_2O$. It has been identified by satellites orbiting Mars near Valles Marineris and Terra Meridiani (Dehouck et al., 2011). On Antarctic

meteorites, it has been identified on Y-74371 (Yabuki et al., 1976), and within other Allan Hill meteorites (Marvin and Motylewski, 1980). It has been studied on the H5 OC LEW 85320, which was collected from Antarctica with alteration crystals visible on the fusion crust. Since being collected and curated at NASA/JSC in a dry, nitrogen environment, LEW 85320 continues to grow new generations of nesquehonite. Stable isotope values for the nesquehonite on LEW 85320 are given in Table 3-1 (Jull et al., 1988, Grady et al., 1989).

Year	Author	Nesquehonite	$\delta^{13}C$ (‰)	$\delta^{18}O$ (‰)
1988	Jull et al.	LEW 85320, 40 (Antarctica)	5.40	9.39
1988	Jull et al.	LEW 85320, 22 (Texas)	4.28	11.35
1989	Grady et al.	LEW 85320 (Antarctica)	7.9	17.9
1989	Grady et al.	LEW 85320 (Texas)	4.2	12.1

Table 3-1: Stable Isotope Values for Nesquehonite on LEW 85320

In the above referenced Grady study, there is a clear stable isotope value difference between the nesquehonite formed in the Antarctic environment and in the Texas curation laboratory. Both studies reflect consistent stable isotope values for the nesquehonite formed in the curation environment. Its formation mechanism remains mysterious however, as in order to continue the creation of nesquehonite in the dry, nitrogen environment at NASA/JSC, remnant water must be in the meteorite. Future generations of nesquehonite will likely be less productive as the water is consumed in curation.

White Druse

The Shergottite EET 79001 is a well-studied martian meteorite with at least 4 different lithologies: Type A (fine grained basalt with small mafic inclusions), Type B (coarser grained, sub-ophitic textured basalt), Type C (shock-melted glass and thin glass veins), and Type X (small mafic inclusions) (NASA, 2017b).

Trapped gas in the shock-melted glass closely correlated to measurements of the martian atmosphere made by the Viking landers, confirming the origin of this meteorite (Bogard and Johnson, 1983, Becker and Pepin, 1984).

Within Type C lithology are white crystals composed of calcite and phosphate. The crystals are enriched in Mg, which is either in the calcite or in the phosphate. There is also a Ca-sulfate mineral present, perhaps gypsum (Gooding and Muenow, 1986). Stable isotope values of this alteration product have been measured, as shown in Table 3-2 (Wright et al., 1988, Clayton and Mayeda, 1988, Jull et al., 1992). Original studies suggested the druse is of martian origin (Gooding and Muenow, 1986, Gooding et al., 1988). First, the petrology suggested the "white druse" is martian since the alteration crystals are in the same lithology as the melted glass containing trapped martian atmospheric gas. Second, the oxygen isotope composition was much different than what would be expected from terrestrial weathering products in Antarctica where the ice typically has a $\delta^{18}O_{water}$ = -35‰ (Dansgaard, 1964), which would create an aqueous equilibrium carbonate with $\delta^{18}O_{carbonate}$ = -5‰ to 0‰ at expected near-freezing temperatures (Chacko et al., 1991). However, subsequent studies of the stable isotope values of nesquehonite on LEW-85320 caused one author to ponder that "carbon and

oxygen isotopic compositions can no longer be considered diagnostic of a [EET 79001 carbonate] pre-terrestrial origin" (Grady et al., 1989).

Year	Authors	White Druse	$\delta^{13}C$ (‰)	$\delta^{18}O$ (‰)
1988	Clayton Mayeda	EETA 79001	9.7	21.0
1988	Wright et al.	EETA 79001	6.8	21.1
1992	Jull et al.	EETA 79001	3.1	20.0

Table 3-2: Stable Isotope Values for White Druse on EET 79001

Weathering Studies of Antarctic Meteorites

Weathering of meteorites in Antarctica can include oxidation, hydration, hydrolysis, solution and carbonation. Oxidation of Fe in metal sulfides and ferrous silicates of OCs is the most common alteration process (Bland et al., 2006). Deposition of white powder (mostly hydrous carbonates) on the surface of meteorites is the second most common form of weathering (Velbel, 1988). This loosely bound carbonate or bicarbonate has been characterized with a $\delta^{13}C = 0 \pm 5‰$ (Swart et al., 1983). Small thin films of water, even if they are only intermittent, in terrestrial microenvironments weather OCs similar to "the role water plays in other terrestrial weathering environments" (Velbel, 2014). Specifically,

> "Terrestrial oxidation of meteoritic sulfides produces sulfuric acid that reacts with anhydrous meteoritic Mg-silicates (e.g., olivine). The acid anion, sulfate, can combine with any cation released by weathering of primary minerals or glass and become incorporated into evaporite minerals occurring as veins or efflorescences such as those long and widely recognized on finds".

This acidification/deposition process could explain how terrestrial, secondary minerals can be found along fractures and seams within meteorites.

A petrographic analysis of Antarctic weathering products (Hallis, 2013), compared two MIL martian Nakhlites (MIL 03346, MIL 090032) to two terrestrial rock samples (MIL 0503, EET 96400). The two terrestrial rocks were collected by the ANSMET team and curated as meteorites, but analysis revealed they were not meteorites. All of the samples contained secondary minerals on externally exposed surfaces including sulfates and iddingsite. Neither of the terrestrial rock samples contained primary sulfur minerals, hence the sulfate source must be wind-blown sea spray and biogenic emissions from the Southern Ocean. Sea spray contributes K, Na, and Ca ions in the secondary assemblages, and also increases the Cl content in iddingsite; however, interior iddingsite in MIL Nakhlites and jarosite within MIL 090136 melt inclusions are likely pre-terrestrial in origin. Sea spray is likely not the source of nesquehonite found on LEW 85320, since it continues to grow in the dry, nitrogen environment while curated at NASA/JSC (Grady et al., 1989). Surface calcite coatings on Antarctic rocks are rare, but those from the Wright Dry Valley region reflect a range of stable isotope values, even on the same rock, with $\delta^{13}C$ from -4.4‰ to +17.6‰, and $\delta^{18}O$ from +0.4‰ to +22.3‰ (Grady et al., 1989).

It is unlikely the sea spray contributes greatly to the creation of terrestrial carbonates on the OC meteorites, but it could be a more significant factor in the creation of terrestrial sulfates. Sea spray deposition has been recorded 1100 km from the coastline on the East Antarctic Plateau (Udisti et al., 2012), which is further inland than

either the Miller Range (MIL) or Elephant Moraine (EET) regions of the Transantarctic Mountains. Halite is also reported far from the coast in dry valley soils (Wentworth et al., 2005). The sea spray sulfates are likely produced predominantly by phytoplankton blooms (Kaufmann et al., 2010).

Carbonate Fractionation Factors

Carbonate precipitation requires that rocks interact with water. The carbonates form in the following process (Morse and Mackenzie, 1990):

$$CO_2\ (g) \leftrightarrow CO_2\ (aq) \qquad \text{eq. 3-1}$$

$$CO_2\ (aq) + H_2O \leftrightarrow H_2CO_3 \qquad \text{eq. 3-2}$$

$$H_2CO_3 \leftrightarrow HCO_3^- + H^+ \qquad \text{eq. 3-3}$$

$$HCO_3^- \leftrightarrow CO_3^{2-} + H^+ \qquad \text{eq. 3-4}$$

$$Ca^{2+}/Fe^{2+}/Mg^{2+} + CO_3^{2-} \leftrightarrow \text{carbonate} \qquad \text{eq. 3-5}$$

The fluid pH drives the distribution of species given in equations 3-2, 3-3 and 3-4, with high pH dominated by CO_3^{2-} and low pH dominated by CO_2 (aq).

Fractionation of oxygen and carbon isotopes happen between the reactants and the products of each equation. Fractionation factors are calculated theoretically or also measured in laboratory experiments, however, the variation in fractionation factors creates an uncertainty in predicted carbonate stable isotope values of 2-5‰ at low temperatures <25°C, especially when the extracted CO_2 is from non-calcite species.

The kinetic fractionation of $\delta^{13}C$ in CO_2 from atmosphere to seawater for eq. 3-1 has been documented as -2.4‰ ± 2‰ (Wanninkhof, 1985) favoring ^{12}C kinetically.

Isotope studies report nearly identical $\delta^{18}O$ fractionation factors from either the atmospheric CO_2 (g) or the fluid CO_2 (aq) to calcite. The predicted $1000\ln\alpha$ for calcite to CO_2 (g) is 42.23‰ at 15°C (Bottinga, 1968, Friedman, 1977), and the measured $1000\ln\alpha$ for calcite to CO_2 (aq) is 42.43‰ at 15°C (Beck et al., 2005).

Theoretical fractionation factors based upon isotopic partition functions were first calculated by Urey (1947). These results were then modified by McCrea (1950) and Bottinga (1968). Subsequently, Chacko (1991) measured calcite exchange with CO_2 at temperatures from 400-950°C and pressures from 1-13 kilobars, then calculated calcite partition function ratios for a temperature range from 273°K to 4000°K. The Chacko study provides both $\delta^{13}C$ and $\delta^{18}O$ calcite fractionation factors. Many older calcite fractionation studies have been collected and documented as a reference guide (Friedman and O'Neil, 1977).

A theoretical study using a physical lattice model to identify reduction partition function ratios for various carbonates demonstrates that calcite may fractionate significantly less than the other carbonates, as seen in Figure 3-1 (Golyshev et al., 1981).

A study of carbon isotope fractionation properties of silicate melts using computations of reduction partition functions predicted differences between calcite and aragonite, Mg-calcite, and dolomite (Deines 2004), and Figure 3-2 demonstrates the impact on $\delta^{13}C$ fractionation for magnesium (Mg) content in calcite. Generally, the calcite fractionates more as Mg content increases.

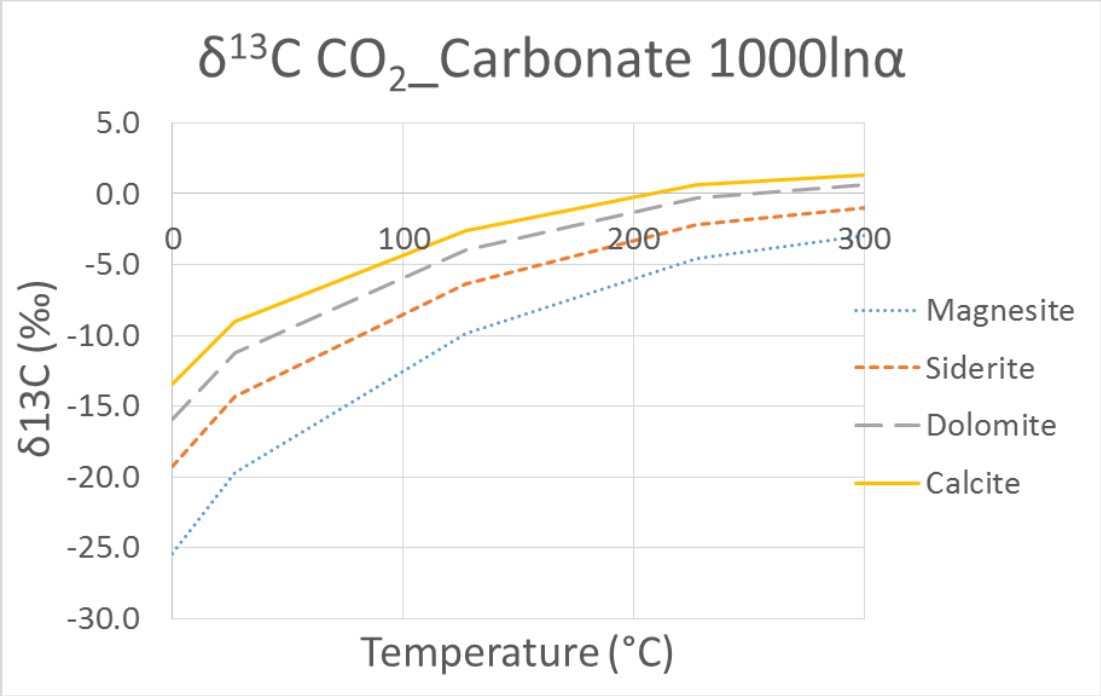

Figure 3-1: $\delta^{13}C$ Fractionation by Carbonate Species (data from Golyshev, 1981)

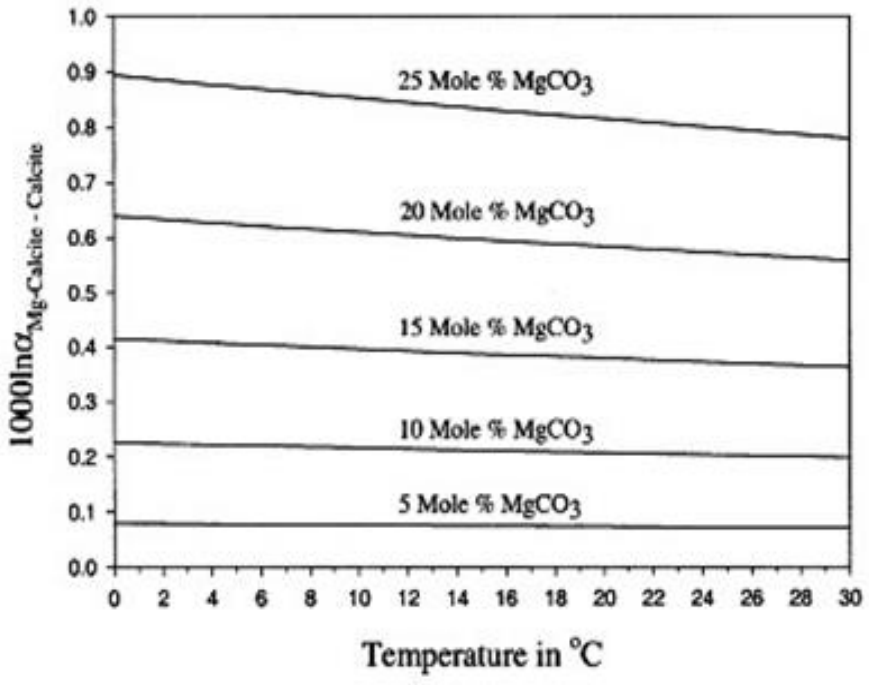

Figure 3-2: $\delta^{13}C$ Fractionation for Mg Content in Calcite (reprinted from Deines, 2004)

Published laboratory carbonate fractionation studies near 0°C are rare. One study used an open-system chemostat technique to produce $\delta^{13}C$ fractionation factors between CO_2 (g) and calcite and aragonite (Romanek et al., 1992). A comparison of these $\delta^{13}C$ results compared to the theoretical studies is given in Figure 3-3, which shows that there is 2-3‰ variation in predicted fractionation of calcite $\delta^{13}C$ at low temperatures.

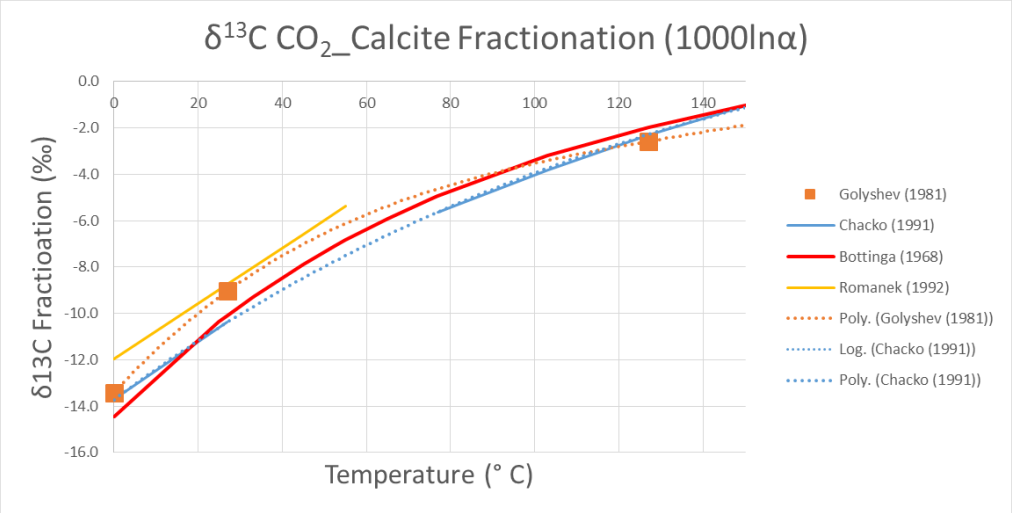

Figure 3-3: $\delta^{13}C$ Fractionation between CO_2 and Calcite

One laboratory study measuring fractionation of phosphoric acid extracted CO_2 from siderite at 33°C to 197°C (Carothers, 1988). This study provides $\delta^{13}C$ fractionation values between siderite and CO_2, and also $\delta^{18}O$ fractionation values between siderite and water. A subsequent study of biogenic siderite from mesophilic and thermophilic iron-reducing bacteria) at 45°C to 75°C measured the $\delta^{13}C$ fractionation between CO_2 (g) and siderite, and created a temperature equation for predicting $\delta^{18}O$ fractionation values to

water (Zhang, 2001). Inorganic siderite was precipitated and studied at 25°C with another study using the chemo-state technique (Jimenez-Lopez and Romanek, 2004). A comparison of the difference in $\delta^{13}C$ fractionation studies is shown in shown in Figure 3-4. Again the calcite fractionates less (~5‰) than the siderite at low temperature.

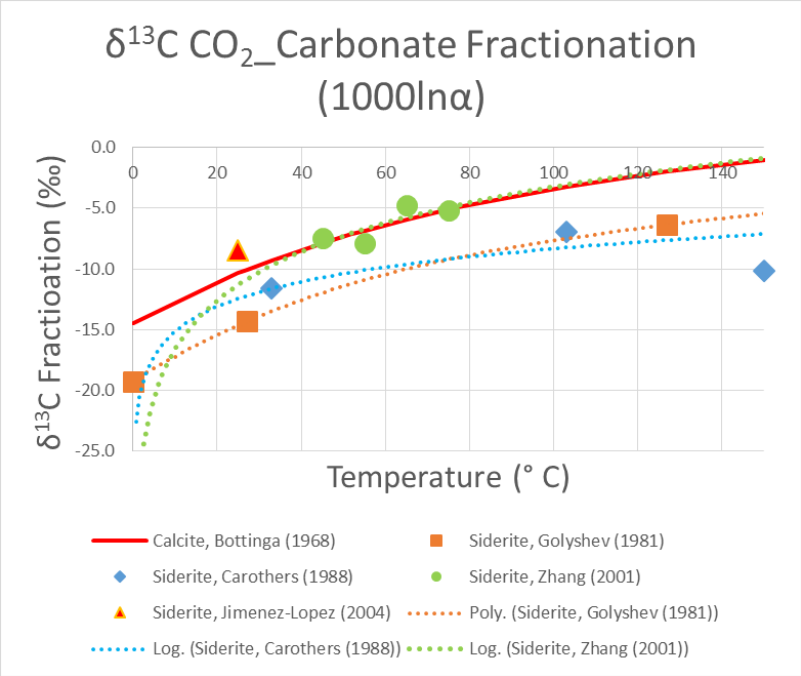

Figure 3-4: $\delta^{13}C$ Fractionation between CO_2 and Calcite or Siderite

A comparison of older acid extraction studies for CO_2 to carbonate $\delta^{18}O$ fractionation factors (given as 1000lnα) is shown in Table 3-3 (data from Rosenbaum and Sheppard, 1986). The difference in $\delta^{18}O$ fractionation between theoretical calcite and siderite, along with more recent siderite laboratory studies, is shown in Figure 3-5. As with the $\delta^{13}C$, the calcite $\delta^{18}O$ fractionates less (~5‰) than the siderite at low temperature.

For magnesite, one laboratory study reported the $\delta^{18}O$ fractionation with water at 25°C, with both a high-Mg and low-Mg experiment (Jimenez-Lopez, et al., 2004). Both magnesites fractionate more than the pure calcite.

	Carbonate	α (25°C)	CO_2: 1000lnα	Study
	Calcite	1.01163	11.56	Rosenbaum & Sheppard (1986)
*	Calcite	1.01025	10.2	Sharma and Clayton (1965)
	Calcite	1.0105	10.52	Land (1980)
*	Dolomite	1.0111	11.04	Sharma and Clayton (1965)
*	Dolomite	1.01169	11.62	Land (1980)
*	Ankerite	1.01098	10.92	Becker (1971)
*	Siderite	1.01169	11.62	Becker and Clayton (1976)
* Composition of carbonate not given				

Table 3-3: $\delta^{18}O$ Fractionation Factors between CO_2 and Calcite or Siderite (data from Rosenbaum and Sheppard, 1986)

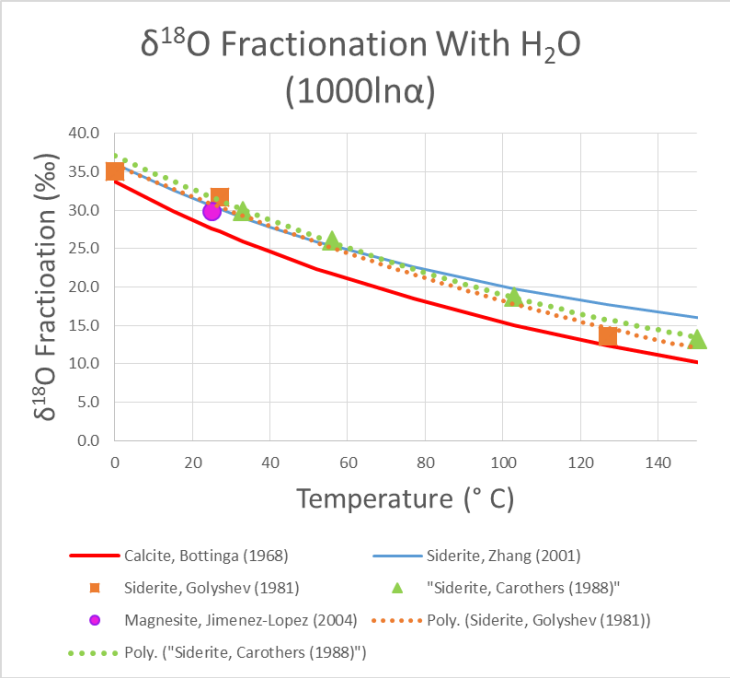

Figure 3-5: $\delta^{18}O$ Fractionation between H_2O and Calcite or Siderite

Stable Isotope Studies of OC Carbonates

Using stable isotope fractionation values for carbonates, calculations can be made to predict either the carbonate stable isotope values, based on known environmental source isotopic values, or (given the carbonate values) the stable isotope values of environmental formation conditions (meteoric water or atmospheric CO_2).

Grady (1989) Study of LEW 85320

The Grady study on LEW 85320 (Grady et al., 1989) employed calcite fractionation factors for the stable isotope fractionation between carbonate and water (Bottinga, 1968, Friedman and O'Neil, 1977). Grady assumed terrestrial carbon and oxygen values for atmospheric CO_2 ($\delta^{13}C$ = -7.5‰, $\delta^{18}O$ = +41‰) to model the carbonate formation. The resulting modeled temperature for carbonate formation, based on $\delta^{13}C$, in Antarctica was -2°C (±4°C), while the temperature for carbonates formed in the Texas curation facility was +16°C (±4°C). The modeled temperatures using $\delta^{18}O$ gave unrealistic results, indicating that the nesquehonite is most likely not in equilibrium with atmospheric CO_2.

From the measured carbonates values, Grady used fractionation factors to calculate a predicted $\delta^{18}O_{meltwater}$ if the meltwater was in equilibrium with the carbonate. The resulting $\delta^{18}O_{meltwater}$ = -17.0‰ to -19.6‰, which is much heavier than the actual Antarctic $\delta^{18}O_{meltwater}$ < -40‰. Grady speculated the oxygen in meltwater exchanges isotopically with silicates in the meteorite.

Next, Grady used the fractionation factors to calculate a predicted $\delta^{18}O_{meltwater}$ if the atmospheric water vapor was in equilibrium with the carbonate. The resulting $\delta^{18}O_{meltwater}$ = -28‰ (also heavier than the Antarctic meltwater). Grady concluded the carbonate must be forming in interactions between meltwater and a heavier oxygen reservoir.

Karlsson (1991) Study of OCs

Another study (Karlsson et al., 1991) compared carbonates from 16 OCs (given as circles in Figure 3-6) to terrestrial Antarctic carbonates (given as boxes in Figure 3-6) and found them indistinguishable isotopically. The authors employed Bottinga calcite fractionation factors (Bottinga, 1968) to conclude the expected $\delta^{13}C$ carbonate values are too heavy for equilibrium with Earth atmospheric CO_2 at 0°C, although they match closely to a formation temperature of 30°C. Regarding $\delta^{18}O$, the authors conclude the wide variation in values is likely from oxygen reservoir mixing between ice melt water ($\delta^{18}O_{SMOW}$ = -37‰) and atmospheric CO_2 ($\delta^{18}O_{SMOW}$ = +41‰). An alternate explanation is the carbonate formed from enriched melt water (from evaporation).

Methodology

Ordinary Chondrite (OC) meteorites were selected from the online NASA ANSMET collection (NASA, 2017b), which contained 16,100 records in the summer of 2013. From this resource, meteorites were selected from regions of Antarctica where martian Nakhlites were collected (MIL, RBT, ALH, EET). The criteria further narrowed

the meteorites to types H4-H6, L4-L6 or LL4-LL6 (no pre-terrestrial aqueous alteration), with mass greater than 10 grams (to provide sufficient sample size), containing external

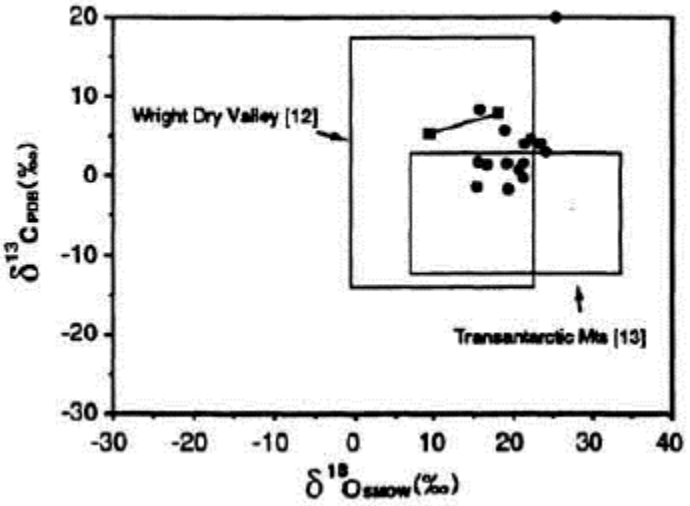

Figure 3-6: Antarctic Carbonates in Rocks and Meteorites (Reprinted from Karlsson et al., 1991)

evaporite deposits (as defined by type "e" with visible white residue on the fusion crust when the meteorite was collected from Antarctica), and collected after 2000 (in order to limit exposure time to the N_2 environment of curation at NASA/JSC). (see discussion of meteorite petrology and weathering types in Chapter 1). The result was a request to the NASA Meteorite Working Group (MWG) dated 8/13/13 for 32 samples (including one for LEW 85320 to repeat the curation nesquehonite study) (see Appendix D).

From the MWG request of 8/13/13, 10 meteorites (divided in 17 samples) were analyzed. The samples were gently crushed and sieved to a size of <700 µm, acidified,

reacted, and extracted to collect CO_2 cryogenically using standard techniques (McCrea, 1950, Al-Aasm et al., 1990, Shaheen et al., 2015).

Samples of ~0.5 g were reacted with 0.7-2.0 ml of 100% H_3PO_4 at 30°C and 150°C. The CO_2 was extracted after three different steps: 1) Rx0 after 1 hour at 30°C; 2) Rx1 after 18 hours at 30°C, and 3) Rx2 after 3 hours at 150°C. The CO_2 was then separated from other condensable gases using a TRACE GC with a Restek HayeSep Q 80/100 6' 2mm stainless column. A description of the design, installation, testing, and validation of the carbonate extraction and measurement system is found in Chapter 2. Based on repeat analysis of standards, the calculated uncertainties for these measurements are $\delta^{13}C = \pm 0.76‰$, $\delta^{18}O = \pm 1.58‰$.

Results

A table of average OC carbonate results is provided in Table 3-4 (note "Ca-rich" carbonates are averages for the Rx0 and Rx1 reactions combined).

OC Carbonates					
	d13C	**stdev (1σ)**	**d18O**	**stdev (1σ)**	**count**
Rx0	4.26	1.90	19.53	4.41	13
Rx1	4.17	1.65	17.40	3.74	15
Rx2**	2.80	1.05	8.75	2.67	11
RBT Ca-rich*	3.89	2.31	20.75	5.52	6
ALH Ca-rich*	5.06	0.60	16.58	3.74	12
MIL Ca-rich*	3.40	1.97	19.14	2.92	10

*"Ca-rich" means Rx0+Rx1

** Excluding ALH 77215, 7/30/15 Tube #380

Table 3-4: Summary of Average OC Carbonate Results

The OC carbonate results are shown in Figure 3-7. It is clear that this stepped extraction process identifies two distinct carbonate species within the OC carbonates. Variability in the results suggest there is much OC terrestrial carbonate heterogeneity (even within the same meteorite); however, some broad observations can be made.

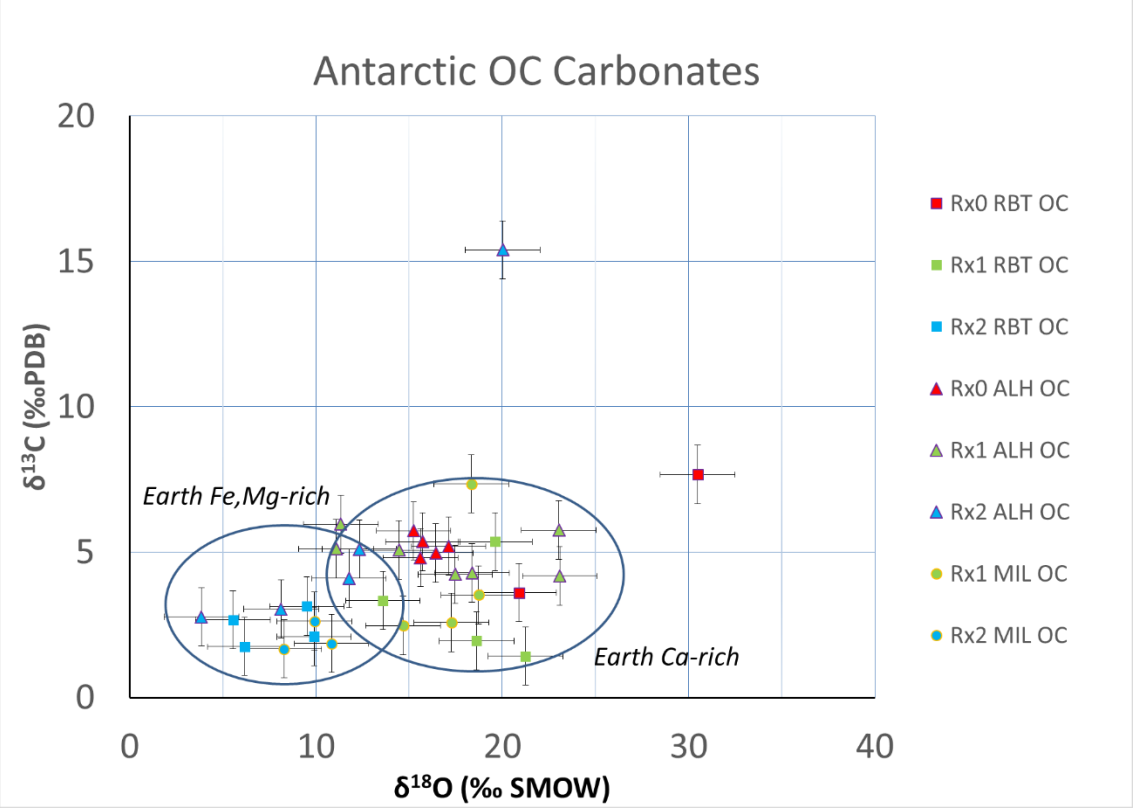

Figure 3-7: Summary of OC Carbonate Results

The Rx0 and Rx1 (low temperature, 30°C) extractions produce CO_2 from Ca-rich carbonates. Based on experiments with carbonate standards (as discussed in Chapter 2), these reactions at 30°C should completely consume the Ca-rich carbonates.

There is wide variability in the $\delta^{18}O$ values for carbonates, ranging from +11.1‰ to +30.5‰. The $\delta^{13}C$ values are somewhat more consistent, ranging from +1.4‰ to +7.7‰ with Ca-rich carbonates grouping between +3‰ to +6‰. Generally, the $\delta^{13}C$ for Rx0 and Rx1 is similar at approximately +4.2‰.

Carbonate Results by Reaction

The Ca-rich carbonates (average of all results from 30°C, Rx0 and Rx1) show a composition distinct from the Fe/Mg-rich group (150°C, Rx2) , as seen in Figure 3-8 (displayed error bars are based on 1σ standard deviation of corrected measurements).

Generally, Rx0 (1 hour) produces $\delta^{18}O$ = +19.53‰ ± 4.41‰ (1σ standard deviation on data), compared to Rx1 (18 hour) $\delta^{18}O$= +17.40 ± 3.74‰ (1σ standard deviation on data), which is ~2‰ heavier. This could be based upon differences in grain size of the Ca-rich carbonates, with the fine grains dissolved first (1 hr) and the coarse grains dissolved more slowly (18 hr). The Rx2 reaction average (Table 3-4) excludes the anomalous data point for ALH 77215, 7/30/15 Tube #380.

The Rx2 high temperature extraction (150°C) produces CO_2 from a different species of carbonate (not Ca-rich). This carbonate is likely either Fe-rich or Mg-rich (it is not possible to identify the cation from stable isotope analysis). This is the first study to identify a distinct Fe-/Mg-rich carbonate population in these meteorites. The Rx2 results suggest the stable isotope values of this carbonate species are independent of region where the OC was collected. The averages for the Rx2 group are

$\delta^{13}C$ = +2.8‰ ± 1.0 ‰ (1σ standard deviation of corrected values), $\delta^{18}O$ = +8.8‰ ± 2.7‰ (1σ standard deviation of corrected values).

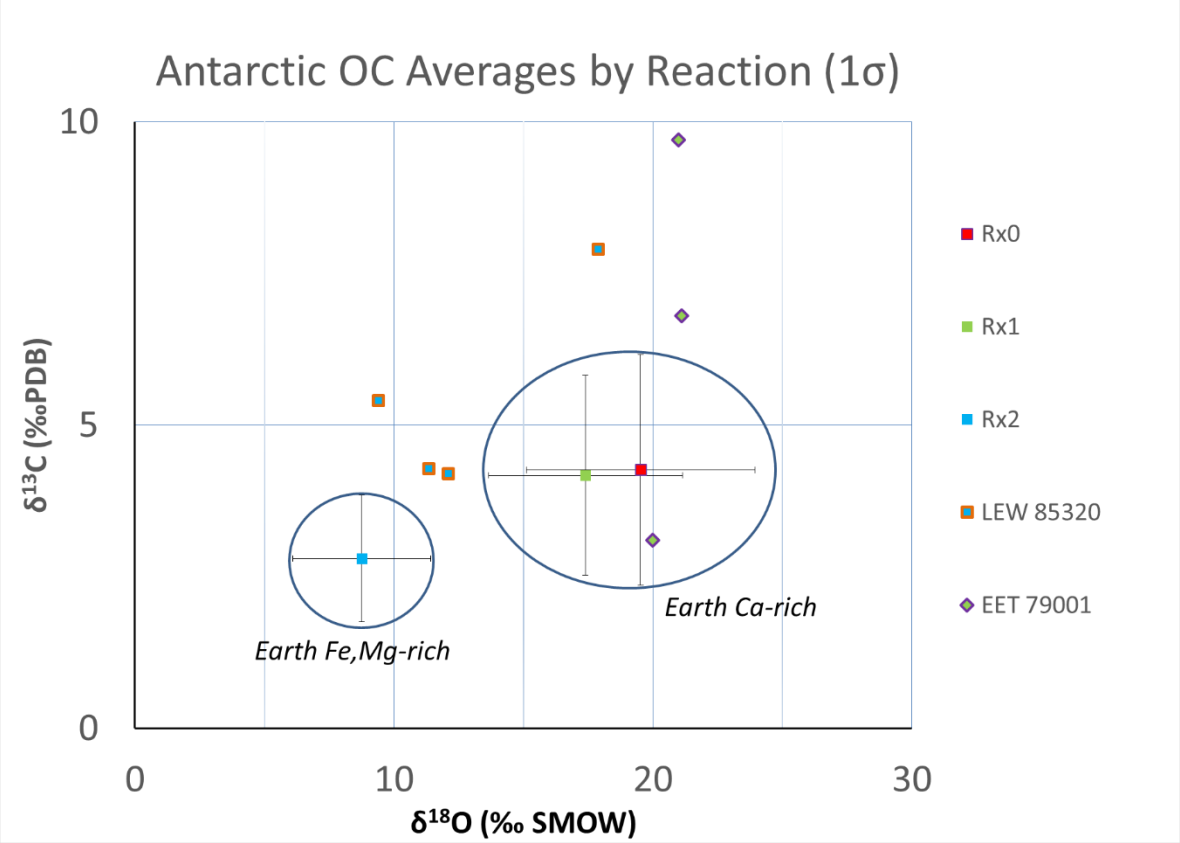

Figure 3-8: OC Carbonate Results by Reaction

Carbonate Results by Region

The OC Ca-rich carbonate results can be averaged by Antarctic collection region. The Fe/Mg-rich results (Rx2) are consistent regardless of region, but the Ca-rich results (Rx0, Rx1) indicate a slight variation based upon where the meteorite resided, as seen in Figure 3-9 (error bars based on 1σ standard deviation of corrected measurements). The

Ca-rich carbonates are similar in regions RBT and MIL, but a slight regional difference can be detected in ALH. The average ALH Rx0/Rx1 average is approximately $\delta^{13}C$ = 1.4‰, or heavier than the average for Ca-rich RBT and MIL. Compared to RBT and MIL, the ALH Ca-rich $\delta^{18}O$ = -3.4‰, or lighter. Regional effects could be due to differences in the availability of sea spray ions, altitude, temperature of carbonate formation, variance in the meteoric water enrichment due to local evaporation, or other unknown glacial impacts. The Rx2 reaction average (Table 3-4) excludes the anomalous data point for ALH 77215, 7/30/15 Tube #380.

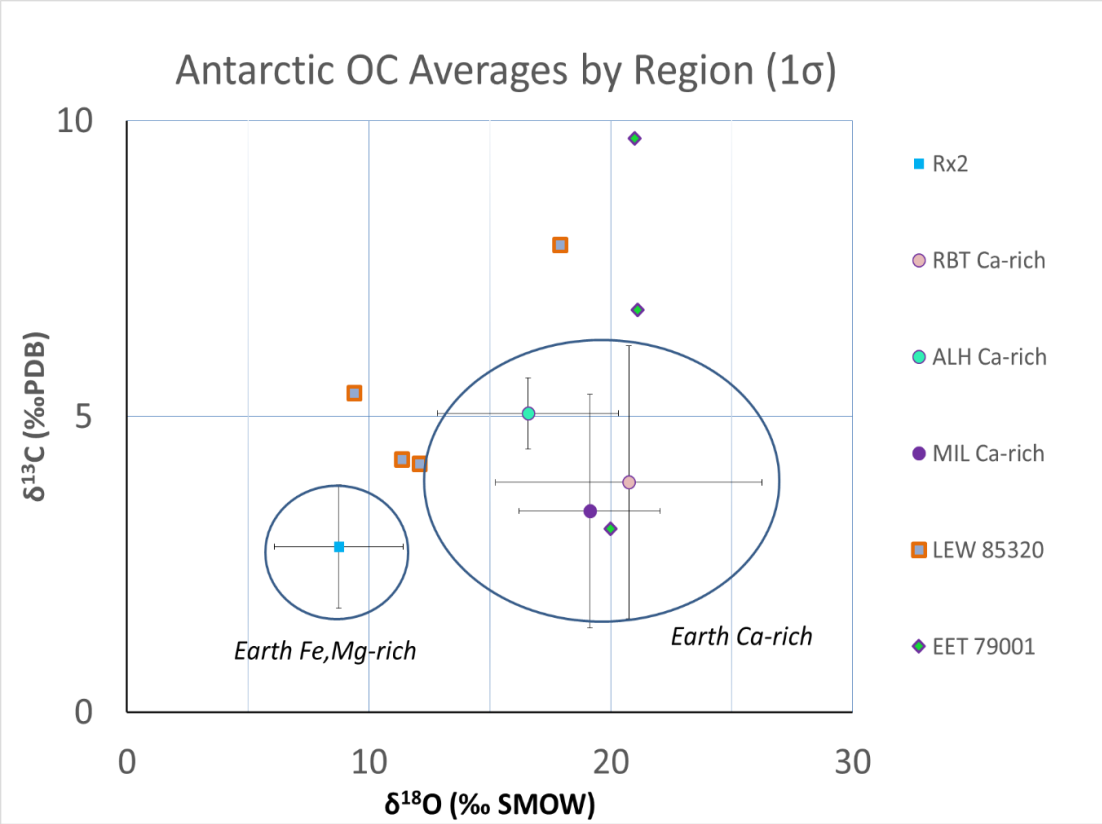

Figure 3-9: OC Carbonate Results by Region

For all results, the stable isotope values were measured and corrected with the appropriate β_{ins} (eq. 2-10) which is calculated by a measurement on repeat carbonate standards that accounts for cumulative fractionation effects introduced during analysis. This includes fractionations created during acid dissolution of the carbonate, as well as small instrumental effects. An additional GC/transfer fractionation offset (eq. 2-11) is applied to account for additional fractionations derived from GC purification steps and is derived from analysis of a standard carbonate mixed with basaltic sand (dataset HIBBs_1). A correlation between GC CO_2 peak and CO_2 sample size, based upon datasets HIBBs_1 and HIBBs_2, is given in eq. 2-12. This correlation provides the estimate of CO_2 sample size. Small CO_2 samples (< 5 μmole) are corrected with offsets based upon dataset HIBBs_2 and calculated in eq. 2-13. All result data tables are color-coded as follows:

- Purple indicates contamination introduced inside the IRMS, which can be identified by R^2 values > 0.5. These were caused by isobaric interferences and these data are discarded from future consideration.
- Orange indicates a small, but acceptable IRMS CO_2 sample size, with the left bellow at 100% expansion measuring < 100 mV.
- Red indicates a IRMS CO_2 sample size too small for accurate analysis, with the left bellow at 100% expansion measuring < 5 mV. These data are discarded from future consideration

Table 3-5 displays the data and corrected results for OCs collected in the Antarctic RBT region, Table 3-6 displays the same for the Antarctic ALH region, and Table 3-7 displays the same for the Antarctic MIL region.

Offset Used	HIBBs_1	HIBBs_1	HIBBs_1	HIBBs_1	HIBBs_1	HIBBs_1
Date	7/6/15	7/7/15	7/23/15	7/23/2015	07/28/15	07/28/15
Meteorite	RBT04298	RBT04298	RBT04298	RBT04298	RBT04149	RBT04149
Type	LL5	LL5	LL5	LL5	H6	H6
Sample Tube (ST)	381	375	25	211	55	25
total wt (µg)	499006	449013	255713	266415	362263	344255
Rx0 FT Pressure (mb)	19.60	0.88	21.36	11.18	3.14	2.00
Rx0 CO2 Peak time			3.83	3.80	3.89	3.90
Rx0 CO2 Peak count			1.3E+06	1.3E+06	7.8E+05	0.0E+00
Rx0 Organic Peak time			17.02	17.69	n/a	n/a
Rx0 Organic Peak count			8.0E+05	3.5E+05	n/a	n/a
Rx0 L100% Signal "clean"			160	155	113	124
Rx0 Correct d13C "clean"			3.126			7.669
Rx0 Correct d18O "clean"			20.901			30.491
Rx0 "clean" R^2 IRMS			0.340	0.685	0.602	0.067
Rx1 FT Pressure (mb)		143.42	129.40	129.56	25.50	17.93
Rx1 CO2 Peak time		3.51	3.75	3.79	3.73	3.77
Rx1 CO2 Peak count		5.4E+06	2.4E+06	2.4E+06	3.1E+06	2.4E+06
Rx1 Organic Peak time		13.78	13.69	13.73	17.25	17.55
Rx1 Organic Peak count		3.5E+06	3.5E+06	3.5E+06	6.0E+04	5.0E+05
Rx1 L100% signal "clean"		1370	320	310	417	407
Rx1 Correct d13C "clean"			1.886	1.361	3.328	5.278
Rx1 Correct d18O "clean"			18.621	21.251	13.593	19.620
Rx1 "clean" R^2 IRMS		0.076	0.072	0.054	0.157	0.028
Rx2 FT Pressure (mb)	22.35	>150	125.64	142.30	130.34	>150
Rx2 CO2 Peak time		3.77	3.82	3.78	3.74	3.69
Rx2 CO2 Peak count		0.0E+00	1.9E+06	1.5E+06	2.8E+06	3.5E+06
Rx2 Organic Peak time		13.45	13.76	13.42	13.75	13.46
Rx2 Organic Peak count		0.0E+00	3.5E+06	3.9E+06	3.5E+06	3.9E+06
Rx2 L100% signal "clean"		268	188	184	337	514
Rx2 Correct d13C "clean"			2.917	1.708	1.798	2.670
Rx2 Correct d18O "clean"			9.514	9.901	6.171	5.545
Rx2 "clean" R^2 IRMS		0.963	0.286	0.457	0.194	0.164
GC peak to sample size						
Basis	HIBBs_2,3	HIBBs_2,3	HIBBs_2,3	HIBBs_2,3	HIBBs_2,3	HIBBs_2,3
Rx0 µm CO2 (Calcite)			2.04	2.04	1.19	0.00
Rx1 µm CO2 (Calcite)			3.96	3.96	5.28	3.87
Rx2 µm CO2 (Sid or Mag)			3.06	2.37	4.70	6.06
Sample µm CO2	0.00		9.06	8.37	11.17	9.93
%carb (assume calcite)	0.000%	0.000%	0.355%	0.314%	0.309%	0.289%
Sample Size Offset						
Basis	HIBBs_2	HIBBs_2	HIBBs_2	HIBBs_2	HIBBs_2	HIBBs_2
Rx0 d13C			0.480	0.480	0.818	
Rx1 d13C			0.060	0.060		0.075
Rx2 d13C			0.222	0.383	-0.048	
FINAL VALUE (Offset, small)						
Rx0 d13C			3.61			7.67
Rx0 d18O			20.90			30.49
Rx1 d13C			1.95	1.42	3.33	5.35
Rx1 d18O			18.62	21.25	13.59	19.62
Rx2 d13C			3.14	2.09	1.75	2.67
Rx2 d18O			9.51	9.90	6.17	5.54

Table 3-5: RBT OC Carbonate Values

Offset Used	HIBBs_1	HIBBs_1	HIBBs_1	HIBBs_1	HIBBs_1	HIBBs_1	HIBBs_1	HIBBs_1	HIBBs_1	HIBBs_1
Date	08/03/15	08/03/15	07/30/15	07/30/15	08/10/15	08/10/15	8/6/15	8/6/15	4/11/16	4/11/16
Meteorite	ALH77214	ALH77214	ALH77215	ALH77215	ALH77215	ALH77215	ALH77299	ALH77299	ALH 77294	ALH 77294
Type	L3.4	L3.4	L3.8	L3.8	L3.8	L3.8	H3.7	H3.7	H5	H5
Sample Tube (ST)	25	55	380	211	375	381	211	380	211	380
total wt (µg)	556010	471442	343948	396985	479736	499130	500413	504679	510214	520291
Rx0 FT Pressure (mb)	16.27	28.98	4.35	13.45	59.56	41.55	86.28	97.40	86.28	116.77
Rx0 CO2 Peak time	3.78	3.72	3.98	3.90	3.89	3.76	3.60	3.56	0.00	3.65
Rx0 CO2 Peak count	2.1E+06	2.8E+06	5.0E+04	1.0E+05	3.4E+05	2.8E+05	4.60E+06	5.10E+06	0.00E+00	2.30E+06
Rx0 Organic Peak time	17.60	16.90	18.02	17.20	15.22	15.58	15.1	14.85	0	13.53
Rx0 Organic Peak count	5.0E+05	9.0E+05	2.3E+05	6.6E+05	2.1E+06	1.7E+06	2.50E+06	2.40E+06	0.00E+00	3.40E+06
Rx0 L100% Signal "clean"	336	578	6	9		38	961	1287		150
Rx0 Correct d13C "clean"	5.581	5.401					4.805	4.970		5.111
Rx0 Correct d18O "clean"	15.241	15.724					15.612	16.430		17.126
Rx0 "clean" R^2 IRMS	0.083	0.064	0.787	0.965		0.584	0.000	0.092		0.438
Rx1 FT Pressure (mb)	53.78	110.71	107.50	135.60	>150	>150	>150	>150	>150	>150
Rx1 CO2 Peak time	3.41	3.57	3.95	3.93	3.86	3.93	3.64	3.58	3.54	3.54
Rx1 CO2 Peak count	4.9E+06	4.6E+06	2.0E+05	2.0E+05	6.8E+05	4.5E+05	4.00E+06	4.60E+06	1.03E+06	8.70E+05
Rx1 Organic Peak time	16.28	14.40	14.04	13.50	11.53	12.46	13.1	12.22	12.86	12.46
Rx1 Organic Peak count	1.3E+06	2.9E+06	3.2E+06	3.8E+06	6.4E+06	5.1E+06	4.20E+06	5.40E+06	3.85E+06	4.30E+06
Rx1 L100% signal "clean"	636	530	53	41	110	73	946	1001	100	85
Rx1 Correct d13C "clean"	5.113	5.962			3.272	4.582		5.070	3.596	3.538
Rx1 Correct d18O "clean"	11.081	11.334			23.085	23.036		14.452	17.477	18.371
Rx1 "clean" R^2 IRMS	0.060	0.155	0.629	0.682	0.012	0.392	0.686	0.352	0.324	0.020
Rx2 FT Pressure (mb)	>150	>150	>150	>150	>150	>150	>150	>150	>150	>150
Rx2 CO2 Peak time	3.60	3.66	3.92	3.87	3.88	3.89	3.67	3.69	3.74	3.46
Rx2 CO2 Peak count	4.4E+06	3.2E+06	4.0E+05	4.0E+05	7.1E+05	6.4E+05	3.30E+06	3.50E+06	9.40E+05	1.08E+06
Rx2 Organic Peak time	11.64	10.82	12.00	12.32	11.10	11.48	11.72	12.02	12.16	11.23
Rx2 Organic Peak count	6.4E+06	7.5E+06	5.6E+06	5.2E+06	7.1E+06	6.4E+06	6.00E+06	5.70E+06	4.95E+06	5.90E+06
Rx2 L100% signal "clean"	856	580	70	48	86	89	672	526	65	55
Rx2 Correct d13C "clean"		3.043	14.142				2.774		3.401	4.496
Rx2 Correct d18O "clean"		8.130	20.023				3.851		11.785	12.335
Rx2 "clean" R^2 IRMS	0.765	0.004	0.298	0.850	0.711	0.974	0.077	0.842	0.171	0.284
GC peak to sample size										
Basis	HIBBs_2,3	HIBBs_2,3	HIBBs_2,3	HIBBs_2,3	HIBBs_2,3	HIBBs_2,3	HIBBs_2,3	HIBBs_2,3	HIBBs_2,3	HIBBs_2,3
Rx0 µm CO2 (Calcite)	3.42	4.70	0.07	0.15	0.51	0.42	8.34	9.44	0.00	3.78
Rx1 µm CO2 (Calcite)	9.00	8.34	0.30	0.30	1.03	0.68	7.08	8.34	1.59	1.34
Rx2 µm CO2 (Sid or Mag)	7.92	5.47	0.60	0.60	1.08	0.97	5.67	6.06	1.45	1.67
Sample µm CO2	20.33	18.52	0.97	1.04	2.62	2.07	21.09	23.85	3.04	6.79
%carb (assume calcite)	0.366%	0.393%	0.028%	0.026%	0.055%	0.041%	0.422%	0.473%	0.060%	0.131%
Sample Size Offset										
Basis	HIBBs_2	HIBBs_2	HIBBs_2	HIBBs_2	HIBBs_2	HIBBs_2	HIBBs_2	HIBBs_2	HIBBs_2	HIBBs_2
Rx0 d13C	0.153	-0.048	2.574	2.135	1.355	1.480				0.090
Rx1 d13C			1.695	1.695	0.907	1.175			0.635	0.746
Rx2 d13C			1.251	1.251	0.879	0.947			0.695	0.603
FINAL VALUE (Offset, small)										
Rx0 d13C	5.73	5.35					4.81	4.97		5.20
Rx0 d18O	15.24	15.72					15.61	16.43		17.13
Rx1 d13C	5.11	5.96			4.18	5.76		5.07	4.23	4.28
Rx1 d18O	11.08	11.33			23.08	23.04		14.45	17.48	18.37
Rx2 d13C		3.04	15.39				2.77		4.10	5.10
Rx2 d18O		8.13	20.02				3.85		11.78	12.33

Table 3-6: ALH OC Carbonate Values

Offset Used	HIBBs_1	HIBBs_1	HIBBs_1	HIBBs_1	HIBBs_1	HIBBs_1	HIBBs_1	HIBBs_1
Date	3/28/16	3/28/16	3/29/16	3/29/16	4/6/16	4/6/16	4/7/16	4/7/16
Meteorite	MIL05001	MIL05001	MIL03338	MIL03338	MIL07005	MIL07005	MIL03429	MIL03429
Type	L5	L5	L5	L5	LL6	LL6	H5	H5
Sample Tube (ST)	375	055	025	381	381	025	055	375
total wt (µg)	424984	486059	448506	615744	503192	511090	505773	516085
Rx0 FT Pressure (mb)		97.2	38.78	38	>150	98.9	27.4	35.86
Rx0 CO2 Peak time		3.58	3.39	3.53	3.76	3.75	3.63	3.57
Rx0 CO2 Peak count		1.20E+06	3.80E+06	3.60E+06	7.30E+05	7.00E+05	3.05E+06	3.75E+06
Rx0 Organic Peak time		13.81	15.86	16.26	11.97	13.81	17.04	16.95
Rx0 Organic Peak count		2.80E+06	1.10E+06	9.00E+05	5.20E+06	3.00E+06	6.00E+05	6.00E+05
Rx0 L100% Signal "clean"		88	396	383	59	50	263	394
Rx0 Correct d13C "clean"		6.004	2.671	3.042	0.598		1.686	2.797
Rx0 Correct d18O "clean"		20.375	17.403	22.596	23.826		16.426	21.725
Rx0 "clean" R^2 IRMS		0.088	0.188	0.072	0.371	0.878	0.082	0.022
Rx1 FT Pressure (mb)	offscale	offscale	71.23	93.62	>150	>150	58.3	43.09
Rx1 CO2 Peak time	3.74	3.74	3.57	3.54	3.53	3.78	3.51	3.53
Rx1 CO2 Peak count	7.80E+05	8.80E+05	2.90E+06	3.40E+06	3.10E+05	4.30E+05	3.65E+06	2.50E+06
Rx1 Organic Peak time	12.21	11.93	15.6	14.16	11.01	10.02	15.16	16.18
Rx1 Organic Peak count	4.80E+06	5.20E+06	2.20E+06	2.60E+06	6.40E+06	8.50E+06	2.00E+06	1.00E+06
Rx1 L100% signal "clean"	49	58	246	186	21	25		271
Rx1 Correct d13C "clean"	6.528		2.547	2.580				3.495
Rx1 Correct d18O "clean"	18.342		14.678	17.268				18.728
Rx1 "clean" R^2 IRMS	0.015		0.030	0.005				0.209
Rx2 FT Pressure (mb)	offscale	offscale	>150	84.34	>150	>150	>150	>150
Rx2 CO2 Peak time	3.75	3.73	3.64	3.71	3.79	3.78	3.67	3.43
Rx2 CO2 Peak count	7.20E+05	7.80E+05	1.55E+06	1.68E+06	4.60E+05	4.30E+05	2.12E+06	2.20E+06
Rx2 Organic Peak time	12.47	12.43	11.05	14.1	10.56	10.02	11.8	12.17
Rx2 Organic Peak count	4.50E+06	4.50E+06	6.40E+06	2.66E+06	7.40E+06	8.50E+06	5.55E+06	4.70E+06
Rx2 L100% signal "clean"	48	473	49	107	30	29	159	185
Rx2 Correct d13C "clean"				1.547			1.521	2.501
Rx2 Correct d18O "clean"				10.846			8.291	9.915
Rx2 "clean" R^2 IRMS	0.584	0.886	0.601	0.035	0.879	0.719	0.112	0.352
GC peak to sample size								
Basis	HIBBs_2,3	HIBBs_2,3	HIBBs_2,3	HIBBs_2,3	HIBBs_2,3	HIBBs_2,3	HIBBs_2,3	HIBBs_2,3
Rx0 µm CO2 (Calcite)	0.00	1.87	6.67	6.26	1.11	1.07	5.18	6.56
Rx1 µm CO2 (Calcite)	1.19	1.35	4.89	5.86	0.46	0.65	6.36	4.14
Rx2 µm CO2 (Sid or Mag)	1.10	1.19	2.46	2.68	0.69	0.65	3.45	3.60
Sample µm CO2	2.29	4.42	14.02	14.80	2.27	2.36	14.99	14.30
%carb (assume calcite)	0.054%	0.091%	0.313%	0.241%	0.045%	0.046%	0.297%	0.277%
Sample Size Offset								
Basis	HIBBs_2	HIBBs_2	HIBBs_2	HIBBs_2	HIBBs_2	HIBBs_2	HIBBs_2	HIBBs_2
Rx0 d13C		0.533			0.861	0.888	-0.109	
Rx1 d13C	0.818	0.739	-0.073		1.415	1.204	-0.239	0.032
Rx2 d13C	0.870	0.818	0.361	0.306	1.161	1.204	0.147	0.121
FINAL VALUE (Offset, small)								
Rx0 d13C		6.54	2.67	3.04	1.46		1.58	2.80
Rx0 d18O		20.37	17.40	22.60	23.83		16.43	21.72
Rx1 d13C	7.35		2.47	2.58				3.53
Rx1 d18O	18.34		14.68	17.27				18.73
Rx2 d13C				1.85			1.67	2.62
Rx2 d18O				10.85			8.29	9.92

Table 3-7: MIL OC Carbonate Values

Discussion

The stable isotope values from this study add to the prior published results for OC carbonates formed in Antarctica. From these new data, $\delta^{13}C$ and $\delta^{18}O$ contribution reservoirs for carbonate formation can be assessed. The graphical results for all completed OC samples is shown in Figure 3-10. Included in the graphic are prior measurements from OC meteorites (Grady et al., 1988, Karlsson et al., 1990, Karlsson et al., 1991), and results for LEW 85320 (Jull et al., 1988, Grady et al., 1989) and EET 79001 (Clayton and Mayeda, 1988, Wright et al., 1988, Jull et al., 1992).

In the prior studies by Grady, OC carbonates were extracted after an 18-hour phosphoric acid reaction (similar to Rx1) and then CO_2 was purified with anhydrous lead ethanoate to solidify H_2S. In the Karlsson study, acidified OC carbonates were extracted after three reactions: 25°C for 1 hr (similar to Rx0), 50°C for 24 hr, and 50°C for 5 days. The Karlsson study results combine all reactions when reporting extracted CO_2 stable isotope values. Prior studies on carbonates from the OC LEW 85320 were made with phosphoric acid extractions of CO_2 (Jull et al., 1988, Grady et al., 1989) and Shergottite EET 79001 (Clayton and Mayeda, 1988, Wright et al., 1988, Jull et al., 1992).

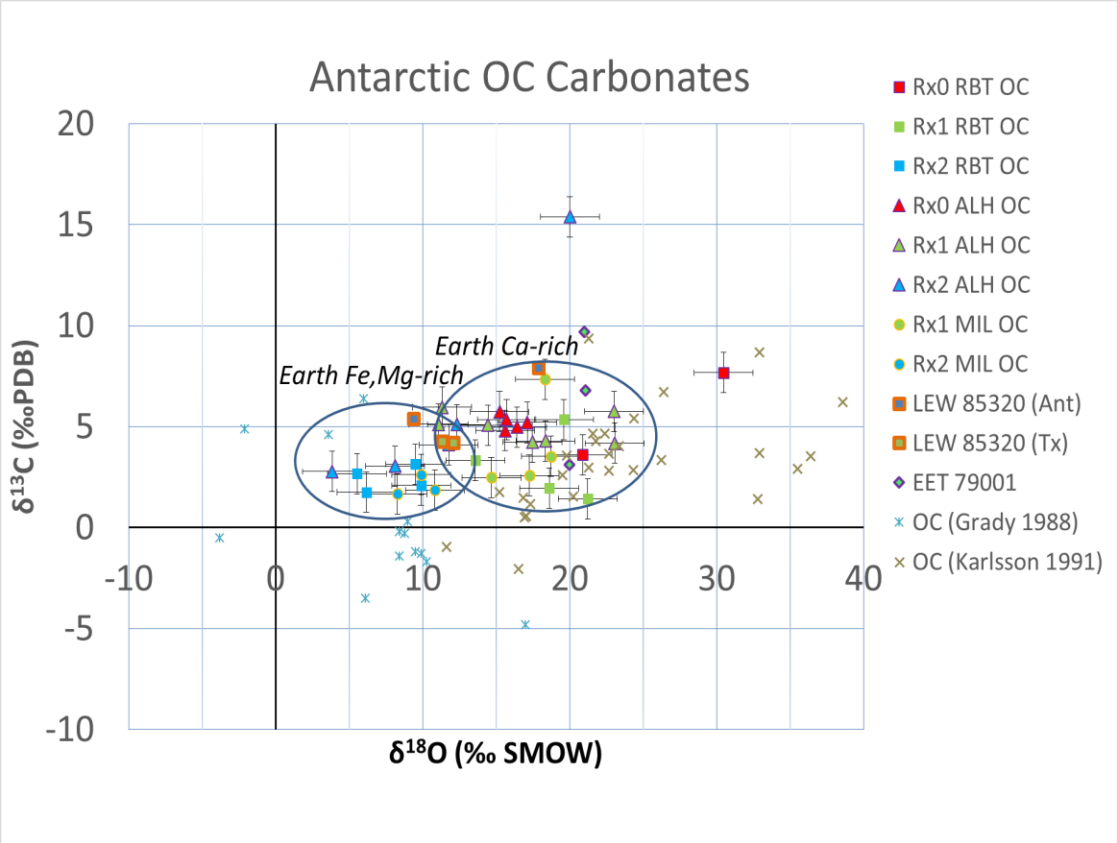

Figure 3-10: Antarctic OC Carbonate Results with Prior Studies

OC Rx2 $\delta^{13}C$ values

The multistep acid extraction procedure measures CO_2 from two different carbonate species. The Fe/Mg-rich (Rx2) carbonates have an average difference of $\delta^{13}C$ = -1.4‰ from the Ca-rich (Rx0/Rx1) carbonates. There are several possible interpretations of the Rx2 data.

The ~1.4‰ difference in $\delta^{13}C$ may represent the constant temperature difference in the carbonate-water fractionation factors between carbon in the atmospheric CO_2 and the carbonate. This interpretation is not consistent with prior, although limited, carbonate fractionation studies (see Figures 3-1, 3-4, and 3-5) that suggest magnesite and

siderite fractionate more in $\delta^{13}C$ and $\delta^{18}O$ than calcite at the same low temperature. If siderite/magnesite fractionates more than calcite at the same temperature, then the expected carbonate $\delta^{13}C$ would be heavier (greater) than the calcite $\delta^{13}C$ values, not lighter (less). The difficulty in evaluating this is complicated by the variability of fractionation factors (up to 2‰) within calcite studies. Not knowing the specific species of carbonate (e.g. magnesite or nesquehonite, which is a hydrated magnesite) complicates the assessment. The $\delta^{13}C$ may simply fall within the error range of this analysis. The consistency of the Rx2 result belies this last conclusion, as shown in Table 3-4 and Figure 3-8. Thus, the Rx2 carbonates are deemed distinct and the $\delta^{13}C$ values might reflect unknown fractionation factors for non-calcite carbonates.

The ~1.4‰ difference in $\delta^{13}C$ might be caused by carbonate species precipitation at different temperatures. Assuming that the Ca-rich and Fe/Mg-rich carbonate fractionation factors are equivalent (which is unlikely true), this represents a difference of approximately +10°C in formation temperature. This suggests that the Fe/Mg-rich carbonates formed in Antarctica at a slightly warmer temperature than the Ca-rich carbonates. Knowing that siderite and magnesite fractionate more than calcite at the same temperature, the Rx2 carbonates may have formed at a much warmer temperature than the Ca-rich carbonates. This could be explained if the Rx2 carbonates formed in the curation facility in Houston, where ambient room temperature for the dry N_2 environmental chamber could be 25°C.

OC Rx2 $\delta^{18}O$ values

The measured average difference in $\delta^{18}O$ between Rx2 and Rx0/Rx1 is approximately -9‰ to -10‰. If the Rx2 carbonates formed at temperatures >10 deg warmer than the Ca-rich carbonates (based on $\delta^{13}C$ interpretation), then the $\delta^{18}O$ values should show a similar signature. The warmer temperature creates less fractionation in both $\delta^{18}O$ and $\delta^{13}C$. Generally, the $\delta^{18}O$ changes 1‰ for each 5°C changes in carbonate formation temperature (near ~25°C) (Grossman, 2012). If this applies to these meteorite carbonates, then there is a ~50°C difference in formation temperature between Rx0/Rx1 carbonates and Rx2 carbonates, which seems unrealistic.

Alternatively, the Rx2 $\delta^{18}O$ average difference of -9‰ to -10‰ from Rx0/Rx1 carbonates could be due to different contributions of two oxygen reservoirs involved in the carbonate formation. This possibility is explored in detail with the development of a $\delta^{18}O$ mixing model (see discussion below).

ALH 77215 values

The measured value for Rx2 on ALH 77215, extraction date 7/30/15, sample tube #380, is completely different from any OC Rx2 other value (see Figures 3-7 and 3-12 highlighted in yellow). The $\delta^{13}C$ = +15.39, $\delta^{18}O$ = +20.02 reflects a carbon source that is +11.2‰ heavier than other OC Rx2 sources (and Rx0 or Rx1 carbon sources). The oxygen source is +11.3‰ than the other OC Rx2 carbonates. This carbonate is possibly non-terrestrial, or the measurements of this carbonate were contaminated in

some undetected manner. The values for this sample are excluded in averages computed for other Rx2 measurements based on reaction and region.

LEW 85320 values

The nesquehonite on LEW 85320 also has reported stable isotope values consistent with terrestrial carbonates; however, the two "Antarctic" values fall into different species (see Table 3-1 and Figure 3-10). The $\delta^{13}C = +5.40‰$, reported by (Jull et al., 1988), is consistent with results for Rx2 Fe/Mg-rich carbonates. Both of the LEW 85320 reported values for nesquehonite growing in "Texas" are consistent with OC terrestrial carbonate values (falling within the overlap between Rx0/Rx1 and Rx2 species). The $\delta^{13}C=+7.9‰$, reported by (Grady et al., 1989), is consistent with results for Rx0/Rx1 Ca-rich carbonate.

EET 79001 values

The reported $\delta^{18}O$ values for "white druse" on Shergottite EET 79001 are consistent with the terrestrial Ca-rich carbonates measured with Rx0/Rx1. Two (of three total) $\delta^{13}C$ values are also consistent with terrestrial Ca-rich carbonates measured with Rx0/Rx1 (see Table 3-2 and Figures 3-10). The $\delta^{13}C = +9.7‰$ reported by (Clayton and Mayeda, 1988) is slightly higher than the other OC carbonate $\delta^{13}C$ values measured in this study. Although prior petrographic studies suggest the "white druse" is martian in origin, comparison with our data from equivalent regions of Antarctica suggest a terrestrial origin.

Antarctic OC Carbonate Formation Temperature

The OC carbonates are created by interactions between cations in the minerals of the meteorite and CO_2 in the Earth's atmosphere, which has a current $\delta^{13}C \approx -8‰$ that is decreasing (getting isotopically lighter) due to the burning of $\delta^{13}C$ fossil fuels (Cuntz, 2011). The OCs contain terrestrial Ca-rich carbonates with $\delta^{13}C$ values clustering between +3‰ and +6‰ (see Figure 3-10). Assuming the carbonates formed when the atmospheric $CO_2‰ = -7.5‰$ (within the past 150 years), the expected calcite $\delta^{13}C$ = +6.09‰ (if formed at 0°C) or $\delta^{13}C$ = +4.38‰ (if formed at 15°C) (using $\Delta_{CO2\_Calcite}$ = -13.59‰ at 273°K and $\Delta_{CO2\_Calcite}$ = -11.88‰ at 288°K) (Chacko et al., 1991). The Rx0/Rx1 Ca-rich $\delta^{13}C$ measurements indicate the carbonate formed in equilibrium with atmospheric CO_2 carbon at temperatures between 0-15°C. This conclusion is consistent with prior Antarctic carbonate formation studies predicting carbonate formation at 0-30°C (Grady et al., 1989, Karlsson et al., 1991).

The Rx2 $\delta^{13}C$ carbonates appear to fractionate less than the Ca-rich carbonates (compared to atmospheric CO_2) in Figure 3-10 (if formed at the same temperature as the Ca-rich carbonates). These carbonates may be similar to the nesquehonite formed on LEW 85320. There are no published fractionation factors for nesquehonite, although one study suggests magnesite fractionates more than calcite at low temperature (see Figure 3-1) (Golyshev et al., 1981).

Antarctic OC Carbonate Formation with a $\delta^{18}O$ Mixing Model

The range of measured $\delta^{18}O$ from OC terrestrial carbonates is approximately +3‰ to +30‰ (see Figure 3-10), which would represent an unrealistic temperature variation in the Antarctic environment. In addition, these values are substantially heavier isotopically than expected if the calcite forms in equilibrium with the Antarctic meteoric water. Using Bottinga $\delta^{18}O$ fractionation factors for calcite and water (Bottinga, 1968), the expected calcite would be $\delta^{18}O < 0$‰ if Antarctic meteoric melt water $\delta^{18}O < -35$‰ (Dansgaard, 1964) and equilibrium fractionation occurs at 0°C-15°C (based on discussion above for $\delta^{13}C$).

A possible explanation for heavier $\delta^{18}O$ in OC carbonates is their formation process. Instead of equilibrium with either the atmosphere or the water, the carbonates may form in a thin-film environment. Thus, the isotopic composition of the carbonates would be dependent on mixing between two different oxygen reservoirs: dissolved atmospheric CO_2 and Antarctic meltwater. Thus the Earth atmospheric CO_2 of heavy $\delta^{18}O \approx +41$‰ in equilibrium with global seawater (Brenninkmeijer et al., 1983) balances the light glacial meteoric water $\delta^{18}O \approx -35$‰ to form intermediate $\delta^{18}O$ carbonates.

A $\delta^{18}O$ mixing model can be created with Earth atmospheric CO_2 and meteoric water as end members. Using fixed contributions of each end member provides predicted values of $\delta^{18}O$ for produced carbonates, thus a parametric study with different fixed contributions provides a tool to interpret the measured OC results.

$\delta^{18}O$ Mixing Model Derivation

Begin with a simple oxygen mixing model of two $\delta^{18}O$ end-members only. Given $\delta^{18}O_{water}$ is the stable isotope value of the melt-water in a thin film around a meteorite, and $\delta^{18}O_{CO2}$ is the stable isotope value of the atmospheric CO_2 (assume the atmospheric CO_2 is well mixed and constant throughout the Earth). Now, let x represent the fraction of $\delta^{18}O$ for melt water in a thin film "bubble" around a meteorite, and let y represent the fraction for $\delta^{18}O$ for CO_2 in the atmospheric "bubble". Then,

$$x + y = 1 \qquad \text{eq. 3-6}$$

The total amount oxygen, $\delta^{18}O_{total}$, is composed of amounts from each end-member:

$$\delta^{18}O_{total} = (x * \delta^{18}O_{water}) + (y * \delta^{18}O_{CO2}) \qquad \text{eq. 3-7}$$

Fractionation factors, α, are well studied for calcite/water/CO_2 systems, although they are not well studied at temperatures near 0°C (Friedman, 1977). Fractionation factors based on near 0°C laboratory studies for other carbonates, such as magnesite, nesquehonite, and siderite, are rare. Calculations for this model are thus made using calcite fractionation factors (which can still result in a difference of 2‰ depending upon which laboratory or theoretical study is employed). Following are the relevant fractionation values (and their source) for this mixing $\delta^{18}O$ model:

$$\delta^{18}O\ \Delta_{CO2\_water} = -45.67‰, \text{ at } 0°C \text{ (Bottinga)} \qquad \text{eq. 3-8}$$

$$\delta^{18}O\ \Delta_{CO2\_water} = -42.26‰, \text{ at } 15°C \text{ (Bottinga)} \qquad \text{eq. 3-9}$$

$$\delta^{18}O\ \Delta_{CO2\_calcite} = -11.68‰, \text{ at } 15°C \text{ (Chacko)} \qquad \text{eq. 3-10}$$

$$\delta^{18}O\ \Delta_{CO2\_calcite} = -11.45‰, \text{ at } 0°C \text{ (Chacko)} \qquad \text{eq. 3-11}$$

Based upon these values, it is possible to calculate the following:

$$\delta^{18}O\ \Delta_{calcite\_water} = -33.78‰, \text{ at } 0°C \quad \text{eq. 3-12}$$

$$\delta^{18}O\ \Delta_{calcite\_water} = -29.94‰, \text{ at } 15°C \quad \text{eq. 3-13}$$

If the calcite forms only in equilibrium with the atmosphere, then

$$\delta^{18}O_{calcite} = \delta^{18}O_{CO2} + \Delta_{CO2\_calcite} \quad \text{eq. 3-14}$$

$$\delta^{18}O_{calcite} = \delta^{18}O_{CO2} - 11.45‰, \text{ at } 0°C \quad \text{eq. 3-15}$$

$$\delta^{18}O_{calcite} = \delta^{18}O_{CO2} - 11.68‰, \text{ at } 15°C \quad \text{eq. 3-16}$$

If the calcite forms only in equilibrium with the water, then

$$\delta^{18}O_{calcite} = \delta^{18}O_{water} + \Delta_{CO2\_calcite} \quad \text{eq. 3-17}$$

$$\delta^{18}O_{calcite} = \delta^{18}O_{water} + 33.78‰, \text{ at } 0°C \quad \text{eq. 3-18}$$

$$\delta^{18}O_{calcite} = \delta^{18}O_{water} + 29.94‰, \text{ at } 15°C \quad \text{eq. 3-19}$$

Thus, the calcite must fall between the two end-members given in eq. 3-15 and eq. 3-18 (at 0°C), or eq. 3-16 and eq. 3-19 (at 15°C). The mixing model output varies based upon the contributions of each end-member in the calcite formation.

$\delta^{18}O$ Mixing Model Application

Begin employment of the mixing model by loading the environmental conditions in Antarctica where the OC carbonates are forming. Assume the carbonate formation happens at 15°C (based upon the analysis of $\delta^{13}C$ values), the $\delta^{18}O_{water}$ = -35‰ (see Figure 1-17) with Antarctica similar to Greenland (Dansgaard, 1964), and $\delta^{18}O_{CO2}$ = +41‰ based on Earth atmospheric equilibrium with seawater (Keeling, 1961). The resulting component mixing of each end-member is shown in Table 3-8. The $\delta^{18}O$

mixing model results, combined with corrected stable isotope values for all OCs, LEW 85320, and EET 79001 are shown in Figure 3-11.

MIXING MODEL		EARTH
OXYGEN		
d18O atmosphere		23.5
d18O H2O (l) - fraction "x"		-35
d18O CO2 (g) - fraction "y"		41
CARBON		
d13C CO2 (g) atmo		-7.5
d13C CaCO3 (atmo) at 0°C		6.09
d13C CaCO3 (atmo) at 15°C		4.38
OUTPUT:		
d18O Analysis (15° C)		
Max d18O Calcite (atmo)		29.32
x	y	
0.0	1.0	29.32
0.1	0.9	25.88
0.2	0.8	22.44
0.3	0.7	19.00
0.4	0.6	15.57
0.5	0.5	12.13
0.6	0.4	8.69
0.7	0.3	5.25
0.8	0.2	1.82
0.9	0.1	-1.62
Min d18O Calcite (water)		-5.06

Table 3-8: Mixing Model Output for Antarctic OC Calcite $\delta^{18}O$

The model predicts that Rx0/Rx1 Ca-rich carbonates form on the Antarctic OCs with 45%-85% contribution of $\delta^{18}O$ from atmospheric CO_2 and the remainder $\delta^{18}O$ from melt water. The Fe/Mg-rich carbonates form with 20%-55% contribution from $\delta^{18}O$ in atmospheric CO_2 and the remainder from $\delta^{18}O$ in melt water.

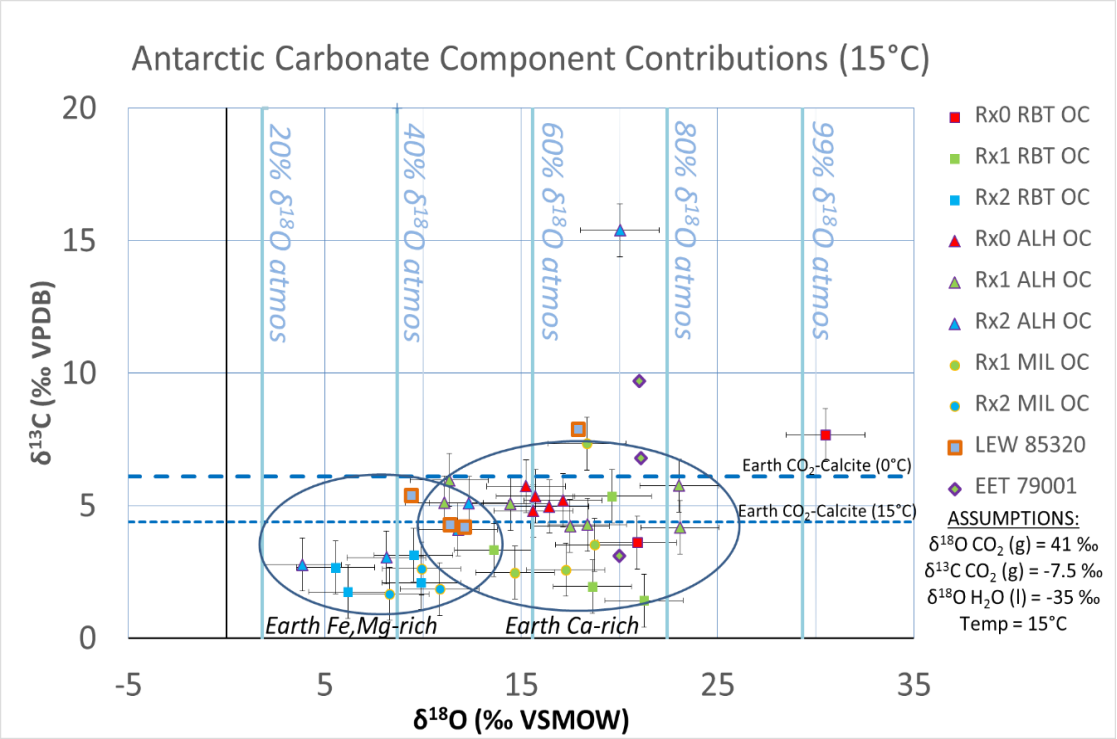

Figure 3-11: Antarctic OC Carbonate Formation $\delta^{18}O$ Sources

Conclusions

OCs assumed to be carbonate-free before arriving on Earth form two distinct carbonate species while resident in Antarctica, a Ca-rich phase and a Mg/Fe-rich phase. Preliminary measurements show that a reaction between the carbonate with phosphoric acid for 1 hour at 30°C (Rx0) and 3 hours at 30°C (Rx1) generate CO_2 from a Ca-rich carbonate (Al-Aasm et al., 1990, Grady et al., 1988, Karlsson et al., 1991, Shaheen et al., 2015).

A reaction at 150°C for 3 hours (Rx2) generates CO_2 from a Fe-rich or Mg-rich carbonate (Al-Aasm 1990, Grady et al., 1988, Shaheen et al., 2015). There are no reported stable isotope fractionation factors for nesquehonite, and few theoretical or

laboratory studies for magnesite and siderite fractionation at low temperatures. Calcite fractionation factors were employed to interpret the Rx2 data.

Much heterogeneity exists with corrected stable isotope values (especially $\delta^{18}O$) for the OC carbonates (see Figure 3-7). Variability exists within a reaction type (see Figure 3-8), within a collection region of Antarctica (see Figure 3-9), and within an individual meteorite (see Tables 3-5, 3-6, 3-7); however, a few broad distinctions are observed.

With all OCs, a Ca-rich carbonate species generates CO_2 from Rx0 that is ~ +2.1‰ (±3.6‰ 1σ based on data) heavier in $\delta^{18}O$ than the CO_2 extracted from Rx1. This variation could be from grain size differences of the Ca-rich carbonate formed on the meteorite. The Ca-rich carbonates $\delta^{13}C$ values suggest formation in equilibrium with atmospheric CO_2 at ~15°C. Using a mixing model of end-members from oxygen in meteoric water and atmospheric CO_2, the $\delta^{18}O$ values suggest a range of 45%-85% oxygen contribution from atmospheric CO_2 at 15°C (see Figure 3-11).

Ca-rich carbonates (Rx0 and Rx1) from region ALH are 1.4‰ (±1.5‰ 1σ based on data) heavier in $\delta^{13}C$ and lighter in $\delta^{18}O$, -3.4‰ (±3.6‰ 1σ based on data), than Ca-rich carbonates (Rx0 and Rx1) in RBT and MIL. This regional variation could be from geographic differences in the creation of meteoric water (Rayleigh distillation) or different temperature of carbonate formation.

Corrected stable isotope values for Rx2 Fe/Mg-rich carbonates are consistent regardless of Antarctic region of collection. They are also distinct from Rx0/Rx1 carbonates, with lighter average values in both $\delta^{13}C$ (-1.3‰±1.5‰ 1σ based on data) and

$\delta^{18}O$ (-10‰±3.6‰ 1σ based on data). This means the Fe/Mg-rich carbonates (Rx2) are fractionating less in $\delta^{13}C$ than the Ca-rich (Rx0/Rx1) carbonates from the Earth atmospheric CO_2 value $\delta^{13}C$ = -7.5‰. Carbonate stable isotope values fractionate less at higher temperature than at cooler temperatures, so the Rx2 carbonates $\delta^{13}C$ values suggest formation in equilibrium with atmospheric CO_2 at >15°C (perhaps +10°C warmer). This assumes calcite fractionation factors. If the Fe/Mg-rich (Rx2) carbonates fractionate more than the Ca-rich (Rx0/Rx1) carbonates, as suggested by one study of magnesites and siderites (Golyshev et al., 1981), then their formation temperature is much warmer, perhaps >20°C. This would be greater than reasonably expected in Antarctica, but consistent with ambient temperatures at the curation facility in Houston, Tx. The Rx2 $\delta^{18}O$ values suggest a range of 25%-65% oxygen contribution from atmospheric CO_2 at 15°C (see Figure 3-11) based upon a mixing model of two end-members (meteoric melt-water and atmospheric CO_2).

One OC meteorite, ALH 77215, demonstrated an anomalous Rx2 stable isotope value significantly heavier in both $\delta^{13}C$ and $\delta^{18}O$ than any other OC Rx2 carbonate. This may represent heterogeneity in the terrestrial Fe/Mg-rich carbonate, or a carbonate from a non-terrestrial origin.

The published stable isotope values for the "white druse" from Shergottite EET 79001 are consistent in $\delta^{18}O \approx +21‰$, but the $\delta^{13}C$ varies from +3‰ to +10‰ (see Figure 3-2) (Clayton and Mayeda, 1988, Wright et al., 1988, Jull et al., 1992). The lighter carbon measurements are consistent with terrestrial Ca-rich carbonates measured from OC Rx0/Rx1 reactions (see Figure 3-8)

The published stable isotope values (see Table 3-1) (Jull et al. 1988, Grady 1989) for nesquehonite from OC LEW 85320 are consistent with terrestrial carbonate results for the OCs in this study. The two "Antarctic" published values for nesquehonite extracted from LEW 85320 before it was transported to the Houston curation facility fall within the Rx0/Rx1 Ca-rich results from this study. The two "Texas" published values for nesquehonite extracted from LEW 85320 fall within the Rx2 Fe/Mg-rich results from this study (but overlap with Rx0/Rx1 Ca-rich results) (see Figure 3-10).

The OCs contain terrestrial carbonates with $\delta^{13}C$ values clustering between +3‰ and +6‰. These Ca-rich (Rx0/Rx1) values are consistent with equilibrium carbonate formation at 15°C with the carbon in Earth's atmospheric CO_2. (see Figure 3-11). The Fe/Mg-rich carbonates appear to fractionate less than the Ca-rich carbonates if they formed at the temperature, but fractionation factors for these carbonates are unknown.

The range of measured $\delta^{18}O$ from OC terrestrial carbonates is approximately +3‰ to +30‰. These values are heavier isotopically than expected if the calcite forms in equilibrium with the oxygen in Antarctic meteoric water. It is proposed that these carbonates formed in an arid, cold climate based upon thin films of melt water on the meteorite interacting with a "bubble" of atmospheric CO_2. A $\delta^{18}O$ carbonate contribution mixing model predicts that Ca-rich carbonates form on the Antarctic OCs with 45%-85% contribution of oxygen from atmospheric CO_2 (assumed $\delta^{18}O$ = +41‰) and the remainder from oxygen in melt water (assumed $\delta^{18}O$ = -35‰). The Fe/Mg-rich carbonates form with 20%-55% contribution from oxygen in atmospheric CO_2.

The predicted low atmospheric contribution to the $\delta^{18}O$ for OC Fe/Mg-rich carbonates (based upon the mixing model) is logically consistent with the "Texas" nesquehonite stable isotope values for LEW 85320, which is being curated in Houston, Tx. in a dry, nitrogen environment yet continues to produce nesquehonite. The LEW 85320 $\delta^{18}O$ source for the nesquehonite is entirely entrapped Antarctic water that is slowly degassing from the meteorite as it sits in N_2 storage.

It is possible that all of the Fe/Mg-rich (Rx2) carbonates formed on the OCs in this study were created in the warmer N_2 curation environment of Houston, Tx, (similar to LEW 85320 nesquehonite). This is suggested by light $\delta^{13}C$ values compared to the Rx0/Rx1 carbonates. The OC Ca-rich (Rx0/Rx1) carbonates, however, likely formed in Antarctica from interactions of meteorite cations, meteoric melt-water, sea-spray aerosols, and atmospheric CO_2 in a thin-film "bubble" microenvironment at about 15°C. This is reinforced by the selection criteria for the OCs in this study. Each OC had visible evaporite deposits on them when collected in Antarctica, although it is unknown if these identified alteration minerals were carbonates, sulfates, or a combination of both.

The $\delta^{18}O$ carbonate contribution mixing model created for OCs from Antarctica may predict oxygen end-member reservoirs on Mars. If martian carbonates form in an arid, thin-film microenvironment similar to the Rx0/Rx1 carbonates in Antarctica, then iteration of the mixing model end-member values can create carbonate predictions to match the measured carbonate stable isotope values.

CHAPTER IV

STUDY OF MILLER RANGE MARTIAN NAKHLITES

Introduction

The martian surface contains features of ancient fluvial systems and evidence of a hydrosphere (Poulet et al., 2005, Lammer et al., 2008) that might have formed carbonates from interaction with the CO_2-rich atmosphere. Meteorites from Mars contain carbonates that can be measured to assess their martian formation environmental conditions with stable isotope analysis (see Chapter 1).

Nakhla is an igneous cumulate clinopyroxenite that crystallized on Mars 1.3-1.4 Ga. A large impact on Mars 11 Mya ejected material into space, and some of it eventually landed on Earth. Nakhla is the type specimen of clinopyroxene cumulate rocks from Mars, which are known as Nakhlites (Nyquist et al., 2001, Park et al., 2009). They are predominantly clinopyroxene-dominated cumulates with large augite and olivine grains. These grains are distinct from the fine matrix material that holds the rock together, known as the intercumulus phase, which consists mostly of "glass and laths of plagioclase, silica, phosphate, and pyroxene" (Udry et al., 2012). The Nakhlites contain martian weathering products that include both clay minerals formed from the hydration of silicates and carbonates, chlorides, and sulfates precipitated in cracks (Grady et al., 2007). The martian brines altering the Nakhlites have been proposed to be from shallow hydrothermal sources or from surface runoff (Bridges and Grady, 2000). Based upon their common cosmic ray exposure ages, they were ejected from Mars by a single large

impact approximately 11 ± 1.5 Ma (Nyquist et al., 2001) and landed on Earth 10,000 – 40,000 years ago (Velbel, 2016).

Nakhla Parent Formation

Several models have been proposed for the formation and evolution of Nakhlites on Mars. The current belief is the Nakhlites all were derived from a set of lava flows or shallow sills with a common source. The location, based upon comparison of crystallization ages to crater count dating, is possibly volcanic zones of Tharsis, Elysium, or Syrtis Major (Treiman, 2005).

The lava flows experienced different cooling rates with depth, and the Nakhlites with the greatest equilibration and least intercumulus phase were slower cooling and derived from a greater formation depth, while those with less equilibration and/or more intercumulus phase were more rapidly cooled and are derived from shallower depths (Day et al., 2006, Mikouchi et al., 2012, McCubbin et al., 2013**).** Stacking the identified Nakhlite meteorites together creates a "lava pile" of different depths of origin for each meteorite. The graded crystallization petrology infers a depth of formation for each Nakhlite.

After the "lava pile" was emplaced, it was infiltrated by fluids to create small amounts of secondary minerals and weathering products. If the water source was on the surface of Mars, the shallowest rocks would have the most aqueous alteration, and the deeper rocks would have the least aqueous alteration. If the water source was a subsurface hydrothermal system, then the rocks closest to the source would experience

the most aqueous alteration. Thus, understanding the placement of the secondary minerals in the lava pile is important for interpreting stable isotope measurements.

Nakhlite Meteorites

The first identified Nakhlites were Nakhla, Lafayette, Governador Valadares, NWA 817, Y000593/Y000749/Y000802 (paired), NWA 998, and MIL 03346 (Treiman, 2005).

Yamato (Y) Y 00593, Y 000749, and Y 000802 were found in 2000 by the 41st Japanese Antarctic Research Expedition. These paired meteorites contain martian iddingsite (like other Nakhlites) which forms from water-rock interaction. They also contain laihunite, which is a "nonstoichiometric olivine-like mineral typically formed as a high-temperature oxidation product under non-equilibrium conditions on Earth" (Noguchi et al., 2009). This implies hot fluids weathering igneous rocks on Mars.

The next three identified Nakhlites (MIL 090030, MIL 090032, and MIL 090136) are paired with MIL 03346 based on mineralogy and petrology (Hallis and Taylor, 2011). MIL 03346 was discovered in 2003, and MIL 090030, MIL 090032, and MIL 090136 were found in 2009 in Antarctica. The four Miller Range meteorites were found in two pairs approximately 4 km apart (see Figure 4-1). Within each pair, the meteorites were located 200m apart. There is great variability in the modal mineral abundances of each meteorite, and single samples of any one meteorite may not be representative of the Miller Range parent body (Udry et al., 2012).

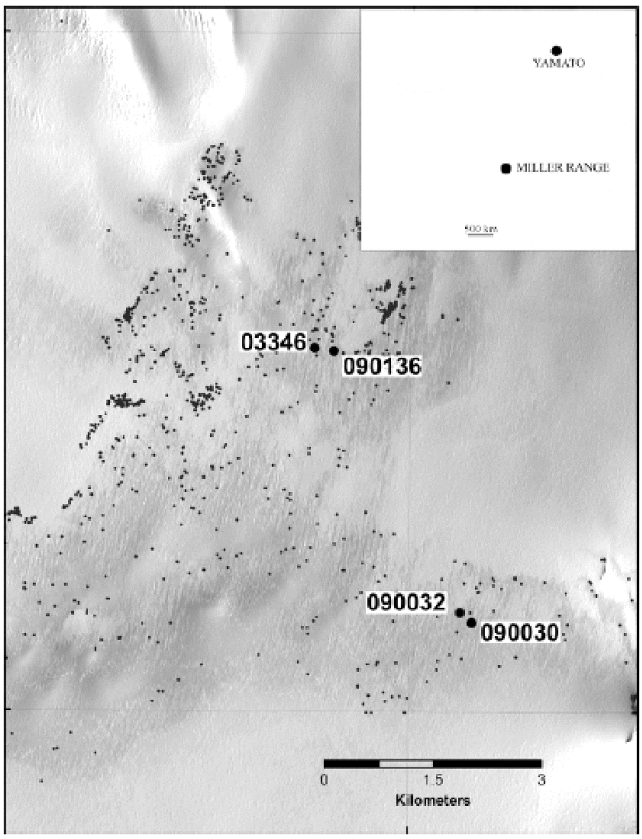

Figure 4-1: Location of Miller Range Nakhlites in Antarctica (reprinted from Udry et al., 2012)

The newest identified Nakhlite, NWA 5790 was found on Earth by nomads in the Sahara Desert in 2010 (Jambon et al., 2016). It is the only Nakhlite lacking iddingsite. This indicates it was not altered aqueously on Mars. This meteorite displays mineralogy from two magma batches before eruption, which complicates the prior models of Nakhlite formation from a single lava flow.

Nakhla Lava Pile

Differences in mineral zoning of each Nakhlite are used to estimate their cooling rates. It is important to ensure the mineral zoning is from diffusion, and not from multiple heating/cooling events, to determine the original formation stratification as the source magma cooled. Diffusion is determined via comparison of zone element concentration to kinetic isotopic fractionation (Sautter et al., 2012). Multiple heating/cooling events are determined by comparison of argon age and closure temperature (~350°C) (Park et al., 2009) to the formation crystallization age of the olivine (Richter et al., 2016).

Prior analysis of MIL 03346 indicate it formed with the other Nakhlites, but underwent rapid cooling prior to complete crystallization (Day et al., 2006). MIL 03346 is distinctive from other Nakhlites in having higher mesostasis (~20% vs. ~10% for others) and lower olivine content (<< ~10% for others). The reported cooling rate, based on Fe-Mg zoning, is 0.8°C/hr placing it at a depth of 1m in the lava pile (Richter et al., 2016). The fastest cooling rate of 11.0°C/hr, found in paired Nakhlites MIL 090030, MIL 090032, and MIL 090136, requires a faster quench than the slowest rates of <0.015°C/hr found in Lafayette and NWA 998 (Mikouchi et al., 2012). The cooling rate for MIL090030/MIL090032/MIL090136 places them shallow, at a depth of 0.3m in the lava pile, which is above MIL 03346 (Mikouchi et al., 2012).

The proposed burial sequence from top to bottom is MIL 03346 (and pairings), NWA 817, Y 000593 (and pairings), Nakhla, GV, Lafayette, and NWA 998 (see Table 4-1) (Day et al., 2006, Changela and Bridges, 2011, Mikouchi et al., 2012). After

identifying NWA 5790, it was initially placed on the top of the lava pile due to its mesostasis similarity to MIL 03346.

Sample	Best fit cooling rate (°C/hr)		Corresponding burial depth (m)*	
	Fe-Mg	Ca	Fe-Mg	Ca
NWA 5790	4.5	0.35	0.4	1-2
MIL090030, 032, 136	11.0	0.75	0.3	1
MIL03346[3]	0.8	0.04	1	4
NWA 817[3]	2.2	0.5	0.5	1-2
Y000593[3]	0.03	0.015	4-5	7
Nakhla[3]	0.04	0.01	4~5	10
Governador Valadares[3]	0.085	0.01	3	10
Lafayette[3]	<0.015	<0.001	>5-6	>30
NWA 998[3]	<0.015	<0.0009	>5~6	>30

*Covered with rock-like material.

Table 4-1: The Nakhla Lava Pile (reprinted from Mikouchi et al., 2012)

Multiple study results show the cumulus phase was first crystallized from a Light Rare Earth element (LREE) depleted mantle source (Treiman, 2005, Day et al., 2006). A recent geochemical analysis of the Nakhlites and Chassignites proposes that they formed from a common magma, but crystallized the intercumulus phase differently (McCubbin et al., 2013). It begins when a) a shallow magma intrusion cooled slightly within the crust, and b) started crystallizing cumulus olivine and some pyroxene, which settled to the bottom of the magma chamber. Then, c) the intrusion was invaded by a Fe^{2+}-rich, Cl-rich, LREE-enriched fluid (possibly crustal, but from a LREE-depleted source) that contaminated the magma as d) orthopyroxenes and augites continued to crystallize. These phases appear to be in geochemical disequilibrium with the olivine with respect to Xe isotopes and REE abundances. As the cooling and crystallization

continues, the magma becomes fluid-saturated, leading to e) degassing of a Cl-rich, Fe^{2+}-rich magmatic fluid phase that migrates upward to the top of the magma body. The sequence is completed as f) the melt solidifies, resulting in the Nakhlite-Chassignite lava pile demonstrated in Figure 4-2.

Figure 4-2: The Nakhla/Chassigny Lava Pile (reprinted from McCubbin et al., 2013)

Further electron microprobe analysis of NWA 5790 identified at least four areas of discrete mineralogy differences from other Nakhlites. Models of different melt compositions were estimated assuming core olivine in equilibrium with the parent melt; whereas prior studies assumed equilibrium with the core augite (Treiman, 2005, Day et al., 2006). Using this approach, the NWA 5790 is placed at the bottom of the total lava pile, but the top of a different lava flow (Jambon et al., 2016). This lowest lava flow

lacks low temperature alteration (no iddingsite formation). At least two, and probably three, different lava flows formed the Nakhlites as shown in Figure 4-3.

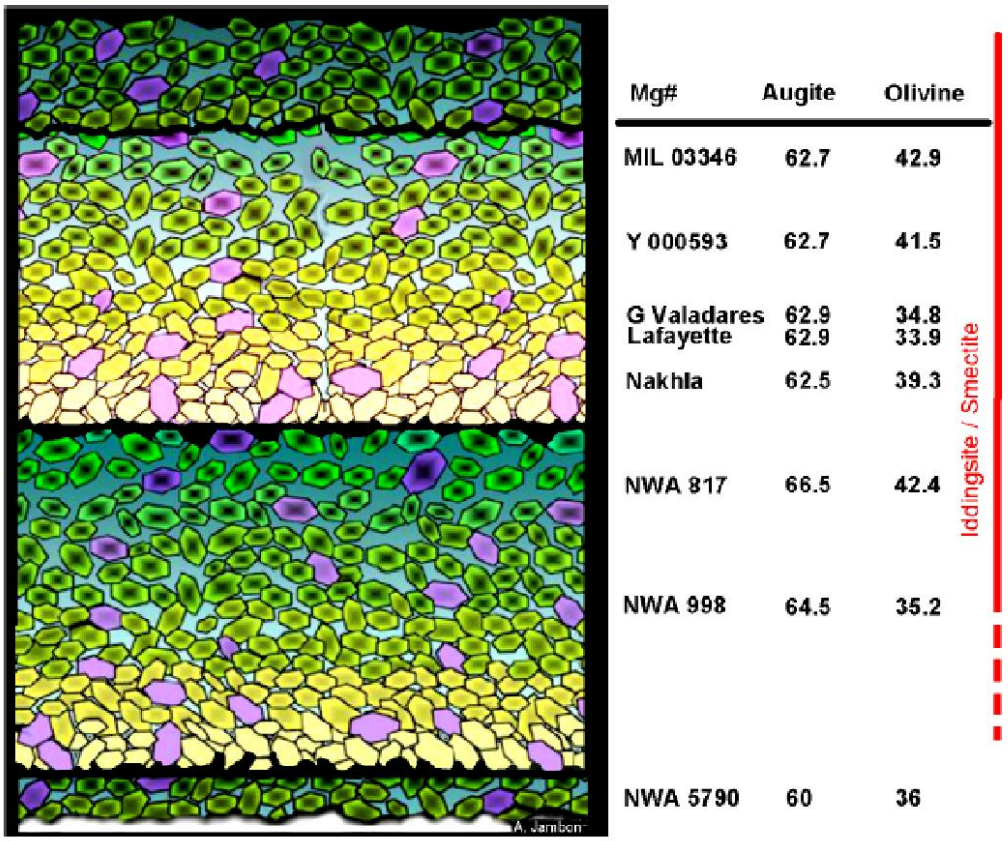

Figure 4-3: The Updated Nakhla Lava Pile (reprinted from Jambom, 2016)

Another study of Nakhlites (Richter et al., 2016) suggests an alternate formation model. The authors suggest Nakhlites crystallized slowly in a crustal magma chamber or thick lava layer, but then they underwent a rapid cooling event. Analysis of the lithium concentration and isotopic fractionation profiles within augite grains in MIL 03346 and NWA 817 creates two possible models to explain the rapid cooling: a) at the

bottom of a lava flow that has erupted onto the martian surface (cooled by contact with the cold surface layer), or b) at the top of a lava layer, such as when a breach of a containment topology drains the magma chamber exposing the mostly crystallized flow to the cold martian atmosphere (See Figure 4-4).

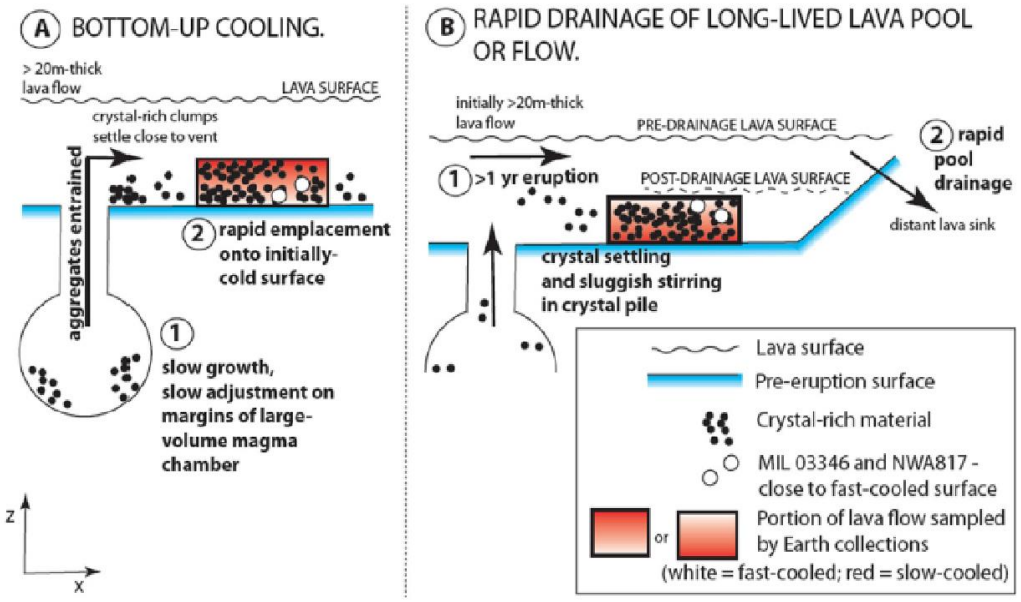

Figure 4-4: Alternate Nakhlite Crystallization Models (reprinted from Richter et al., 2016)

Secondary Alteration

Ion microprobe analysis of thin sections from the Nakhla meteorite reveals multiple chemically heterogeneous species both within grains and between grains (Saxton et al., 1998). The carbonates appear in cracks and crushed zones of the rock, and have crystals <100 µm (Bridges et al., 2001). Martian carbonates predominantly include cations of Ca, Fe, Mg and Mn forming varieties of calcite, siderite, magnesite,

rhodochrosite and ankerite. Carbonate chemistry varies with each class of martian meteorite, indicating separate deposition sequences (Niles et al., 2013).

Martian meteorites are also altered by shock impact. Shergottites, for example, include unique shocked minerals of maskelynite, stishovite, and ringwoodite (Nyquist et al., 2001).

Gypsum

This is an alteration product created as a hydrated form of calcium sulfate (chemical formula $CaSO_4 * 2H_2O$). It is reported in martian Nakhlites MIL-03346/090030 based on a Raman spectra that shows broad H_2O-related peaks, which differentiate the mineral from anhydrite (Hallis and Taylor, 2011). Gypsum is often found in SNC meteorites. On Shergottite EET 79001, the "white druse" (containing gypsum) has been reported to be a martian alteration product (Gooding and Muenow, 1986, Gooding, 1992).

Laihunite

This is an opaque, black alteration product created in olivine from high-temperature oxidation under non-equilibrium conditions found on Earth (Banfield et al., 1990). The chemical formula is $Fe^{2+}(Fe^{3+})_2(SiO_4)_2$. Found in the paired Nakhlites Y000593/Y000749, laihunite is suspected of being formed in a "fluid-assisted high temperature oxidation event" (Noguchi et al., 2009).

Jarosite

This is an alteration product forming tiny crystals of yellow to brown color. It forms in acid environments such as terrestrial mine drainage, sulfate soils, or during "alteration of volcanic rocks by sulfur-rich fluids near volcanic vents" (Fulignati et al., 2002). The chemical formula is $KFe^{3+}_3(OH)_6(SO_4)_2$ (Friedman, 2017). It was identified by the Mars rover Opportunity in the Meridiani Planum (Squyres et al., 2004), and has been identified elsewhere on Mars as well (Madden, 2004). As a hydrous iron sulfate, it persists only in arid climates, and water vapor causes it to decompose to hematite (Barrón, 2006). It has been reported in martian meteorites, for Nakhlites Y000593/749 and MIL 03346, and Shergottites RBT 0462 and QUE 94201;however, MIL 090136 contains interior jarosite, which could represent pre-terrestrial weathering on Mars (Hallis, 2013).

Iddingsite

Iddingsite (chemical formula $MgO * Fe_2O_3 * 4\ H_2O$, but MgO can be substituted for CaO in the ratio of 1:4) (Ross, 1925) is an alteration product of olivine found when basalts are weathered by liquid water. A major constituent of iddingsite in Y000593/Y000749 is phyllosilicate, perhaps smectite (Noguchi et al., 2009). It forms as a phenocryst, which is a secondary crystal relatively larger in size than the primary crystals of the parent igneous rock. Often found in martian Nakhlites, the presence of iddingsite could indicate interactions with liquid water on the surface of Mars from 1.3 Ga to 650 Ma ago (Swindle et al., 2000).

Iddingsite is found in many Nakhlites (Treiman, 2005), but not NWA-5790 (Jambon et al., 2016). It is speculated the Nakhla lava pile was infused with liquid water approximately 620 mya, which dissolved olivine and mesostasis glass, then deposited iddingsite and salt minerals (Treiman, 2005).

Terrestrial Complications

The Nakhlites also contain terrestrial minerals formed in Antarctica since they landed approximately 10,000 years ago (Treiman, 2005). For example, MIL 03346 contains both martian carbonates (iddingsite) and terrestrial sulfates. The terrestrial sulfates are located on exposed surfaces and along fractures (Stopar et al., 2013). The meteorite also contains olivine phenocrysts (etch-pits) with corrosion features that match terrestrial weathered olivines. A comparison of interior and exterior olivine indicates there has been more surface aqueous alteration from Antarctic weathering during its terrestrial residence than occurred during 500,000 - 1.0 billion years after iddingsite formation on Mars (Velbel, 2016).

One theory for Antarctic meteorite weathering is from slightly alkaline sea-spray. This aerosol, which is found far inland on Antarctica, deposits Ca^{+}, Na^{+}, and SO_4^{2-} ions on the meteorite. Then, when the meteorite is exposed on the surface of Antarctic glaciers, the high albedo rock absorbs sunlight and melts a small amount of ice to form liquid water. This water combines with the cations and anions to form carbonates and sulfuric acid which alters the meteorite mineralogy (Hallis, 2013).

Mars Fluids and Carbonate Formation Conditions

Many theories have been developed to model the conditions under which martian carbonates are precipitated. The meteorite ALH 84001 is well studied; however, it is much older than the Nakhlites and likely formed in a different location. Nonetheless, the researchers have interpreted measurements on ALH 84001 to propose radically different carbonate formation theories on Mars (see broad discussion in Niles et al., 2005). In a broad sense, many of the features of carbonate mineral formation in martian meteorites are common to all meteorite types.

Carbonate Formation Models based on Temperature

Some models speculate that high temperature fluids (>200°C) are necessary to create the minerals observed in ALH 84001. The model then requires rapid cooling to create the variation in measured $\delta^{18}O$ values (Eiler et al., 2002). Whether the fluids are heated by impact events (Harvey and McSween, 1996, Scott et al., 1997, Scott and Knot, 1998) or hydrothermal fluids (Gleason et al., 1997, Kring et al., 1998), the high temperature formation theories fail to explain a lack of observed chemical weathering in the silicate phases of ALH 84001 (Treiman, 1995). Unlike ALH 84001, the Nakhlites do contain iddingsite as an aqueous alteration product of olivine. Another criticism of the high temperature formation followed by rapid cooling model is the reported $\delta^{13}C$ values, which do not vary enough to support the necessary temperature range. Lastly, this theory fails to provide a plausible geologic process for continuous carbonate deposition in a cooling environment, where reduced temperature would likely result in

cessation of carbonate formation (Friedman, 1970, Dandurant et al., 1982, Usdowski, 1982).

The wide variation in martian meteorite carbonate $\delta^{18}O$ values can also be explained by low fluid/rock ratio interactions with CO_2-rich fluids over short duration periods (Leshin et al., 1998). Evaporation models have also been proposed that were based on observed petrographic and isotopic data (McSween and Harvey, 1998, Warren, 1998), although the lack of abundant sulfates and other salts in ALH 84001 is problematic (carbonates should be more Mg-rich since Mg is more soluble than Ca, which is not reflected in the data) (Niles et al., 2005). Low temperature terrestrial hydrothermal fluids (<70°C to +190°C) form carbonate globules similar to those in ALH 84001 (Treiman et al., 2002).

Carbonate Formation Analog from High pH Terrestrial Springs

Large carbonate oxygen isotope variations have also been observed in high-pH terrestrial spring environments, which can be formed from low temperature serpentization of ultramafic rocks (creating extremely alkaline fluids pH > 12). When these CO_2-free solutions are exposed to atmospheric CO_2, it rapidly dissolves in the solution and subsequently forms carbonates (see eq. 3-1 to 3-5). The carbonates in this environment form rapidly, favoring strong kinetic fractionation. The initial carbonates are very light (meaning more negative $\delta^{13}C$ and $\delta^{18}O$ values), due to the kinetic enrichment of ^{12}C and ^{16}O. The initial carbonate values for $\delta^{13}C$ are depleted up to ~27.5‰ and the $\delta^{18}O$ are depleted by 16.9‰ (Clark et al., 1992). The carbonates

gradually reach equilibration and the pH is lowered as the carbonates continue to precipitate (Niles et al., 1995). The carbonates formed at equilibrium are much less negative $\delta^{13}C$ and $\delta^{18}O$ values than the initial carbonates and form a set of carbonates with a wide range of co-variant carbon and oxygen isotopic compositions.

Carbonate Formation from Mixing of Different Reservoirs

A theoretical calculation of $\delta^{18}O_{water}$ for Mars has been published. Using a mass balance model of hot oxygen (1000°C from ancient, volcanic outgassing) and cold oxygen (at 0°C for carbonate formation) to explain carbonate values on EET 79001 ($\delta^{18}O_{calcite}$ = +21.0‰) one study used estimates of Mars bulk silicate ($\delta^{18}O_{silicate}$ = +4.2‰) and known Bottinga calcite fractionation factors to predict the $\delta^{18}O_{water}$ (Clayton and Mayeda, 1988). The resulting range of $\delta^{18}O_{water}$ = -37.6‰ to +6.4‰ creates the measured carbonate value if the mole fraction of outgassed vapor is 80% water (the remaining 20% is CO_2). Next, a study was made using ion microprobe results of the Nakhla meteorite siderite found within the mesostasis ($\delta^{18}O_{siderite}$ = +34‰ ± 1‰) (Saxton, 1998). The predicted $\delta^{18}O_{water}$ = -5‰ to +34‰ if formation is at 0°C.

Triple oxygen isotope analysis ($\delta^{17}O$, $\delta^{18}O$, $\Delta^{17}O$) of ALH 84001 and two Nakhlites (Nakhla and Lafayette) demonstrates that martian carbonates formed from an atmospheric oxygen reservoir (CO_2) not in equilibrium with the silicate phases within the meteorites (Farquhar et al., 1998, Farquhar and Thiemens, 2000). In addition, carbon isotope enrichment (increased $\delta^{13}C$) of ALH 84001 and Nakhlite carbonates is likely derived from atmospheric CO_2 which is enriched in ^{13}C due to preferential loss of ^{12}C

from the martian atmosphere following the loss of the planet's magnetic field 4 billion years ago (Jakosky et al., 1994, Niles et al., 2012).

One study suggests the Miller Range (MIL) Nakhlites were altered by a different fluid on Mars than the fluid that altered the meteorite Nakhla (Hallis and Taylor, 2011). A different study of Y000593/Y000749 finds the minerals laihunite and jarosite present, which suggests **a** formation temperature of 400°C to 800°C based on terrestrial analogy (Banfield et al., 1990). A newer study, however, concludes it more likely that laihunite in the Yamato Nakhlites formed during emplacement with a small amount of hydrothermal water rather than a subsequent alteration event (Noguchi et al., 2009). Additionally, the formation of jarosite requires an acid environment with arid conditions afterwards, otherwise the jarosite decomposes to ferric oxyhydroxides in the presence of water (Madden et al., 2004). A recent SEM/TEM study of the meteorite Nakhla indicates the martian carrier water was opaline silica, which supports the hypothesis that Nakhlites formed at an ancient martian hot spring (Lee and MacLaren, 2016).

This dissertation proposes an alternate theory for martian carbonate formation in the Nakhlites. Using terrestrial carbonates formed on OC meteorites collected in Antarctica, it is possible to demonstrate that a cold, arid environment produces carbonates with a wide range of $\delta^{18}O$ values created by mixing between oxygen reservoirs in a thin-film of water and dissolved CO_2 (see Chapter 3). A similar mixing model has been proposed for carbonates in ALH 84001 (Niles et al., 2005). This possibility is explored in detail below (see Discussion section for MIL Nakhlite Carbonate $\delta^{18}O$ Values, below).

Previous Martian Meteorite Stable Isotope Measurements

Procedures using phosphoric acid extraction of ground whole rock samples have historically been employed to measure stable isotopes of carbonates (McCrea, 1950). This general procedure was used to study terrestrial carbonates on OCs collected from Antarctica (see Chapter 3). The difficulty of this process is separating the derived CO_2 from water and other gases (often sulfides), then measuring the stable isotope values on very small amounts of CO_2 the samples. Older stable isotope studies of Nakhlites and Chassigny showed a wider variability in $\delta^{13}C$ than in $\delta^{18}O$ (Table 4-2) (Wright et al., 1992):

Sample	Concentration (ppm C)	$\delta^{13}C_{PDB}$ (‰)	$\delta^{18}O_{SMOW}$ (‰)
Governador Valadares	26.8	+11	+24
Lafayette	10.0	+1	+26
Nakhla (1)	29.0	+9	+23
Nakhla (2)	15.0	+6	+26
Chassigny	2.5	−5	+29

Table 4-2: Prior Stable Isotope Values (reprinted from Wright et al., 1992)

A more recently published study also shows the variability of martian carbonate $\delta^{13}C$ results (see Figure 4-5) (Hu et al., 2015). One interpretation of the wide variability of results is they represent combinations of multiple martian carbonate species and terrestrial secondary carbonates that have not been properly separated and identified (Niles et al., 2012).

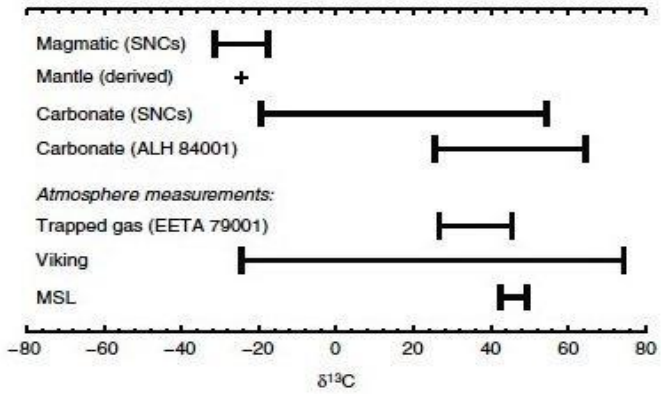

Figure 4-5: Published Mars Carbonate $\delta^{13}C$ Values (reprinted from Hu 2015)

ALH 84001 is a martian meteorite originally classified as a Howardite-Eucrite-Diogenite (HED) meteorite (Dreibus et al., 1994), but now categorized as distinct. It formed 3.9 Ga and has carbonates representing early martian environmental conditions from the ancient atmosphere and crust (~4.5 Ga) (Borg et al., 1999). It has extensive carbonate zoning with Mg-rich crystal faces that are overgrown with Ca, Fe-rich bands. Initial phosphoric acid extractions on this meteorite (Romanek et al., 1994) involved the removal of CO_2 continuously from a reaction vessel during the first 4 hours of the reaction, followed by sequential aliquots extracted from the sealed vessel after 16 hours, and then again after 24 hours. The stable isotope measurements of the Mg-rich carbonate were attributed to the weighted mean of the 4-16 hour and 16-24 hour aliquots. The Ca/Fe-rich carbonate stable isotope values were calculated using first-order dissolution kinetics based on the procedure. The results identify both carbonates enriched in ^{13}C ($\delta^{13}C$ = +40-42‰) from formation equilibrium interactions with the martian atmosphere. The oxygen values were calculated based on mixing between two end members of $\delta^{18}O$ = +13.3‰ for the Ca/Fe-rich carbonates and $\delta^{18}O$ = +22.3‰ for

the Mg-rich carbonates. The authors conclude both carbonates were deposited in an open-system with a low-temperature fluid in the martian crust, although the temperature of the mineralization varied (Table 4-3) (Romanek et al., 1994).

Stable isotope measurements of ALH 84001 and Nakhla carbonates were made using an acid etching procedure (Wright et al., 1988) to measure the $\delta^{13}C$ and $\delta^{18}O$. The summarized values for Nakhla are $\delta^{13}C = +35‰$ and $\delta^{18}O \sim +15 \pm 5‰$, and for ALH 84001 are $\delta^{13}C = +41‰$ and $\delta^{18}O \sim +15 \pm 5‰$. Since Nakhla is a fall collected from the Sahara Desert, the carbonate values are thought to be less likely to reflect terrestrial contamination.

TABLE 1 Isotopic composition of ALH84001 carbonate

(*a*) Measured values*

Aliquot	$\delta^{13}C$ (‰)	$\delta^{18}O$ (‰)	Yield (μg of C)
0–4 h	+40.3	+16.4	4.32
4–16 h	+41.9	+22.6	2.55
16–24 h	+41.5	+21.4	0.79

(*b*) Calculated endmembers†

Composition	$\delta^{13}C$ (‰)	$\delta^{18}O$ (‰)	Yield (μg of C)
Ca,Fe-rich	+39.5	+13.3	1.50
Mg-rich	+41.8	+22.3	6.16

Table 4-3: Prior ALH 84001 Stable Isotope Values (reprinted from Romanek et al., 1994)

ALH 84001 has been on Earth ~13,000 years based on ^{14}C activity (Jull et al., 1989). Analysis of both $\delta^{13}C$ and $^{14}C/^{12}C$ ratio in ALH 84001 found a correlation for the carbonates: if $\delta^{13}C > 45‰$, the $^{14}C/^{12}C$ ratio is lower than expected for terrestrial

carbonates and thus indicates martian origin, but if $\delta^{13}C$ <5‰ the $^{14}C/^{12}C$ ratio is enriched indicating terrestrial origin. There is no similar correlation for $\delta^{18}O$ since oxygen is easily exchanged isotopically (Jull et al., 1995).

The difference in oxygen isotope ratios for ^{17}O and ^{18}O uniquely identifies the planet of origin for silicate crystallization based on mass dependent fractionation. The relationship for Mars $\Delta^{17}O$ (based on eq. 1-6) is an offset from the TFL of approximately +0.321‰ (Franchi et al., 1999). Stepwise vacuum pyrolysis has extracted water from martian meteorites to measure their $\delta^{17}O$ and $\delta^{18}O$ values. Analysis of seven SNC meteorites identified martian water that created carbonates not in equilibrium with the martian host rock; thus, two separate oxygen reservoirs on Mars must exist. The authors speculated on a distinct martian depleted ^{17}O oxygen pool in the lithosphere separate from enriched ^{17}O in the atmosphere and/or hydrosphere (Karlsson et al., 1992). Subsequent analysis of the martian ALH 84001 speculated the atmospheric ^{17}O anomaly was created by the photodecomposition of ozone and the exchange between CO_2 and O. The $\delta^{18}O = +18.3 \pm 0.4$‰ for this sample (Farquhar et al., 1998). Lafayette and Nakhla samples were also evaluated and the authors concluded the Mars carbonates were formed in a low temperature environment without large reservoirs of liquid water in a long-lived, oxidized, reactive surface environment. (Farquhar and Thiemens, 2000). The results identified different isotope values for martian carbonates and silicates in the meteorites (Table 4-4).

Sample	Mass g	Method	CO_2 Yield μmol	$\delta^{18}O$ ‰	$\delta^{17}O$ ‰	$\Delta^{17}O$ ‰
Nakhla.23 j-146	0.90872	25°C AC	0.8	na	na	na
Nakhla.23 j-146bx1p235	0.90872	150°C AC	4.0	31.48	17.34	1.04
Nakhla USNM 426 j-193x1p323	1.93557	H_2O-soluble SO_4	2.0	3.72	0.60	1.33
Nakhla USNM 426 b-36	0.00237	silicate LF	na	4.41	2.61	0.32
Lafayette USNM 1505 j-179	1.04148	25°C AC	0.9	na	na	na
Lafayette USNM 1505 j-179bx1p254	1.04148	150°C AC	3.7	27.64	14.99	0.74
Lafayette USNM 1505 b-34	0.00314	silicate LF	na	4.38	2.60	0.33
ALH 84001.137 b-38	0.00129	silicate LF	na	4.74	2.76	0.30

Here na is not applicable. AC is phosphoric acidification. LF is silicate laser fluorination.

Table 4-4: Prior Nakhlite Oxygen Isotope Values (reprinted from Farquhar and Thiemens, 2000)

The next study (Grady et al., 2007), using an enhanced phosphoric acid extraction procedure with a GC clean-up (to separate sulfur-bearing gases from the CO_2), does not profoundly reduce the range of isotopic values. The acidification was conducted at a single temperature of 72°C, so distinct carbonate species could not be extracted. Petrographic analysis indicated the carbonates were mostly siderite. The Nakhlite samples displayed two orders of magnitude difference in carbonate concentration, with MIL 03346 containing the least (and suspected of containing terrestrial carbonates due to the significantly lower stable isotope values). The authors further suggested that MIL 03346 might have formed at the base of a magma flow (not exposed on the surface of the flow but cooled on the bottom in contact with the cold martian regolith) different than the other Nakhlites (Table 4-5).

Sample	Depth[1]	Yield[2]	$\delta^{13}C$ (‰)	$\delta^{18}O$ (‰)
MIL 03346	1	1	+10.3	+18.7
Y 000593	2	60	+42.0	+26.6
Nakhla	3	27	+51.5	+33.6
GV	4	26	+24.6	+31.3
Lafayette	5	17	+24.8	+29.1

Table 4-5: Updated Nakhlite Stable Isotope Values (reprinted from Grady et al., 2007)

Terrestrial carbonates have a typical value $\Delta^{17}O$=0 ‰, while martian carbonates have values from $\Delta^{17}O$=0.6-0.9 ‰ (average 0.7‰). The meteorite ALH 84001 has a carbonate value of $\Delta^{17}O$=0.7‰. The meteorite Nakhla has $\Delta^{17}O$ > 0.9‰ (Farquhar and Thiemens, 2000). The oxygen source for the carbonates is not CO_2 from the silicates, with a $\Delta^{17}O$=0.32‰ (Franchi et al., 1999). The $\Delta^{17}O$ values of the carbonates have been interpreted as being derived from MIF of in the martian atmosphere (Shaheen et al., 2015) (see Figure 4-6).

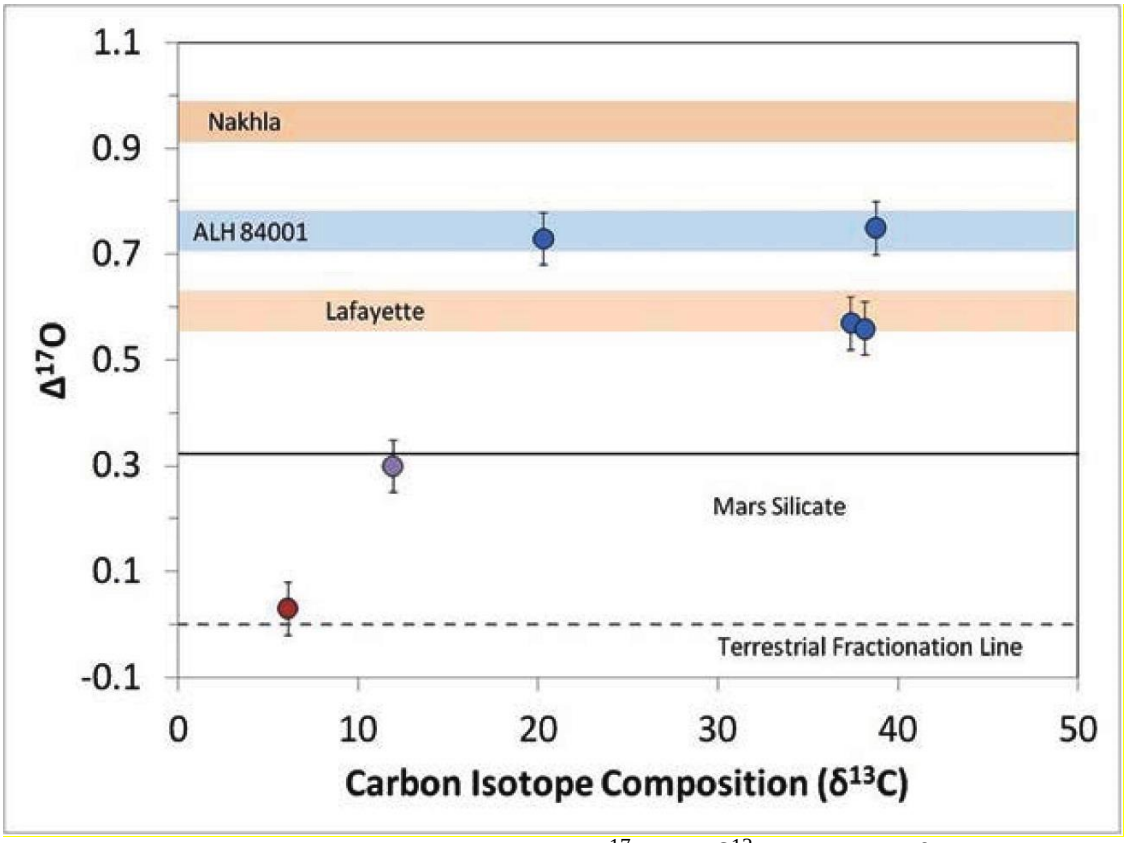

Figure 4-6: Carbonate Planetary Origin using $\Delta^{17}O$ and $\delta^{13}C$ (reprinted from Shaheen et al., 2015)

Ion microprobe analysis of ALH 84001 provides stable isotope measurements of carbonate grain spots 10 to 30 μm in diameter. This procedure is useful to distinguish carbonate species that may be lost in averaging of CO_2 isotope values from acidification extractions of whole rock samples. The microprobe results show a range of values of $\delta^{13}C$ = +27‰ to +64‰ PDB (Niles et al., 2005), which is consistent with the range from bulk rock acidification extraction analysis. These values are much higher than any terrestrial carbonate $\delta^{13}C$ values from OC analysis ($\delta^{13}C$ < +10‰), indicating a carbon

reservoir of martian origin likely exists at $\delta^{13}C > +30‰$ (Romanek et al., 1994, Jull et al., 1995, Jull et al., 1998).

Other ion microprobe measurements of ALH 84001 also show strong correlation between $\delta^{18}O$ and magnesium concentration. When a post-formation aqueous event forms carbonates within the martian rock, the carbonates do not follow this general Mg trend. Discovery of Ca-rich carbonate inclusions in this meteorite, with unique isotopic signatures varying from the expected Mg-rich carbonate minerals, reflects post-formation changes to the martian atmosphere. Although their $\Delta^{17}O$ anomaly is consistent with all martian carbonates, variation in the $\delta^{17}O$ and $\delta^{18}O$ reflect post-formation changes to the martian hydrosphere. ALH 84001 carbonates possess two distinct values: for Ca-rich carbonates $\delta^{13}C=+11.94‰$, while for Fe-Mg carbonates the $\delta^{13}C=+38‰$. These results suggest the carbon isotopic composition of the martian atmosphere has varied substantially since the ALH 84001 meteorite formed ~3.9 Ga. (Shaheen et al., 2015).

A study combining stepped acid extraction technique (12 hours at 25°C for Ca-rich carbonates and 3 hours at 150°C for Fe-Mg-Mn-rich carbonates), fluorination to measure ^{17}O, and ion microprobe analysis of carbonates in ALH 84001 generated measurements of all five carbonate stable isotopes (^{12}C, ^{13}C, ^{16}O, ^{17}O, ^{18}O) (Table 4-6) (Shaheen et al., 2015). If $\Delta^{17}O > 0$, then the carbonates were not formed on Earth. If $\Delta^{17}O = +0.321$, then the carbonate was formed on Mars, as shown in Figures 1-9 and 4-6 (Franchi et al., 1999, Shaheen et al., 2015). The martian carbonates from ALH 84001 reflect formation conditions from the ancient martian climate ~ 4.0 Ga (Gaines et al.,

2009). Stable isotope values from MIL Nakhlite carbonates are much younger, probably 0.5-1.0 Ga (based on speculated iddingsite deposition at 620 mya) (Treiman, 2005).

Sample	Treatment	% CO_3 by mass	CO_2 µmole	O_2 µmole	$\delta^{13}C$	$\delta^{17}O'$*	$\delta^{18}O'$*	$\Delta^{17}O$
ALH84001C	1 h at 25 °C	0.0079	2.69	2.58	6.09	19.16	36.51	0.03
ALH84001C**	12 h at 25 °C	0.01	3.45	3.36	20.27	14.14	25.60	0.73
ALH84001C†	3 h at 150 °C	0.145	14.56	13.8	38.77	11.99	21.46	0.75
ALH84001C‡	Laser fluorination					2.54	4.17	0.36
ALH84001A	3 h at 150 °C	0.13	6.08	5.15	37.37	12.59	22.93	0.57
ALH84001B**	12 h at 25 °C	0.014	0.735	0.65	11.94	18.33	34.42	0.30
ALH84001B†	3 h at 150 °C	0.12	6.09	4.15	38.14	12.17	22.16	0.56
ALH_302_9	SIMS	—	—	—	—	—	17.4 ± 2.0	—
ALH_302_15	SIMS	—	—	—	—	—	20.3 ± 2.2	—

Table 4-6: Updated ALH 84001 Stable Isotope Values (reprinted from Shaheen et al., 2015)

Methodology

The four Miller Range Nakhlite meteorites, MIL 03346, MIL 090030, MIL 090032, and MIL 090136, collected in Antarctica were sampled for stable isotope analysis. The samples were gently crushed and sieved to a size of <700 µm, acidified, reacted, and extracted to collect CO_2 cryogenically using standard techniques (McCrea, 1950, Al-Aasm et al., 1990, Shaheen et al., 2015). Samples of ~1.2g and were reacted with 1.2-1.5 ml of 100% H_3PO_4 at 30°C and 150°C. The CO_2 was extracted at three different steps: 1) Rx0 after 1 hour at 30°C; 2) Rx1 after 18 hours at 30°C, and 3) Rx2 after 3 hours at 150°C. The CO_2 was then separated from other condensable gases using a TRACE GC with a Restek HayeSep Q 80/100 6' 2mm stainless column. A description of the design, installation, testing, and validation of the carbonate extraction and

measurement system is found in Chapter 2. The total error for this analysis is $\delta^{13}C$ = ±0.76‰, $\delta^{18}O$ = ±1.58‰.

The four Antarctic Miller Range (MIL 03346, MIL 090030, MIL 090032, and MIL 090136) Nakhlites contain low carbonate concentrations (avg. 0.006% by wt), as determined from a correlation of known CO_2 standard samples sizes to GC peak count (see Chapter 2). The largest MIL Nakhlite sample, MIL 090032 Rx2 Sample Tube #380 6/13/16, contained 0.87 µmoles of CO_2 with a 100% left bellow signal of 56 mv.

Because of the low carbonate concentrations, the IRMS signal for each sample was very small, ranging from 20 mv to 300 mv (with a fully compressed left bellow) for these Nakhlites. The MAT 253 was modified to capture 100% of the GC purified CO_2 from each Collection Tube (CT). The left bellow pressure gauge was replaced with a small, stainless steel finger tube that fit within a small dewar of liquid N_2, thus allowing a complete transfer of sample from the CT to the IRMS. A relative scale for IRMS sample size is inferred (during the run) from the signal of the uncompressed bellow (100% left bellow), but an actual correlation with GC CO_2 peak size (see eq. 2-12) is used to predict the sample size afterwards. No successful IRMS Rx0 runs were completed on the MIL Nakhlites due to minute amount of carbonate dissolved in 1 hour.

Results

A summary of results for the Nakhlite carbonates from the Antarctic Miller Range are given in Table 4-7, and detailed results are given in Table 4-8. The IRMS machine accuracy for very small signal size was verified with known standard calcite

samples of equivalent size run concurrently with the Nakhlites. A "small sample" size offset is created to correct the $\delta^{13}C$ values for any sample < 5 µmoles (µm) (see Chapter 2 for explanation).

	Meteorite	Reaction	Signal (mv)	d13C avg	d18O avg
MIL	00346	Rx1	46	38.27	26.56
		Rx2	132-216	36.46	9.78
MIL	090030	Rx1	37-200	n/a	n/a
		Rx2	180	26.08	19.12
MIL	090032	Rx1	20-28	31.35	15.77
		Rx2	151-271	41.14	14.60
MIL	090136	Rx1	5	n/a	n/a
		Rx2	80-118	n/a	n/a
	ALL	Rx1	20-200	33.65	19.37
	ALL	Rx2	132-271	36.26	13.57

* Not including MIL 090136 (contaminated runs)

Table 4-7: Summary of Average Miller Range (MIL) Nakhlite Results

Samples with a 100% left bellow signal < 5 mv were discarded as untrustworthy (colored in red on Table 4-8). If a sample run on the IRMS generated a series of measurements that created a line (as determined by the plotted result R^2 value > 0.5), then the run was deemed "contaminated" and the result was not considered valid (colored in purple on Table 4-8). The IRMS measurements for $\delta^{13}C$ and $\delta^{18}O$ are not expected to co-vary in a linear manner during any run (consisting of 10 sequential measurements in "dual inlet' mode), and laboratory experience has shown that linear IRMS runs represent residual contamination in the sample bellows.

MILLER RANGE NAKHLITE RESULTS

Offset Used	HIBBs_1	HIBBs_1	HIBBs_1	HIBBs_1	HIBBs_1	HIBBs_1	HIBBs_1	HIBBs_1
Date	5/23/16	5/31/16	6/2/16, 6/3/16	6/2/16, 6/3/16	6/2/16, 6/6/16	06/09/16	06/13/16	6/15/16
Meteorite	MIL03346	MIL03346	MIL090030	MIL090030	MIL090030	MIL090032	MIL090032	MIL090136
Type	NAK	NAK	NAK	NAK	NAK	NAK	NAK	NAK
Sample Tube (ST)	055	380	966	966	211	375	380	211
total wt (µg)	957863	1369828	1239599	1239599	1095220	1369607	1383163	1359563
Rx0 FT Pressure (mb)	0.4	0.3	3.000	0.000	1.300	0.500	2.96	2.6
Rx0 CO2 Peak time	3.79	3.77	3.72	0.00	3.67	3.65	3.65	3.66
Rx0 CO2 Peak count	1.60E+04	1.50E+04	1.0E+04	0.0E+00	1.2E+04	5.5E+04	4.20E+04	8.00E+03
Rx0 Organic Peak time	0	0	0.00	0.00	0.00	0.00	0	0
Rx0 Organic Peak count	0.00E+00	0.00E+00	0.0E+00	0.0E+00	0.0E+00	0.0E+00	0.00E+00	0.00E+00
Rx0 L100% Signal "clean"					2	6	2	2
Rx0 Correct d13C "clean"					-8.031	15.401	6.135	-16.267
Rx0 Correct d18O "clean"					5.159	28.273	14.532	3.328
Rx0 "clean" R^2 IRMS					0.211	0.744	0.091	0.480
Rx1 FT Pressure (mb)	0.08	1.95	0.240	0.000	1.100	0.380	0.7	0.25
Rx1 CO2 Peak time	3.68	3.69	3.70	0.00	3.72	3.64	3.67	3.65
Rx1 CO2 Peak count	1.00E+04	1.00E+04	1.0E+04	0.0E+00	1.0E+04	5.5E+04	4.00E+04	3.00E+04
Rx1 Organic Peak time		0	0.00	0.00	0.00	0.00	0	0
Rx1 Organic Peak count		0.00E+00	0.0E+00	0.0E+00	0.0E+00	0.0E+00	0.00E+00	0.00E+00
Rx1 L100% signal "clean"		5	6	0	2	3	6	
Rx1 Correct d13C "clean"		34.640	21.505		12.422	24.570	32.893	
Rx1 Correct d18O "clean"		26.557	22.175		17.027	17.561	13.983	
Rx1 "clean" R^2 IRMS		0.181	0.970		0.563	0.110	0.000	
Rx2 FT Pressure (mb)	5.556	10.87	12.975		11.465	11.700	10.83	13.94
Rx2 CO2 Peak time	3.77	3.65	3.62		3.64	3.61	3.71	3.72
Rx2 CO2 Peak count	3.90E+05	5.70E+05	5.6E+05	3.8E+05	4.0E+05	4.8E+05	5.70E+05	6.10E+05
Rx2 Organic Peak time	17.39	16.99	16.70		16.90	16.80	0	16.93
Rx2 Organic Peak count	2.50E+05	4.20E+05	5.5E+05		4.6E+05	4.5E+05	0.00E+00	4.30E+05
Rx2 L100% signal "clean"	25	39	55	28	2	32	56	16
Rx2 Correct d13C "clean"	36.575	34.009	-5.081	24.799	70.720	41.785	38.344	58.569
Rx2 Correct d18O "clean"	11.653	7.906	-20.446	19.117	31.015	14.363	14.829	37.696
Rx2 "clean" R^2 IRMS	0.447	0.090	0.000	0.292	0.022	0.048	0.098	0.633
GC peak to sample size								
Basis (7.48, 1.47)	HIBBs_2,3	HIBBs_2,3	HIBBs_2,3	HIBBs_2,3	HIBBs_2,3	HIBBs_2,3	HIBBs_2,3	HIBBs_2,3
Rx0 µm CO2 (Calcite)	0.02	0.02	0.01	0.00	0.02	0.08	0.06	0.01
Rx1 µm CO2 (Calcite)	0.01	0.01	0.01	0.00	0.01	0.08	0.06	0.04
Rx2 µm CO2 (Sid or Mag)	0.56	0.83	0.84	0.57	0.60	0.72	0.86	0.92
Sample µm CO2	0.60	0.86	0.87	0.57	0.63	0.88	0.98	0.98
%carb (assume calcite)	0.006%	0.006%	0.007%	0.005%	0.006%	0.006%	0.007%	0.007%
Sample Size Offset								
Basis (0.9286, -0.631)	HIBBs_2	HIBBs_2	HIBBs_2	HIBBs_2	HIBBs_2	HIBBs_2	HIBBs_2	HIBBs_2
Rx0 d13C	3.329	3.370	3.591		3.476	2.514	2.684	3.732
Rx1 d13C	3.626	3.626	3.591		3.591	2.514	2.715	2.897
Rx2 d13C	1.296	1.048	1.039	1.281	1.251	1.133	1.022	0.978
FINAL VALUE (Offset, small)								
Rx0 d13C								
Rx0 d18O								
Rx1 d13C		38.27				27.08	35.61	
Rx1 d18O		26.56				17.56	13.98	
Rx2 d13C	37.87	35.06		26.08		42.92	39.37	59.55
Rx2 d18O	11.65	7.91		19.12		14.36	14.83	37.70

Table 4-8: Detail of Miller Range (MIL) Nakhlite Results

This study successfully measured two values for Rx2 (Mg/Fe-rich carbonate) and one combined value for Rx0/Rx1 (Ca-rich carbonate). For MIL 090030, one sample run for Rx0 was completed with an IRMS signal too small to be trustworthy. Both of two sample runs for Rx1 were contaminated with the run $R^2 > 0.5$. Three Rx2 samples runs were completed, but only one successful value was measured (one run contaminated and one run with a too small IRMS signal). With MIL 090032, two sample Rx0 runs were completed with one too small IRMS signal and one contaminated with $R^2 > 0.5$. Two successful sample runs for Rx1 and Rx2 were completed. MIL 090136 had one Rx0 sample run completed with a too small IRMS signal. No sample runs for Rx1 were successfully completed. One sample run for Rx2 was completed with suspected contamination $R^2 = 0.633$.

Discussion

The paired Miller Range (MIL) Nakhlites (MIL 03346, MIL 090030, MIL 090032, and MIL 090036) contain very small amount of carbonate, averaging about 0.006% carbonate by weight. Rx1 reactions generated 0.04 to 0.08 μm of CO_2 from Ca-rich carbonates, and Rx2 reactions generated 0.57 to 0.98 μm of CO_2 from Fe/Mg-rich carbonates. This is much less than the amount of terrestrial carbonates on studied OCs collected in Antarctica (which averaged 0.21% carbonate by weight in Chapter 3). The OCs were selected based upon visible alteration minerals on their fusion crust and the samples were taken from the fusion crust. The martian meteorites were sampled from the interior of the meteorite to minimize possible terrestrial contamination.

The MIL Nakhlite carbonate results have some common characteristics with the terrestrial carbonates measured on OCs. Both have similar $\delta^{18}O$ range of values which suggests a similar formation process. The martian carbonates have a bigger range in $\delta^{13}C$ than the range observed in the OCs. This might be caused by carbonate formation at multiple periods influenced by an evolving martian atmosphere. Combined with prior studies that report martian meteorite stable isotope values, however, it is clear the OCs are different in $\delta^{13}C$ (see Figure 4-7).

Only one previous stable isotope measurement of a MIL Nakhlite carbonate is reported. MIL 03346 values were reported as $\delta^{13}C$ = +10.3‰ ± 2‰ and $\delta^{18}O$ = +18.7‰ ± 2‰ (Grady et al., 2007). These prior values are not consistent with the measured MIL Nakhlite carbonate results in this study, but are consistent with terrestrial carbonates formed on OCs (see Figure 4-7).

As with the OCs, the MIL Nakhlites appear to be two distinct species of carbonates. The Ca-rich carbonate from the Rx1 reaction has $\delta^{13}C_{avg}$ = 33.6‰ ± 5.8‰ (1σ stdev on the data) and $\delta^{18}O_{avg}$ = 19.4‰ ± 6.5‰ (1σ stdev on the data). The Fe/Mg-rich carbonate from the Rx2 reaction (excluding the contamination value from MIL 090136) has $\delta^{13}C_{avg}$ = 36.3‰ ± 6.4‰ (1σ stdev on the data), and $\delta^{18}O_{avg}$ = 13.6‰ ± 4.2‰ (1σ stdev on the data). The distinction between the MIL species is much less than in the OC species.

The $\delta^{13}C$ for all MIL samples (and many of the other martian results) is from +20‰ to +50‰ heavier than the OC samples, indicating a clearly different carbon reservoir for carbonate formation. The prior reported value for MIL 03346 (Grady et al.,

2007) is grouped with the results identified as terrestrial in origin (based on Chapter 3 conclusions), along with LEW 85320 and EET 79001 carbonates.

The range of $\delta^{18}O$ values for these martian carbonate samples, including the MIL Nakhlites, is similar to the OC terrestrial carbonates.

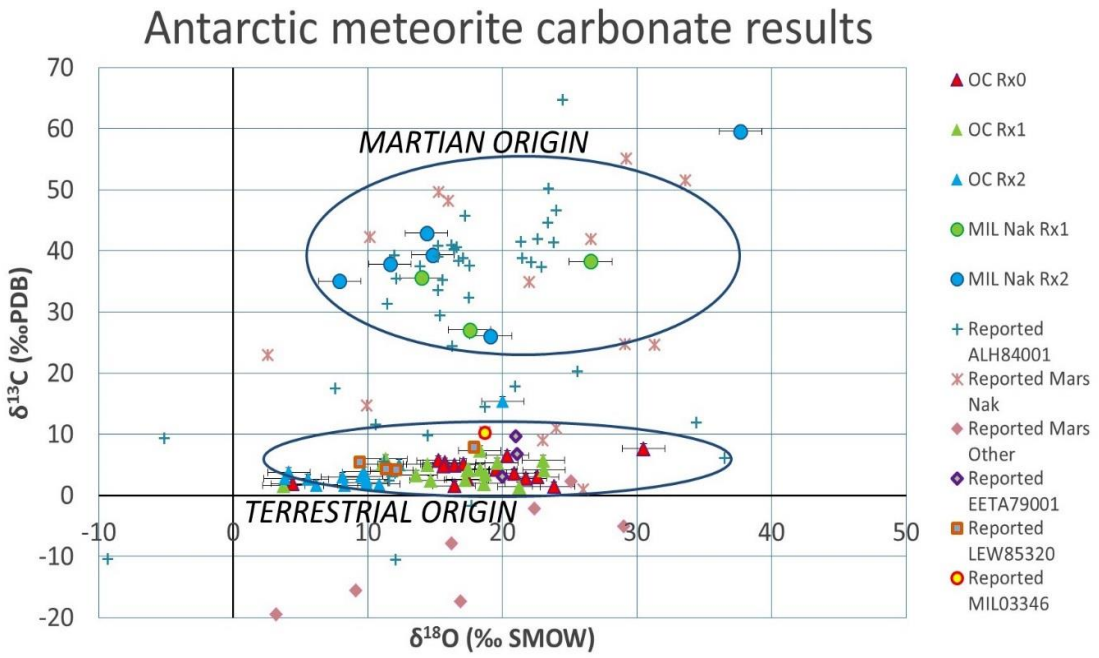

Figure 4-7: Study Nakhlite and OC Meteorite Results with Previously Reported Values

The martian carbonates, both past studies and results from this research, are shown in a labelled ellipse "*MARTIAN ORIGIN*" on Figure 4-7. Excluding the outlier (MIL 090136 possible contamination), the MIL Nakhlite data does not show covariance between the oxygen and carbon isotope values. It is possible, however, to infer a covariance when the prior study data is added from other Nakhlites. If a covariance exists, it is possible to interpret the Nakhlite data as forming from an evaporating brine

or high pH fluid with a general trend of increasing carbonate $\delta^{13}C$ and $\delta^{18}O$ values. This covariance does not appear in the OC terrestrial carbonate data, where the $\delta^{13}C$ is fixed by equilibrium with the Earth's atmospheric CO_2 and the $\delta^{18}O$ is variable based on contribution of different oxygen reservoirs (see discussion in Chapter 3 on $\delta^{18}O$ mixing model). Data values between the "*TERRESTRIAL ORIGIN*" region and the "*MARTIAN ORIGIN*" region possibly represents mixing of extracted CO_2 between both sources.

The parent lava pile was invaded by martian fluids approximately 620 mya (Treiman, 2005) and created carbonates (e.g. Iddingsite) and sulfates (e.g. Jarosite) in the subsurface. Oxygen $\Delta^{17}O$ analysis of Nakhlites and ALH 84001 reflects that the CO_2 in martian carbonate creating fluids was not in equilibrium with silicates (Farquhar et al., 1998, Farquhar and Thiemens, 2000). Thus, the CO_2 source was likely atmospheric CO_2 dissolved in the thin-film water, and not from a magmatic CO_2 reservoir.

High pH fluid is created from low temperature serpentization of ultramafic rocks, which could have happened in the lava pile (Niles et al., 2005, Clark et al., 1992). On Mars, it is possible the fluid became enriched in atmospheric CO_2 on the surface, then invaded the lava pile beneath the surface. On Earth, when this process happens in terrestrial springs, the carbonates that form experience kinetic fractionation leading to a large range in isotope values (see Chapter 3 discussion on "Carbonate Formation Analog from High pH Terrestrial Springs"). The MIL Nakhlite carbonates do not demonstrate a high range of values in $\delta^{13}C$, nor do they display extreme ^{18}O depletion, as expected with kinetic carbonate formation in the CO_2-rich, high pH fluid. Thus, it is assumed the carbonates form in equilibrium with the fluid.

Martian Nakhlite Carbonate Formation Model

The martian subsurface water, containing dissolved CO_2, may have formed thin-films on the rock grains that precipitated carbonates similar to the process that created terrestrial carbonates on OCs collected in Antarctica (see Chapter 3). The relative consistency in carbon values ($\delta^{13}C \sim +40‰$) suggest equilibrium formation with dissolved atmospheric CO_2, as seen with the OC carbonates collected in Antarctica. The wide range in $\delta^{18}O$ values is possible if the equilibrium carbonate formation occurred over a wide range of temperatures, if the process is kinetically dominated, or if the carbonate exchanged oxygen isotopes with two different reservoirs (dissolved CO_2 in the water, and the water itself). This latter explanation is feasible in a very low water/rock environment, such as the thin-film analog of meltwater on Antarctic OC meteorites.

MIL Nakhlite Carbonate $\delta^{13}C$ Values

If the MIL Nakhlite calcite formed in equilibrium with dissolved atmospheric CO_2 in subsurface fluid on Mars at <~15°C (the formation temperature of carbonates on OCs in Antarctica), then the expected Ca-rich (Rx0/Rx1) carbonate $\delta^{13}C$ values can be predicted using fractionation factors (see eq. 1-3) and measurements of the martian atmosphere. The current martian atmospheric CO_2, as measured by MSL, is $\delta^{13}C = 46‰ \pm 4‰$, and $\delta^{18}O = 48‰ \pm 5‰$ (Webster et al., 2013). The Chacko $\delta^{13}C$ fractionation factors for calcite and atmospheric CO_2 (Chacko et al., 1991) are $1000\ln\alpha = -13.59‰$ at 0°C, and $1000\ln\alpha = -11.88‰$ at 15°C. Thus, the expected martian Ca-rich carbonate values should be $\delta^{13}C_{calcite} = 59.6‰$ at 0°C and $\delta^{13}C_{calcite} = 57.9‰$ at 15°C. For the MIL

Nakhlites, the expected carbonate is +25‰ heavier for Rx1 (Ca-rich carbonates), and +22‰ for Rx2 (Fe/Mg-rich carbonates). The Nakhlite carbonate $\delta^{13}C$ values are more consistent with equilibrium formation in an atmospheric CO_2 of $\delta^{13}C$ = +30‰ (see Figure 4-8). It should be noted the value for the Rx2 run on MIL 090036 ($\delta^{13}C$ = +59.71‰, but suspected of being contaminated) is close to the expected value if the carbonate formed in equilibrium with the most recently published value for the modern Mars atmosphere.

The difference between expected equilibrium $\delta^{13}C$ values and what is measured in the MIL Nakhlites may be explained by kinetic fractionation that favors creation of ^{13}C depleted carbonates ($\delta^{13}C$ = -27.5‰ relative to their equilibrium compositions), as found in terrestrial springs with high pH fluids (Clark et al., 1992) (discussion above and in Chapter 3). This should produce carbonates demonstrating a clear covariant relationship that spans the range between equilibrium and kinetic $\delta^{13}C$ values. This might be consistent with the MIL Nakhlite data when the measurement from MIL 090036 is considered, but as discussed above, this data point is likely affected by isobaric contamination. Taking into account all previous measurements of Nakhlite carbonates, a covariant trend may exist consistent with a high pH formation model; however, the range of Nakhlite $\delta^{18}O$ values is greater than predicted even with the kinetic high pH model.

In summary, there are three possible explanations for measured MIL Nakhlite $\delta^{13}C_{calcite}$ values:

a. The Nakhlite Ca-rich carbonates formed in equilibrium with an older, denser Mars atmospheric with $\delta^{13}C \approx +30‰$ (consistent with loss to space)

b. The Nakhlite Ca-rich carbonates formed in equilibrium with the modern Mars atmosphere, but the reported modern martian atmospheric CO_2 $\delta^{13}C$ is incorrect, and the actual $\delta^{13}C$ value is $\approx +30‰$

c. The martian carbonates did not form in equilibrium with the measured modern Mars atmosphere, but were formed kinetically in a high pH solution.

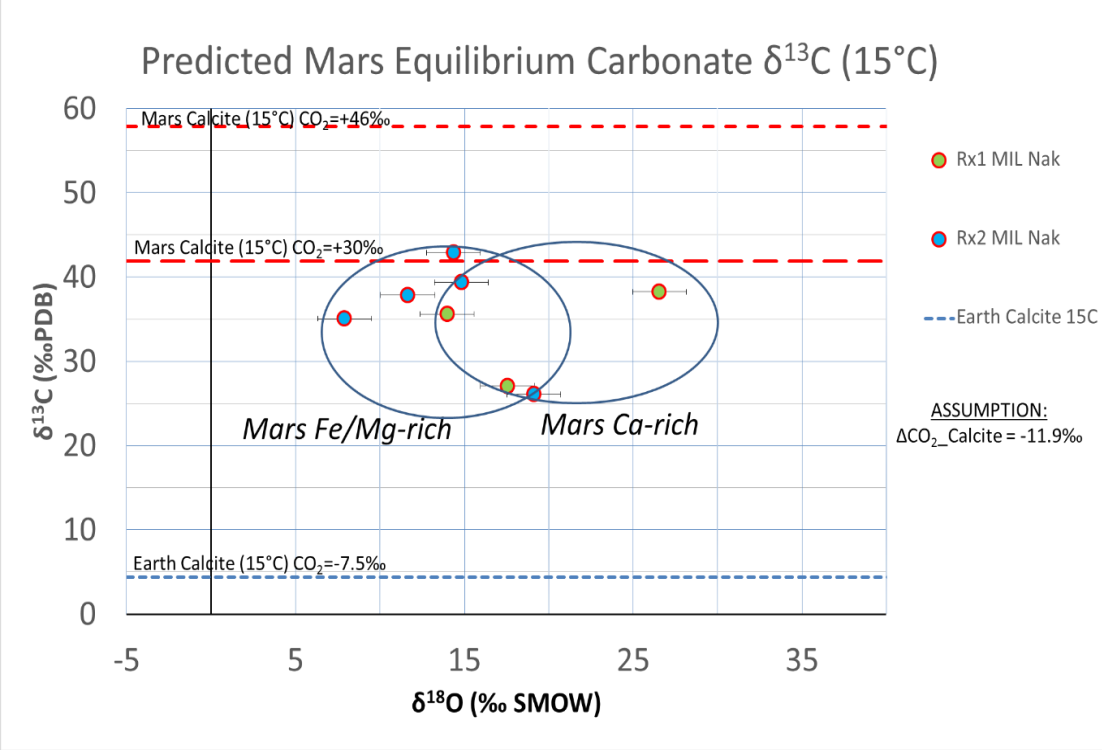

Figure 4-8: Predicted Mars Equilibrium Carbonate $\delta^{13}C$ at 15°C

MIL Nakhlite Carbonate $\delta^{18}O$ Values

The MIL Nakhlite carbonates vary in $\delta^{18}O$ from +7.9‰ to +26.6‰ (not including the MIL 090036 Rx2 suspected contamination measurement). This is not typical for formation from hydrothermal environments, because carbonates formed in aqueous systems would have consistent $\delta^{18}O$ values based upon the formation temperature and $\delta^{18}O$ of the water.

Previously reported stable isotope values for Nakhlites also reflect the wide variability in carbonate $\delta^{18}O$ values. The $\delta^{18}O$ of martian Nakhlite carbonates varies from +26-+36‰ (Saxton et al., 2000, Vicenzi and Eiler, 1998). The large range in $\delta^{18}O$ observed in the Nakhlites (~20‰) is difficult to explain even using the kinetic models. The OC results show an even wider oxygen range ($\delta^{18}O$ ~28‰) when formed in meltwater of pH ~ 0. These wide ranges suggest a formation environment where carbonates formed in a thin-film melt-water, with both the water and the dissolved CO_2 providing oxygen contribution to carbonate formation (Chapter 3). This cold, lower water/rock environment is also analogous to what might be encountered on Mars ~1 Ga. A mixing model with two end-members (meteoric water and dissolved atmospheric CO_2) can predict equilibrium calcite $\delta^{18}O$ values for oxygen contribution from each reservoir (see Figure 3-11). The Ca-rich carbonates appear to form in $\delta^{13}C$ equilibrium with dissolved atmospheric CO_2 at 15°C, which provides a formation temperature for the fractionation factors employed in the $\delta^{18}O$ mixing model. For the OCs, the results show a difference in reservoir contribution based upon reaction type:

OC Rx0/Rx1 (Ca-rich): 45%-85% $\delta^{18}O$ from dissolved atmospheric CO_2

OC Rx2 (Fe/Mg-rich): 20%-55% $\delta^{18}O$ from dissolved atmospheric CO_2

Since the Nakhlite samples were taken from the interior of the meteorite, the sea spray input to Ca-rich carbonate is zero and all the carbonate cations are presumed martian (this is supported by the $\delta^{13}C$ results).

If the MIL Nakhlite carbonates formed on Mars in a thin-film microenvironment like the Rx0/Rx1 Ca-rich carbonates on the Antarctic OCs, then assume the mixing contributions of $\delta^{18}O$ from each end member oxygen reservoir (meteoric water and dissolved CO_2) is the same on Mars as in the OCs. The oxygen contributions for each MIL Nakhlite carbonate species is thus:

Rx0/Rx1 Ca-rich: 35%-85% $\delta^{18}O$ from dissolved atmospheric CO_2

Rx2 Fe/Mg-rich: 20%-60% $\delta^{18}O$ from dissolved atmospheric CO_2

The $\delta^{18}O$ mixing model predicts the martian meteoric water $\delta^{18}O_{water}$ = -30‰ (see Figure 4-9). Note this value falls within the predicted regions for $\delta^{18}O_{water}$ from theoretical predictions (Clayton and Mayeda, 1988).

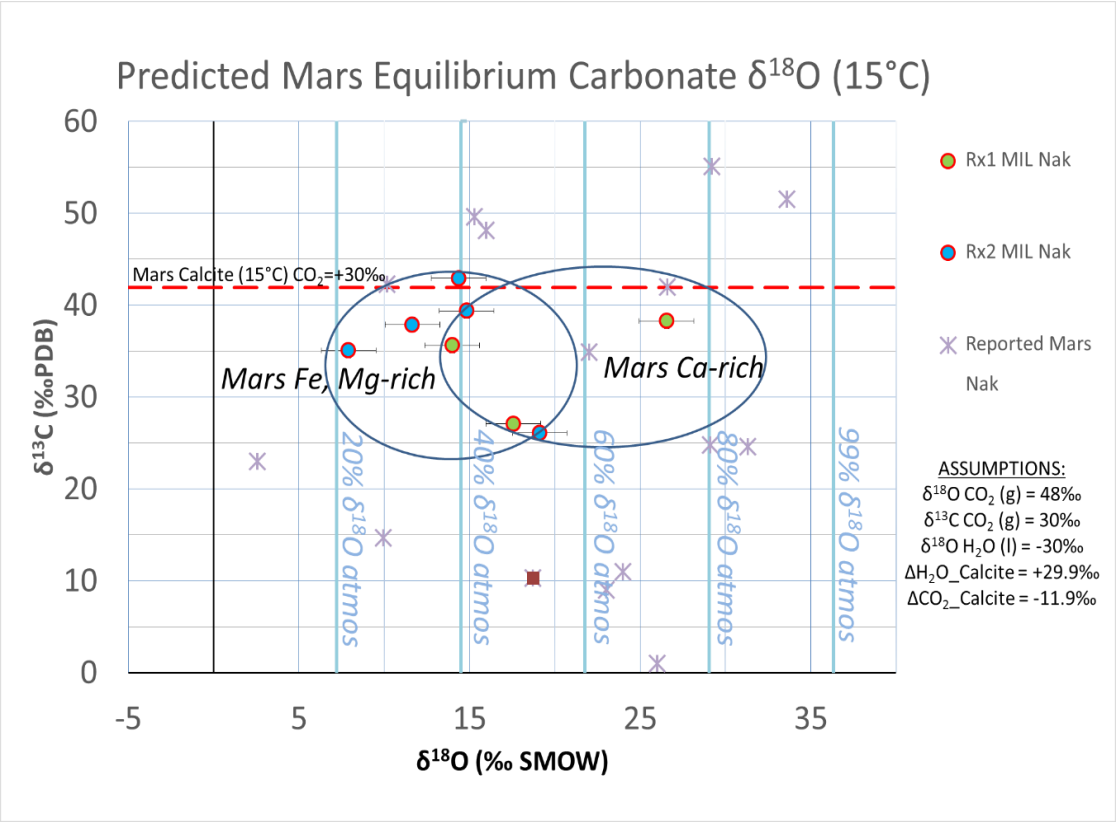

Figure 4-9: Predicted Mars Equilibrium Carbonate $\delta^{18}O$ Mixing at 15°C

Conclusions

MIL Nakhlites possess carbonates that are significantly different from terrestrially formed carbonates on OCs, with a difference of from +20‰ to +50‰ in $\delta^{13}C$. The Nakhlite $\delta^{18}O$ value range is similar to OC terrestrial carbonates. Prior studies of Nakhlites and other martian meteorites report results consistent with the measured MIL Nakhlite stable isotope values (see Figure 4-7).

From the nine successful IRMS measurements, it is concluded the MIL Nakhlites contain two species of carbonates. The Ca-rich carbonate from the Rx1 reaction has $\delta^{13}C_{avg}$ = 33.6‰ ± 5.8‰ (1σ stdev on the data) and $\delta^{18}O_{avg}$ = 19.4‰ ± 6.5‰ (1σ stdev

on the data). The Fe/Mg-rich carbonate from the Rx2 reaction (excluding the contamination value from MIL 090136) has $\delta^{13}C_{avg}$ = 36.3‰ ± 6.4‰ (1σ stdev on the data), and $\delta^{18}O_{avg}$ = 13.6‰ ± 4.2‰ (1σ stdev on the data). The isotopic difference between these two species is less than measured with the OC terrestrial carbonates.

A prior reported result for carbonates in MIL 03346 are inconsistent with the measured values in this study. The prior values for MIL 03346, LEW 85320, and EET 79001 more closely resemble measured stable isotope values for the OCs terrestrial carbonates than for the MIL Nakhlite carbonates (see Figure 4-7), although values with $\delta^{13}C$>10‰ could represent a mixture of CO_2 from carbonates that are from both terrestrial and non-terrestrial sources.

MIL Nakhlite Ca-rich carbonates are not formed in equilibrium with the current Mars atmospheric CO_2 of $\delta^{13}C$ = +46‰, as measured by the Curiosity rover (Mahaffy, 2013) at any reasonable Mars formation temperature. Kinetic fractionation could create lighter carbonate isotope values. The Ca-rich carbonates could have formed in equilibrium with Mars atmospheric CO_2 of $\delta^{13}C$ = +30‰ at 15°C (see Figure 4-7, which is the formation temperature for OC terrestrial carbonates (see Chapter 3). The Nakhlites formed approximately 1.3 Ga (Nyquist 2001) and martian fluids infused the lava pile perhaps 620 mya (Treiman, 2005). Loss of atmosphere to space enriches the remaining stable isotopic values of atmospheric CO_2 (Owen, 1988). The Nakhlite carbonates formed during the Amazonian period, but it is not known if Mars atmospheric loss during this time is sufficient for the $\delta^{13}C$ to increase from +30‰ (carbonate formation) to +46‰ (measured modern Mars atmosphere value).

The wide variability in the MIL Nakhlite carbonate $\delta^{18}O$ values do not resemble expected values for equilibrium formation in an aqueous environment, even for kinetic processes in a high pH fluid. The wide range of values is similar to measured $\delta^{18}O$ terrestrial carbonates formed on the OCs collected in Antarctica. The OC terrestrial carbonates may have formed in a thin-film environment with small amount of trapped melt-water and dissolved atmospheric CO_2 acting as reservoir end-members for oxygen in carbonate formation.

If the carbonates on the Nakhlites formed on Mars in a similar process to the terrestrial carbonates on the OCs in Antarctica, the $\delta^{18}O$ mixing model can be employed to predict formation environmental conditions as: (see Figure 4-9):

$\delta^{18}O$ atmospheric CO_2 = +48‰ (Mahaffy, 2013)

$\delta^{18}O$ water on Mars = -30‰

$\delta^{13}C$ atmospheric CO_2 = +30‰

Carbonate formation temperature = 15°C

CHAPTER V

SUMMARY AND FUTURE WORK

Summary

Two species of terrestrial carbonates were identified on OC meteorites collected in Antarctica. Using OCs with no extraterrestrial carbonate (assumed from their petrological type of 3-6) but with visible terrestrial, alteration minerals (Weathering type "e") on the fusion crust. A Ca-rich and a Fe/Mg-rich carbonate were extracted and measured on the IRMS. These meteorites have a max carbonate content of 0.47% by weight, with an average of 0.21%.

OC carbonates may have formed in a thin-film of meltwater created as the black rock heated on the surface of the ice. The terrestrial meltwater, in direct contact with the atmosphere, contained dissolved atmospheric CO_2. The Ca-rich carbonate likely formed in equilibrium with dissolved atmospheric CO_2 at approximately 15°C (see Figure 3-11). The Fe/Mg-rich carbonates are slightly lighter than the Ca-rich carbonate $\delta^{13}C$ and $\delta^{18}O$ (see Figure 3-10). They may have formed in Antarctica or in the curation facility at NASA/JSC, where the meteorites are stored in a dry N_2 (gas) environment at room temperature. Studies of another OC, LEW 85320, suggest a hydrated Mg-rich mineral, nesquehonite, is growing on the meteorite in the curation facility from outgassing glacial meltwater that is entrained in the grains (see Table 3-1). The measured Fe/Mg-rich carbonates on the OCs may be forming in a similar manner as nesquehonite on LEW 85320.

The range of $\delta^{18}O$ values for the OC carbonates are too heavy for equilibrium formation with Antarctic meteoric water. A new formation model for Antarctic carbonates suggests mixing of oxygen reservoirs from both the meltwater and the dissolved CO_2 in the thin-film. Each species of carbonate has a slightly different mix of oxygen reservoir contributions (see Figure 3-11).

Two species of carbonates were identified on martian Nakhlites collected from the Miller Range in Antarctica. A Ca-rich and a Fe/Mg-rich carbonate were extracted and measured on the IRMS from samples taken from the interior of the meteorites. These meteorites have a max carbonate content of 0.007% by weight, with an average of 0.006%. The carbonates on the MIL Nakhlites are distinct in $\delta^{13}C$ from the OCs, but have a similar range of $\delta^{18}O$ values (see Figure 4-7). These meteorites have a consistent carbonate content of ~0.006% by weight. This low carbonate content was a challenge to extract, separate, and measure in this study.

The Nakhlite carbonates may have also formed in a low water/rock, cold (near 0°C) environment like the OCs. This proposed subsurface martian carbonate formation model is different from other models of large surface lacustrine or marine environments, or from subsurface hydrothermal systems. The Nakhlite carbonates formed in the subsurface. The Nakhlite lava pile may have been infiltrated by water containing dissolved martian atmospheric CO_2 that created thin-films around grains of the parent basalt. The martian crust during the Amazonian period is cold with no residual volcanic or radioactive heat, so the Antarctic formation environment is a good analog for Nakhlite carbonates. As with the OCs, the Ca-rich carbonates may form in $\delta^{13}C$ equilibrium with

the dissolved atmospheric CO_2, while the $\delta^{18}O$ reflects a mixing of contribution from both meteoric melt-water and dissolved atmospheric CO_2.

A kinetic carbonate formation model can also explain the MIL Nakhlite carbonate values if formed in a high pH fluid. This model is consistent with kinetic formation from the modern atmospheric CO_2 as measured by the Curiosity rover. This model predicts carbonates that are up to -27.5‰ (lighter) in $\delta^{13}C$ (Clark et. al, 1992) than the current, measured martian values CO_2 $\delta^{13}C$ = 46‰ (Mahaffy et al., 2013) (see Figure 4-7). This is sufficient to explain the variation in Nakhlite $\delta^{13}C$ stable isotope values; however, the Nakhlite $\delta^{18}O$ range of value is difficult to explain with this model.

This study characterizes distinct terrestrial and martian carbonates based on a difference in $\delta^{13}C$ (see Figure 4-7). Using data from the OC carbonate stable isotope values, evaluation of prior martian meteorite measurements indicates some of these carbonates may be terrestrial in origin, specifically EET 79001 "white druse" (Clayton and Mayeda, 1988, Wright et al., 1988, Jull et al., 1992) See Table 3-2) and MIL 03346 (Grady et al., 2007). The prior reported values for nesquehonite on LEW 85320 (Jull et al., 1988, Grady et al., 1989) (see Table 3-1) are consistent with terrestrial carbonates measured in this study, indicating that some terrestrial carbonates may form after collection in Antarctica.

Future Work

Ion microprobe analysis of the meteorite samples could provide specific mineralogy and stable isotope values for specific grains of carbonate (if they can be

located within the ground meteorite sample), which would be useful as a comparison to the "bulk" carbonate values derived in this dissertation research. This would be easier for the OCs, which were selected due to visible evaporite deposits on the fusion crust, than with the MIL Nakhlites, which have much lower carbonate content than the OCs.

A new stable isotope study of the nesquehonite on LEW 85320 would provide a "3rd generation" value for this terrestrial carbonate, and aid interpretation of the OC Rx2 results.

The 2nd MWG request (dated 3/4/16, see Appendix D) requests OC EET samples from the fusion crust and from within the meteorite. The purpose of this request is to compare stable isotope results from the terrestrial carbonates (on the fusion crust) to any interior carbonates (which are assumed to be null, since this type of meteorite is assumed to be carbonate free before landing on Earth, type 4-6). If any carbonates exist within the meteorite, it is assumed they are secondary, terrestrial alteration products. A stable isotope analysis of the inside and outside of the EET OCs will constrain this assumption.

Every MIL Nakhlite sample was divided so that at least two extractions and IRMS runs could be completed, except for MIL 090036. The only stepped acid extraction stable isotope value for this meteorite is $\delta^{13}C$ = 59.547‰ and $\delta^{18}O$ = 37.696‰ on a run with R2 = 0.633 (suspected of contamination). Although it is available, time constraints prevented the extraction and measurement on the 2nd sample. This sample will be acidified, extracted and run on the IRMS for comparison to the above measurements.

Measurements of $\delta^{17}O$ can identify the carbonate planetary origin (Franchi et al., 1999), but creating the laboratory equipment to measure this stable isotope value has been difficult in the NASA LEAL. Work has been underway for the past 5 years to create an extraction process using BrF_5 to generate O_2 from CO_2 (Clayton and Mayeda, 1963). Eventually, the MIL Nakhlite carbonates will be sampled with this new laboratory apparatus to establish their $\delta^{17}O$ values and verify their planet or origin.

REFERENCES

ABRAMOV, O. & MOJZSIS, S. J. 2016. Thermal effects of impact bombardments on Noachian Mars. *Earth and Planetary Science Letters,* 442**,** 108-120.

AL-AASM, I. S., TAYLOR, B. E. & SOUTH, B. 1990. Stable isotope analysis of multiple carbonate samples using selective acid-extraction. *Chemical Geology,* 80**,** 119-125.

ANDERSON, T. F. A., M.A. 1983. Stable isotopes of carbon and oxygen and their application to sentimentologic and paleoenvironmental studies. *In:* M. A. ARTHUR, E. A. (ed.) *Stable Isotopes in Sedimentary Geology* Tulsa, Ok: SEPM

ASSONOV, S. S. & BRENNINKMEIJER, C. A. M. 2001. A new method to determine the O-17 isotopic abundance in CO2 using oxygen isotope exchange with a solid oxide. *Rapid Communications in Mass Spectrometry,* 15**,** 2426-2437.

ATREYA, S. K., MAHAFFY, P. R. & WONG, A.-S. 2007. Methane and related trace species on Mars: Origin, loss, implications for life, and habitability. *Planetary and Space Science,* 55**,** 358-369.

BANDFIELD, J. L., GLOTCH, T. D. & CHRISTENSEN, P. R. 2003. Spectroscopic identification of carbonate minerals in the martian dust. *Science,* 301**,** 1084-1087.

BANFIELD, J. F., VEBLEN, D. R. & JONES, B. F. 1990. Transmission Electron-Microscopy of Subsolidus Oxidation and Weathering of Olivine. *Contributions to Mineralogy and Petrology,* 106**,** 110-123.

BAO, H., THIEMENS, M. H., FARQUHAR, J., CAMPBELL, D. A., LEE, C. C.-W., HEINE, K. & LOOPE, D. B. 2000. Anomalous 17O compositions in massive sulphate deposits on the Earth. *Nature,* 406**,** 176-178.

BARONI, M., THIEMENS, M. H., DELMAS, R. J. & SAVARINO, J. 2007. Mass-independent sulfur isotopic compositions in stratospheric volcanic eruptions. *Science,* 315**,** 84-87.

BARRÓN, V., TORRENT, J. & GREENWOOD, J. P. 2006. Transformation of jarosite to hematite in simulated Martian brines. *Earth and Planetary Science Letters,* 251**,** 380-385.

BATALHA, N. E., KOPPARAPU, R. K., HAQQ-MISRA, J. & KASTING, J. F. 2016. Climate cycling on early Mars caused by the carbonate–silicate cycle. *Earth and Planetary Science Letters,* 455**,** 7-13.

BAUCH, D., ERLENKEUSER, H. & ANDERSEN, N. 2005. Water mass processes on Arctic shelves as revealed from δ18O of H2O. *Global and Planetary Change,* 48**,** 165-174.

BAUMGARTNER, L. P. & VALLEY, J. W. 2001. Stable isotope transport and contact metamorphic fluid flow. *Reviews in Mineralogy and Geochemistry,* 43**,** 415-467.

BECKER, R. H. 1971. *Carbon and Oxygen Isotope Ratios in Iron-formation and Associated Rock from the Hammersley Range of Western Australia and Their Implications,* Universaity of Chicago.

BECKER, R. H. & CLAYTON, R. N. 1976. Oxygen isotope study of a Precambrian banded iron-formation, Hamersley Range, Western Australia. *Geochimica et Cosmochimica Acta,* 40**,** 1153-1165.

BECKER, R. H. & PEPIN, R. O. 1984. The Case for a Martian Origin of the Shergottites - Nitrogen and Noble-Gases in Eeta-79001. *Earth and Planetary Science Letters,* 69**,** 225-242.

BENDER, M., SOWERS, T. & LABEYRIE, L. 1994. The Dole effect and its variations during the last 130,000 years as measured in the Vostok ice core. *Global Biogeochemical Cycles,* 8**,** 363-376.

BIBRING, J.-P., LANGEVIN, Y., POULET, F., GENDRIN, A., GONDET, B., BERTHÉ, M., SOUFFLOT, A., DROSSART, P., COMBES, M. & BELLUCCI, G. 2004. Perennial water ice identified in the south polar cap of Mars. *Nature,* 428**,** 627-630.

BIBRING, J. P., LANGEVIN, Y., GENDRIN, A., GONDET, B., POULET, F., BERTHE, M., SOUFFLOT, A., ARVIDSON, R., MANGOLD, N., MUSTARD, J., DROSSART, P. & THE, O. T. 2005. Mars surface diversity as revealed by the OMEGA/Mars Express observations. *Science,* 307**,** 1576-1581.

BINZEL, R., REDDY, V. & DUNN, T. 2015. The near-Earth object population: Connections to comets, main-belt asteroids, and meteorites. *Asteroids IV,* 1**,** 243.

BLAND, P. A., ZOLENSKY, M. E., BENEDIX, G. K., SEPHTON, M. A. & MCSWEEN, H. Y. 2006. Weathering of Chondritic Meteorites. *In:* LAURETTA, D. S. (ed.) *Meteorites and the Early Solar System II.*

BOGARD, D. D. & JOHNSON, P. 1983. Martian Gases in an Antarctic Meteorite. *Science,* 221**,** 651-654.

BOGARD, D. D. & PARK, J. 2008. 39Ar-40Ar dating of the Zagami Martian shergottite and implications for magma origin of excess 40Ar. *Meteoritics and Planetary Science,* 43**,** 1113-1126.

BORG, L. E., CONNELLY, J. N., NYQUIST, L. E., SHIH, C. Y., WIESMANN, H. & REESE, Y. 1999. The age of the carbonates in martian meteorite ALH84001. *Science,* 286**,** 90-94.

BOTTINGA, Y. 1968. Calculation of fractionation factors for carbon and oxygen isotopic exchange in the system calcite-carbon dioxide-water. *The Journal of Physical Chemistry,* 72**,** 800-808.

BOUVIER, A., BLICHERT-TOFT, J., VERVOORT, J. D. & ALBAREDE, F. 2005. The age of SNC meteorites and the antiquity of the Martian surface. *Earth and Planetary Science Letters,* 240**,** 221-233.

BOUVIER, A., BLICHERT-TOFT, J., VERVOORT, J. D., GILLET, P. & ALBARÈDE, F. 2008. The case for old basaltic shergottites. *Earth and Planetary Science Letters,* 266**,** 105-124.

BOYNTON, W. V., FELDMAN, W. C., SQUYRES, S. W., PRETTYMAN, T. H., BRUCKNER, J., EVANS, L. G., REEDY, R. C., STARR, R., ARNOLD, J. R., DRAKE, D. M., ENGLERT, P. A. J., METZGER, A. E., MITROFANOV, I., TROMBKA, J. I., D'USTON, C., WANKE, H., GASNAULT, O., HAMARA, D. K., JANES, D. M., MARCIALIS, R. L., MAURICE, S., MIKHEEVA, I., TAYLOR, G. J., TOKAR, R. & SHINOHARA, C. 2002. Distribution of hydrogen in the near surface of Mars: Evidence for subsurface ice deposits. *Science,* 297**,** 81-85.

BRENNINKMEIJER, C., KRAFT, P. & MOOK, W. 1983. Oxygen isotope fractionation between CO 2 and H 2 O. *Chemical Geology,* 41**,** 181-190.

BRIDGES, J. C., CATLING, D. C., SAXTON, J. M., SWINDLE, T. D., LYON, I. C. & GRADY, M. M. 2001. Alteration Assemblages in Martian Meteorites: Implications for Near-Surface Processes. *Space Science Reviews,* 96**,** 365-392.

BRIDGES, J. C. & GRADY, M. M. 2000. Evaporite mineral assemblages in the nakhlite (martian) meteorites. *Earth and Planetary Science Letters,* 176**,** 267-279.

BROECKER, W. & OVERSBY, V. 1971. Distribution of trace isotopes between coexisting phases. *Chemical Equilibrium in the Earth, McGraw-Hill, New York***,** 150-170.

CAROTHERS, W. W., ADAMI, L. H. & ROSENBAUER, R. J. 1988. Experimental oxygen isotope fractionation between siderite-water and phosphoric acid liberated CO2-siderite. *Geochimica et Cosmochimica Acta,* 52**,** 2445-2450.

CARR, M. H. 1996. *Water on Mars,* New York, Oxford University Press.

CASPER, M. 2017. *Meteorites Inc.* [Online]. Available: http://www.caspermeteorites.com/.

CATLING, D. C. 1999. A chemical model for evaporites on early Mars: Possible sedimentary tracers of the early climate and implications for exploration. *Journal of Geophysical Research-Planets,* 104**,** 16453-16469.

CHACKO, T., MAYEDA, T. K., CLAYTON, R. N. & GOLDSMITH, J. R. 1991. Oxygen and carbon isotope fractionations between CO2 and calcite. *Geochimica et Cosmochimica Acta,* 55**,** 2867-2882.

CHANGELA, H. G. & BRIDGES, J. C. 2011. Alteration assemblages in the nakhlites: Variation with depth on Mars. *Meteoritics & Planetary Science,* 45**,** 1847-1867.

CHASSEFIÈRE, E., LANGLAIS, B., QUESNEL, Y. & LEBLANC, F. 2013. The fate of early Mars' lost water: the role of serpentinization. *Journal of Geophysical Research: Planets,* 118**,** 1123-1134.

CHEVRIER, V. F. & RIVERA-VALENTIN, E. G. 2012. Formation of recurring slope lineae by liquid brines on present-day Mars. *Geophysical Research Letters,* 39.

CHIODINI, G., CALIRO, S., AIUPPA, A., AVINO, R., GRANIERI, D., MORETTI, R. & PARELLO, F. 2011. First 13C/12C isotopic characterisation of volcanic plume CO2. *Bulletin of volcanology,* 73**,** 531-542.

CHRISTENSEN, P. R., BANDFIELD, J. L., HAMILTON, V. E., RUFF, S. W., KIEFFER, H. H., TITUS, T. N., MALIN, M. C., MORRIS, R. V., LANE, M. D., CLARK, R. L., JAKOSKY, B. M., MELLON, M. T., PEARL, J. C., CONRATH, B. J., SMITH, M. D., CLANCY, R. T., KUZMIN, R. O., ROUSH, T., MEHALL, G. L., GORELICK, N., BENDER, K., MURRAY, K., DASON, S., GREENE, E., SILVERMAN, S. & GREENFIELD, M. 2001. Mars Global Surveyor Thermal Emission Spectrometer experiment: Investigation description and surface science results. *Journal of Geophysical Research-Planets,* 106**,** 23823-23871.

CLARK, B. C., BAIRD, A. K., ROSE, H. J., TOULMIN, P., KEIL, K., CASTRO, A. J., KELLIHER, W. C., ROWE, C. D. & EVANS, P. H. 1976. Inorganic Analyses of Martian Surface Samples at Viking Landing Sites. *Science,* 194**,** 1283-1288.

CLARK, I. D., FONTES, J. C. & FRITZ, P. 1992. Stable isotope disequilibria in travertine from high pH waters - laboratory investigations and field observations from Oman. *Geochimica et Cosmochimica Acta,* 56**,** 2041-2050.

CLARK, I. D. & FRITZ, P. 1997. *Environmental isotopes in hydrogeology*, CRC press.

CLAYTON, R. N. & MAYEDA, T. K. 1988. Isotopic composition of carbonate in EETA 79001 and its relation to parent body volatiles. *Geochimica et Cosmochimica Acta,* 52**,** 925-927.

CLAYTON, R. N. & MAYEDA, T. K. 1999. Oxygen isotope studies of carbonaceous chondrites. *Geochimica et Cosmochimica Acta,* 63**,** 2089-2104.

COPLEN, T. B. 1988. Normalization of oxygen and hydrogen isotope data. *Chemical Geology: Isotope Geoscience Section,* 72**,** 293-297.

COPLEN, T. B., BRAND, W. A., GEHRE, M., GRONING, M., MEIJER, H. A. J., TOMAN, B. & VERKOUTEREN, R. M. 2006. New guidelines for delta C-13 measurements. *Analytical Chemistry,* 78**,** 2439-2441.

CRAIG, H. 1957. Isotopic Standards for Carbon and Oxygen and Correction Factors for Mass-Spectrometric Analysis of Carbon Dioxide. *Geochimica Et Cosmochimica Acta,* 12**,** 133-149.

CRAIG, H. 1961. Isotopic Variations in Meteoric Waters. *Science,* 133**,** 1702-&.

CRAIG, H. & GORDON, L. Isotopic oceanography: Deuterium and oxygen 18 variations in the ocean and the marine atmosphere, Stable Isotopes in Oceanographic Studies and Paleotemperatures E. Proceedings of the Spoleto Conference E. Tongiorgi, 1965. 9-130.

CUNTZ, M. 2011. Carbon cycle: A dent in carbon's gold standard. *Nature,* 477**,** 547-548.

DANDURAND, J. L., GOUT, R., HOEFS, J., MENSCHEL, G., SCHOTT, J. & USDOWSKI, E. 1982. Kinetically controlled variations of major components and carbon and oxygen isotopes in a calcite-precipitating spring. *Chemical Geology*, 36**,** 299-315.

DANSGAARD, W. 1964. Stable isotopes in precipitation. *Tellus,* 16**,** 436-468.

DARLING, D. 2017. *Asteroids* [Online]. Available: http://www.daviddarling.info/encyclopedia/A/asteroid.html.

DAY, J., TAYLOR, L. A., FLOSS, C. & MCSWEEN, H. Y. 2006. Petrology and chemistry of MIL 03346 and its significance in understanding the petrogenesis of nakhlites on Mars. *Meteoritics & Planetary Science,* 41**,** 581-606.

DEBAILLE, V., BRANDON, A. D., O/'NEILL, C., YIN, Q. Z. & JACOBSEN, B. 2009. Early martian mantle overturn inferred from isotopic composition of nakhlite meteorites. *Nature Geosci,* 2**,** 548-552.

DEHOUCK, E., CHEVRIER, V., GAUDIN, A., MANGOLD, N., MATHÉ, P. & ROCHETTE, P. 2011. ROLE OF SULFIDE-WEATHERING IN THE FORMATION OF SULFATES OR CARBONATES ON MARS. *Lunar Planet. Sci., XLII*.

DEINES, P. 2004. Carbon isotope effects in carbonate systems. *Geochimica et Cosmochimica Acta,* 68**,** 2659-2679.

DICKENS, G. R. 2011. Down the Rabbit Hole: toward appropriate discussion of methane release from gas hydrate systems during the Paleocene-Eocene thermal maximum and other past hyperthermal events. *Clim. Past,* 7**,** 831-846.

DOLE, M. 1936. The Relative Atomic Weight of Oxygen in Water and in Air A Discussion of the Atmospheric Distribution of the Oxygen Isotopes and of the Chemical Standard of Atomic Weights. *Journal of Chemical Physics,* 4**,** 268-275.

DREIBUS, G., BURGHELE, A., JOCHUM, K. P., SPETTEL, B., WLOTZKA, F. & WANKE, H. Chemical and mineral composition of ALH 84001: A martian orthopyroxenite. Meteoritics, July 1, 1994 1994. 29, 461.

EDWARDS, C. S. & EHLMANN, B. L. 2015. Carbon sequestration on Mars. *Geology,* 43**,** 863-866.

EHLMANN, B., BERGER, G., MANGOLD, N., MICHALSKI, J., CATLING, D., RUFF, S., CHASSEFIÈRE, E., NILES, P., CHEVRIER, V. & POULET, F. 2013. Geochemical Consequences of Widespread Clay Mineral Formation in Mars' Ancient Crust. *Space Science Reviews,* 174**,** 329-364.

EILER, J. M. 2001. Oxygen Isotope Variations of Basaltic Lavas and Upper Mantle Rocks. *Reviews in Mineralogy and Geochemistry,* 43**,** 319-364.

EILER, J. M., VALLEY, J. W., GRAHAM, C. M. & FOURNELLE, J. 2002. Two populations of carbonate in ALH84001: Geochemical evidence for discrimination and genesis. *Geochimica et Cosmochimica Acta,* 66**,** 1285-1303.

EMILIANI, C. 1955. Pleistocene temperatures. *The Journal of Geology***,** 538-578.

EMILIANI, C. & SHACKLETON, N. J. 1974. The Brunhes epoch: isotopic paleotemperatures and geochronology. *Science,* 183**,** 511-514.

EPSTEIN, S. & LOWENSTAM, H. A. 1953. Temperature-Shell-Growth Relations of Recent and Interglacial Pleistocene Shoal-Water Biota from Bermuda. *The Journal of Geology,* 61**,** 424-438.

EUGSTER, O., BUSEMANN, H., LORENZETTI, S. & TERREBILINI, D. 2002. Ejection ages from krypton-81-krypton-83 dating and pre- atmospheric sizes of martian meteorites. *Meteoritics & Planetary Science,* 37**,** 1345-1360.

FAIRBANKS, R. G. 1989. A 17, 000-year glacio-eustatic sea level record: influence of glacial melting rates on the Younger Dryas event and deep-ocean circulation. *Nature,* 342**,** 637-642.

FAIREN, A. G., FERNANDEZ-REMOLAR, D., DOHM, J. M., BAKER, V. R. & AMILS, R. 2004. Inhibition of carbonate synthesis in acidic oceans on early Mars. *Nature,* 431**,** 423-426.

FANALE, F. P., SALVAIL, J. R., BRUCE BANERDT, W. & STEVEN SAUNDERS, R. 1982. Mars: The regolith-atmosphere-cap system and climate change. *Icarus,* 50**,** 381-407.

FARQUHAR, J. & THIEMENS, M. H. 2000. Oxygen cycle of the Martian atmosphere-regolith system: Δ17O of secondary phases in Nakhla and Lafayette. *Journal of Geophysical Research: Planets,* 105**,** 11991-11997.

FARQUHAR, J., THIEMENS, M. H. & JACKSON, T. 1998. Atmosphere-Surface Interactions on Mars: Δ17O Measurements of Carbonate from ALH 84001. *Science,* 280**,** 1580-1582.

FASSETT, C. I. & HEAD, J. W. 2008. The timing of martian valley network activity: Constraints from buffered crater counting. *Icarus,* 195**,** 61-89.

FAURE, G. 1986. *Principles of isotope geology,* New York, John Wiley & Sons.

FORGET, F., WORDSWORTH, R., MILLOUR, E., MADELEINE, J.-B., KERBER, L., LECONTE, J., MARCQ, E. & HABERLE, R. M. 2013. 3D modelling of the early martian climate under a denser CO< sub> 2</sub> atmosphere: Temperatures and CO< sub> 2</sub> ice clouds. *Icarus,* 222**,** 81-99.

FORMISANO, V., ATREYA, S., ENCRENAZ, T., IGNATIEV, N. & GIURANNA, M. 2004. Detection of methane in the atmosphere of Mars. *Science,* 306**,** 1758-1761.

FRANCHI, I. A., WRIGHT, I. P., SEXTON, A. S. & PILLINGER, C. T. 1999. The oxygen-isotopic composition of Earth and Mars. *Meteoritics & Planetary Science,* 34**,** 657-661.

FRIEDMAN, H. 2017. *Minerals.net* [Online]. Available: http://www.minerals.net/mineral/jarosite.aspx.

FRIEDMAN, I. 1970. Some investigations of the deposition of travertine from Hot Springs--I. The isotopic chemistry of a travertine-depositing spring*1. *Geochimica et Cosmochimica Acta,* 34**,** 1303-1315.

FRIEDMAN, I. & O'NEIL, J. 1977. Compilation of Stable Isotope Fractionation Factors of Geochemical Interest. *Data of Geochemistry,* 6.

FULIGNATI, P., SBRANA, A., LUPERINI, W. & GRECO, V. 2002. Formation of rock coatings induced by the acid fumarole plume of the passively degassing volcano of La Fossa (Vulcano Island, Italy). *Journal of volcanology and geothermal research,* 115**,** 397-410.

GAINES, S. M., EGLINTON, G. & RULLKOTTER, J. 2009. *Echos of Life - What Fossil Molecules Reveal about Earth History,* New York, New York, Oxford University Press, Inc.

GENDRIN, A., MANGOLD, N., BIBRING, J.-P., LANGEVIN, Y., GONDET, B., POULET, F., BONELLO, G., QUANTIN, C., MUSTARD, J., ARVIDSON, R. & LEMOUELIC, S. 2005. Sulfates in Martian Layered Terrains: The OMEGA/Mars Express View. *Science,* 307**,** 1587-1591.

GEOGRAPHIC, N. 2013. *If All the Ice Melted* [Online]. Available: http://ngm.nationalgeographic.com/2013/09/rising-seas/if-ice-melted-map.

GHASHGHAIE, J. & BADECK, F. W. 2014. Opposite carbon isotope discrimination during dark respiration in leaves versus roots–a review. *New Phytologist,* 201**,** 751-769.

GLEASON, J. D., KRING, D. A., HILL, D. H. & BOYNTON, W. V. 1997. Petrography and bulk chemistry of Martian orthopyroxenite ALH84001: Implications for the origin of secondary carbonates. *Geochimica et Cosmochimica Acta,* 61**,** 3503-3512.

GOLYSHEV, S. I., PADALKO, N. L. & PECHENKIN, S. A. 1981. Fractionation of Stable Isotopes of Carbon and Oxygen in Carbonate Systems. *Geokhimiya***,** 1427-1441.

GOODING, J. L. 1992. Soil Mineralogy and Chemistry on Mars - Possible Clues from Salts and Clays in Snc Meteorites. *Icarus,* 99**,** 28-41.

GOODING, J. L. & MUENOW, D. W. 1986. Martian Volatiles in Shergottite Eeta 79001 - New Evidence from Oxidized Sulfur and Sulfur-Rich Aluminosilicates. *Geochimica Et Cosmochimica Acta,* 50**,** 1049-1059.

GOODING, J. L., WENTWORTH, S. J. & ZOLENSKY, M. E. 1988. Calcium-Carbonate and Sulfate of Possible Extraterrestrial Origin in the Eeta-79001 Meteorite. *Geochimica Et Cosmochimica Acta,* 52**,** 909-915.

GOODING, J. L., WENTWORTH, S. J. & ZOLENSKY, M. E. 1991. Aqueous alteration of the Nakhla meteorite. *Meteoritics,* 26**,** 135-143.

GRADY, M., ANAND, M., GILMOUR, M., WATSON, J. & WRIGHT, I. Alteration of the Nakhlite Lava Pile: Was water on the surface, seeping down, or at depth, percolating up? Evidence (such as it is) from carbonates (abstract# 1826). Lunar and Planetary Institute Conference Abstracts, 2007. 38.

GRADY, M. M. 2000. *Catalogue of Meteorites Reference Book with CD-ROM,* Cambridge University Press.

GRADY, M. M., GIBSON, E., WRIGHT, I. & PILLINGER, C. 1989. The formation of weathering products on the LEW 85320 ordinary chondrite: Evidence from carbon and oxygen stable isotope compositions and implications for carbonates in SNC meteorites. *Meteoritics,* 24**,** 1-7.

GRADY, M. M. & WRIGHT, I. 2006. The carbon cycle on early Earth - and on Mars? *Philosophical Transactions of the Royal Society B-Biological Sciences,* 361**,** 1703-1713.

GRADY, M. M., WRIGHT, I. P., SWART, P. K. & PILLINGER, C. T. 1988. The carbon and oxygen isotopic composition of meteoritic carbonates. *Geochimica et Cosmochimica Acta,* 52**,** 2855-2866.

GROSSMAN, E. 2010. Oxygen isotope stratigraphy. A New Geologic Time Scale. Cambridge Univeristy Press.

GROSSMAN, E. L., MII, H.-S. & YANCEY, T. E. 1993. Stable isotopes in Late Pennsylvanian brachiopods from the United States: Implications for Carboniferous paleoceanography. *Geological Society of America Bulletin,* 105**,** 1284-1296.

GROTZINGER, J. P., CRISP, J., VASAVADA, A. R., ANDERSON, R. C., BAKER, C. J., BARRY, R., BLAKE, D. F., CONRAD, P., EDGETT, K. S. & FERDOWSKI, B. 2012. Mars Science Laboratory mission and science investigation. *Space science reviews,* 170**,** 5-56.

HABERLE, R. M. 1998. Early Mars climate models. *Journal of Geophysical Research-Planets,* 103**,** 28467-28479.

HABERLE, R. M., MCKAY, C. P., SCHAEFFER, J., CABROL, N. A., GRIN, E. A., ZENT, A. P. & QUINN, R. 2001. On the possibility of liquid water on present-day Mars. *J. Geophys. Res.,* 106**,** 23317-23326.

HALLIS, L. J. 2013. Alteration assemblages in the Miller Range and Elephant Moraine regions of Antarctica: Comparisons between terrestrial igneous rocks and Martian meteorites. *Meteoritics and Planetary Science,* 48**,** 165-179.

HALLIS, L. J. & TAYLOR, G. J. 2011. Comparisons of the four Miller Range nakhlites, MIL 03346, 090030, 090032 and 090136: Textural and compositional observations of primary and secondary mineral assemblages. *Meteoritics & Planetary Science,* 46**,** 1787-1803.

HALLIS, L. J., TAYLOR, G. J., NAGASHIMA, K., HUSS, G. R., NEEDHAM, A. W., GRADY, M. M. & FRANCHI, I. A. 2012. Hydrogen isotope analyses of alteration phases in the nakhlite martian meteorites. *Geochimica et Cosmochimica Acta,* 97**,** 105-119.

HARVEY, R. P. & MCSWEEN, H. Y. 1996. A possible high-temperature origin for the carbonates in the Martian meteorite ALH84001. *Nature,* 382**,** 49-51.

HOEFS, J. 2009. Stable isotope geochemistry. Springer Berlin Heidelberg.

HOFFMAN, S. J. & BUSSEY, B. 2016. Human Mars Landing Site and Impacts on Mars Surface Operations.

HOLM, N. G. & CHARLOU, J. L. 2001. Initial indications of abiotic formation of hydrocarbons in the Rainbow ultramafic hydrothermal system, Mid-Atlantic Ridge. *Earth and Planetary Science Letters,* 191**,** 1-8.

HOURDIN, F. D. R., FORGET, F. & TALAGRAND, O. 1995. The sensitivity of the Martian surface pressure and atmospheric mass budget to various parameters: A comparison between. *Journal of Geophysical Research,* 100**,** 5501-5523.

HU, R., KASS, D. M., EHLMANN, B. L. & YUNG, Y. L. 2015. Tracing the fate of carbon and the atmospheric evolution of Mars. *Nature communications,* 6.

HUDSON, J. 1977. Stable isotopes and limestone lithification. *Journal of the Geological Society,* 133**,** 637-660.

HUDSON, J. D. & ANDERSON, T. F. 1989. Ocean temperatures and isotopic compositions through time. *Earth and Environmental Science Transactions of the Royal Society of Edinburgh,* 80**,** 183-192.

HUROWITZ, J. A., MCLENNAN, S. M., TOSCA, N. J., ARVIDSON, R. E., MICHALSKI, J. R., MING, D. W., SCHRODER, C. & SQUYRES, S. W. 2006. In situ and experimental evidence for acidic weathering of rocks and soils on Mars. *Journal of Geophysical Research-Planets,* 111.

INSTITUTION, S. 2017. *ANSMET, the Antarctic Search for Meteorites* [Online]. Available: http://mineralsciences.si.edu/research/meteorites/antarctica/.

JAKOSKY, B. M. & JONES, J. H. 1997. The history of Martian volatiles. *Reviews of Geophysics,* 35**,** 1-16.

JAKOSKY, B. M., PEPIN, R. O., JOHNSON, R. E. & FOX, J. L. 1994. Mars Atmospheric Loss and Isotopic Fractionation by Solar-Wind- Induced Sputtering and Photochemical Escape. *Icarus,* 111**,** 271-288.

JAKOSKY, B. M. & PHILLIPS, R. J. 2001. Mars' volatile and climate history. *Nature,* 412**,** 237-244.

JAMBON, A., SAUTTER, V., BARRAT, J.-A., GATTACCECA, J., ROCHETTE, P., BOUDOUMA, O., BADIA, D. & DEVOUARD, B. 2016. Northwest Africa 5790: Revisiting Nakhlite Petrogenesis. *Geochimica et Cosmochimica Acta,* 190**,** 191-212.

JIMENEZ-LOPEZ, C. & ROMANEK, C. S. 2004. Precipitation kinetics and carbon isotope partitioning of inorganic siderite at 25 degrees C and 1 atm. *Geochimica Et Cosmochimica Acta,* 68**,** 557-571.

JIMENEZ-LOPEZ, C., ROMANEK, C. S., HUERTAS, F. J., OHMOTO, H. & CABALLERO, E. 2004. Oxygen isotope fractionation in synthetic magnesian calcite. *Geochimica et Cosmochimica Acta,* 68**,** 3367-3377.

JOACHIMSKI, M., BREISIG, S., BUGGISCH, W., TALENT, J., MAWSON, R., GEREKE, M., MORROW, J., DAY, J. & WEDDIGE, K. 2009. Devonian climate and reef evolution: insights from oxygen isotopes in apatite. *Earth and Planetary Science Letters,* 284**,** 599-609.

JULL, A., ENGLERT, P., DONAHUE, D. & LINICK, T. Trends in carbon-14 terrestrial ages of Antarctic meteorites from different sites. Lunar and Planetary Science Conference, 1989. 20.

JULL, A. J. T., BECK, J. W. & BURR, G. S. 2000. Isotopic evidence for extraterrestrial organic material in the Martian meteorite, Nakhla. *Geochimica et Cosmochimica Acta,* 64**,** 3763-3772.

JULL, A. J. T., CHENG, S., GOODING, J. L. & VELBEL, M. A. 1988. Rapid Growth of Magnesium-Carbonate Weathering Products in a Stony Meteorite from Antarctica. *Science,* 242**,** 417-419.

JULL, A. J. T., COURTNEY, C., JEFFREY, D. A. & BECK, J. W. 1998. Isotopic evidence for a terrestrial source of organic compounds found in martian meteorites Allan Hills 84001 and Elephant Moraine 79001. *Science,* 279**,** 366-369.

JULL, A. J. T., DONAHUE, D. J., SWINDLE, T. D., BURKLAND, M. K., HERZOG, G. F., ALBRECHT, A., KLEIN, J. & MIDDLETON, R. Isotopic Studies Relevant to the Origin of the "White Druse" Carbonates on EETA 79001. Lunar and Planetary Institute Science Conference Abstracts, March 1, 1992 1992. 23, 641.

JULL, A. J. T., EASTOE, C. J., XUE, S. & HERZOG, G. F. 1995. Isotopic composition of carbonates in the SNC meteorites Allan Hills 84001 and Nakhla. *Meteoritics,* 30**,** 311-318.

KAHN, M. I., OBA, T. & KU, T.-L. 1981. Paleotemperatures and the glacially induced changes in the oxygen-isotope composition of sea water during late Pleistocene and Holocene time in Tanner Basin, California. *Geology,* 9**,** 485-490.

KARLSSON, H. R., JULL, A. J. T., SOCKI, R. A. & GIBSON, E. K., JR. 1991. Carbonates in Antarctic Ordinary Chondrites: Evidence for Terrestrial Origin. *Lunar and Planetary Institute Science Conference Abstracts.*

KARLSSON, H. R., SOCKI, R. A., GIBSON JR, E. K. & BALAFAS, J. S. 1990. Stable isotopic compositions of carbonates in Antarctic ordinary chondrites: Indicators of terrestrial weathering? *Meteoritics,* 25**,** 375.

KARLSSON, K. R., CLAYTON, R. N., GIBSON, E. K. & MAYEDA, T. K. 1992. Water in SNC Meteorites - Evidence for a Martian Hydrosphere. *Science,* 255**,** 1409-1411.

KAUFMANN, P., FUNDEL, F., FISCHER, H., BIGLER, M., RUTH, U., UDISTI, R., HANSSON, M., DE ANGELIS, M., BARBANTE, C. & WOLFF, E. W. 2010. Ammonium and non-sea salt sulfate in the EPICA ice cores as indicator of biological activity in the Southern Ocean. *Quaternary Science Reviews,* 29**,** 313-323.

KEELING, C. D. 1961. The concentration and isotopic abundances of carbon dioxide in rural and marine air. *Geochimica et Cosmochimica Acta,* 24**,** 277-298.

KEELING, C. D. 1979. The Suess effect: 13Carbon-14Carbon interrelations. *Environment International,* 2**,** 229-300.

KOCH, P. L., ZACHOS, J. C. & GINGERICH, P. D. 1992. Correlation between isotope records in marine and continental carbon reservoirs near the Paleocene Eocene boundary.

KOROCHANTSEVA, E. V., SCHWENZER, S. P., BUIKIN, A. I., HOPP, J., OTT, U. & TRIELOFF, M. 2011. 40Ar-39Ar and cosmic-ray exposure ages of nakhlites—Nakhla, Lafayette, Governador Valadares—and Chassigny. *Meteoritics & Planetary Science,* 46**,** 1397-1417.

KRING, D. A., SWINDLE, T. D., GLEASON, J. D. & GRIER, J. A. 1998. Formation and relative ages of maskelynite and carbonate in ALH84001. *Geochimica et Cosmochimica Acta,* 62**,** 2155-2166.

KROOPNICK, P. 1985. The distribution of 13 C of ΣCO 2 in the world oceans. *Deep Sea Research Part A. Oceanographic Research Papers,* 32**,** 57-84.

KROOPNICK, P. & CRAIG, H. 1972. Atmospheric Oxygen: Isotopic Composition and Solubility Fractionation. *Science,* 175**,** 54-55.

LAMMER, H., CHASSEFIÈRE, E., KARATEKIN, Ö., MORSCHHAUSER, A., NILES, P., MOUSIS, O., ODERT, P., MÖSTL, U., BREUER, D., DEHANT, V., GROTT, M., GRÖLLER, H., HAUBER, E. & PHAM, L. 2013. Outgassing History and Escape of the Martian Atmosphere and Water Inventory. *Space Science Reviews,* 174**,** 113-154.

LAMMER, H., KASTING, J. F., CHASSEFIERE, E., JOHNSON, R. E., KULIKOV, Y. N. & TIAN, F. 2008. Atmospheric Escape and Evolution of Terrestrial Planets and Satellites. *Space Science Reviews,* 139**,** 399-436.

LAMMER, H., SELSIS, F., PENZ, T., AMERSTORFER, U. V., LICHTENEGGER, H. I. M., KOLB, C. & RIBAS, I. 2005. Atmospheric Evolution and the History of Water on Mars. *In:* TOKANO, T. (ed.) *Water on Mars and Life.* Berlin Heidelberg: Springer-Verlag.

LAND, L. S. 1980. The isotopic and trace element geochemistry of dolomite: the state of the art.

LEE, M. & MACLAREN, I. 2016. Identifying the Carrier of Martian Water in the Nakhla Meteorite. *Microscopy and Microanalysis,* 22**,** 1806-1807.

LESHIN, L. A., MCKEEGAN, K. D., CARPENTER, P. K. & HARVEY, R. P. 1998. Oxygen isotopic constraints on the genesis of carbonates from Martian meteorite ALH84001. *Geochimica Et Cosmochimica Acta,* 62**,** 3-13.

LUZ, B., BARKAN, E., BENDER, M. L., THIEMENS, M. H. & BOERING, K. A. 1999. Triple-isotope composition of atmospheric oxygen as a tracer of biosphere productivity. *Nature,* 400**,** 547-550.

MADDEN, M. E. E., BODNAR, R. J. & RIMSTIDT, J. D. 2004. Jarosite as an indicator of water-limited chemical weathering on Mars. *Nature,* 431**,** 821-823.

MAHAFFY, P. R., WEBSTER, C. R., ATREYA, S. K., FRANZ, H., WONG, M., CONRAD, P. G., HARPOLD, D., JONES, J. J., LESHIN, L. A. & MANNING, H. 2013. Abundance and isotopic composition of gases in the martian atmosphere from the Curiosity rover. *Science,* 341**,** 263-266.

MALIN, M. C. & EDGETT, K. S. 2000. Sedimentary Rocks of Early Mars. *Science,* 290**,** 1927-1937.

MARSHALL, C. P., FAIRBRIDGE, R. W. & GROSSMAN, E. 1999. *Encyclopedia of geochemistry: Oxygen Isotopes*, Springer.

MARVIN, U. & MOTYLEWSKI, K. Mg-carbonates and sulfates on Antarctic meteorites. Lunar and Planetary Science Conference, 1980. 11, 669-670.

MATEO, M. A., CEBRIÁN, J., DUNTON, K. & MUTCHLER, T. 2006. Carbon flux in seagrass ecosystems. *Seagrasses: Biology, ecology and conservation.* Springer.

MAUERSBERGER, K., ERBACHER, B., KRANKOWSKY, D., GÜNTHER, J. & NICKEL, R. 1999. Ozone isotope enrichment: Isotopomer-specific rate coefficients. *Science,* 283**,** 370-372.

MCBRIDGE, K. M. & RIGHTER, K. 2011. The 100th Anniversary of the Fall of Nakhla: The Subdivision of BM1913, 25.

MCCREA, J. M. 1950. On the Isotopic Chemistry of Carbonates and a Paleotemperature Scale. *The Journal of Chemical Physics,* 18**,** 849.

MCCUBBIN, F. M., ELARDO, S. M., SHEARER, C. K., SMIRNOV, A., HAURI, E. H. & DRAPER, D. S. 2013. A petrogenetic model for the comagmatic origin of chassignites and nakhlites: Inferences from chlorine-rich minerals, petrology, and geochemistry. *Meteoritics & Planetary Science,* 48**,** 819-853.

MCKAY, D. S., GIBSON, J., EVERETT K., THOMAS-KEPRTA, K. L., VALI, H., ROMANEK, C. S., CLEMETT, S. J., CHILLIER, X. D. F., MAECHLING, C. R. & ZARE, R. N. 1996. Search for Past Life on Mars: Possible Relic Biogenic Activity in Martian Meteorite ALH84001. *Science,* 273**,** 924-930.

MCSWEEN, H. Y. & HARVEY, R. P. 1998. An evaporation model for formation of carbonates in the ALH84001 Martian meteorite. *International Geology Review,* 40**,** 774-783.

MIKOUCHI, T., MAKISHIMA, J., KURIHARA, T., HOFFMANN, V. & MIYAMOTO, M. Relative burial depth of nakhlites revisited. Lunar and Planetary Science Conference, 2012. 43, 2363.

MILLER, M. 2002. Isotopic fractionation and the quantification of 17O anomalies in the oxygen three-isotope system. *Geochimica et cosmochimica acta,* 66**,** 1881-1889.

MILONE, E. F. & WILSON, W. J. 2008. Meteorites, Asteroids and the Age and Origin of the Solar System. *Solar System Astrophysics.* Springer.

MORRIS, R. V., RUFF, S. W., GELLERT, R., MING, D. W., ARVIDSON, R. E., CLARK, B. C., GOLDEN, D. C., SIEBACH, K., KLINGELHOFER, G., SCHRODER, C., FLEISCHER, I., YEN, A. S. & SQUYRES, S. W. 2010. Identification of Carbonate-Rich Outcrops on Mars by the Spirit Rover. *Science,* 329**,** 421-424.

MORSE, J. W. & MACKENZIE, F. T. 1990. *Geochemistry of sedimentary carbonates*, Elsevier.

MUEHLENBACHS, K. & CLAYTON, R. N. 1976. Oxygen Isotope Composition of the Oceanic Crust and Its Bearing on Seawater. *J. Geophys. Res.,* 81**,** 4365-4369.

MUMMA, M. J., VILLANUEVA, G. L., NOVAK, R. E., HEWAGAMA, T., BONEV, B. P., DISANTI, M. A., MANDELL, A. M. & SMITH, M. D. 2009. Strong Release of Methane on Mars in Northern Summer 2003. *Science,* 323**,** 1041-1045.

NASA. 2017a. *Mars* [Online]. Available: http://mars.nasa.gov/.

NASA. 2017b. *The Martian Meteorite Compendum* [Online]. NASA. Available: http://curator.jsc.nasa.gov/antmet/mmc/.

NICKELL, L. 1993. A tribute to Hugo P. Kortschak: The man, the scientist and the discoverer of C4 photosynthesis. *Photosynthesis Research,* 35**,** 201-204.

NILES, P. 2017. *What kinds of beer will they serve on Mars?* [Online]. Available: http://beeronmars.blogspot.com/.

NILES, P. B., CATLING, D. C., BERGER, G., CHASSEFIÈRE, E., EHLMANN, B. L., MICHALSKI, J. R., MORRIS, R., RUFF, S. W. & SUTTER, B. 2012. Geochemistry of Carbonates on Mars: Implications for Climate History and Nature of Aqueous Environments. *Space Science Reviews,* 174**,** 301-328.

NILES, P. B., LESHIN, L. A. & GUAN, Y. 2005. Microscale carbon isotope variability in ALH84001 carbonates and a discussion of possible formation environments. *Geochimica et Cosmochimica Acta,* 69**,** 2931-2944.

NOGUCHI, T., NAKAMURA, T., MISAWA, K., IMAE, N., AOKI, T. & TOH, S. 2009. Laihunite and jarosite in the Yamato 00 nakhlites: Alteration products on Mars? *J. Geophys. Res.,* 114.

NYQUIST, L. E., BOGARD, D. D., SHIH, C. Y., GRESHAKE, A., STOFFLER, D. & EUGSTER, O. 2001. Ages and geologic histories of Martian meteorites. *Space Science Reviews,* 96**,** 105-164.

OWEN, T., MAILLARD, J. P., DEBERGH, C. & LUTZ, B. L. 1988. Deuterium on Mars - the Abundance of Hdo and the Value of D/H. *Science,* 240**,** 1767-1770.

OZE, C. & SHARMA, M. 2005. Have olivine, will gas: Serpentinization and the abiogenic production of methane on Mars. *Geophysical Research Letters,* 32.

PARK, J., GARRISON, D. H. & BOGARD, D. D. 2009. 39 Ar–40 Ar ages of martian nakhlites. *Geochimica et Cosmochimica Acta,* 73**,** 2177-2189.

PERRY JR, E. C. 1968. The oxygen isotope chemistry of ancient cherts. *Earth and Planetary Science Letters,* 3**,** 62-66.

PETIT, J.-R., JOUZEL, J., RAYNAUD, D., BARKOV, N., BARNOLA, J.-M., BASILE, I., BENDER, M., CHAPPELLAZ, J., DAVIS, M. & DELAYGUE, G. 1999. Climate and atmospheric history of the past 420,000 years from the Vostok ice core, Antarctica. *Nature,* 399**,** 429-436.

PILSON, M. E. 2012. *An Introduction to the Chemistry of the Sea*, Cambridge University Press.

POLLACK, J. B., KASTING, J. F., RICHARDSON, S. M. & POLIAKOFF, K. 1987. The Case for a Wet, Warm Climate on Early Mars. *Icarus,* 71**,** 203-224.

POPP, B. N., ANDERSON, T. F. & SANDBERG, P. A. 1986. Brachiopods as indicators of original isotopic compositions in some Paleozoic limestones. *Geological Society of America Bulletin,* 97**,** 1262-1269.

POULET, F., BIBRING, J. P., MUSTARD, J. F., GENDRIN, A., MANGOLD, N., LANGEVIN, Y., ARVIDSON, R. E., GONDET, B. & GOMEZ, C. 2005. Phyllosilicates on Mars and implications for early martian climate. *Nature,* 438**,** 623-627.

QUAY, P., EMERSON, S., WILBUR, D., STUMP, C. & KNOX, M. 1993. The δ18O of dissolved O2 in the surface waters of the subarctic Pacific: a tracer of biological productivity. *Journal of Geophysical Research: Oceans (1978–2012),* 98**,** 8447-8458.

RAVEN, J. A. & EDWARDS, D. 2001. Roots: evolutionary origins and biogeochemical significance. *Journal of Experimental Botany,* 52**,** 381-401.

RAYMOND, S. N., QUINN, T. & LUNINE, J. I. 2006. High-resolution simulations of the final assembly of Earth-like planets I. Terrestrial accretion and dynamics. *Icarus,* 183**,** 265-282.

RICHTER, F., CHAUSSIDON, M., MENDYBAEV, R. & KITE, E. 2016. Reassessing the cooling rate and geologic setting of Martian meteorites MIL 03346 and NWA 817. *Geochimica et Cosmochimica Acta,* 182**,** 1-23.

RIGHTER, K., CORRIGAN, C., MCCOY, T. & HARVEY, R. 2014. *35 seasons of US Antarctic meteorites (1976-2010): a pictorial guide to the collection,* John Wiley & Sons.

ROBERTS, J. A., KENWARD, P. A., FOWLE, D. A., GOLDSTEIN, R. H., GONZÁLEZ, L. A. & MOORE, D. S. 2013. Surface chemistry allows for abiotic precipitation of dolomite at low temperature. *Proceedings of the National Academy of Sciences,* 110**,** 14540-14545.

ROMANEK, C. S., GRADY, M. M., WRIGHT, I. P., MITTLEFEHLDT, D. W., SOCKI, R. A., PILLINGER, C. T. & GIBSON, E. K. 1994. Record of fluid-rock interactions on Mars from the meteorite ALH84001. *Nature,* 372**,** 655-657.

ROMANEK, C. S., GROSSMAN, E. L. & MORSE, J. W. 1992. Carbon Isotopic Fractionation in Synthetic Aragonite and Calcite - Effects of Temperature and Precipitation Rate. *Geochimica et Cosmochimica Acta,* 56**,** 419-430.

ROSENBAUM, J. & SHEPPARD, S. M. F. 1986. An Isotopic Study of Siderites, Dolomites and Ankerites at High-Temperatures. *Geochimica Et Cosmochimica Acta,* 50**,** 1147-1150.

SALTZMAN, M. R., GROESSENS, E. & ZHURAVLEV, A. V. 2004. Carbon cycle models based on extreme changes in delta C-13: an example from the lower Mississippian. *Palaeogeography Palaeoclimatology Palaeoecology,* 213**,** 359-377.

SAUTTER, V., TOPLIS, M. J., LORAND, J. P. & MACRI, M. 2012. Melt inclusions in augite from the nakhlite meteorites: A reassessment of nakhlite parental melt and implications for petrogenesis. *Meteoritics & Planetary Science,* 47**,** 330-344.

SAXTON, J. M., LYON, I. C., CHATZITHEODORIDIS, E. & TURNER, G. 2000. Oxygen isotopic composition of carbonate in the Nakhla meteorite: Implications for the hydrosphere and atmosphere of Mars. *Geochimica et Cosmochimica Acta,* 64**,** 1299-1309.

SAXTON, J. M., LYON, I. C. & TURNER, G. 1998. Oxygen Isotopic Composition of Nakhla Siderite: Implications for Martian Volatiles. *Meteoritics & Planetary Science, vol. 33, p. A172,* 33**,** 172.

SCOTT, E. R. D. & KROT, A. N. 1998. Formation of preimpact, interstitial carbonates in the Allan Hills 84001 Martian meteorite. *In:* ANONYMOUS (ed.) *61st Meteoritical Society meeting; abstracts.* Fayetteville, AR, United States: Meteoritical Society.

SCOTT, E. R. D., KROT, A. N. & YAMAGUCHI, A. 1997. Formation of carbonates in Martian meteorite Allan Hills 84001 from shock melts. *Meteoritics & Planetary Science,* 32**,** A117-A118.

SHACKLETON, N. J. 2000. The 100,000-Year Ice-Age Cycle Identified and Found to Lag Temperature, Carbon Dioxide, and Orbital Eccentricity. *Science,* 289**,** 1897-1902.

SHAHEEN, R., NILES, P. B., CHONG, K., CORRIGAN, C. M. & THIEMENS, M. H. 2015. Carbonate formation events in ALH 84001 trace the evolution of the Martian atmosphere. *Proceedings of the National Academy of Sciences,* 112**,** 336-341.

SHARMA, T. & CLAYTON, R. N. 1965. Measurement of 18O/16O ratios of total oxygen of carbonates. *Geochimica Et Cosmochimica Acta,* 29**,** 1347-&.

SHARP, Z. 2007. *Principles of stable isotope geochemistry*, Pearson education Upper Saddle River, NJ.

SOCIETY, M. 2017. *Meteorites* [Online]. Available: http://meteoriticalsociety.org/.

SQUYRES, S. W., GROTZINGER, J. P., ARVIDSON, R. E., BELL, J. F., CALVIN, W., CHRISTENSEN, P. R., CLARK, B. C., CRISP, J. A., FARRAND, W. H., HERKENHOFF, K. E., JOHNSON, J. R., KLINGELHOFER, G., KNOLL, A. H., MCLENNAN, S. M., MCSWEEN, H. Y., MORRIS, R. V., RICE, J. W., RIEDER, R. & SODERBLOM, L. A. 2004. In situ evidence for an ancient aqueous environment at Meridiani Planum, Mars. *Science,* 306**,** 1709-1714.

STOPAR, J. D., TAYLOR, G. J., VELBEL, M. A., NORMAN, M. D., VICENZI, E. P. & HALLIS, L. J. 2013. Element abundances, patterns, and mobility in Nakhlite Miller Range 03346 and implications for aqueous alteration. *Geochimica et Cosmochimica Acta,* 112**,** 208-225.

SWART, P., GRADY, M. & PILLINGER, C. 1983. A method for the identification and elimination of contamination during carbon isotopic analyses of extraterrestrial samples. *Meteoritics,* 18**,** 137-154.

SWINDLE, T. D., TREIMAN, A. H., LINDSTROM, D. J., BURKLAND, M. K., COHEN, B. A., GRIER, J. A., LI, B. & OLSON, E. K. 2000. Noble gases in iddingsite from the Lafayette meteorite: Evidence for liquid water on Mars in the last few hundred million years. *Meteoritics & Planetary Science,* 35**,** 107-115.

TAO, K., ROBBINS, J. A., GROSSMAN, E. L. & O'DEA, A. 2013. *Quantifying upwelling and freshening in nearshore tropical American environments using stable isotopes in modern gastropods* [Online].

THIEMENS, M. H. 1999. Mass-independent isotope effects in planetary atmospheres and the early solar system. *Science,* 283**,** 341-345.

THIEMENS, M. H., JACKSON, T. L. & BRENNINKMEIJER, C. A. M. 1995. Observation of a Mass-Independent Oxygen Isotopic Composition in Terrestrial Stratospheric Co2, the Link to Ozone Chemistry, and the Possible Occurrence in the Martian Atmosphere. *Geophysical Research Letters,* 22**,** 255-257.

TREIMAN, A. H. 1995. A petrographic history of Martian meteorite ALH84001 - 2 shocks and an ancient age. *Meteoritics,* 30**,** 294-302.

TREIMAN, A. H. 2005. The nakhlite meteorites: Augite-rich igneous rocks from Mars. *Chemie der Erde-Geochemistry,* 65**,** 203-270.

TREIMAN, A. H., AMUNDSEN, H. E. F., BLAKE, D. F. & BUNCH, T. 2002. Hydrothermal origin for carbonate globules in Martian meteorite ALH84001: A terrestrial analogue from Spitsbergen (Norway). *Earth and Planetary Science Letters,* 204**,** 323-332.

TWELKER, E. T. J. 2017. The Meteorite Market. Available: http://meteoriticalsociety.org/

UDISTI, R., DAYAN, U., BECAGLI, S., BUSETTO, M., FROSINI, D., LEGRAND, M., LUCARELLI, F., PREUNKERT, S., SEVERI, M. & TRAVERSI, R. 2012. Sea spray aerosol in central Antarctica. Present atmospheric behaviour and implications for paleoclimatic reconstructions. *Atmospheric Environment,* 52**,** 109-120.

UDRY, A., MCSWEEN JR, H. Y., LECUMBERRI-SANCHEZ, P. & BODNAR, R. J. 2012. Paired nakhlites MIL 090030, 090032, 090136, and 03346: Insights into the Miller Range parent meteorite. *Meteoritics & Planetary Science,* 47**,** 1575-1589.

UREY, H. C. 1947. The Thermodynamic Properties of Isotopic Substances. *Journal of the Chemical Society***,** 562-581.

UREY, H. C. & CRAIG, H. 1953. The composition of the stone meteorites and the origin of the meteorites. *Geochimica et Cosmochimica Acta,* 4**,** 36-82.

UREY, H. C., LOWENSTAM, H. A., EPSTEIN, S. & MCKINNEY, C. R. 1951. Measurement of paleotemperatures and temperatures of the Upper Cretaceous of England, Denmark, and the southeastern United States. *Geological Society of America Bulletin,* 62**,** 399-416.

USDOWSKI, E. 1982. Reactions and equilibria in the systems CO2-H2O and CaCO3-CO2- H2O (O-degrees-C-50-degrees-C) - a review. *Neues Jahrbuch Fur Mineralogie-Abhandlungen,* 144**,** 148-171.

VAN SCHMUS, W. & WOOD, J. A. 1967. A chemical-petrologic classification for the chondritic meteorites. *Geochimica et Cosmochimica Acta,* 31**,** 747IN7755-754IN10765.

VELBEL, M. A. 1988. The Distribution and Significance of Evaporitic Weathering Products on Antarctic Meteorites. *Meteoritics,* 23**,** 151-159.

VELBEL, M. A. 2014. Terrestrial weathering of ordinary chondrites in nature and continuing during laboratory storage and processing: Review and implications for Hayabusa sample integrity. *Meteoritics & Planetary Science,* 49**,** 154-171.

VELBEL, M. A. 2016. Aqueous Corrosion of Olivine in the Mars Meteorite Miller Range (MIL) 03346 During Antarctic Weathering: Implications for Water on Mars. *Geochimica et Cosmochimica Acta*.

VERKOUTEREN, R. M. 1999. Preparation, characterization, and value assignment of carbon dioxide isotopic reference materials: RMs 8562, 8563, and 8564. *Analytical Chemistry,* 71**,** 4740-4746.

VICENZI, E. P. & EILER, J. 1998. Oxygen Isotopic Composition and High-Resolution Secondary Ion Mass Spectrometry Imaging of Martian Carbonate in Lafayette Meteorite. *Meteoritics and Planetary Science Supplement,* 33**,** 159.

WANNINKHOF, R. 1985. Kinetic fractionation of the carbon isotopes 13C and 12C during transfer of CO2 from air to seawater. *Tellus B,* 37**,** 128-135.

WARREN, P. H. 1998. Petrologic evidence for low-temperature, possibly flood evaporitic origin of carbonates in the ALH84001 meteorite. *Journal of Geophysical Research-Planets,* 103**,** 16759-16773.

WASSON, J. T. 1985. Meteorites: their record of early solar-system history.

WASSON, J. T. 2012. *Meteorites: Classification and properties*, Springer Science & Business Media.

WATSON, L. L., HUTCHEON, I. D., EPSTEIN, S. & STOLPER, E. M. 1994. Water on Mars - Clues from Deuterium/Hydrogen and Water Contents of Hydrous Phases in Snc Meteorites. *Science,* 265**,** 86-90.

WEBSTER, C. R. Mars atmospheric escape recorded by H, C and O isotope ratios in carbon dioxide and water measured by the Sam Tunable Laser Spectrometer on the Curiosity Rover. LPSC, 2013 Woodlands, TX.

WENTWORTH, S. J., GIBSON, E. K., VELBEL, M. A. & MCKAY, D. S. 2005. Antarctic Dry Valleys and indigenous weathering in Mars meteorites: Implications for water and life on Mars. *Icarus,* 174**,** 383-395.

WHITICAR, M. 1996. Stable isotope geochemistry of coals, humic kerogens and related natural gases. *International Journal of Coal Geology,* 32**,** 191-215.

WICKRAMASINGHE, C. 2015. Comment on Liquid Water and Life on Mars. *Astrobiol Outreach,* 3**,** e111.

WIECHERT, U. H., HALLIDAY, A. N., PALME, H. & RUMBLE, D. 2004. Oxygen isotope evidence for rapid mixing of the HED meteorite parent body. *Earth and Planetary Science Letters,* 221**,** 373-382.

WINGATE, L., SEIBT, U., MONCRIEFF, J. B., JARVIS, P. G. & LLOYD, J. 2007. Variations in 13C discrimination during CO2 exchange by Picea sitchensis branches in the field. *Plant, Cell & Environment,* 30**,** 600-616.

WOOD, C. A. & ASHWAL, L. D. 1981. SNC meteorites: Igneous rocks from Mars. *Proc. Lunar Planet. Sci. B,* 12**,** 1359-1375.

WORDSWORTH, R., KALUGINA, Y., LOKSHTANOV, S., VIGASIN, A., EHLMANN, B., HEAD, J., SANDERS, C. & WANG, H. 2017. Transient reducing greenhouse warming on early Mars. *Geophysical Research Letters*.

WRAY, J. J., MURCHIE, S. L., BISHOP, J. L., EHLMANN, B. L., MILLIKEN, R. E., WILHELM, M. B., SEELOS, K. D. & CHOJNACKI, M. 2016. Orbital evidence for more widespread carbonate-bearing rocks on Mars. *Journal of Geophysical Research: Planets,* 121**,** 652-677.

WRIGHT, I. P., GRADY, M. M. & PILLINGER, C. T. 1988. Carbon, Oxygen and Nitrogen Isotopic Compositions of Possible Martian Weathering Products in EETA-79001. *Geochimica Et Cosmochimica Acta,* 52**,** 917-924.

WRIGHT, I. P., GRADY, M. M. & PILLINGER, C. T. 1992. Chassigny and the Nakhlites - Carbon-Bearing Components and Their Relationship to Martian Environmental-Conditions. *Geochimica Et Cosmochimica Acta,* 56**,** 817-826.

YABUKI, H., OKADA, A. & SHIMA, M. 1976. Nesquehonite found on the Yamato 74371 meteorite. *Sci. Pap. Inst. Phys. Chem. Res., Vol. 70, No. 1, p. 22-29,* 70**,** 22-29.

ZACHOS, J., PAGANI, M., SLOAN, L., THOMAS, E. & BILLUPS, K. 2001. Trends, rhythms, and aberrations in global climate 65 Ma to present. *Science,* 292**,** 686-693.

ZAHNLE, K., FREEDMAN, R. S. & CATLING, D. C. 2011. Is there methane on Mars? *Icarus,* 212**,** 493-503.

ZHANG, C. L., HORITA, J., COLE, D. R., ZHOU, J. Z., LOVLEY, D. R. & PHELPS, T. J. 2001a. Temperature-dependent oxygen and carbon isotope fractionations of biogenic siderite. *Geochimica et Cosmochimica Acta,* 65**,** 2257-2271.

ZHANG, H.-F., MENZIES, M. A., MATTEY, D. P., HINTON, R. W. & GURNEY, J. J. 2001b. Petrology, mineralogy and geochemistry of oxide minerals in polymict xenoliths from the Bultfontein kimberlites, South Africa: implication for low bulk-rock oxygen isotopic ratios. *Contributions to Mineralogy and Petrology,* 141**,** 367-379.

APPENDIX A

ACRONYMS

ALH	Allan Hills region of Antarctica
ANSMET	Antarctic Search for Meteorites (group funded by NSF)
Bya	Billion years ago (dating in geologic time)
CAI	Calcium-Aluminum Inclusions (component of chondrites)
CC	Carbonaceous Chondrite
CRISM	Compact Reconnaissance Imaging Spectrometer for Mars (CRISM) instrument of MRO for identification of martian surface minerals
CT	Collection Tube, used to store CO_2 gas for transfer between components
CT_k	A specific CT used for YIELD calculations. The volume is known from measurements of the ST filled with water compared to the empty weight. This volume is 7.121 ml ± 0.302 ml (2σ standard deviation)
DIC	Dissolved Inorganic Carbon
DSR	Differentiated Silicate-Rich meteorites
EC	Enstatite Chondrite
EET	Elephant Moraine region of Antarctica
FT_c	Finger Tube located on the carbonate extraction line
FT_i	Finger Tube replacing the IRMS left bellow (sample) pressure gauge
Ga, Gy	Billion years ago, on Mars (dating in geologic time)
GEL	Global Equivalent Layer, measurement of water volume on Mars
GC	Gas Chromatography, or Gas Chromatograph (instrument). For this analysis, the instrument is a TRACE GC with a Restek HayeSep Q 80/100 6’ 2mm stainless column
GV	Governador Valadares, a martian Nakhlite meteorite

HED	Howardite-Eucrite-Diogenite type of meteorite which may have formed on the asteroid 4 Vesta
HIBB	Hawaiian Island Basalt sand
HIBBs	HIBB terrestrial regolith spiked with a known carbonate standard
IR	Infra-red spectrum of light (wavelengths from 0.7- 1000 microns)
IRMS	Isotope Ratio Mass Spectrometer. For this analysis the IRMS is a Thermo Mat 253 instrument running dual inlet mode
JSC	Johnson Space Center, a NASA facility located in Houston, Tx.
LEAL	Light Element Analysis Laboratory, at NASA-JSC in Houston, Tx.
LHB	Late Heavy Bombardment period, from 3.8-4.1 Ga depending on models
LREE	Light Rare Earth Elements (including Lanthanum, Cerium, Praseodymium, Neodymium, Promethium, and Samarium)
MDF	Mass Dependent Fractionation
MGS	Mars Global Surveyor (launched 11/7/96, lost 4/13/07 in Mars orbit)
MIF	Mass Independent Fractionation
MIL	Miller Range region of Antarctica
MR_c	Mole Ratio of carbonate reaction acidified in phosphoric acid (=1.0)
MW_c	Molecular Weight of carbonates (calcite = 110.09 g/mole, siderite = 115.86 g/mole)
MWG	Meteorite Working Group
MPL	Meteorite Processing Lab, located at NASA/JSC in Houston, Tx.
MRO	Mars Reconnaissance Orbiter (launched 8/12/2005)
Mya	Million years ago (dating in geologic time)
NADW	North Atlantic Deep Water

NASA	National Aeronautics and Aerospace Administration
NSF	National Science Foundation
OC	Ordinary Chondrite
PAH	Polycyclic Aromatic Hydrocarbons (important for ALH-84001)
PC	Personal Computer (Windows Operating System, various versions)
P_{FTc}	Pressure reading from the carbonate extraction line Finger Tube gauge
P_p	Predicted Pressure
RBT	Robertson Bay region of Antarctica
Rx0	The first reaction in stepped extractions: 30°C for 1 hour. This reaction is targeted to extract terrestrial, fine-grained calcite that formed on the meteorites after they landed in Antarctica
Rx1	The second reaction in stepped extractions: 30°C for 18 hours. This reaction is targeted to extract in-situ calcites
Rx2	The third reaction in stepped extractions: 150°C for 3 hours. This reaction is targets to extract ins-situ magnesites and/or siderites
SNC	"Shergotty – Nakhla – Chassigny" group of martian meteorites
Sol	One martian day, equivalent to 24 hours 39 minutes on Earth. One martian year is 668 sols, or 687 Earth days
ST	Sample Tube, used to react acid with the regolith in a side-arm vessel
SEM	Scanning Electron Microscope/Microscopy
TEM	Transmission Electron Microscope/Microscopy
TES	Thermal Emission Spectrometer: Instrument on the MGS mapping the martian surface with infrared scans
TFL	Terrestrial Fractionation Line, based on correlation of $\delta^{17}O$ v $\delta^{18}O$ in silicates for each planet
Ya, ya	Years ago (dating) – billion years ago (bya), million years ago (mya)

APPENDIX B

SUPPLEMENTAL CARBONATE METHODOLOGY

Detailed Procedure

Sample Preparation

This section provides the detailed procedure for preparing each sample, extracting the CO_2, and measuring the carbonate stable isotopes. Detailed discussion of individual components of the procedure is provided afterwards. A worksheet developed to document each step of the process, and record sample results, is given in Appendix C. In general, the laboratory procedure to measure stable isotope values on CO_2 from acidified meteorite carbonates is as follows:

1. Crush meteorites, weigh samples, then acidify samples with known amount of phosphoric acid (H_3PO_4) in a Sample Tube (ST),
2. Heat the ST for designated period at designated temperature,
3. Extract CO_2 from ST on the Carbonate Extraction Line, measure CO_2 Yield (only for carbonate standards) and capture the CO_2 in a Collect Tube (CT),
4. Move the CT to the GC, load the CO_2 into the GC inlet loop, purify the CO_2 with a GC run, log the CO_2 peak and any other peaks, capture the purified CO_2 in the GC outlet loop, then transfer the purified CO_2 back to the CT,
5. Move the CT to the IRMS, load the purified CO_2 into the left bellow (using a dewar on the installed small finger tube for meteorite samples), adjust and record the IRMS left/right bellow pressure and signal, run the IRMS, and

record the raw $\delta^{13}C$, raw $\delta^{18}O$, and R^2 for the run (to assess if the sample is contaminated).

Each solid rock sample is first ground with a mortar and pestle. The meteorite powder is sieved for weighing. Each sample is carefully weighed into a clean Sample Tube (ST) and a small, measured volume of 100% phosphoric acid (from 0.5 ml to 1.5 ml depending on sample size) is loaded into the ST side-arm. Note this acid has been in the LEAL laboratory for over 10 years; the purity was not tested before the experiments. The ST is heated to the desired temperature before mixing the acid with the sample in vacuo, as shown in Figure B-1.

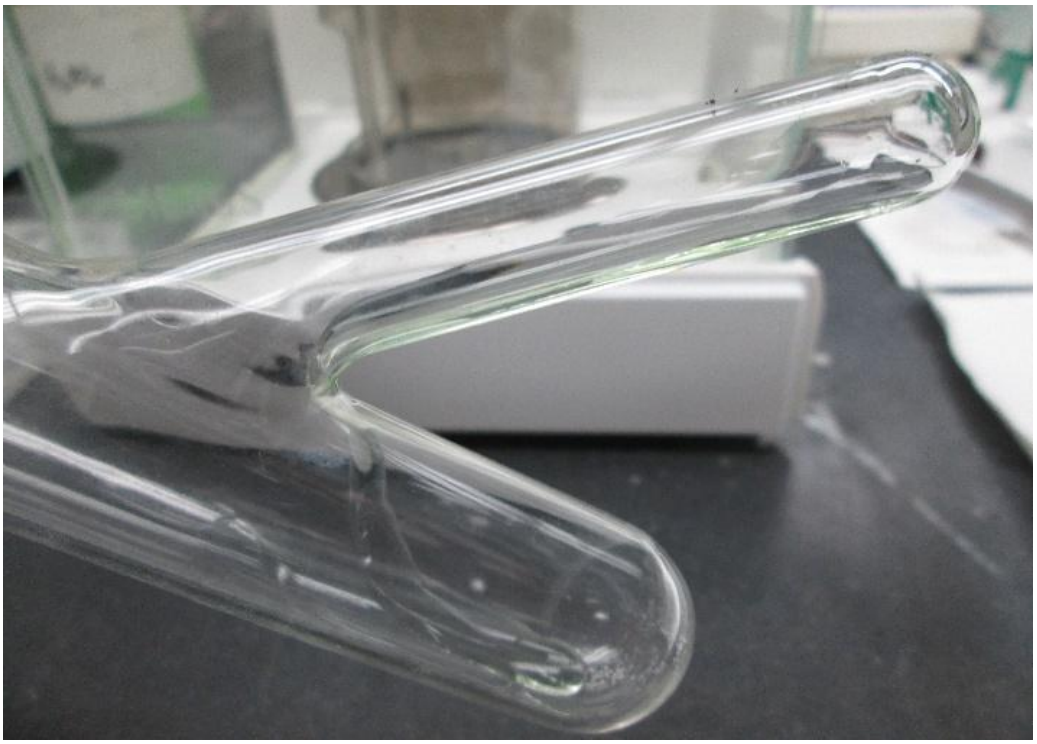

Figure B-1: ST Containing Ground Sample and Acid

Samples are heated to 30°C with either a water bath (Figure B-2) or the custom built heater block at 150°C (Figure B-3). The heater block is used only for Rx2 samples. Once the sample and acid are mixed, cryogenic extractions of CO_2 are completed at the desired time intervals. For multi-carbonate extractions, the ST is returned to the heating source immediately after Rx0 or Rx1 and the reaction continues.

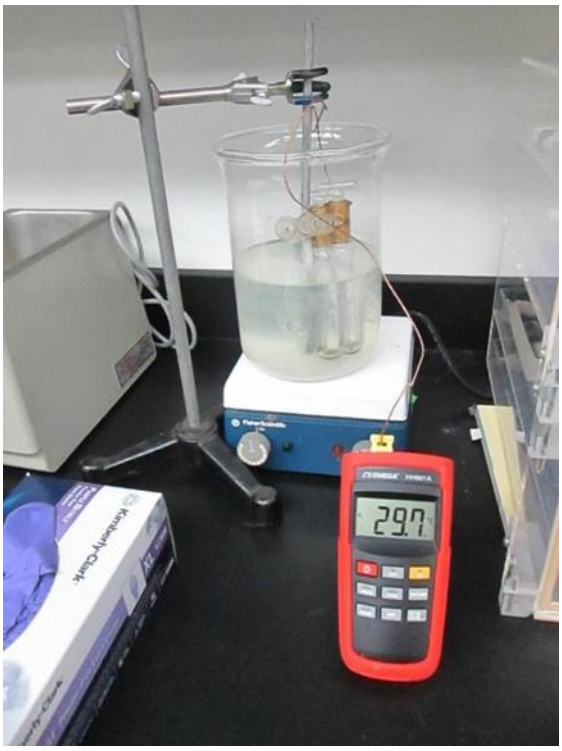

Figure B-2: Heating ST in Water Bath

Figure B-3: Heating ST in Heater Block

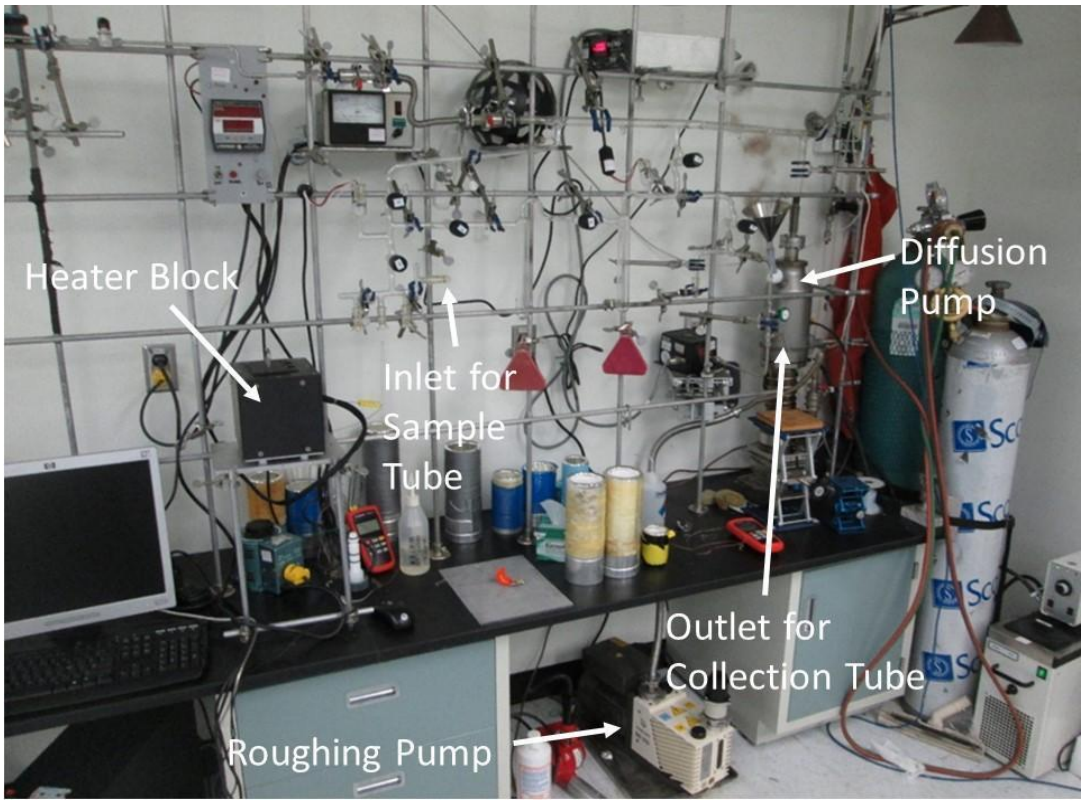

Figure B-4: LEAL Carbonate Extraction Line

CO_2 Extraction

The LEAL Carbonate extraction line is displayed in Figure B-4. Multi-step extractions separate different species of carbonates (Al-Aasm et al., 1990), with a first extraction after reaction (Rx) Rx1 at 30°C for 12-24 hours (to extract calcite), and then Rx2 at 150°C for 3 hours (to extract magnesite and/or siderite). This process is modified for meteorites to include an extra step. An early extraction, Rx0, after 1 hour at 30°C, has been shown to isolate terrestrial Ca-rich carbonates that are a contamination from meteorites collected in Antarctica (Shaheen et al., 2015). The Rx0 extraction was not performed on carbonate standards.

The cryogenic capture of CO_2 progressed in two steps for each extraction. The first step requires a dewar of chilled methanol at approximately -40°C placed on the left pyrex tube, and a dewar of liquid N_2 on the right pyrex tube of the carbonate extraction line (see Figure B-5). Water and some condensable gases are frozen into the left pyrex tube, while CO_2 and condensable gas with a freezing point above the temperature of liquid N_2 (-196°C) are frozen into the right pyrex tube. Incondensable gas, composed of sulfur-rich compounds and organics, is pumped away to bring the system back to vacuum of approximately 1 μbar.

Figure B-5: Dewars on Carbonate Extraction Line

The second step begins by isolating the frozen CO_2 in the right pyrex tube, then swapping the liquid N_2 dewar for the chilled alcohol dewar. As the right pyrex tube warms, the CO_2 melts and refreezes in the carbonate line FT_c within a small dewar of liquid N_2. The CO_2 is isolated by closing valves on the system. Additional water and condensable gas are trapped in the right dewar, and are then thawed and pumped away (along with any remaining incondensable gas). The YIELD of CO_2 is determined with carbonate standard samples of known mass (and moles of CO_2). The frozen CO_2 in the FT_c, is allowed to expand into a known volume connected to a pressure gauge. The associated pressure, P_{FTc} is recorded and the moles of extracted gas are calculated using the ideal gas law (see detailed discussion under section "Predicting Sample CO_2 YIELD, below). Finally, the CO_2 is refrozen into a Collection Tube (CT) for transfer to either the IRMS or the GC.

CO_2 Purification

All of the meteorites samples were transferred to the GC for purification before stable isotope measurements were made on the IRMS. This is due to the presence of condensable gases that transfer with the CO_2 into the CT.

This pressure derived method of determining Yield from the carbonate standards, based on the ideal gas law, proved inaccurate when extracting CO_2 from the meteorites. Acidification of meteorite samples created condensable sulfur-bearing and organic gases that mixed with the thawed CO_2 to create a false pressure reading. For the meteorite samples, an alternate method for predicting moles of CO_2 is made. The CO_2 from carbonate standard samples of known size is run through the GC, and the peak size for the CO_2 is recorded. A correlation was made to predict meteorite CO_2 sample size based upon the GC CO_2 peak size (see detailed discussion under section "Correlate GC CO_2 Peak Count to Sample Size, below).

Loading the CO_2 into the GC required the construction of new stainless steel inlet and outlet loops to capture the CO_2 with dewars of liquid N_2 (these loops became contaminated over time with organic or condensable gas residue from meteorite reactions, and were replaced as the martian samples were analyzed). To load the CO_2 on the GC, the loops are first evacuated to baseline (approximately 1 μbar of pressure). The CO_2 from the CT is frozen to the inlet loop, and then isolated with valves. The GC carrier gas, Helium, is then loaded into the inlet loop with the frozen CO_2. The dewar is removed, and the CO_2 thaws and mixes with the Helium. This creates a "slug" of

sample that moves into the GC and creates a well-defined CO_2 peak (see Figure B-6). Other gases are seen passing through the GC with distinctly different retention times.

Purified CO_2 is cryogenically captured in the GC outlet loop and transferred to the CT. The CO_2 GC collection time was iterated to maximize CO_2 capture without collecting other gases. The NASA1 calcite, Ordinary Chondrites, and initial martian Nakhlites collected CO_2 for 4 minutes total (collection started at 2.5 minutes and ended at 6.5 minute retention time in the GC run). Martian Nakhlite MIL 090136 displayed an odd peak at 4.8 min which is possibly N_2O, a gas not seen in other samples (see Figure B-7). The collection time for this meteorite was adjusted as 2.5 min to 4.8 min (2.3 min total). After collecting the CO_2 in the GC outlet loop, the CO_2 is cryogenically transferred to the CT and then then moved to the IRMS for stable isotope measurements.

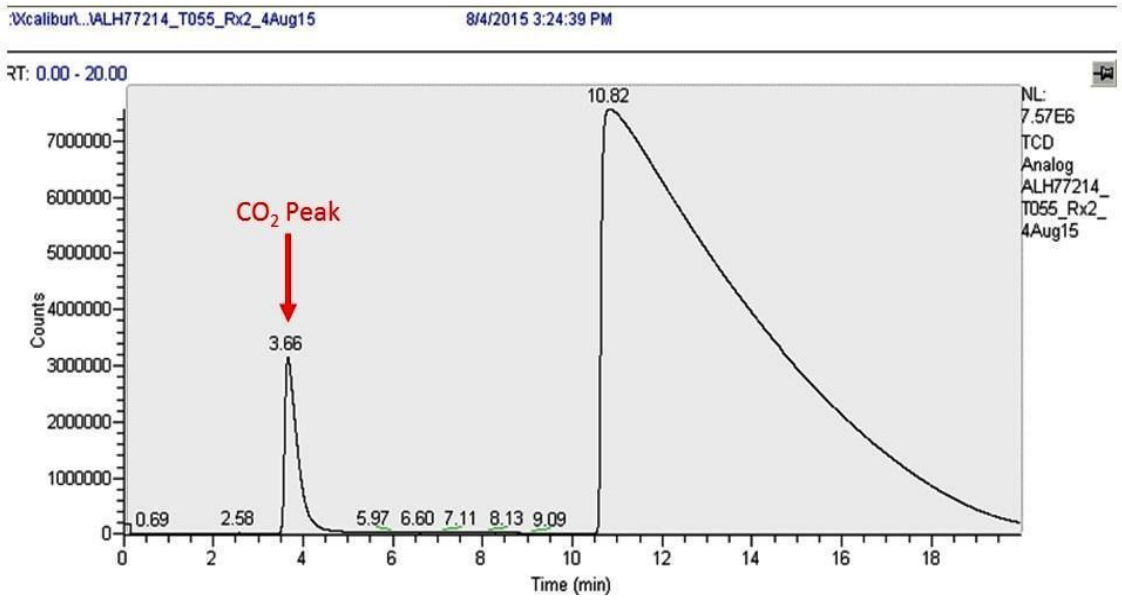

Figure B-6: GC CO_2 Peak Assessment for OC ALH 77214

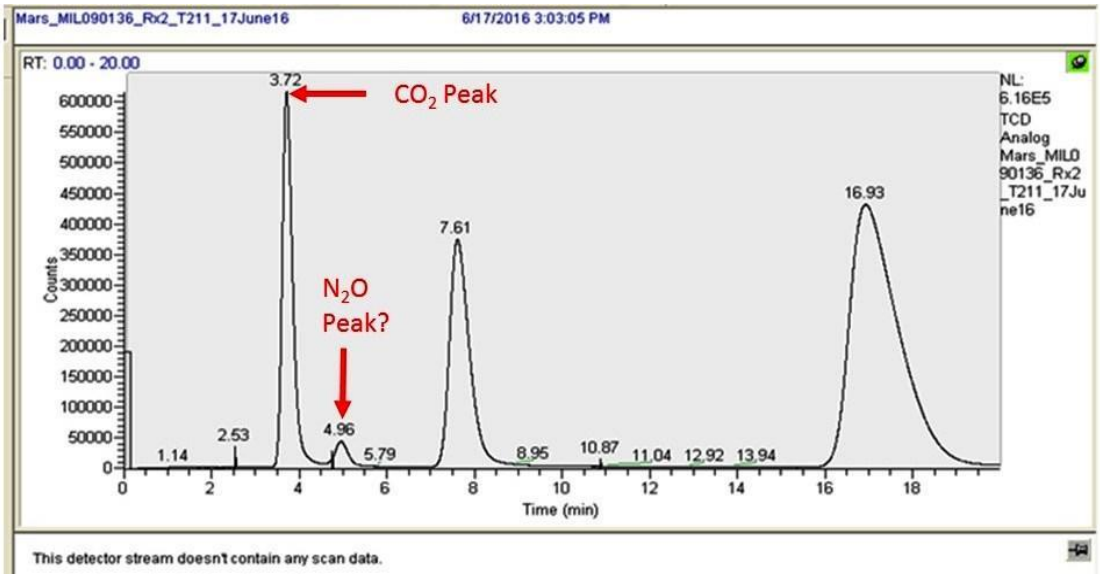

Figure B-7: Nakhlite MIL 090136 Rx2 GC Run

The Nakhlite meteorite samples display GC CO_2 peaks consistently from retention times of 3.4 min. to 4.0 min (see Figure B-8). The Nakhlites also create GC peaks from retention times of 11 min. to 18 min., which are not from CO_2. These peaks are created by unknown gases that are created with the Nakhlite acidification, but not seen mixed with the CO_2 from the carbonate standards or OC samples (see Figure B-9). No diagnostic analysis of these unknown gases was performed, but they smelled of sulfur-bearing compounds when run through the GC.

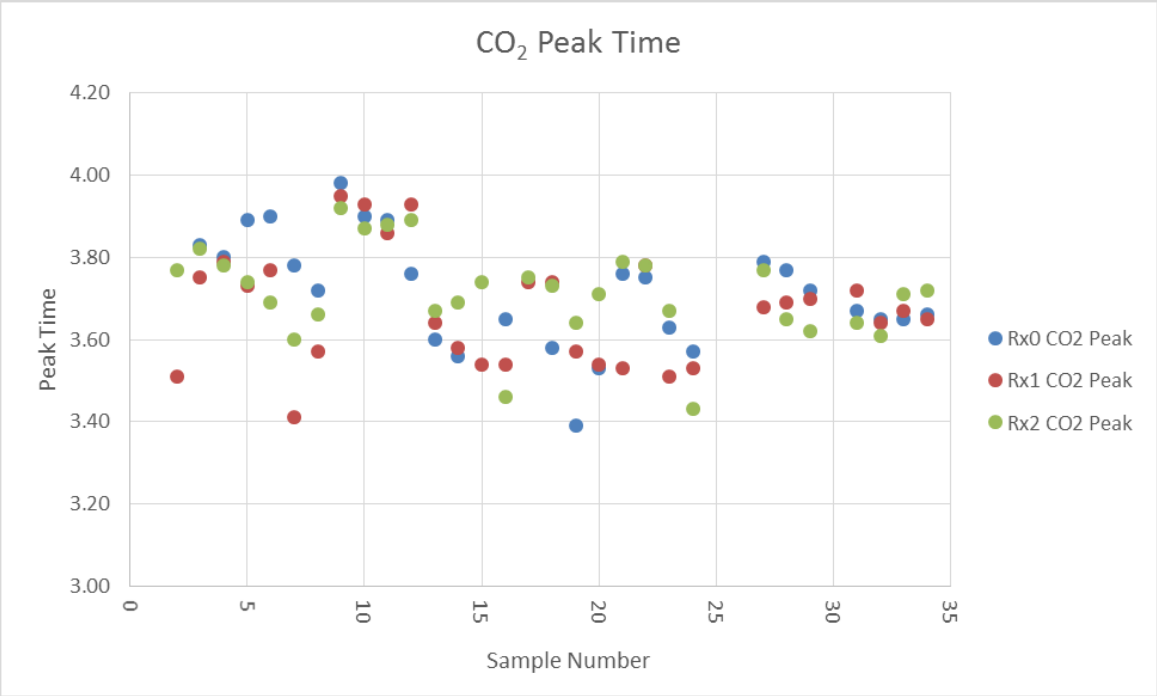

Figure B-8: Summary of All Nakhlite GC CO_2 Peak Times

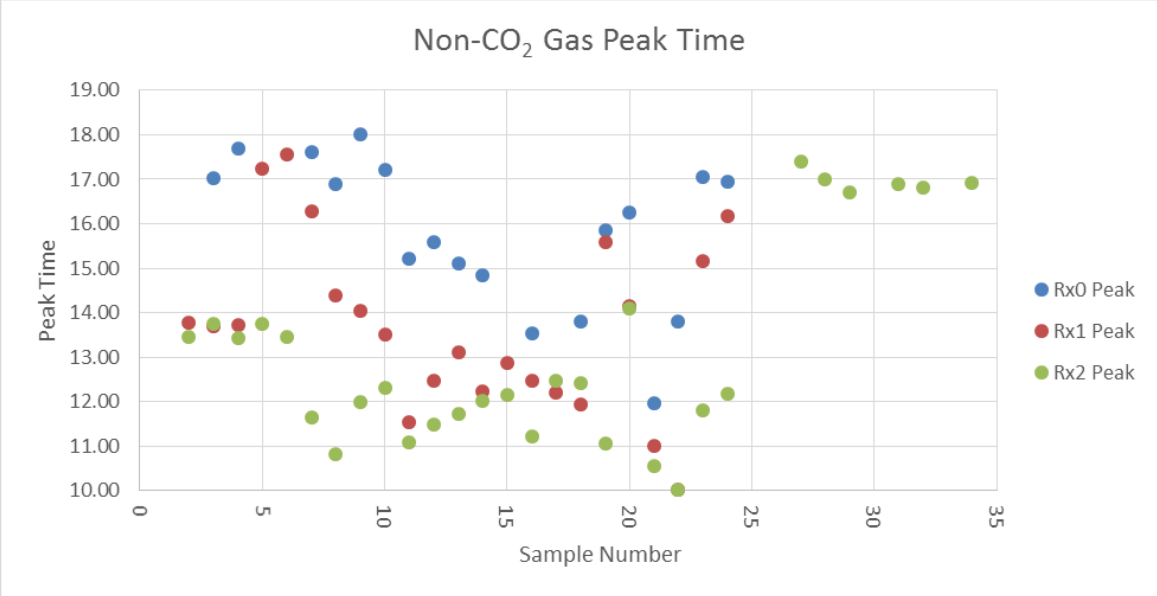

Figure B-9: Summary of All Nakhlite GC non-CO_2 Peak Times

Stable Isotope Measurements

The LEAL instrument configuration, including the Thermo MAT 253 Isotope Ratio Mass Spectrometer (IRMS) and Gas Bench, is shown in Figure B-10. The IRMS measures the stable isotopes of carbon and oxygen in CO_2. When run in "dual inlet" mode, the machine measures the difference in isotope values for CO_2 from a sample as compared to the CO_2 from a reference gas with known $\delta^{13}C$ and $\delta^{18}O$ values. A "Zero-enrichment" run, or "CO_2-zero", is initially run with the CO_2 reference gas as sample. If the results indicate the measured sample value is the same as the reference gas, then the machine is ready to measure unknown CO_2 samples.

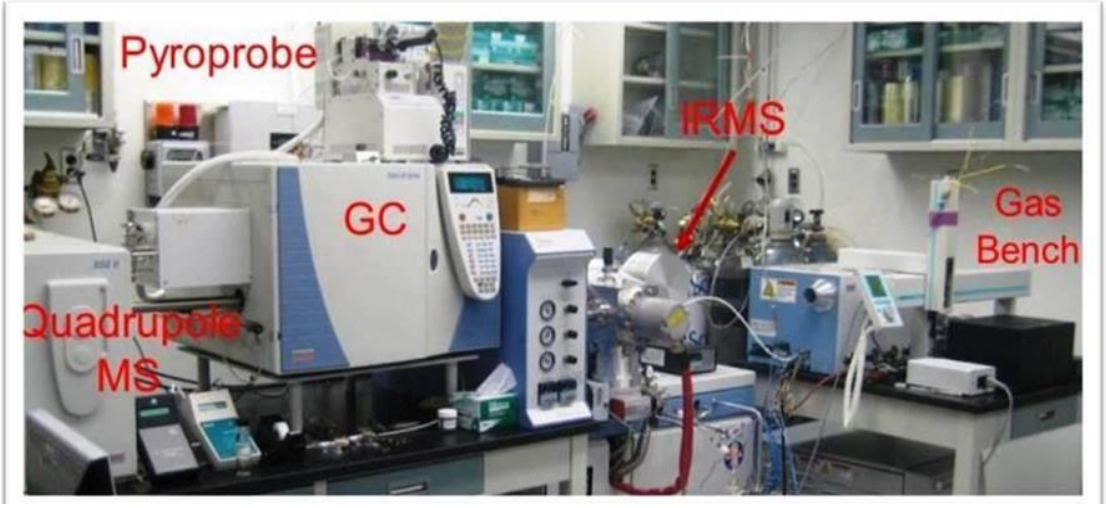

Figure B-10: LEAL IRMS and Gas Bench Configuration

The IRMS is prepared for sample measurements by loading the left bellow with CO_2 from either the carbonate extraction line, or the GC. To accomplish this, the CT containing sample CO_2 is connected to the IRMS on the left inlet port (see Figure B-11).

For large CO_2 samples, the sample gas is expanded from the CT into the left bellow at ambient temperature. For small CO_2 samples (such as from the meteorites), a small FT is attached to the left bellow (replacing the pressure gauge). The CO_2 is cryogenically transferred to the FT using a small dewar of liquid N_2. The FT is then thawed and the sample CO_2 gas is compared to the reference CO_2 gas to calculate sample $\delta^{13}C$ and $\delta^{18}O$ values.

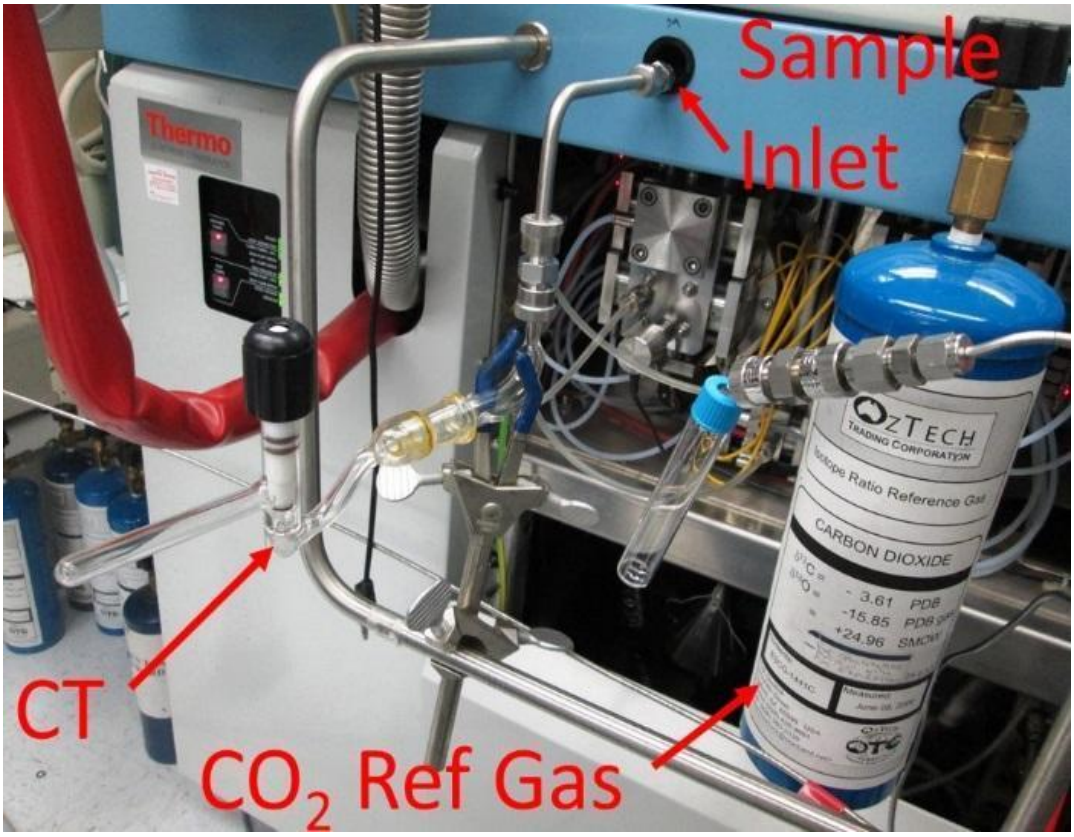

Figure B-11: IRMS Inlet Configuration

Building and Installing Apparatus for the NASA LEAL

The NASA Light Element Analysis Laboratory (LEAL) is a stable isotope measurement facility originally constructed at NASA's Johnson Space Center (JSC) to conduct analysis of lunar rocks returned to Earth with the Apollo astronauts. The facility had a inoperative carbonate extraction line that was modified for this study beginning in 2013. Much of the line consists of custom made glass tubing that requires skilled glass blowing to link the components (see Figure B-12). The glass components are connected to pumps and stainless steel tubing with couplings that require maintenance and monitoring to ensure atmospheric gas is not leaking into the line.

Figure B-12: Construction of the glass carbonate extraction line

One of the first new additions to the line is inlet tubing to connect with side arm Sample Tubes (ST). Each custom made ST is designed with two reservoirs: one to hold the solid sample and one to hold acid (see Figure B-13). The ST is tipped to allow the acid to mix with the sample and begin the reaction that creates CO_2 (see Figure B-1).

Figure B-13: ST Connected to the Carbonate Extraction Line

Another new addition to the extraction line is a stainless steel "Finger Tube". The FT is placed in a dewar of liquid Nitrogen (N2) at -196°C to cryogenically trap the sample CO_2. The FT is then isolated from the carbonate extraction line and the CO_2 gas is allowed to thaw and expand into a known volume. A pressure gauge on this FT volume is used to measure the amount of CO_2 for calculation of sample Yield. New connections were added to allow the sample gas to be cryogenically captured in Collection Tubes (CT) after determining Yield (see Figure B-14).

A new heater block with finger heaters and a Variac controller was designed for heating the STs to 150°C, which is necessary for separating different carbonate species in stepped extractions. This custom hardware was designed and fabricated to fit the STs. (see Figure B-3).

A chilled water system was attached to the molecular diffusion pump on the carbonate extraction line to provide sufficient cooling for desired operations. The system operates continuously at approximately $1x10^{-6}$ bars (1 μbar) of pressure.

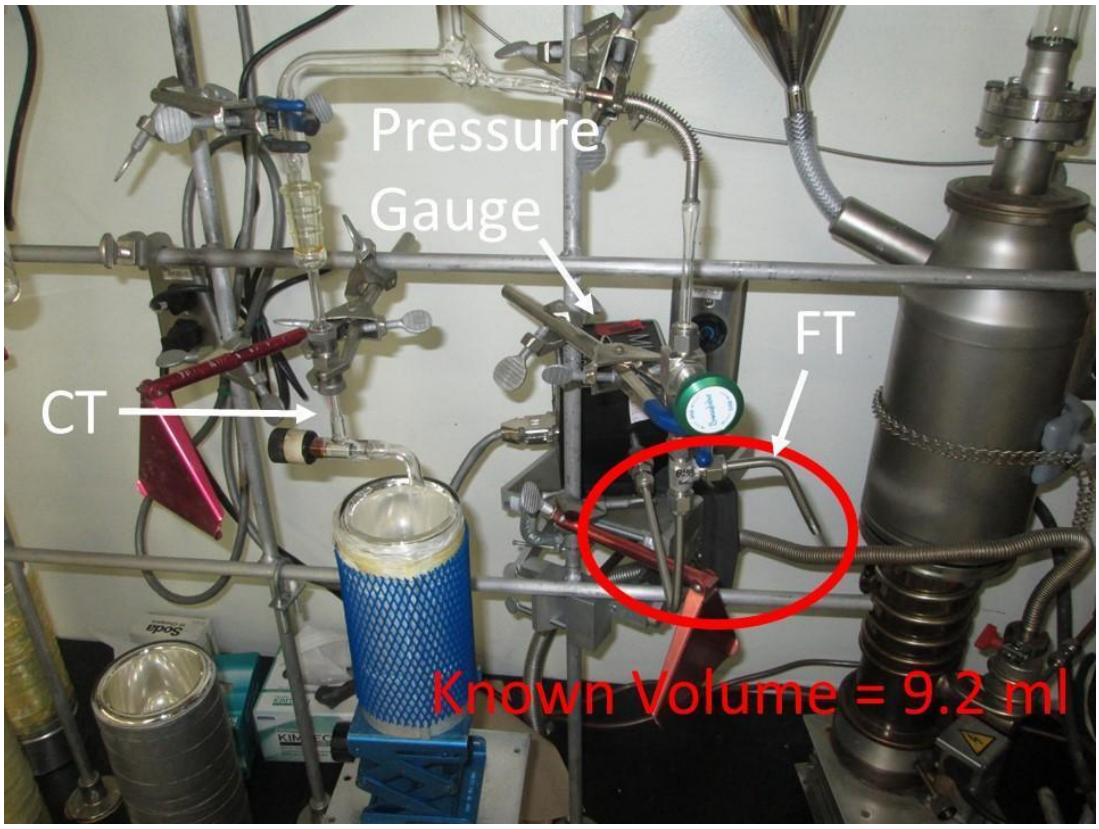

Figure B-14: FT_c on the Carbonate Extraction Line

In order to purify the extracted gas and isolate the CO_2 from other condensable gases, a GC was needed. An older, surplus GC was acquired from government surplus. Much effort was expended updating the software and connecting the instrument to an available, but outdated, laboratory personal computer (PC). A custom stainless steel inlet/outlet system was designed and created to connect a CT to the GC for loading sample gas and collecting purified CO_2. Once the GC was operational, procedures were developed to identify the optimal Helium (He) carrier gas flow rate and to concentrate the sample gas as a "slug" of input to the GC. Correction factors for this GC fractionation were determined and applied to the meteorite samples.

Several minor components were fabricated from wood to simplify operations in the laboratory. Custom stands were manufactured for each ST (see Figure B-15), and a GC cover was installed to provide a stable platform for dewars and CT jack stands.

Figure B-15: Custom ST Stands

Issues with Existing Equipment

Pump Maintenance

Laboratory equipment requires continuous maintenance and repair. Experiment measurements were frequently interrupted due to failures of equipment and the inherent delay in ordering and installing parts. Pumps on the carbonate extraction line, the GC, and the IRMS work continuously. Oil changes are necessary to replace fouled lubricant and ensure the systems operates at extremely low vacuum. Roughing pumps on the carbonate line (1 unit), and on the IRMS (3 units) provide vacuum sufficient for the 2^{nd} stage pumps (Diffusion and Turbo) to operate and generate the highest level of vacuum.

IRMS

The MAT 253 IRMS is an instrument capable of generating reliable stable isotope measurements on carbonates. This study is attempting to measure CO_2 samples that are much smaller than the manufacturer design. To ensure that all of the CO_2 sample small volume is captured, the left bellow (assigned as "sample" in dual inlet operations) pressure sensor was replaced with a custom made stainless steel FT. This allowed a small dewar of liquid N_2 to be applied to the FT, and the CO_2 was cryogenically trapped from the CT. It was noted after several meteorite sample runs that the FT was contaminated with residual material causing incorrect blank runs on the IRMS. New, smaller FTs were manufactured and installed on the IRMS as the old FTs became corrupt. The loss of a pressure gauge on the left bellow was not an impact

during the sample runs, but the pressure gauge was required whenever the IRMS system required re-calibration of the bellows.

The meteorite samples provided very small volumes of CO_2 for analysis. The recommended signal for stable isotope measurements of the IRMS is 2000 mv (2 volts), but many of the meteorite samples were analyzed with signals from 200-500 mv. To ensure this low signal provided accurate stable isotope values, carbonate standards of 1-2 µmole carbonate size (which creates 1-2 µmole CO_2) were measured. These samples provided a signal range comparable to the meteorite sample signals, and a correction factor was created to offset the stable isotope values for such small volumes of CO_2.

A modification to the IRMS was made for the martian meteorite samples. A small stainless steel "finger tube" was installed on the left sample bellow, replacing the pressure gauge. This allowed a small dewar of liquid N_2 to freeze 100% of the sample CO_2 from the inlet CT to the IRMS. This allowed carbonates samples of 1-5 µmole to be measured on the system.

The IRMS ion source is an electrical filament that is consumed with use. An annual preventative maintenance procedure, performed by a Thermo MAT 253 technician, frequently replaced the source filament and adjusted the lens alignment on the ion source. The inability to create a stable signal on the IRMS made experiments impossible, and much time was lost diagnosing and repairing the instrument.

Glassware

Meteorite acidification creates deposits on STs that can't be cleaned with available acids. The "stained" STs run with carbonate standards demonstrate no impact on the resulting stable isotope measurements of CO_2. Eventually these STs will need to be physically repolished to remove the deposits.

Water Leaks in Facility

The LEAL is a government facility located in a building constructed in the 1960s. The lab is located underneath an air-handler unit providing air conditioning to the building. Periodically, buildup of scale in the secondary overflow pans on the A/C condenser units causes water to flow into the ceiling of the LEAL, and to fall onto benches and equipment beneath the light fixtures (see Figure B-16).

Figure B-16: LEAL Water Overflow Event

The LEAL configuration has changed significantly over the years. Much of the layout is the result of "add-on" components without overall planning of the system. Safety inspection modifications have slowly improved the layout of the lab floor space.

APPENDIX C

CARBONATE EXTRACTION WORKSHEET

	Sample:	ST1 No:	ST2 No:
1	SAMPLE PREP Date/Time:		
	Grinding Notes:		
	Regolith wt (µg)		
	Acid Volume (ml): Pump to (µm Hg):		
	Lab Temp/Humidity:		
2	Rx0 Temp:	Hours:	Hours:
3	Rx0 Extract Date/Time:		
	P1 Measure, Slurry Temp: Incond Open/Closed: Pump down:		
	P2 Measure, Baseline: Incond: Pump down:		
	Carbonate FT P (mb):		
4	Rx0 GC Date/Time:		
	Xfer to Inlet(min): Load He to Inlet (sec): GC Time Open: GC Time Closed: CO2 Peak time: CO2 Peak count: Organic Peak time: Organic Peak count: Pump away He to: Xfer to CT(min):		
5	Rx0 CO2-ZERO Run/L100		
	d13C: d18O:		
6	Rx0 IRMS Run/L100		
	d13C: d18O: R2:		
7	Rx0 Comments:		
8	Rx1 Temp:	Hours:	Hours:
9	Rx1 Extract Date/Time:		
	P1 Measure, Slurry Temp: Incond Open/Closed: Pump down:		
	P2 Measure, Baseline: Incond: Pump down:		
	Carbonate FT P (mb):		

10	Rx1 GC Date/Time:		
	Xfer to Inlet(min): Load He to Inlet (sec): GC Time Open: GC Time Closed: CO2 Peak time: CO2 Peak count: Organic Peak time: Organic Peak count: Pump away He to: Xfer to CT(min):		
11	Rx1 CO2-ZERO Run/L100		
	d13C: d18O:		
12	Rx1 IRMS Run/L100		
	d13C: d18O: R2:		
13	Rx1 Comments:		
14	Rx2 Temp:	Hours:	Hours:
15	Rx2 Extract Date/Time:		
	P1 Measure, Slurry Temp: Incond Open/Closed: Pump down:		
	P2 Measure, Baseline: Incond: Pump down:		
	Carbonate FT P (mb):		
16	Rx2 GC Date/Time:		
	Xfer to Inlet(min): Load He to Inlet (sec): GC Time Open: GC Time Closed: CO2 Peak time: CO2 Peak count: Organic Peak time: Organic Peak count: Pump away He to: Xfer to CT(min):		
17	Rx2 CO2-ZERO Run/L100		
	d13C: d18O:		
18	Rx2 IRMS Run/L100		
	d13C: d18O: R2:		
19	Rx2 Comments:		

APPENDIX D

METEORITE SAMPLE REQUESTS

MWG Request Dated 8/13/2013

Antarctic Meteorite Sample Request Form

1a) Name of person requesting samples: Dr. Michael Evans
1b) Signature:
2) Professional Title: NASA Pathways PhD Student
3) Date: 8/13/2013
4) Institution: Johnson Space Center
5) Address: Mail Code KR, 2101 NASA Parkway, Houston, Tx. 77058
6) Telephone: 281-483-3171
7) E-mail: Michael.E.Evans@NASA.gov

(8) Meteorite	(9) Class	(10) Form	(11) No.	(12) Mass/Size	(13) Minimum mass/size	(14) Remarks and notes	Weathering
MIL 03334	H6	Chip	1	4025.900	1g-3g	For new study on weathering	B/CE
MIL 03335	L5	Chip	1	2283.300	1g-3g	For new study on weathering	B/CE
MIL 03336	L5	Chip	1	969.800	1g-3g	For new study on weathering	BE
MIL 03337	LL5	Chip	1	1564.700	1g-3g	For new study on weathering	A/BE
MIL 03338	L5	Chip	1	1597.300	1g-3g	For new study on weathering	A/BE
MIL 03362	LL5	Chip	1	400.200	1g-3g	For new study on weathering	BE
MIL 03374	L5	Chip	1	71.271	1g-3g	For new study on weathering	B/CE
MIL 03395	H5	Chip	1	20.003	1g-3g	For new study on weathering	B/CE
MIL 03429	H5	Chip	1	27.269	1g-3g	For new study on weathering	B/CE
MIL 05001	L5	Chip	1	3055.500	1g-3g	For new study on weathering	BE
MIL 05002	H5	Chip	1	21490.000	1g-3g	For new study on weathering	CE
MIL 05005	L5	Chip	1	1127.800	1g-3g	For new study on weathering	BE
MIL 05006	L5	Chip	1	1234.800	1g-3g	For new study on weathering	BE
MIL 05008	H5	Chip	1	330.900	1g-3g	For new study on weathering	B/CE
MIL 05022	L5	Chip	1	235.700	1g-3g	For new study on weathering	B/CE
MIL 05027	LL6	Chip	1	67.520	1g-3g	For new study on weathering	A/BE
MIL 05045	L5	Chip	1	283.400	1g-3g	For new study on weathering	B/CE
MIL 05047	LL5	Chip	1	289.700	1g-3g	For new study on weathering	A/BE
MIL 05107	LL6	Chip	1	18.683	1g-3g	For new study on weathering	A/BE
MIL 07005	LL6	Chip	1	75.000	1g-3g	For new study on weathering	A/BE
RBT 04149	H6	Chip	1	94.734	1g-3g	For new study on weathering	CE
RBT 04298	LL5	Chip	1	43.956	1g-3g	For new study on weathering	BE
ALHA 77299	H3.7	Chip	1	260.700	1g-3g	Repeat Grady (1988) study results	A
ALHA 77214	L3.4	Chip	1	2111.000	1g-3g	Repeat Grady (1988) study results	C
ALHA 77215	L3.8	Chip	1	819.600	1g-3g	Repeat Grady (1988) study results	B
ALHA 77278	LL3.7	Chip	1	312.900	1g-3g	Repeat Grady (1988) study results	A
ALHA 77294	H5	Chip	2	1351.000	1g-3g	Repeat Karlsson (1990) study results	AE
ALHA 78134	H4	Chip	1	458.30	1g-3g	Repeat Karlsson (1990) study results	B/C
ALHA 77231	L6	Chip	2	9270.00	1g-3g	Repeat Karlsson (1990) study results	A/BE
ALHA 77262	H4	Chip	2	861.50	1g-3g	Repeat Karlsson (1990) study results	B/CE
EET 83202	L5-6	Chip	1	1231.20	1g-3g	Repeat Karlsson (1990) study results	A/B
LEW 85320	H5	Chip	2	110200.00	1g-3g	Repeat Karlsson (1990) and Socki (1992) study results	Be

1

15) Title of Research

Characterization of the terrestrial carbonates found in Antarctica ordinary chondrite meteorites using stable isotopes analysis

16) Purpose of Study/Scientific rationale

This proposed study seeks to identify a distinctive oxygen isotope signature for terrestrial carbonate weathering on meteorites collected from Antarctica. When this signature is identified, it can be applied to future studies of meteorite carbonates to isolate the terrestrial weathering from the insitu carbonate (extraterrestrial) species. Minerals such as nesquehonite ($MgCO_3 \bullet 3H_2O$) form on the exterior surface and in cracks of Antarctic meteorites when they come into contact with terrestrial water and atmospheric CO_2 in cold temperatures (Kloprogge et al., 2003). It is proposed that these terrestrial carbonate species have a oxygen isotope value (and possibly a carbon isotope value) that is distinct from the bulk rock values determined by prior researchers (Grady et al., 1988, Velbel, 1988, Karlsson, 1991, Socki et al., 1992). It is hoped that knowledge of this unique terrestrial carbonate isotopic signature can then be applied to these past studies to discern a more accurate evaluation of the non-terrestrial carbonate isotope values.

Using a newly constructed laboratory experiment at NASA Johnson Space Center Light Element Analysis Laboratory (LEAL), a high precision study of triple-oxygen isotopes will be completed on the selected ordinary chondrite meteorites. Precise measurement of the triple-oxygen isotope ratios ($^{16}O/^{17}O/^{18}O$) will yield better mass-independent fractionation calculations of $\Delta^{17}O$ to identify the mineral source. Comparison of the measured bulk rock carbonate $\delta^{17}O$, $\delta^{18}O$, and $\delta^{13}C$ values against published values will build confidence in the new equipment. Once it is determined that the LEAL equipment and procedure yields accurate results, new evaluation of evaporate deposits on the selected ordinary chondrites will be undertaken to meet the goals of this study.

This research is being conducted by Dr. Michael E. Evans as a Pathways Graduate Student working towards a PhD in Oceanography from Texas A&M University (TAMU). NASA scientists and TAMU faculty are collaborating to guide Dr. Evans in this effort. NASA/ARES/Dr. Paul Niles is his primary technical advisor and TAMU/Oceanography/Dr. Piers Chapman is his primary academic advisor. Experiments conducted in the LEAL will be under the supervision of experienced isotope geochemists Richard A. Socki and Post-Doctorate Fellow Dr. Tao Sun. This proposed study is the 1st component of the planned research for the PhD thesis by Dr. Evans, which will include a future meteorite request for Martian meteorite samples.

17) Planned measurements and collaborators

All experiments will be conducted at the NASA/JSC LEAL facility in Houston, Tx.

Collaborator	Institute	Method	Mass required
Dr. Piers Chapman	Texas A&M University	Review results only with PhD Committee for Michael Evans	n/a

The samples will be carefully processed in the LEAL with supervision by experienced meteorite isotope geochemists. The general procedure follows prior analysis completed on Martian meteorites (Agee et al., 2013) (Farquhar and Thiemens, 2000):

1. Grind the meteorite chip containing carbonates/evaporites to a fine powder
2. Divide the ground meteorite chip sample into three separate containers. Load the powder from each container into an evacuation vessel and mixed with H_3PO_4 at a vacuum pressure of approximately 10^{-6} Torr for a pre-determined time interval at a pre-determined temperature. This

reaction produces CO_2. Each combination of time and temperature dissolves distinct carbonates within the sample. The digestions are:

a. 1 hour at 25°C
b. 12 hours at 25°C
c. 3 hours at 150°C

3. Measure the $\delta^{13}C$ of a portion of the created CO_2 gas for each sample in the IRMS. Cryogenically re-capture the remaining CO_2.
4. Create pure O_2 gas by combining the CO_2 gas with Bromine Pentafluoride (BrF_5) in a closed Nickel-alloy reaction chamber at 800°C for 48 hours
5. Measure the $\delta^{17}O$ and $\delta^{18}O$ of the created O_2 gas from each sample on the IRMS
6. Calculate the $\Delta^{17}O$ of each sample

18) Reason(s) for choosing the particular samples requested

Samples are requested from the ALHA, EET, and LEW meteorites to replicate published isotope analysis and verify the accuracy of the LEAL experimental system. For each of these meteorites, it is requested that a 1-3 gram chip be provided including bulk rock carbonates as provided to prior studies. If the meteorite is listed as having evaporates, then a second chip request of 1-3 grams is requested to concentrate only on the evaporite carbonates (ALHA 77294, 77231, 77262, and LEW 85320).

Samples are requested from MIL and RBT based upon a selection criteria focused on testing evaporate carbonates. A 1-3 gram chip is requested from the surface/cracks each of these meteorite where the carbonates exist. The steps in selecting these samples followed this sequence:

- Start with the NASA Meteorite Database (16,100 records) at:
  http://curator.jsc.nasa.gov/antmet/us_clctn.cfm
- Select only meteorites with evaporate weathering (850 records)
  Desire OC with obvious carbonates visible likely from Antarctic exposure
- Select only meteorites with type H4-H6, L4-L6, or LL4-LL6 (597 records)
  Desire OC with no pre-terrestrial weathering (no aqueous alteration)
- Select only meteorites from sites ALH, EET, MIL, LEW, RBT, or PCA (246 records)
  Desire OC collected from sites where Martian meteorites have been located
- Select only meteorites with mass > 10 grams (189 records)
  Desire OC with enough mass to provide chips for analysis
- Select only meteorites collected after 2000 (22 records)
  Desire OC with limited time exposure to pure nitrogen gas storage environment that might promote secondary carbonate formation

19) Basis for estimating mass requested

The isotope analysis on the MAT 253 IRMS in the LEAL requires at least 5 µmole CO_2. Analysis of the Martian meteorite EETA 79001 provides a rare publication stating expected CO_2 yield based on meteorite chip sample size. In this study, 29.3 mg chip containing calcite generated 1.33 µmole CO_2. (Clayton and Mayeda, 1988). Thus for EETA 79001, a chip of at least 120 mg would be required to generate sufficient carbon dioxide for analysis on the LEAL MAT 253. Since each sample must be analyzed with 3 different acid digestions, at least 360 mg of EETA 79001 would be required (A sample from EETA 79001 is NOT being requested).

This study is completing analysis of weathered ordinary chondrites. The expected yield of CO_2 per sample size is at least the equivalent of EETA 79001, and likely greater due to the visible evidence of evaporates. Thus, sample chips of 1-3g are requested from each of the specified meteorites. This will at least 3-4 times more than the minimum amount required for the analysis.

20) Special preparations
As stated above, each chip should contain visible evaporites (preferably $CaCO_3$ minerals) from the external surface of the meteorite except for the few samples to be evaluated as bulk rock carbonates. Dr. Evans will be returning to NASA/JSC in January 2014 for a co-op tour lasting until August 2014, and he would like to participate in the sample collection process (if possible).

21) Effects on samples
Each sample will be ground to a powder and digested with acid to generate carbon dioxide gas from insitu carbonates. The residual powder will be retained in the LEAL and returned to the designated location upon completion of the analysis.

22) Certification of research advisor (required only when requester has not yet received an undergraduate or graduate degree).

I certify that the student submitting this request has access to the laboratories required to complete the research.

Name: Dr. Paul Niles Signature:

Institution: NASA/JSC/ARES Address 2101 NASA Parkway, Houston, Tx.

Telephone: (281) 483-7860 E-mail: Paul.B.Niles@NASA.gov

References:

AGEE, C. B., WILSON, N. V., MCCUBBIN, F. M., ZIEGLER, K., POLYAK, V. J., SHARP, Z. D., ASMEROM, Y., NUNN, M. H., SHAHEEN, R., THIEMENS, M. H., STEELE, A., FOGEL, M. L., BOWDEN, R., GLAMOCLIJA, M., ZHANG, Z. & ELARDO, S. M. 2013. Unique Meteorite from Early Amazonian Mars: Water-Rich Basaltic Breccia Northwest Africa 7034. *Science,* 339, 780-785.

CLAYTON, R. N. & MAYEDA, T. K. 1988. Isotopic composition of carbonate in EETA 79001 and its relation to parent body volatiles. *Geochimica et Cosmochimica Acta,* 52, 925-927.

FARQUHAR, J. & THIEMENS, M. H. 2000. Oxygen cycle of the Martian atmosphere-regolith system: Δ17O of secondary phases in Nakhla and Lafayette. *Journal of Geophysical Research: Planets,* 105, 11991-11997.

GRADY, M. M., WRIGHT, I. P., SWART, P. K. & PILLINGER, C. T. 1988. The Carbon and Oxygen Isotopic Composition of Meteoritic Carbonates. *Geochimica Et Cosmochimica Acta,* 52, 2855-2866.

KARLSSON, H. R. J., A. J. T; SOCKI, R. A.; GIBSON, JR., E. K. Carbonates in Antarctic Ordinary Chondrites: Evidence for Terrestrial Origin. Lunar and Planetary Institute Science Conference Abstracts, 1991. 689.

KLOPROGGE, J. T., MARTENS, W. N., NOTHDURFT, L., DUONG, L. V. & WEBB, G. E. 2003. Low temperature synthesis and characterization of nesquehonite. *Journal of Materials Science Letters,* 22, 825-829.

SOCKI, R., ROMANEK, C., GIBSON JR, E. & ALLTON, J. 1992. Hydrogen and Oxygen Isotope Exchange in Hydrated Carbonates from an H-5 Chondrite: Clues to the Formation of Weathering Products on LEW85320. *Meteoritics,* 27, 290.

VELBEL, M. A. 1988. The Distribution and Significance of Evaporitic Weathering Products on Antarctic Meteorites. *Meteoritics,* 23, 151-159.

MWG Request Dated 3/4/16

Antarctic Meteorite Sample Request Form

1a) Name of person requesting samples: Dr. Michael Evans

1b) Signature:

2) Professional Title: NASA Pathways PhD Student

3) Date: 3/4/16

4) Institution: Johnson Space Center

5) Address Mail Code XI3, 2101 NASA Parkway, Houston, Tx. 77058

6) Telephone: 281-483-3276

7) E-mail: Michael.E.Evans@NASA.gov

(8) Meteorite	(9) Class	(10) Form	(11) No.	(12) Mass/Size	(13) Minimum mass/size	(14) Remarks and notes	Weathering
EET 96034	L6	Chip	2	311.400	1g-3g	New study on weathering	Be
EET 96279	LL6	Chip	2	45.300	1g-3g	New study on weathering	Ce
EET 99412	H5	Chip	2	250.000	1g-3g	New study on weathering	Ce
EET 99425	H5	Chip	2	61.900	1g-3g	New study on weathering	B/Ce
MIL 03346	Nak	Chip	1	715.200	1g-3g	New study on weathering	B
MIL 090030	Nak	Chip	1	452.6	1g-3g	New study on weathering	B
MIL 090032	Nak	Chip	1	532.2	1g-3g	New study on weathering	B
MIL 090136	Nak	Chip	1	171	1g-3g	New study on weathering	B

15) Title of Research

Stable isotopic measurements of martian carbonates interpreted with measurements of terrestrial weathering in ordinary chondrites collected from Antarctica

16) Purpose of Study/Scientific rationale

This proposed study continues research initiated with a Meteorite Working Group (MWG) request form I submitted in August 2013. The requested samples were delivered to NASA/JSC/P. Niles from 2014 to 2015. I have now studied terrestrial carbonates formed on the exterior of carbonate-free Ordinary Chondrites (H, L, and LL alteration types 4-6) collected in Antarctica from the RBT and ALH sites. This research has been presented at the 2015 American Geophysical Union (AGU) annual conference in a poster session. I will again present my research at a poster session during the 2016 Lunar Planetary Science Conference (LPSC). A summary of these results in given in Figure 1, which reflects the documented measurements of carbonate $\delta^{13}C$ and $\delta^{18}O$ on martian meteorites compared to carbonates in the OCs completed by my study (Clayton and Mayeda, 1988, Wright et al., 1988, Wright et al., 1992, Wright et al., 1998, Jull et al., 1995, Jull et al., 1997, Jull et al., 2000, Romanek et al., 1994, Niles, 2005, Grady et al., 2007). It is apparent that some prior research has reported carbonate values for martian meteorites that is likely terrestrial carbonate contamination (specifically ALH84001, EET 79001, Nakhla, and Lafayette).

My results show that stepped extraction of CO_2 from OCs in Antarctica reflect 1) different species of terrestrial carbonates that form on the meteorites (Ca-rich and Fe-rich or Mg-rich, and 2) regionality in Ca-rich carbonates based on where the meteorites were collected (for RBT and ALH). OC samples from MIL will be also completed before the LPSC in March 2016. I will assess OC terrestrial carbonates from sites in Antarctica where known martian meteorites have been collected to better differentiate terrestrial carbonates from martian carbonates. I am thus requesting additional OCs from EET to compare with documented measurements from EETA 79001.

1

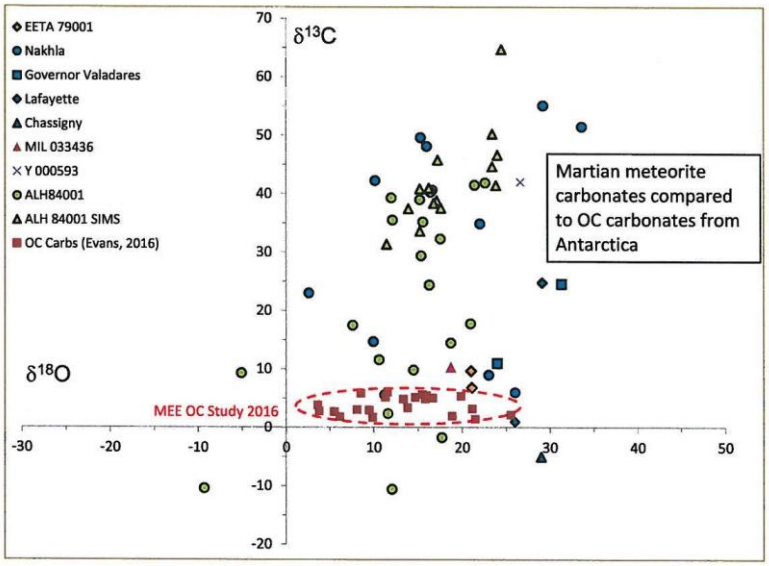

Figure 1: Martian meteorite carbonates and OC carbonate isotopic value comparison

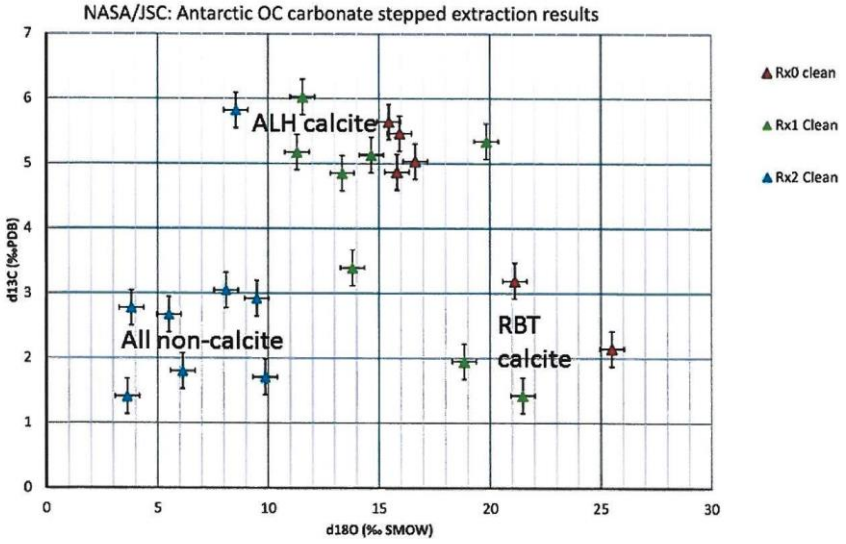

Figure 2: OC secondary carbonates from Antarctica reflect regional and petrographic differences

2

In addition, I request samples of each known martian Nakhlite collected from the Miller Range. To date, only one carbonate measurement has been completed on MIL 033436 (Grady et al., 2007), and this value is likely a mixture of terrestrial contamination and martian carbonate (see Figure 1). The measurement was made on a sample with very low CO_2 yield in a single H_3PO_4 extraction at 72°C. No carbonate stable isotope measurements using a stepped extraction technique (as described below) have been documented for MIL 090030, 090032, or 090136. These MIL meteorites are all paired (Hallis and Taylor, 2011) and petrographic analysis identified siderite in MIL 03346 (Grady et al., 2007), and either jarosite or siderite in MIL 090032 (Hallis et al., 2014). The martian carbonate is heterogeneous and a very small weight percentage of each meteorite, so samples of each paired meteorite is necessary.

The results of this research will identify 1) if the MIL Nakhlites contain any carbonates, 2) what the $\delta^{13}C$ and $\delta^{18}O$ values are for the different species of carbonates, and 3) if the carbonates resemble terrestrial contamination, in-situ martian carbonates, or a mixture of the two.

This research is being conducted by Dr. Michael E. Evans as a NASA Pathways Graduate Student working towards a PhD in Oceanography from Texas A&M University (TAMU). NASA scientists and TAMU faculty are collaborating to guide Dr. Evans in this effort. NASA/ARES/Dr. Paul Niles is his primary technical advisor and TAMU/Oceanography/Dr. Piers Chapman is his primary academic advisor.

17) Planned measurements and collaborators
All experiments will be conducted at the NASA/JSC LEAL facility in Houston, Tx.

Collaborator	Institute	Method	Mass required
Dr. Piers Chapman	Texas A&M University	Review results with PhD Committee for Michael Evans	n/a

The samples will be carefully handled in the LEAL with procedures developed for the ordinary chondrites from the 2013 request. The general procedure follows prior analysis completed on Martian meteorites (Agee et al., 2013) (Farquhar and Thiemens, 2000):

1. Gently grind the meteorite chip containing carbonates/evaporites to coarse powder
2. Divide the sample powder into at least 2 separate quantities for separate analysis (conduct at least two measurements on each sample)
3. Load the sample into a sample tube, load ~0.5 ml H_3PO_4 into a side arm on the sample tube, and vacuum the sample tube to approximately 0.002 Torr (2.6×10^{-3} mbar). Pre-heat the tube to 30°C and allow the H_3PO_4 to react with the sample. This reaction produces CO_2. Each combination of time and temperature dissolves distinct carbonates within the sample. The reactions are:
   a. 1 hour at 30°C
   b. 18 hours at 30°C
   c. 3 hours at 150°C
4. Cryogenically extract the CO_2 from the sample tube at each step, and measure the thawed CO_2 $\delta^{13}C$ and $\delta^{18}O$ on the IRMS

18) Reason(s) for choosing the particular samples requested
As with the first request from 2013, Ordinary Chondrites (OCs) were selected as follows:

- Start with the NASA Meteorite Database at:
  http://curator.jsc.nasa.gov/antmet/us_clctn.cfm
- Select only meteorites with evaporate weathering
  Desire OC with obvious carbonates visible likely from Antarctic exposure
- Select only meteorites with type H4-H6, L4-L6, or LL4-LL6

Desire OC with no pre-terrestrial weathering (no aqueous alteration). It is assumed these meteorites contain no insitu carbonates from formation

- Select only meteorites with mass > 10 grams
  Desire OC with enough mass to provide chips for analysis
- Select only meteorites collected after 1999
  Desire OC with limited time exposure to pure nitrogen gas storage environment that might promote secondary carbonate formation during curation

The four EET meteorite samples are requested to study the stable isotope difference between carbonates on the fusion crust and interior via bulk-rock analysis (using the stepped extraction technique). This provides insight into the extent of terrestrial contamination to the OC. The site EET was selected to provide proximity to EETA79001, which has been extensively studied with documented results (Carr et al., 1985, Clayton and Mayeda, 1988, Wright et al., 1988, Jull et al., 1992). For each of these meteorites, it is requested that a 1-3 gram chip be from the fusion crust where carbonates are present, and also a 1-3 gram chip of carbonates from the interior of the rock.

The four MIL Nakhlites are requested to study the bulk-rock stable carbonate stable isotopes using the stepped extraction technique, which has not previously been accomplished. For each of these martian meteorites, it is requested that a 1-3 gram chip of carbonates from the interior of the rock be provided.

19) Basis for estimating mass requested

The OCs I have studied have carbonates that are assumed to be 100% terrestrial contamination, with no extra-terrestrial carbonates. The MAT 253 Isotope Ratio Mass Spectrometer (IRMS) manufacturer recommends 5-10 μmole CO_2 for analysis, but I have demonstrated reasonable measurements from 1 μmole CO_2 extracted from these meteorites. In order to create at least 1 μmole CO_2 for each extraction step, I require at least 0.5g of OC ground sample. For verification of results, at least two measurements of each sample is desired; thus, a total of >1g OC sample is requested.

The martian meteorites will contain carbonates formed on Mars and terrestrial carbonates from Antarctic contamination. The amount of CO_2 extracted in each step will be at least 1 μmole for a 0.5g sample (based on the OC terrestrial contamination analysis) and perhaps up to 5-10 μmole CO_2 including martian carbonate. Prior research reflects great heterogeneity in martian carbonates, and provided samples may contain none. Thus a total of >1g martian sample is requested for each MIL meteorite to complete at least two measurements of each meteorite.

20) Special preparations

As stated above, each EET chip should contain visible evaporites (preferably $CaCO_3$ minerals) from the external surface. The interior chips from the EET and MIL meteorites should be as pristine as possible without evidence of any alteration. Dr. Evans is available to assist in selecting samples at NASA/JSC.

21) Effects on samples

Each sample will be ground to a powder and digested with acid to generate carbon dioxide gas from insitu carbonates. The residual powder, if any, will be retained in the LEAL and returned to the designated location upon completion of the analysis.

22) Certification of research advisor (required only when requester has not yet received an undergraduate or graduate degree).

I certify that the student submitting this request has access to the laboratories required to complete the research.

Name: Dr. Paul Niles Signature: 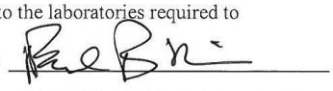

Institution: NASA/JSC/ARES/XI3 Address 2101 NASA Parkway, Houston, Tx.
Telephone: (281) 483-7860 E-mail: Paul.B.Niles@NASA.gov

AGEE, C. B., WILSON, N. V., MCCUBBIN, F. M., ZIEGLER, K., POLYAK, V. J., SHARP, Z. D., ASMEROM, Y., NUNN, M. H., SHAHEEN, R., THIEMENS, M. H., STEELE, A., FOGEL, M. L., BOWDEN, R., GLAMOCLIJA, M., ZHANG, Z. & ELARDO, S. M. 2013. Unique Meteorite from Early Amazonian Mars: Water-Rich Basaltic Breccia Northwest Africa 7034. *Science,* 339, 780-785.

CARR, R. H., GRADY, M. M., WRIGHT, I. P. & PILLINGER, C. T. 1985. Martian atmospheric carbon-dioxide and weathering products in SNC meteorites. *Nature,* 314, 248-250.

CLAYTON, R. N. & MAYEDA, T. K. 1988. Isotopic composition of carbonate in EETA 79001 and its relation to parent body volatiles. *Geochimica et Cosmochimica Acta,* 52, 925-927.

FARQUHAR, J. & THIEMENS, M. H. 2000. Oxygen cycle of the Martian atmosphere-regolith system: Δ17O of secondary phases in Nakhla and Lafayette. *Journal of Geophysical Research: Planets,* 105, 11991-11997.

GRADY, M. M., ANAND, M., GILMOUR, M., WATSON, J. & WRIGHT, I. 2007. Alteration of the Nakhlite Lava Pile: was water on the surface, seeping down, or at depth, percolating up? Evidence (such as it is) from carbonates.

HALLIS, L., ISHII, H., BRADLEY, J. & TAYLOR, G. 2014. Transmission electron microscope analyses of alteration phases in martian meteorite MIL 090032. *Geochimica et Cosmochimica Acta,* 134, 275-288.

HALLIS, L. J. & TAYLOR, G. J. 2011. Comparisons of the four Miller Range nakhlites, MIL 03346, 090030, 090032 and 090136: Textural and compositional observations of primary and secondary mineral assemblages. *Meteoritics & Planetary Science,* 46, 1787-1803.

JULL, A. J. T., BECK, J. W. & BURR, G. S. 2000. Isotopic evidence for extraterrestrial organic material in the Martian meteorite, Nakhla. *Geochimica et Cosmochimica Acta,* 64, 3763-3772.

JULL, A. J. T., DONAHUE, D. J., SWINDLE, T. D., BURKLAND, M. K., HERZOG, G. F., ALBRECHT, A., KLEIN, J. & MIDDLETON, R. 1992. Isotopic Studies Relevant to the Origin of the "White Druse" Carbonates on EETA 79001. *Lunar and Planetary Institute Science Conference Abstracts.*

JULL, A. J. T., EASTOE, C. J. & CLOUDT, S. 1997. Isotopic composition of carbonates in the SNC meteorites, Allan Hills 84001 and Zagami. *Journal of Geophysical Research-Planets,* 102, 1663-1669.

JULL, A. J. T., EASTOE, C. J., XUE, S. & HERZOG, G. F. 1995. Isotopic composition of carbonates in the SNC meteorites Allan Hills 84001 and Nakhla. *Meteoritics,* 30, 311-318.

NILES, P. B. 2005. *Evaluation of the formation environment of the carbonates in Martian meteorite ALH84001.* Dissertation, Arizona State University.

ROMANEK, C. S., GRADY, M. M., WRIGHT, I. P., MITTLEFEHLDT, D. W., SOCKI, R. A., PILLINGER, C. T. & GIBSON, E. K. 1994. Record of fluid-rock interactions on Mars from the meteorite ALH84001. *Nature,* 372, 655-657.

WRIGHT, I. P., GRADY, M. M. & PILLINGER, C. T. 1988. Carbon, Oxygen and Nitrogen Isotopic Compositions of Possible Martian Weathering Products in EETA-79001. *Geochimica Et Cosmochimica Acta,* 52, 917-924.

WRIGHT, I. P., GRADY, M. M. & PILLINGER, C. T. 1992. Chassigny and the Nakhlites - Carbon-Bearing Components and Their Relationship to Martian Environmental-Conditions. *Geochimica Et Cosmochimica Acta,* 56, 817-826.

WRIGHT, I. P., GRADY, M. M. & PILLINGER, C. T. 1998. Further carbon-isotopic measurements of carbonates in Allan Hills 84001. *Meteoritics & Planetary Science,* 33, A169-A169.